# Calcium oxalate modulation of tubular epithelial cell mitochondria: Oxidative vulnerability due to restricted glutathione homeostasis.

A thesis submitted to the University of London for the degree of

Doctor of Philosophy

By

Eirini Meimaridou BSc, MPhil

Institute of Urology and Nephrology

University College London

May 2007





ProQuest LLC
789 East Eisenhower Parkway
P.O. Box 1346
Ann Arbor, MI 48106-1346

# ABSTRACT

Calcium oxalate (COM) crystals are the commonest component of kidney stones. These arise mainly in the distal tubules and collecting ducts. To gain further insight for the cellular damage in terms of oxidative stress caused by COM deposition, *in vitro* and *in vivo* model studies were performed.

*In vitro*

In renal distal tubule cells, COM and free oxalate treatment caused a 3- and 2- fold increase respectively in superoxide ($O_2^{\bullet-}$) formation, originating from mitochondria. This was measured by lucigenin chemiluminescence in digitonin permeabilised cells. However, hydroxyapatite produced a much lower but significant enhancement of $O_2^{\bullet-}$, whilst other micro-particles, uric acid crystals, brushite, zymosan, and latex beads had no effect. When EDTA was omitted during $O_2^{\bullet-}$ monitoring, COM induced mitochondrial $O_2^{\bullet-}$ was ablated indicating a requirement for the release of free oxalate.

Mitochondrial oxalate uptake was studied by employing different oxalate transport inhibitors. Omitting phosphate from the media or using mersalyl both of which block dicarboxylate transport, caused a significant decrease in the $O_2^{\bullet-}$ formation evoked by COM treatments.

Using the membrane potential sensitive-probe tetramethylrhodamine methyl ester (TMRM) together with confocal microscopy, evidence is presented that in cells where COM binding had occurred a marked change in the mitochondrial membrane potential ($\Delta\psi_m$) occurred.

COM also modulated intracellular $Ca^{2+}$ signalling as demonstrated using the $Ca^{2}$-sensitive dye Fura-2 AM, and this was via a non-mitochondrial mechanism.

*In Vivo*

Using a rat model of crystalluria and renal stones initiated by treatment with ethylene glycol (EG) and 1, 25-dihydroxycholecalciferol (DHC), nephrolithiasis arose in kidneys and this was linked to oxidative stress. In the EG + DHC treated animals where crystalluria was evident, this oxidative insult was manifest by a decrease in total and mitochondrial glutathione concentration, as well as an increased activity of glucose-6-phosphate dehydrogenase.

Severe kidney damage at the mitochondria level was a further observation, indicated by the diminished $O_2$ consumption resulting in a lowered $O_2^{\cdot -}$ production. In addition, histopathological analysis revealed increased renal tubular pathology characterised by obstruction, distension and interstitial inflammation. The above findings were not observed in hyperoxaluria (EG) or calciuria (DHC) and are therefore a direct effect of crystal formation in kidney distal tubules that have implications in kidney stone disease which are discussed.

# ACKNOWLEDGEMENTS

Firstly, I would like to express my enormous gratitude to my supervisor Dr John Hothersall to whom I am indebted for his guidance and patience throughout the course of this study. I could not have asked for a better supervisor! I would also like to thank Dr Alberto Noronha-Dutra for his good advice and encouragement. I also thank Dr Jake Jacobson for the collaborative work with the confocal microscopy studies.

My time at the Institute of Urology and Nephrogy has been made very special and memorable by many people. I would like to thank Dr Theodossis Theodossiou and Veronique Blanc who have made my time here entertaining and enjoyable. Especially I would like to thank my dearest friend Dr Tahirah Alam for her patience, constant support and for sharing the most amazing and un-forgetful moments!

I would also like to thank Kelly Vetsika and Dr Kristie Theodorakou who have been great friends and relentless in their badgering me to finish this thesis – well now it's done!

For his amazing support, patience, and understanding I am grateful to Bilal, who have put up with my emotional ups and downs over the past couple of years.

Finally, I would like to thank my father Vassilis, my mother Fotini and my sister Antonia for their support and love. This work would never have been possible if it was not for them.

# TABLE OF CONTENTS

# LIST OF TABLES

## CHAPTER 1



## CHAPTER 2



## CHAPTER 7

# LIST OF FIGURES

## CHAPTER 1



## CHAPTER 2

# CHAPTER 3

## CHAPTER 4



## CHAPTER 5

## CHAPTER 6

## CHAPTER 7

## LIST OF ABBREVIATIONS

| | |
|---|---|
| $\Delta\psi_m$ | mitochondrial transmembrane potential |
| $^1O_2$ | singlet oxygen |
| ADP | adenosine diphosphate |
| AEBSF | 4-(2-Aminoethyl) enzenesulfonylfluoride |
| ANT | adenine nucleotide translocator |
| ATP | adenosine triphosphate |
| BCA | bicinchoninic acid |
| BSA | bovine serum albumin |
| BSC-1 | epithelial cells of African green monkey kidney origin |
| BSO | L-buthionine-sulfoximine |
| CaOx | calcium oxalate |
| CCCP | carbonylcyanide m-chlorophenylhydrazone |
| CCD | charge-coupled device |
| cDNA | complementary DNA |
| CL | chemiluminescence |
| COD | calcium oxalate dehydrate |
| COM | calcium oxalate monohydrate |

| | |
|---|---|
| Cu – SOD | copper superoxide dismutase |
| DCC | dicarboxylate carrier |
| DCCD | *N,N'* dicyclohexylcarbodiimide |
| DHC | 1, 25-dihydroxycholecalciferol |
| DMEM | Dulbecco's modified eagle's minimal essential medium |
| DMSO | dimethyl sulfoxide |
| DNA | Deoxyribonucleic acid |
| DPI | diphenyleneiodonium |
| DTNB | 5,5'-dithiobis-2-nitrobenzoic acid |
| EDTA | ethylenediaminetetraacetic acid |
| EG | ethylene glycol |
| EGTA | Ethylene glycol-bis(2-aminoethylether)-*N,N,N',N'*-tetraacetic acid |
| FAD | flavin adenine dinucleotide |
| FCS | fetal calf serum |
| G6PDH | Glucose-6-phosphate dehydrogenase |
| GAGs | glycosaminoglycans |
| GPx | glutathione peroxidase |
| GR | glutathione reductase |
| GSH | glutathione |

| | |
|---|---|
| GSSG | glutathione disulfide |
| H & E | haematoxylin and eosin |
| h | hour |
| $H_2O_2$ | hydrogen peroxide |
| HA | hydroxyapatite |
| HEPES | 4-(2-hydroxyethyl)-1-piperazineethanesulfonic acid, 4-(2-hydroxyethyl)-1-piperazineethanesulphonic acid |
| HK | human kidney |
| HOCl | hyperchlorous acid |
| Hsp | Heat shock protein |
| IMAC | Inner Membrane Anion Channel |
| IMCD | inner medullary collecting duct |
| IαI | inter- α – inhibitor |
| JC-1 | 1,1',3,3'-tetraethylbenzimidazolylcarbocyanine iodide |
| LB | latex beads |
| LDCL | lucigenin-derived chemiluminescence |
| LLCPK | Lewis lung carcinoma pig kidney cells |
| MDCK | Madin darby canine kidney |

| | |
|---|---|
| min | minute |
| Mn – SOD | manganese superoxide dismutase |
| MnTMPyP | Mn(III)tetrakis(1-methyl-4-pyridyl porphyrin) |
| MOPS | 4-Morpholinepropanesulfonic acid |
| MPA | metaphosphoric acid |
| MTT | 3-(4,5-dimethylthiazol-2-yl)-2,5-diphenyltetrazolium bromide |
| MW | molecular weight |
| $NAD^+$ | Nicotinamide adenine dinucleotide |
| NADPH | nicotinamide adenine dinucleotide phosphate, reduced form |
| NaOx | sodium oxalate |
| NDGA | Nordihydroguaiaretic acid |
| NO | nitric oxide |
| $O_2^{\bullet-}$ | superoxide |
| OGC | Oxoglutarate carrier |
| $OH^{\bullet}$ | hydroxyl radical |
| $OONO^-$ | peroxynitrite |
| OPN | osteopontin |
| PBS | phosphate buffer saline |

| | |
|---|---|
| PS | phosphotidylserine |
| PT | permeability transition |
| PTF1 | prothrombin fragment 1 |
| PUFA | polyunsaturated fatty acids |
| RB | respiration buffer |
| ROS | reactive oxygen species |
| RPMI medium | Roswell Park Memorial Institute media |
| s | second |
| SEM | scanning electron microscope |
| SFM | serum free medium |
| SOD | superoxide dismutase |
| SOD | superoxide dismutase |
| STD | standard deviation |
| THP | Tamm-Horsfall protein |
| TMRM | tetramethylrhodamine methyl ester |
| TNB | 5-thiol-2-nitrobenzoic acid |
| TTFA | thenoyl trifluoracetone |
| UA | uric acid |
| $UQ_{10}$ | ubisemiquinone |
| VDAC | voltage – dependent anion channel |

| | |
|---|---|
| γ – GCS | γ – glutamylcysteine synthase |

# PUBLICATIONS ARISING FROM THIS WORK

## PAPERS:

**E. Meimaridou**, Edgar Lobos John Hothersall. Renal oxidative vulnerability due to changes in mitochondrial – glutathione and energy homeostasis in a rat model of calcium oxalate urolithiass. *Am J Physiol Renal Physiol.* **294**: (4): F31-40, 2006

**E. Meimaridou**, W. Robertson, JS Hothersall. Effect of crystalline and other micro-articles on renal epithelial cell superoxide production: Role of oxalate release in Calcium Oxalate specific response. *Free Radic Biol Med.* **38**:(12): 1553-64, 2005

**Meimaridou E**, Robertson WG, Hothersall JS. Oxalate-mediated $O_2^{\bullet-}$. production. In: Gohel MDI, Au DWT, eds. Kidney stones: inside and out. Kowloon, Hong Kong Polytechnic University Press, pp26-28, 2004

## ABSTRACTS:

**Meimaridou E**, Robertson WG, Hothersall JS. Dicarboxylate transporter: role in calcium oxalate mediated mitochondrial O2. production. Urol Res 2004;32(2):143.

**E. Meimaridou**, W. Robertson and JS Hothersall. Intracellular Origins Of MDCK Cell Superoxide production in Response to Exposure to Calcium Oxalate. *Urolithiasis* 2001;

**E. Meimaridou** and JS Hothersall. Oxidative Stress during Calcium Oxalate Nephrolithiasis in Rats. Free Radical Research 2003; 37 Supplement 1:84

# CHAPTER 1

## INTRODUCTION

## 1.1 UROLITHIASIS

Urolithiasis is the medical term for kidney stone disease and is one of the most painful urological disorders. Renal stone disease is an ancient and common affliction, whose clinical occurrence and presentation was first described in the *Aphorisms of Hippocrates*. Scientists have also found evidence of kidney stones in a 7,000-year old Egyptian mummy [http://kidney.niddk.nih.gov/kudiseases/pubs/stonesadults/]. Recently, reports have shown that renal stones occur once in a lifetime in 15 % of white men and 6 % of all women [Goodman, HO., *et al.*, 1995]. Patients that have been diagnosed with kidney stone disease face a considerable risk of becoming recurrent stone formers, and for this reason it is desirable to provide an efficient stone preventive treatment [Tiselius, HG., & Hojgaard, I., 1999]. Most kidney stones pass out of the body without any intervention by a physician. Stones that cause lasting symptoms or other complications may be treated by various techniques most of which do not involve major surgery. However, in order to understand the patho - physiological mechanisms of stone disease, allowing more effective diagnosis and treatment, stone composition should be analysed and mechanisms of crystallisation and crystal-cell interaction need to be understood.

## 1.2 KIDNEY STONE COMPOSITION

The major crystalline substances that have been identified in urinary calculi are shown in Table 1.1. Studies conducted using x-ray power diffraction have identified six major groups of kidney stones constituents: calcium oxalate (monohydrate, and dihydrate), calcium phosphate (hydroxyapatite and brushite), bacterial induced (struvite), purines and their salts (uric acid), and cystine.

**Table 1. 1 Crystalline substances that occur most frequently in urinary calculi.**

| CHEMICAL NONMENCLATURE | CHEMICAL FORMULA |
|---|---|
| **Calcium Oxalate Monohydrate** | $CaC_2O_4 \bullet H_2O$ |
| **Calcium Oxalate Dihydrate** | $CaC_2O_4 \bullet (2 + x) H_2O$ |
| **Basic calcium Hydrogen Phosphate (hydroxyapatite)** | $Ca_5 (PO_4)_3 (OH)$ |
| **Calcium Hydrogen Phophate (brushite)** | $CaHPO_4 \bullet 2H_2O$ |
| **Magnesium Ammonium Phosphate (struvite)** | $Mg(NH_4)(PO_4) \bullet 6H_2O$ |
| **Uric Acid** | $C_5H_4N_4O_3$ |

### 1.2.1 CALCIUM OXALATE STONES

Urine is usually supersaturated with calcium and oxalate ions that nucleate to form calcium oxalate crystals [Coe, FL., & Parks, JH., 1988]. Previous studies of renal stones or fragments of stones recovered after shock wave lithotripsy have shown that the most common constituent of kidney stones is the calcium oxalate monohydrate (COM) [Figure 1.1A]. In addition, calcium oxalate dihydrate (COD) crystals [Figure 1.1 B] are the most common crystals found in the urine [Tiselius, HG., & Hojgaard, I.,

1999; Lieske, JC., & Deganello, S., 1999]. COD crystals are metastable and once formed tend to undergo a phase transition to COM, which is the thermodynamically stable hydrate and most abundant crystal found in kidney stones [Coe, FL., & Parks, JH., 1988]. In this way the association of COD crystals with renal cells could result in the formation of COM stones. Recent studies have demonstrated that COM crystals can bind rapidly to the surface of renal epithelial cells [Lieske, JC., *et al.,* 1995; Riese, RJ., *et al.,* 1988] and be internalised [Lieske, JC., *et al.,* 1992; Lieske, JC., & Toback, FG., 1993]. The attachment mechanism and internalisation of COM crystals will be discussed in detail in the following sections.

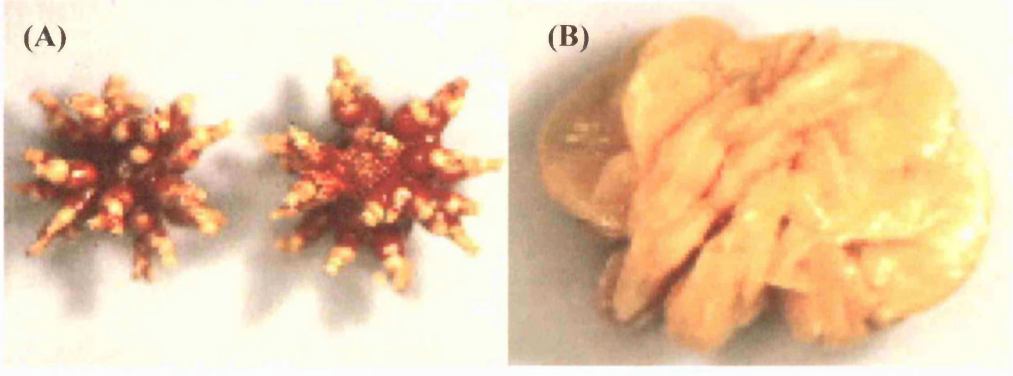


**Figure 1. 1 Calcium oxalate stones.** Scanning electron micrographs of (A) calcium oxalate monohydrate and (B) calcium oxalate dihydrate crystals as adapted from http://www.herringlab.com/photos/Urinary/Oxalates/Com

### 1.2.2 URIC ACID STONES

Uric acid stones [Figure 1.2 A] are smooth, round, yellow-orange and nearly radiographically transparent. High purine diet, containing organ meats and fish, result in hyperuricosuria, and in combination with low urine volume and low urinary pH (resulting from impaired renal ammonia production), can lead to uric acid formation [Colussi, G., *et al.,* 2000]. Even in the absence of elevated serum or urinary uric acid concentrations, uric acid can precipitate out in acid urine. Furthermore, hyperuricaemic disorders including gout, myeloproliferative disorders, tumor lysis syndrome, and inborn errors of metabolism result in an increased filtered load of uric acid and thus, hyperuricosuria [Rumsby, G., 2000]. As with all stones, certain drugs may enhance stone formation, and in the case of uric acid stones, hyperuricosuric agents include low dose salicytates, probenecid, and thiazides.

### 1.2.3 STRUVITE STONES

Radiographs show struvite stones as large, gnarled, and laminated. They are associated with substantial morbididty including bleeding, obstruction, and urinary tract infection. Signs of struvite stones [Figure 1.2 B] include urinary pH greater than 7 and urease that grows bacteria on culture. Struvite stones which develop if urine is alkaline, have a raised concentration of ammonium, contain trivalent phosphate, and contain urease produced by bacteria [Cohen, TD., & Preminger, GM., 1996].

### 1.2.4 CYSTINE STONES

Cystine stones [Figure 1.2 C], caused by an inborn, heritable renal defect. The tubular reabsorption of the amino acids cystine, arginine, lysine, and ornithine is reduced, even though only cystine is poorly soluble [Shekarriz, B., & Stoller, ML., 2002; Knoll, T., *et al.,* 2003]. Cystine stone formation might occur only in infancy, although

the first manifestation mostly occurs in the second decade [Singh, A., *et al.,* 1998; Slavkovic, *et al.,* 2002]. They are greenish-yellow, flecked with shiny crystallites, and are moderate radio opaque with a rounded appearance. Calcium stones are more dense than vertebral bodies, whereas cystine stones are less dense. People who are homozygous for cystinuria (an autosomal recessive disorder) excrete more than 600 mg per day of insoluble cystine. Low urinary dilution and a high intake of animal protein, as well as sodium chloride, increase the urinary excretion of cystine. More than half the stones in cystinuria are of mixed composition, and many patients have associated physiological problems, such as hypercalciuria, hyperuricosuria, and hypercitraturia [Sakhee, K., *et al.,* 1989].

### 1.2.5 CALCIUM PHOSPHATE STONES

Hydroxyapatite crystals [Figure 1.2 D] are often present in the urine. Randall's plaques, which are submucosal calcifications on the human renal papillary surface, have been proposed as early sites of stone formation that seem to arise from a calcium phosphate nucleus [Prien, EL., 1975]. Hydroxyapatite crystals appear to bind to the anions anchored on the apical surface of the kidney epithelial cells in culture. Hydroxyapatite crystals also interact with microvilli on the apical renal cell surface, undergo internalisation, and subsequently appear within membrane-lined vesicles [Lieske, JC., *et al.,* 1999]. These results suggest that the interactions of hydroxyapatite with renal cells are regulated by the structure or function of soluble anions in tubular fluid and those anions anchored to the cell surface could be critical determinants of hydroxyapatite crystal retention in the nephron.

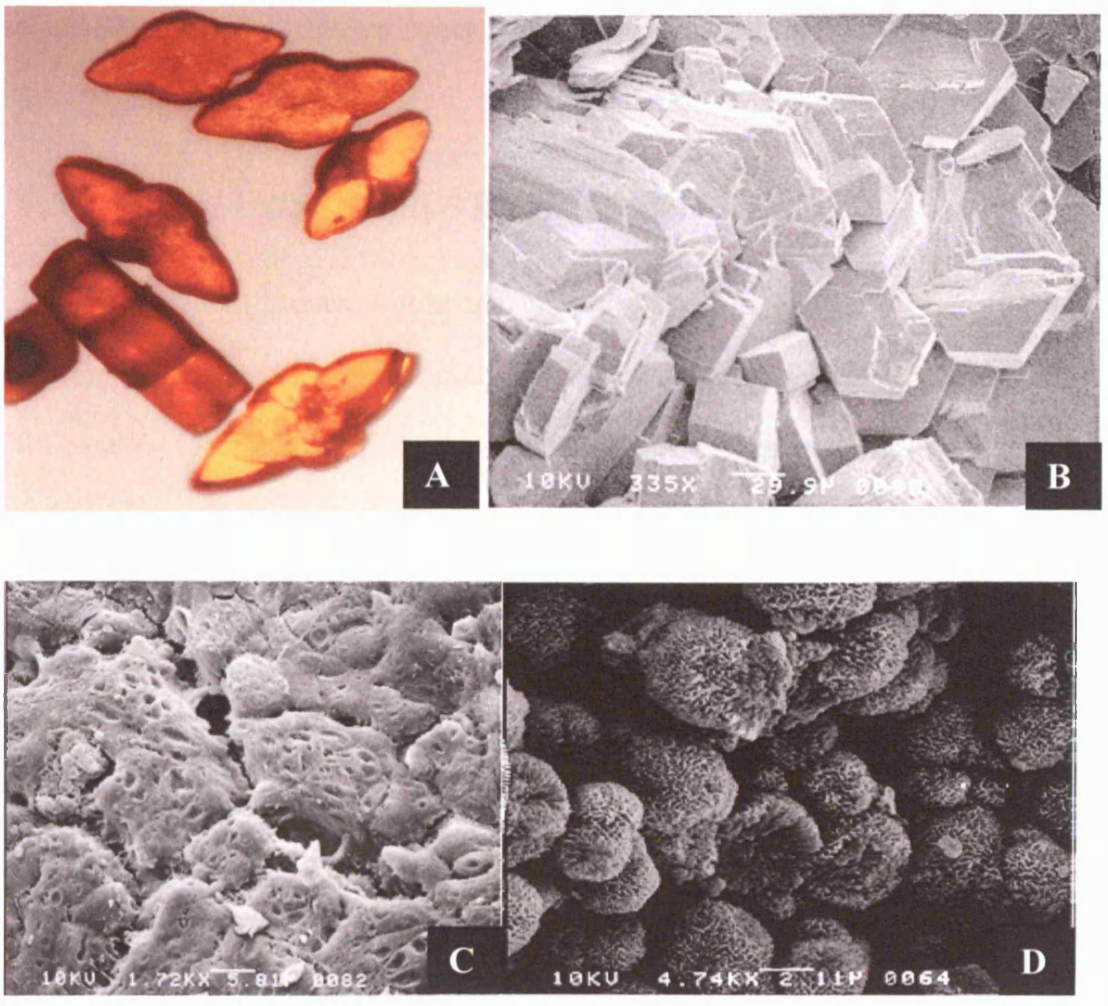


**Figure 1. 2 Different types of kidney stones.** Scanning electron micrographs of (A) uric acid dihydrate, (B) cystine stones, (C) magnesium ammonium phosphate (struvite), and (D) calcium phosphate (hydroxyapatite) kidney stone as adapted from http://www.herringlab.com/photos/Urinary/Oxalates/Com.

Information about the composition of the specific types of kidney stones allows improvements in medical treatment to prevent that particular type of stone to form, and thereby to prevent recurrent kidney stone attacks. In addition, such information could shed light on the mechanism of kidney stone formation, another important factor to be investigated in order to eliminate the risks of kidney stone development.

## 1.3 MECHANISMS OF STONE FORMATION

The formation of stones within the urinary tract is a multifaceted and complex process. Supersaturation of the urine with respect to calcium oxalate is a prerequisite for calcium oxalate urinary stone formation. Urine supersaturation though is not the only determinant factor for urinary stone formation. Both stone-forming patients and healthy subjects share the common phenomenon of supersaturated urine and crystalluria [Robertson, WG., 1969; Elliot, JS., & Rabinowitz, IN., 1976]. This finding led to the concept that the precipitation of COM crystals by itself poses no problem as long as the particles formed are allowed to pass freely through the urinary tract. Problems occur only when the particles are retained and allowed to form the nidus of a stone. The movement through the urinary tract at a speed lower than that of the urinary flow is defined as retention. Retention can occur because the particles become too big to pass freely through the renal tubules, by adhesion to the tubular cells, and by trapping of particles at sites of disturbed urinary flow. When the size of the particle is the decisive factor for the mechanism of stone formation, the process is defined as the free particle mechanism. This is in contrast to the fixed particle mechanism, where adhesion plays a dominant role.

The chances of forming stone through a free particle mechanism were calculated by Finlayson and Reid [Finlayson, B., & Reid, S., 1978]. These studies were based on

average normal values for oxalate excretion, kidney structure and nephron dimensions, and they claimed that the "free-particle" model was unlikely to occur. They also claimed that there was not sufficient time to allow crystals to grow large enough and become trapped before they were extruded. Instead, they suggested that the nuclei of CaOx, resulting from supersaturation of the tubular fluid, are attached to epithelial cells lining the tubule due to the damage that has occurred, either as a result of the abrasive action of the crystals or as a consequence of an infection.

This "fixed-particle" model was reassessed more recently by Kok and Khan [Kok, DJ., & Khan, SR., 1994], taking into account new evidence on tubule dimensions and the flow rates of tubular fluid. These authors formed a compromise between the "free" and "fixed"-particle models. They proposed that the "free-particle" model could be possible in the case where crystal agglomeration occurred, since the latter constitutes the fastest means by which particles may become large within a short space of time.

More recently, Robertson [Robertson, WG., 2004] examined the probability that crystals can indeed become large enough at some point in the nephron by introducing three new hydrodynamic factors that may lead to the delay of crystal passage. This latest model takes into account that crystals may move at different speeds in relation to the fluid flow rate at the central axis of the tubule, and crystals moving adjacent to the tubule walls move more slowly than crystals at tubule axis. In addition, it was suggested that crystal transit may be delayed more in tubules with long loops of Henle, and crystals may stop moving or even fall backwards in the upward-draining sections of the tubule. Finally, Robertson proposed that if these hydrodynamic factors are operative in the human kidney, it is possible that the "free-particle" model might still be a mechanism by which CaOx stones are initiated.

### 1.3.1 CALCIUM OXALATE CRYSTAL ADHERE TO RENAL EPITHELIAL CELLS

Studies using diverse cultured renal epithelial cells have demonstrated that calcium oxalate monohydrate (COM) crystals, the most common crystal in human stones, rapidly adhere to molecules on the apical surface [Lieske, JC., *et al.,* 1995; Lieske, JC., *et al.,* 1996; Riese, RJ., *et al.,* 1988; Riese, RJ., *et al.,* 1992; Verkoelen, CF., *et al.,* 1996] and are internalised [Lieske, JC., *et al.,* 1992; Lieske, JC., *et al.,* 1993]. The COM crystal surface behaves as if it were positively charged [Lieske, JC., *et al.,* 1995] and the apical kidney tubular cell surface functions as if it were negatively charged [Lieske, JC., *et al.,* 1996]. It has been proposed that anionic molecules on the cell surface, by acting as receptors for COM crystals [Lieske, JC., *et al.,* 1996; Bigelow, MW., *et al.,* 1997], and specific anions in tubular fluid by binding to the crystal surface and blocking its adhesion to the cell [Verkoelen, CF, *et al.,* 1996], have each emerged as potentially critical determinants of stone formation.

Lieske and Deganello [Lieske, JC., & Deganello, S., 1999], in their attempt to understand how renal cells respond to crystals and how these processes might result in stone formation, have proposed a potential mechanism of cell-crystal interaction in the nephron [Figure 1.3]. Calcium oxalate or calcium phosphate crystals can either nucleate in luminal fluid or potentially form on the surface of renal cells. In the case where crystals nucleate in tubular fluid can be coated by soluble ions (glycosaminoglycans, citrate, proteins), or adhere to anchored anions on the cell surface. These in turn bind to candidate receptors such as glycoproteins, phospholipids, or glycolipids. Once attached to their surface, crystals can be internalised by cells and eventually appear in membrane lined vacuoles. Crystals may

then be dissolved within the cells or possibly become situated in the interstitium. The outcome of this series of events could determine whether a crystal is flushed out of the nephron or is retained in the kidney with the potential to initiate stone formation.

While studies were performed on interaction between crystals and renal tubular cells [Lieske, JC., *et al.,* 1992; Weissner, JH., *et al.,* 1987], other studies were based on the cell-surface substances responsible for crystal attachment.

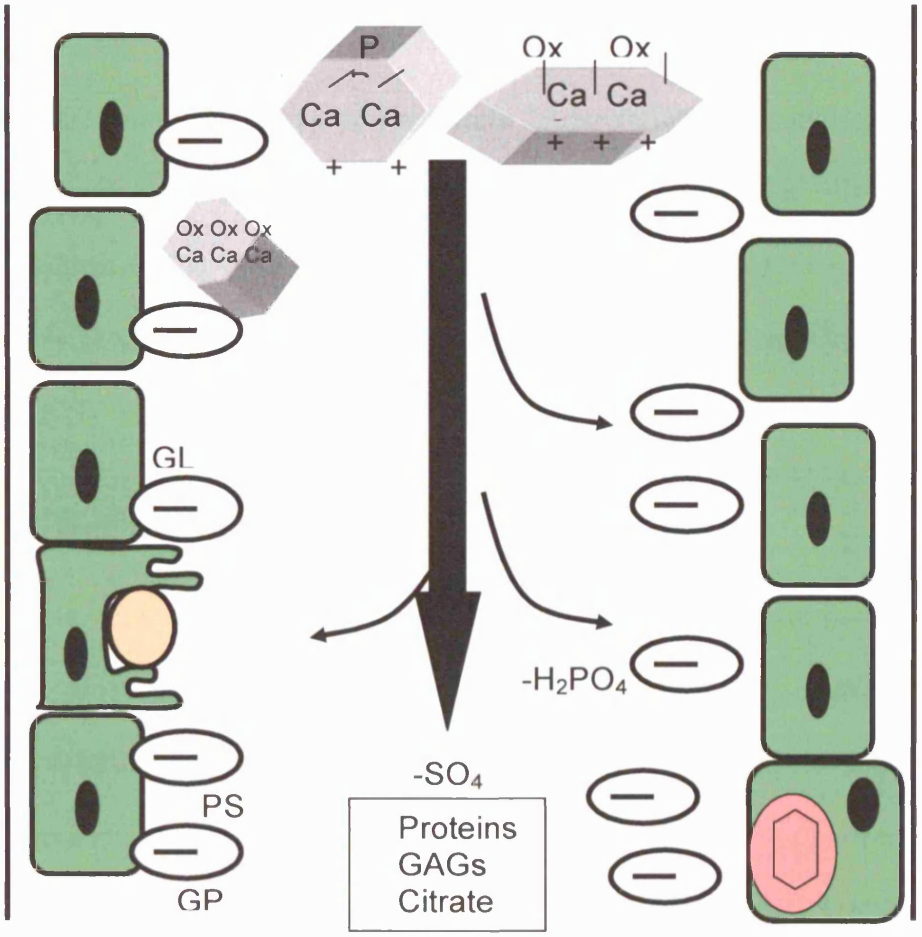


**Figure 1. 3 Proposed mechanism of nucleation, growth and adhesion of calicium oxalate crystals in the renal tubule, adapted from Lieske, JC., et al., 2000.** Calcium oxalate or calcium phosphate crystals nucleate in tubular fluid or on the tubular cell surface. Crystals that are nucleated in tubular fluid can either be coated by soluble ions (proteins, GAGs) or adhere to ions of the tubular cell surface. These can then be flushed out of the nephron or be retained in the kidney and develop a kidney stone. Oxalate crystals that anchor on the tubular surface, can be internalised by the cells. These crystals may then be dissolved within the tubular cells or possibly become translocated in the interstitium.

## *1.4 CRYSTAL BINDING MOLECULES*

Observations made in kidneys derived from hyperoxaluric rats and stone-forming patients suggested that under pathological conditions, renal tubular cells express cell-surface molecules that have an affinity for crystals. These surface molecules were described as crystal-binding molecules and fall into four main groups: phosphatidylserine, sialic acid, extra-cellular matrix molecules, and hyaluronan.

### 1.4.1 PHOSPHATIDYLSERINE

The possible role of plasma-membrane phospholipids in the attachment of COM crystals to primary cultures of inner medullary collecting duct (IMCD) was first investigated by Mandel's group [Weissner, JH., *et al.,* 2001; Bigelow, MW., *et al.,* 1997]. Specifically, these authors, by exogenously adding phospholipid liposome suspensions or by exposing IMCD cells to a calcium ionophore (A23187), were able to induce alteration in the membrane lipid composition of the cells. Both of these approaches have revealed that the expression of phosphatidylserine at the cell surface greatly enhanced crystal binding. Further experiments on treating phosphatidylserine-expressing cells with the apoptotic marker annexin V, a $Ca^{2+}$-dependent binding protein with a high affinity for phosphatidylserine, have revealed similar results, indicating low levels of crystal binding. Based on these observations, Bigelow and his group [Bigelow, MW., *et al.,* 1997] proposed that crystal retention might be caused under pathological conditions by the appearance of phosphatidylserine at the surfaces of epithelial cells lining the collecting ducts. The same effect of phosphatidylserine exposure and crystal binding was also shown by the group of Scheid [Cao, LC., *et al.,* 2001] when they treated Madin-Darby canine kidney (MDCK) cells with toxic oxalate concentrations.

### 1.4.2 SIALIC ACID

In 1996, Lieske *et al.* [Lieske, JC., *et al.,* 1996] described the adherence of COM crystals to wild type MDCK cells. When these cells were incubated with positively charged compounds, crystal binding was reduced. This suggested that crystals adhere to negatively charged cell surface components [Lieske, JC., *et al.,* 1996]. Pre-treatment of the crystals with these cationic compounds did not influence crystal binding, indicating that they affected the cell surface rather than the crystal surface. Since most of the cell surface of the negative charge is attributable to terminal sialic acid residues, these investigators subsequently studied the effect of sialidase on crystal binding. This treatment significantly reduced the binding of the crystals. In addition, pre-treatment of the MDCK cells with sialic acid-specific lectins could also reduce crystal binding. Therefore, it has been suggested that crystals can bind to sialic acid.

As it has been described earlier in section 1.3.1, Lieske *et al.* have proposed a possible interaction mechanism where one population of anions anchor to the apical plasma membrane and the other free in tubular fluid. Both of these populations are deemed as competitors for the crystal surface. To determine whether or not crystals bind to the renal tubular surface, further investigation is required on the alterations in the quality and quantity of either population of ions.

### 1.4.3 EXTRACELLULAR MATRIX MOLECULES

Other potential crystal binding molecules are those of the extra-cellular matrix. Kohri *et al.* [Kohri, *et al.,* 1991] observed that calcium oxalate crystals adhere to collagen type IV-positive cell clumps in primary cultures of IMCD cells. This observation led to the speculation that renal tubular basement membrane collagen IV is a potential

crystal-binding molecule. Further investigations [Yamate, T., *et al.*, 1992] have shown that when wild-type MDCK cells were exposed to osteopontin resulted in increased crystal deposition on the cell surfaces. The fluorescence intensity of osteopontin at the cell surface could be reduced by osteopontin antibodies and therefore reducing crystal binding. From these observations, it was proposed that osteopontin might serve as a crystal binding molecule.

### 1.4.4 HYALURONAN

Besides sialic acid, glycosaminoglycans (GAGs) also make a substantial contribution to the overall negative charge of the cell surface. These molecules have therefore frequently been postulated as potential crystal-binding molecules. Hyaluronan is a principal component of stone matrix GAG content, and it participates in one or more stages of renal stone formation. The multiple roles attributable to hyaluronan in renal stone formation may be a consequence of its various size-related functions. The high molecular mass (100 kDa) forms that stabilise matrix architectures [Laurent, TC., & Fraser, JRE., 1992; Knudson, W., *et al.*, 1993; Scott, JE., *et al.*, 1991] can coat crystals and thus block crystal-crystal or crystal-cell interaction. However, the lower molecular mass forms can mediate crystal-cell adhesion and crystal nucleation [McKee, CM., *et al.*, 1996; McKee, CM., *et al.*, 1997; Oertli, B., *et al.*, 1998].

Although hyaluronan is usually found in the medullary and papillary interstitium of the normal kidney [Wells, AF., *et al.*, 1990; MacPhee, PJ., 1998], it has also been demonstrated [Wessler, E., 1971; Hansen, C., *et al.*, 1997; Lokeshwar, VB., *et al.*, 1997] that a minor component may be found in normal urine. The urinary hyaluronan is predominantly in the range of 10 kDa [Lipkin, GW., *et al.*, 1993]. Studies [Gustafson, S., *et al.*, 1997] have shown that renal and extra-renal high molecular

mass hyaluronan is rarely excreted in the urine. However, in the case of injury or inflammation of renal tissues, degradation of high molecular mass hyaluronan to lower molecular fragments occurs [Saari, H., 1991; Kreil, G., 1995]. The latter may become signal molecules that upregulate expression of adhesion molecules in renal tubular epithelial cells [Oertli, B., *et al.,* 1998]. In addition, these low molecular fragments of hyaluronan, produced as a secondary product of injury or inflammation, may become involved in the crystallisation of urinary calcium oxalate as a prelude to cell-crystal adhesion and crystal-crystal aggregation, leading to renal stone formation.

Having described various candidate crystal-binding molecules that determine the susceptibility of the renal tubular cell surface to crystal binding, other investigations have focused on the effects of stone matrix proteins responsible for inhibiting or promoting kidney stone formation.

## 1.5 KIDNEY STONE PROTEINS

Urolithiasis researchers have been searching for synthetic or natural occurring substances that can inhibit crystallisation of calcium salts. A number of urinary components have been identified as inhibitors and those can be divided into low- and high-molecular weight substances [Ryall, RL., 1997]. It has been suggested that high-molecular weight substances and especially proteins may have an important role in the prevention of stone disease [Ryall, RL., 1995]. Studying proteins that have been identified in human calculi have suggested that the presence of these proteins in stone matrices play a role (as either inhibitors or promoters) in stone pathogenesis. Therefore, analysis of stone matrix proteins to assess their roles in kidney stone formation is of great value. As it has been discussed in earlier sections healthy human urine does not under physiological conditions contain proteins. The presence of

proteins in the urine can arise as a result of tissue trauma. Therefore, studying proteins included in calcium oxalate crystals precipitated from fresh healthy human urine *in vitro* might yield important information of the role of these proteins in stone formation. In the following paragraphs a few of these proteins will be discussed according to their potential role in kidney stone formation.

### 1.5.1 TAMM-HORSFALL PROTEIN

Tamm-Horsfall protein (THP) is a glycoprotein present abundantly in human urine. Urinary excretion occurs by proteolytic cleavage of the large ectodomain of the glycosyl phosphatidylinositol-anchored counterpart exposed at the luminal cell surface of the thick ascending limb of Henle's loop [Chakraborty, J., *et al.*, 2003; Serafini-Cessi, F., *et al.*, 2003]. THP of normal subjects inhibits the aggregation, but has little effect on nucleation and growth of CaOx crystals [Worcester, EM., *et al.*, 1988]. However, THP activity is influenced by its own concentration, urinary pH and ionic strength, playing a role in crystal formation depending on the environmental conditions [Hess, B., 1994]. Moreover, THP isolated from the urine of recurrent stone formers sometimes becomes a promoter of CaOx aggregation due to a tendency to self-aggregation, which removes it from effective interaction with CaOx monohydrate crystals [Hess, B., *et al.*, 1991]. THP is a macromolecule and has been extensively studied, sometimes with paradoxical results concerning CaOx crystallization, depending on the conditions and methods employed. Most authors agree that THP is a weak inhibitor of nucleation and growth, but in solutions with high pH, low ionic strength, and low concentrations of divalent ions, the glycoprotein acts as a powerful inhibitor of CaOx crystal aggregation [Dussol, B., & Berland, Y., 1996].

### 1.5.2 OSTEOPONTIN

It has been proposed that osteopontin (OPN) is involved in stone formation as a component of the stone matrix [Yamate, T., *et al.,* 1999]. Initially these authors performed sequencing of the cDNA of proteins in the stone matrix of calcium oxalate calculi and they found that OPN was present [Kohri, K., *et al.,* 1992; Umekawa, T., *et al.,* 1995]. In addition they observed that the OPN expression in renal distal tubular cells was increased in renal stone-forming rats [Kohri, K., *et al.*, 1993]. According to these observations they suggested a dual action of OPN. Firstly, OPN playing a role in binding with calcium and secondly OPN may be contributing to the cell adhesion. Furthermore, the same authors [Yamate, T., *et al.,* 1999] have reported that calcium oxalate crystal adhesion on the surface of MDCK cells increased when OPN was added to MDCK cells [Yamate, T., *et al.,* 1996]. To further evaluate the effect of OPN on the adhesion of calcium oxalate crystals to MDCK cells, they suppressed the urolithic activity of OPN. When they pre-treated MDCK cells with OPN, and thrombin, which is an OPN inhibitor, scanning electron micrographs revealed that the degree of CaOx crystal deposition was suppressed between 40 % to 80 %. These findings led to the conclusion that OPN is essential for crystal deposition on MDCK cells, and plays an important role as a component of extracellular matrices.

### 1.5.3 PROTHROMBIN FRAGMENT 1

Prothrombin fragment 1 (PTF1) has been identified as a crystal matrix protein [Stapleton, AMF., & Ryall, RL., 1995; Nishio, T., *et al.,* 1998] that exhibits strong inhibitory effects on calcium oxalate crystallisation. PTF1 is localised to lithogenic regions of renal tubules [Stapleton, AMF., *et al.* 1993] and has a potent inhibitory activity against calcium oxalate crystal growth and crystal aggregation, under

inorganic aqueous conditions [Grover, PK, *et al.,* 1998] and in undiluted human urine *in vitro* [Ryall, RL., *et al.,* 1995]. Evidence to support a direct role for the protein in stone pathogenesis requires demonstration that synthesis of the protein is influenced by the formation of crystals or stones within the urinary tract. Recently, PTF1 was found in calcium phosphate crystals generated in urine and in the stone matrix of CaOx [Stapleton, AMF., *et al.,* 1996]. Urinary PTF1 strongly inhibits CaOx crystal aggregation; therefore its abundance in urine is believed to prevent urinary stone formation [Suzuki, K., *et al.,* 1994; Doyle, IR., 1995]. Reports have also showed that PTF1 strongly inhibited the crystal growth of CaOx at a physiological concentration in urine [Bezeaud, A., & Guillin, MC., 1984].

### 1.5.4 BIKUNIN

A factor that may explain the difference between stone and non-stone forming patients is that normal human urine is more efficient in inhibiting the formation and aggregation of calcium oxalate crystals. Numerous studies have shown that normal urine contains macromolecular substances capable of preventing and reducing calcium oxalate crystal formation and aggregation [Ryall, RL., & Stapleton, AMF., 1995; Atmani, F., *et al.,* 1998; Khan, SR., 1997]. One substance that has attracted attention is inter-α-inhibitor (IαI) and its various components, particularly the light chain called bikunin. IαI is composed of three distinct polypeptide chains: two heavy chains H1 and H2, and bikunin. The bikunin chain originates from a common α1-microglobulin/bikunin precursor, which is separated into two polypeptides by post-translational cleavage. Free bikunin is found in plasma as well as in urine. Urinary bikunin, obtained from human or rat urine, was shown to be a potent inhibitor of calcium oxalate growth [Atmani, F., *et al.,* 1996]. When the same inhibitor was

isolated from the urine of stone formers it showed less inhibitory activity towards calcium oxalate growth [Atmani, F., *et al.,* 1996]. In addition, further studies have shown that during calcium oxalate nephrolithiasis increased levels of bikunin were synthesized [Atmani, F., *et al.,* 1996]. Furthermore, bikunin is thought to be a calcium-binding protein [Kobayashi, H., *et al.,* 1998] and is likely that the inhibitory action against crystal adhesion may depend on the binding of bikunin to the crystal surface.

### 1.5.5 ANNEXIN II

A critical step for the development of kidney stones is the attachment of newly formed crystals to renal epithelial cells. Annexin II has been shown to be the most prominent crystal-binding protein [Kleinamnn, JG, & Soronika, EA., 1999]. It is present on the apical cell surface and is an intrinsic membrane bound protein. It has been demonstrated that when IMCD cells are exposed to oxalate there is enhanced $^{(14)}C$ - oxalate crystal binding and increased exposure of phosphotidylserine (PS) on the cell membrane [Cao, LC., *et al.,* 2001; Weissner, JH., *et al.,* 1999]. Further studies have also shown that treatment of IMCD cells with PS-containing liposomes enhanced $^{(14)}C$ - oxalate crystal binding. Annexin-II binds to anionic phospholipids, and to COM crystals. According to these observations it is therefore, possible that enhanced COM crystal binding to cells under conditions where PS is exposed could be related to increased Annexin-II present on the cell surface [Kumar, V., *et al.,* 2003]. These authors have also suggested that Annexin-II not only mediates adhesion of COM crystals to renal cells, but it could also play a role in their subsequent internalisation.

It has been proposed that deposition of crystals in the renal tubules is associated with injury to the tubular epithelium. In order to evaluate the mechanisms involved in crystal retention within the kidneys, it is necessary to understand how epithelial injury and the subsequent process of wound healing could lead to increased crystal binding.

## 1.6 IMPACT OF EPITHELIAL INJURY ON CRYSTAL- CELL INTERACTION

The idea that renal tubular cell injury might play a role in urolithiasis is supported by several lines of evidence: (1) it was observed that in clinical idiopathic calcium oxalate stone formers increased levels of brush border and lysosomal enzymes of renal epithelial origin were excreted in their urine [Baggio, BG., *et al.*, 1983], (2) increased urinary enzyme levels and renal tubular apical membranes were also found in experimental models of stone disease [Hackett, RLP., *et al.*, 1994; Khan SR., *et al.*, 1989], and (3) calcium oxalate crystals are able to adhere to injured urothelium of the rat bladder [Gill, WB., *et al.*, 1981; Khan, SR., *et al.*, 1984].

Further studies of crystal deposition in association with renal epithelial injury have also showed that epithelial cells lining the crystal-containing tubules suffered damage [Khan, SR., 1991; Khan, SR., & Hackett, RL., 1985; Khan, SR., *et al.*, 1979; Khan, SR., *et al.*, 1982]. The first observed phenomena occurred in the proximal tubules where the brush border was distorted by clubbing of the microvilli, blebs were formed and focal loss of the brush border. Progressive changes in the cells resulted in their ultimate death and detachment from the basement membrane. Furthermore, a number of dividing cells were found in the epithelial lining of the tubules. Many of them were seen in close proximity to the cell surface and in association with the microvilli. Some were found attached to the injured cells. At later stages, many crystals were found in

the intracellular spaces and also attached to the denuded basement membrane. Renal cellular injury is indicated by an increase of urinary excretion enzymes such as, γ-glutamyl transpeptidase, alkaline phosphatase, and *N*-acetyl-β-glucosaminidase [Khan, SR., *et al.,* 1989; Khan, SR., *et al.,* 1992].

Similar studies were performed by Hackett *et al.* [Hackett, RL., *et al.,* 1994], showing that when MDCK cells were exposed to calcium oxalate crystals, this resulted in detachment and shedding of the cells from their substrates. This was indicated by elevated levels of γ-glutamyl transpeptidase, leucine aminopeptidase, and *N*-acetyl-β-glucosaminidase found in the culture media indicative of cellular injury. The cells remaining attached appeared injured, showing blebbing and swelling of the microvilli, with their eventual loss. In addition, cell-to-cell contacts appeared stretched with widened intracellular space. As a result of these phenomena, crystals became attached to the cells and microvilli and some of them were internalised whilst others were found in the intracellular spaces. Other studies included the effect of calcium oxalate crystals in a proximal origin cell line (LLCPK). The effect of crystal deposition was the same, exhibiting morphological changes including vacuolisation [Menson, M, *et al.,* 1993].

Hyperoxaluria in the absence of calcium oxalate crystal deposition in the kidneys also appears to be injurious to renal epithelial cells. Thus, it is important to understand how free oxalate is associated with urolithiasis.

### 1.6.1 OXALATE IS ASSOCIATED WITH INJURY OF RENAL EPITHELIAL CELLS

Oxalate is a small dicarboxylic ion $\begin{matrix} COO^- \\ \| \\ COO^- \end{matrix}$ ($C_2O_4^{2-}$) that is freely filtered at the glomerulus. Dietary oxalate is a major contributor to urinary oxalate excretion in most individuals. Studies have indicated that dietary oxalate can contribute up to 50 % to the daily urinary oxalate excretion [Holmes, RP., *et al.,* 1995; Assimos, *et al.,* 1997]. Calcium oxalate crystals have an increased propensity to form in the presence of hyperoxaluria, even in the absence of elevated calcium [Seftel, A., & Resnick, MI., 1990], suggesting a prominent role for oxalate. *Oxalobacter forminogenes* is a bacterium colonising the gastrointestinal tracts of vertebrates, including humans [Allison, MJ., *et al.,* 1985]. This bacterium has an important symbiotic relationship with its hosts in regulating oxalic acid absorption through the intestine, as well as oxalic acid levels in the plasma [Doane, LA., *et al.,* 1989; Hatch, M., & Freel, RW., 1996]. Further studies [Han, JZ, *et al.,* 1995 Kwak, C., *et al.,* 2003] have indicated that the absence of *O. forminogenes* can lead to a significant increase in the absorption of oxalate from the gut, thereby increasing the levels of urinary oxalate excretion, especially when the diet is rich in oxalate. The absence of *O. forminogenes* from the gut appears to be a risk factor for absorptive hyperoxaluria and its subsequent complications, including nephrolithiasis.

The amount of oxalate that is excreted in the urine not only depends on the intestinal absorption, but on the dietary intake, endogenous production, and renal transport [Larsson, L., & Tiselius, HG., 1987; Menon, M., & Mahle, CJ., 1982; Menon, M., & Koul, H., 1992; Wandzilak, TR., & Williams, HE., 1990; Williams, AW., & Wilson, DM., 1990; Williams, HE., & Wandzilak, 1989; Senekjian, HO., & Weinman, EJ.,

1982]. The endogenous production of oxalate predominantly derives from the metabolism of glyoxylate and ascorbate and contributes importantly to the amount of oxalate that is excreted in the urine [Menon, M., & Mahle, CJ., 1982; Menon, M., & Koul, H., 1992; Senekjian, HO., & Weinman, EJ., 1982].

The mechanism by which oxalate promotes stone formation is not yet clear. The majority of the patients with calcium oxalate stone disease show a small, but a definite, increase in urinary oxalate excretion, but few have been diagnosed with hyperoxaluria [Tiselius, HG., 1980]. However, the probability of stone formation and the severity of stone disease are directly proportional to urinary oxalate levels [Elliot, JS., *et al.,* 1976]. Elevated urinary oxalate levels can lead to calcium oxalate crystallisation, but not necessarily to stone formation. Therefore, the mechanism through which oxalate promotes stone formation is clearly more complex than a simple increase in crystal formation. Moreover, presence of crystals in the urine does not appear to be a distinguishable difference between stone formers and healthy subjects. Crystal formation is not an indication of symptomatic stone disease, since most of the solid particles crystallising within the urinary tract will be excreted freely. Studies by Robertson [Robertson, WG., 1969] have concluded that crystalluria does not indicate kidney stone disease. Therefore, the mechanism by which oxalate promotes crystal retention has been the focus of studies for several years.

Previous reports [Barker, G., & Simmons, NL., 1981] have suggested that oxalate transport may be altered by morphological or functional changes of renal epithelial cells. Oxalate transport across cellular membranes is mediated by anion–exchange transport proteins. A defect in the structure of these transport proteins could explain augmented transcellular oxalate transport. Aronson [Aronson, PS., Kuo SM., 1994]

demonstrated that difference in the structure of band-3-related transport protein would alter the affinity of a transport system for oxalate in such a way that oxalate absorption in the intestine and secretion in the kidney is increased.

Two proposed mechanisms were developed to explain crystal retention. The first one includes the direct entry of oxalate into the renal tubular cells to promote crystal formation within the tubular cells. Alternatively, an increased oxalate flux would result in cellular proliferation and or damage that could promote crystal retention [Khan, SR., & Hackett, RL., 1993; Khan, SR., *et al.,* 1990]. Specifically, during cell proliferation cell-cell contacts are minimised, mitosis then reduces cell adhesion to the extra-cellular matrix and exposes previously masked basolateral membrane domains to tubular fluid, thereby favouring crystal retention.

As previously mentioned, oxalate is a dicarboxylate that is freely filtered at the glomerulus and undergoes both reabsorption and secretion in the proximal tubule, with secretion dominating under normal conditions [Aronson, PS., 1989]. *In vitro* studies [Koul, HK., *et al.,* 1999; Scheid, C., *et al.,* 1996; Khan, SR., *et al.,* 1999] have demonstrated that exposure of elevated levels of oxalate led to progressive changes in the morphology and cell viability. Furthermore, it has been shown [Koul, HK., *et al.,* 1999] that proximal tubular cells are more susceptible to oxalate challenges than the cells of the collecting duct epithelium. An injury to cells of the proximal tubular epithelium may provide substrate for heterogeneous nucleation of crystals in the collecting ducts where urine is concentrated and calcium oxalate is metastable. Scheid [Scheid, C., *et al.,* 1996] has provided evidence that oxalate is toxic to proximal tubule cells. These authors treated LLCPK cells, an epithelial cell line with characteristics of proximal tubular cells, to high concentrations ($\geq$ 350 $\mu$M) of oxalate

and have showed changes in morphology and viability of these cells. This is at a concentration of oxalate that is likely to be higher than might occur in the normal kidney, but within the range that might be found in hyperoxaluria or in end-stage renal disease. The same group also suggested that a possible mechanism by which hyperoxaluria may promote crystal retention relies on the increase of turnover of renal epithelial cells that provides cellular debris for nucleation and retention of calcium oxalate crystals.

Having discussed the injurious effect of oxalate on LLCPK cells, it is worthwhile mentioning whether cellular death may be necrotic or apoptotic. There are specific differences when a cell undergoes necrosis or apoptosis. During apoptosis cells shrink, cell membrane remains intact, phosphatidylserine of the plasma membrane flips from inside to the cell surface, chromatin in the nucleus condenses, and DNA fragments. During necrosis, cells swell, vacuoles enlarge, mitochondria become swollen, plasma membranes are compromised, and blebbing may occur on cell surfaces. However, cells undergoing necrosis, do not exhibit either an increase in phosphatidylserine on the cell surface or condensation of chromatin and DNA fragmentation. Cells undergoing apoptosis detach from the basement membrane and break into smaller bodies that are phagocytosed by the neighbouring cells, whereas necrotic cells rupture and release their contents into the surrounding area. Consequently, cell necrosis can provoke an inflammatory response, whereas cell death by apoptosis shows a reduced incidence.

Renal epithelial cells of proximal tubular origin exposed to oxalate have been reported to follow both mechanisms of cell death [Lieberthal, W., *et al.,* 1996]. When LLCPK cells were exposed to oxalate for 24 h and 48 h, apoptotic cells start accumulating and

being phagocytosed by the neighbouring healthy cells, while the plasma membrane is still intact. However, the clearance of apoptotic cells was interrupted and cells went through a process of secondary necrosis [Lieberthal, W., & Hughes, H., 1993; Lieberthal, W., *et al.,* 1996; Schwartzman, RA., & Cidlowski, JA., 1993]. Apoptosis of renal epithelial cells in response to oxalate may play a significant role in nephrolithiasis. Exposure of annexin binding phosphatidylserine to the cell surface, a mechanism described as an apoptotic marker, results in attracting calcium and acting as a site for attachment of calcium oxalate crystals to the cell surfaces [Bigelow, MW., *et al.,* 1996].

In addition, oxalate has been reported to induce lipid peroxidation. Lipid peroxidation refers to the oxidative damage of unsaturated fatty acid molecules by free radicals. This injury to a cell alters membrane permeability, impairs the transport of ions, and results in the inability of the cells to maintain a normal ionic environment [Scheid, CR, *et al.,* 1996 (a); Scheid, CR., *et al.,* 1996 (b)]. There has long been an association between urolithiasis and free radicals, and the study of the latter is important to understand their role in the mechanism of action and their implication in the pathogenesis of kidney stone disease.

## 1.7 REACTIVE OXYGEN SPECIES (ROS)

Many natural occurring molecules require metabolic activation to form reactive intermediates in order to exert their toxicity. It is known that many of these intermediates are free radicals, with at least one unpaired electron in the outermost shell, and are capable of independent existence. The free radicals formed may be carbon, nitrogen or oxygen centred and have been implicated in the action of a wide range of structurally and pharmacologically diverse compounds with an equally broad range of toxicities including carcinogenesis, mutagenesis, cell necrosis and lipid peroxidation [Mason, 1982; Mason & Chignell, 1982; Trush *et al.*, 1982]. Other intermediates derived from free radicals in which electrons are paired can also be cytotoxic. Both classes are referred to as Reactive Oxygen Species (ROS). These species because of their high reactivity can undergo a number of reactions including: (i) electron transfer to molecular oxygen generating superoxide anion radical and other active oxygen species, (ii) hydrogen atom abstraction leading to autoxidation of polyunsaturated fatty acids and (iii) covalent binding to tissue macromolecules by radical addition to carbon-carbon double bonds or by radical combination [Smith., *et al.*, 1984]. ROS include a number of chemically reactive molecules derived from oxygen. Some are extremely reactive, such as the hydroxyl radical and singlet oxygen whilst others are less reactive such as superoxide and hydrogen peroxide.

Free radicals and ROS can readily react with many biomolecules, starting a chain reaction of free radical formation. In order to stop this chain reaction, a newly formed radical must either react with another free radical scavenger or antioxidant.

**Table 1. 2 ROS molecules and their sources**

| ROS Molecule | Main cellular sources |
|---|---|
| Superoxide ($O_2^{\bullet-}$) | Leakage of electrons form the electron transport chain<br>Activated Phagocytes<br>Xanthine Oxidase<br>Flavoenzymes |
| Hydrogen peroxide ($H_2O_2$) | From $O_2^{\bullet-}$ via superoxide dismutase (SOD)<br>NADPH-oxidase<br>Glucose oxidase<br>Xanthine oxidase |
| Hydroxyl Radical ($^{\bullet}OH$) | From $O_2^{\bullet-}$ and $H_2O_2$ via transition metals ($Fe^{2+}$ or $Cu^{+}$) |
| Nitric oxide (NO)<br><br>Peroxynitrite ($OONO^-$) | Nitric oxide synthases<br><br>NO and $O_2^{\bullet-}$ |
| Singlet Oxygen ($^1O_2$) | Photochemical reactions between light, oxygen, and photosensitizers eosinophils |

The most familiar intracellular and extra-cellular forms of ROS are listed in Table 1.2, along with their main sources of production. The main reaction steps in the single electron reduction of molecular oxygen are shown below [1]:

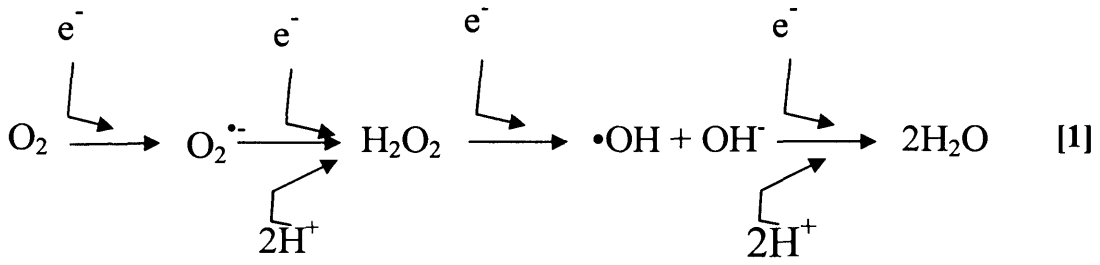


[1]

In the following sections the main ROS molecules will be discussed in terms of pathways of formation and their cellular effects.

### 1.7.1 SUPEROXIDE ($O_2^{\bullet-}$)

The superoxide anion produced from molecular oxygen by the addition of an electron is, in spite of being a free radical, not highly reactive. It is not able to penetrate through the lipid membranes and therefore it is normally enclosed in the compartment in which it is produced. Superoxide can be produced enzymatically by flavoenzymes such as xanthine oxidase or by enzymes such as lipoxygenase and cyclooxygenase [Kuppusamy, P., & Zweier, JL., 1989; McIntyre, *et al.,* 1999]. However, the majority of superoxide that is produced in most eukaryotic cells originates from the mitochondrial respiratory chain and is produced by a nonenzymatic mechanism. Ubisemiquinone ($UQ_{10}$) species generated during electron transfer in the respiratory chain donate electron to oxygen and provide a constant source of superoxide [2]:

$$UQ_{10}^{-} + O_2 = O_2^{-} + UQ_{10} \qquad [2]$$

Under normal circumstances, the rate of generation of superoxide from mitochondria is rather low and does little damage. However, there are circumstances, such as ingested chemicals that act as radical amplifiers, medically applied high concentrations of oxygen, or during periods of perfusion of tissues with oxygen

following ischemia, where high rates of superoxide do occur. $O_2^{\bullet-}$ formation is also affected by the NADH/$NAD^+$ ratio. Disturbances in the ratio of $NAD^+$ to NADH have significant implications in the regulation of electron flow. As the flow of electrons during state 4 respiration is coupled to ATP function, $\Delta\psi_m$ (membrane potential across the inner mitochondrial membrane) and the NADH/$NAD^+$ ratio determine the rate of electron leakage to $O_2^{\bullet-}$ at complex III.

Under normal rates of superoxide production, superoxide dismutase (SOD) acts as a defence mechanism to successfully and efficiently remove the superoxide. Superoxide dismutases were the first ROS-metabolising enzymes discovered [McCord, JM., & Fridovich, I., 1969]. In eukaryotic cells $O_2^{\bullet-}$ can be metabolised to hydrogen peroxide by two metal containing SOD isoenzymes, an 80 - kDa tetrameric Mn - SOD present in mitochondria, and the cytosolic 32 - kDa dimeric Cu / Zn - SOD. Both of SOD catalyse the same reaction [3]:

$$2H^+ + O_2^- + O_2^- \xrightarrow{\text{SOD}} H_2O_2 + O_2 \qquad [3]$$

However, the presence of increased Cu / Zn – SOD, at the same time as catalysing efficient removal of superoxide, it leads to rapid synthesis of hydrogen peroxide, which itself can be damaging. Increased production of hydrogen peroxide in the cytosolic compartments or subsequent production of $^{\bullet}OH$ radical by the Fenton reactions has been suggested as responsible for making the Cu / Zn – SOD overexpressing mice more susceptible to radiation, infection and other stresses [Golenser, J., *et al.*, 1998; Gahtan, E., *et al.*, 1998]. Therefore, overexpression of superoxide dismutases can be as problematic as underexpression.

### 1.7.2 HYDROGEN PEROXIDE ($H_2O_2$)

$H_2O_2$ is not a free radical, but is nonetheless highly important mostly because of its ability to penetrate biological membranes, and is mainly formed by dismutation of superoxide. It plays a radical forming role as an intermediate in the production of more reactive ROS molecules, including hyperchlorous acid (HOCl) in inflammatory cells [4]:

$$H^+ + Cl^- + H_2O_2 \longrightarrow HOCl + H_2O \qquad [4]$$

$H_2O_2$ once produced by the above mechanism is removed by at least three antioxidant enzyme systems, namely catalases, glutathione peroxidases, and peroxiredoxins [Chae, E., *et al.*, 1999; Mates, *et al.*, 1999]. Catalase, present in the peroxisomes of nearly all aerobic cells, serves to protect the cell from the toxic effects of hydrogen peroxide by catalysing its decomposition into molecular oxygen and water without the production of free radicals. However the most important is glutathione peroxidase by oxidising glutathione (GSH) and therefore reducing cytosolic $H_2O_2$ to $H_2O$ (reaction 5).

$$H_2O_2 + 2\ GSH \rightarrow GSSG + 2\ H_2O \qquad [5]$$

### 1.7.3 HYDROXYL RADICAL ($^{\bullet}OH$)

Due to its strong reactivity with biomolecules, $^{\bullet}OH$ is believed by some to be capable of causing more damage to biological systems than any other ROS [Betteridge, DJ., 2000; Halliwell, B., 1987]. The radical is formed from hydrogen peroxide in a

reaction catalysed by metal ions ($Fe^{2+}$ or $Cu^{+}$), often bound in complex with different proteins or other molecules. This is known as the Fenton reaction [6]:

$$H_2O_2 + Cu^{+}/Fe^{2+} \longrightarrow {}^{\bullet}OH + OH^{-} + Cu^{2+}/Fe^{3+} \qquad [6]$$

Superoxide also plays an important role in connection with Reaction 5 by recycling the metal ions. Transition metals may be released from proteins such as ferritin and the [4Fe - 4S] centre of different dehydrases by reactions with $O_2^{\bullet-}$ [Harris, LR., *et al.*, 1994] [7]:

$$Cu^{2+}/Fe^{3+} + O_2^{\bullet-} \longrightarrow Cu^{+}/Fe^{2+} + O_2 \qquad [7]$$

## 1.7.4 NITRIC OXIDE ($NO^{\bullet}$)

Nitric oxide represents an odd member of the free radical family and is similar to $O_2^{\bullet-}$ in several aspects in that it does not readily react with most biomolecules despite its unpaired electron. On the other hand it easily reacts with other free radicals, generating mainly less reactive molecules, thus in fact functioning as a free radical scavenger. $NO^{\bullet}$ for example, has been shown to inhibit lipid peroxidation in cell membranes [Rubbo, H., *et al.*, 2000; Hogg, N., & Kalyanaraman, B., 1998]. However, if $O_2^{\bullet-}$ is produced in large amounts and parallel with NO, the two react with each other very rapidly ($1.6 \times 10^{-10}$ $Mol^{-1}$ $s^{-1}$) to yield peroxynitrite ($OONO^{-}$), which is highly cytotoxic [Meckman, JS., & Koppenol, WH., 1996]. In physiologic concentrations $NO^{\bullet}$ functions mainly as an intracellular messenger stimulating guanylate cyclase and protein kinases, thereby relaxing smooth muscle in blood

vessels, among other effects. $NO^{\bullet}$ has the ability to cross cell membranes and can thereby also transmit signals to other cells [Ignarro, LJ., 1990]. When produced in larger amounts it becomes an important factor in redox control of cellular function [Wink, DA., & Mitchell, JB., 1998]. The total effect of $NO^{\bullet}$ on the redox status of cells is multifaceted, though, in conclusion, in many respects it seems to function as an antioxidant and not as an oxidant [Halliwell, B., 1996].

## 1.7.5 SINGLET OXYGEN ($^1O_2$)

Singlet oxygen ($^1O_2$) is a highly reactive form of molecular oxygen that may harm living systems by oxidising critical organic molecules. It originates as a consequence of photochemical reactions between light, oxygen, and light-reactive substances called photosensitizers [Foote, CS., 1968]. Biological $^1O_2$, however, may also arise from non-photochemical sources such as the neutrophil respiratory burst and membrane lipid peroxidative chain reactions [Cadenas, E., 1989]. The macrophage myeloperoxidase catalyse the halide driven reduction of hydrogen peroxide, to form the oxidant hyperchlorus acid (HOCl). HOCl then reacts with $H_2O_2$ to form $^1O_2$ [8]:

$$H_2O_2 + BrCl^- \longrightarrow HOCl + OH^- \qquad [8]$$

$$H_2O_2 + HOCl \longrightarrow {}^1O_2 + Cl^- + H^+$$

In vitro studies have shown that $^1O_2$ oxidises macromolecules such as lipids, nucleic acids, and protein, depending on its intracellular site of formation, and promotes detrimental processes such as lipid peroxidation, membrane damage, and cell death.

## 1.7.6 LIPID PEROXIDATION

Biological macromolecules, such as lipids, proteins, and DNA are all targets for free radical injury [Shewfelt, & Purvis, 1995]. Polyunsaturated fatty acids (PUFA), the main components of membrane lipids, are susceptible to peroxidation. Lipid peroxidation is one of the most investigated consequences of the free radical action on the membrane structure and function. The idea of lipid peroxidation as a solely destructive process has changed during the last decade. It has been shown that lipid hydroperoxides and oxygenated products of lipid degeneration as well as lipid peroxidation initiators (free radicals) can participate in the signal transduction cascade [Tarchevskii, 1992].

Hydroxyl radicals and singlet oxygen can react with the methylene groups of PUFA forming conjugated dienes, lipid peroxyl radicals and hydroperoxides [Smirnoff, 1995], [9 and 10]:

$$PUFA\ H + X^{\bullet} \longrightarrow PUFA^{\bullet} + X\text{-}H \qquad [9]$$

$$PUFA\bullet + O_2 \longrightarrow PUFA\text{-}OO^{\bullet} \qquad [10]$$

The peroxyl radical formed is highly reactive and is able to propagate the chain reaction [11]:

$$PUFA\text{-}OO^{\bullet} + PUFA\text{-}H \longrightarrow PUFA\text{-}OOH + PUFA^{\bullet} \qquad [11]$$

The formation of conjugated dienes occurs when free radicals attack the hydrogens of methylene groups that separates double bonds and leads to rearrangement of the bonds [Recknagel, 1984]. The lipid hydroperoxides produced (PUFA- OOH) can

undergo reductive cleavage by reduced metals, such as $Fe^{2+}$, according to the following equation [12]:

$$Fe^{2+}complex + PUFA\text{-}OOH \longrightarrow Fe^{3+}\ complex + OH^{-} + PUFA\text{-}O^{\bullet} \quad \textbf{[12]}$$

The lipid alkoxyl radical produced, PUFA- $O^{\bullet}$, can initiate additional chain reactions [Buettner, 1993] [13]:

$$PUFA\text{-}O^{\bullet} + PUFA\text{-}H \longrightarrow PUFA\text{-}OH + PUFA^{\bullet} \quad \textbf{[13]}$$

## 1.8 SITES OF FREE RADICALS PRODUCTION

The superoxide anion radical and hydrogen peroxide, respectively, the products of the univalent and bivalent reduction of oxygen, are produced during normal aerobic metabolism and constitute physiological intracellular metabolites. Several reactions in biological systems contribute to the steady state concentrations of $O_2^{\bullet-}$ and $H_2O_2$, although mitochondria seem to be quantitatively the most important cellular source.

Mitochondria, which are present in virtually all-eukaryotic cells, are membrane-bound organelles that convert energy to forms that can be used to drive cellular reactions. It is estimated that 1 - 2 % of oxygen reacting with the respiratory chain leads to the formation of $O_2^{\bullet-}$.

In eukaryotic mitochondria, electrons are fed into the electron transport chain from reduced substrates such as glycerol phosphate, fatty acids, NADH or succinate. Large membrane bound enzymes, such as glycerol phosphate dehydrogenase, NADH-Q oxidoreductase (Complex I) or succinate-Q oxidoreductase (Complex II) pass electrons down the gradient of redox potential to the mobile lipid-soluble carrier, ubiquinone (UQ). From UQ, the electrons pass down through UQ-cytochrome *c*

oxidoreductase (Complex III) to the final acceptor, oxygen. Coupling of this series of energy-releasing oxidation reactions to the energy-demanding reactions of ATP synthesis is accomplished by a chemiosmotic mechanism. As electrons flow down their chemical gradient, Complex I, Complex III and complex IV pump protons from the mitochondrial matrix to the intermembrane space, against their electrochemical gradient. This active proton pumping sets up a proton-motive force which, consists mostly of an electrical gradient (membrane potential), accompanied by a small chemical gradient (pH difference). The proton-motive force that drives protons back into the matrix through the mitochondrial ATP synthase, results in ATP synthesis. The resulting chemiosmotic proton circuit is the mechanism of oxidative phosphorylation.

Therefore, oxidative phosphorylation in the mitochondria is carried out by four electron-transporting complexes (I-IV) and one $H^+$- translocating ATP synthetic complex (complex V). Two of these complexes have been shown to be responsible for much of the superoxide generated by mitochondria: complex I, the NADH-ubiquinone oxidoreductase, and complex III, the ubiquinonol-cytochrome c oxidoreductase [Beyer, R., 1991; Takeshiga, K., & Minakami, S., 1979]. A series of electron carriers, that are conserved from prokaryotes through to higher mammals, conduct electrons derived from the oxidation of NADH through a series of iron - sulphur centres to finally reduce ubiquinone during which protons are pumped from the matrix space to the outside of the mitochondrial membrane. Semiquinones generated within complex I have been identified as the likely donors for transforming $O_2$ to $O_2^{\bullet-}$.

Complex III of the mitochondrial respiratory chain is another site of $O_2^{\bullet-}$ production. Complex III (ubiquinol-cytochrome c oxidoreductase) is responsible for receiving reducing equivalents, which are generated in complexes I and II and contained in ubiquinol, and transferring them through reactions with cytochrome *b*, the Rieske iron-sulphur protein, and then cytochrome $c_1$ to the final electron acceptor *cytochrome c*. The Rieske iron-sulphur protein accepts one electron from ubiquinone (Q), forming a semiquinone. The latter reduces the first cytochrome *b* haem ($b_L$), which donates one electron to the second cytochrome *b* haem ($b_H$) to reduce ubiquinone and eventually form ubisemiquinone ($UQH^{\bullet}$), which is the source of $O_2^{\bullet-}$.

The concentration of $QH^{\bullet}$ in the electron transport chain is an important determinant of ROS production. Agents that increase respiration rate, such as uncouplers or ADP have long been known to decrease ROS production by isolated mitochondria [Boveris, A., & Chance, B., 1973]. However, inhibitors of electron transport can either increase or decrease ROS production depending on their site of action, so ROS production is not linearly related to the rate of electron transport. However, it shows a steep dependence on the magnitude of the proton-motive force in isolated mitochondria [Liu, SS., 1997; Korshunof, SS., *et al.*, 1997]. Uncouplers and ATP synthesis lower proton-motive force by increasing its consumption. The proton-motive force would affect ROS production by altering the redox state of UQ; at high proton-motive force respiration slows, so electrons would accumulate at Q instead of passing down the electron transport chain to oxygen. This would increase the steady-state concentration of $QH^{\bullet}$ and so increase the rate of mitochondrial ROS production. Inhibitors of electron transport lower proton-motive force, but they also affect the redox state of the UQ pool: those that are expected to increase the oxidation of the UQ

pool decrease ROS production and those that are expected to increase the reduction of the UQ pool increase ROS production.

### 1.8.1 COMPLEX I AND SUPEROXIDE PRODUCTION

Mammalian complex I is a large macromolecular assembly of proteins comprising thirty four subunits encoded by the nuclear DNA and seven subunits encoded by mitochondrial DNA [Shoffner, JM., & Wallace, DC., 1995]. Semiquinones generated within complex I have been identified as potential donors for transforming $O_2$ to $O_2^{\bullet-}$, although the exact mechanism of how and where these semiquinones are generated by the complex I components is yet to be fully elucidated [Boveris, A., & Chance, B., 1977; Du, G., *et al.,* 1998]. The sites within complex I where semiquinones are generated are thought to be in proximity to inhibition sites within the complex for the quinone analogue inhibitors such as rotenone [Boveris, A., & Chance, B., 1977; Du, G., *et al.,* 1998] [Figure 1.4]. The detailed mechanisms of how complex I functions to transport electrons linked to vectorial proton transport are not yet clear. It is likely that rotenone and other complex I inhibitors increase $O_2^{\bullet-}$ and $H_2O_2$ production from mitochondria at complex I, possibly by blocking a site where semiquinone donates an electron to an acceptor [Pitkanen, S., *et al.,* 1996; Pitkanen, S., & Robinson, BH., 1996]. In addition, it has been shown that diphenyleneiodonium (DPI) a mitochondrial inhibitor of complex I, resulted in decreased oxidative phosphorylation [Holland, PC., *et al.,* 1973; Ragan, CI., & Bloxham, DP., 1977]. Majander *et al.* [Majander, A., *et al.,* 1994] further demonstrated that DPI inhibits the reduction of iron-sulfur clusters of the complex I possibly through irreversibly reacting with flavoenzymes.

Deficiency or inhibition of mitochondrial complex I has been associated with clinical studies. Tomomi *et al.* [Tomomi, I., *et al.,* 1999] provided evidence for the increased production of $O_2^{\bullet-}$ at the complex I site in the mitochondria isolated from failing cardiac myocytes. It has also been reported that excessive superoxide production in a family with cataracts is linked to complex I deficiency on the mitochondrial respiratory chain [Pitkanen, SF., *et al.,* 1995]. It has also been demonstrated that NADH / NADPH oxidase is the predominant $O_2^{\bullet-}$ source in both endothelial and smooth muscle cells [Griendling, KK., *et al.,* 1994; Mohazzab-H, KM., *et al.,* 1994].

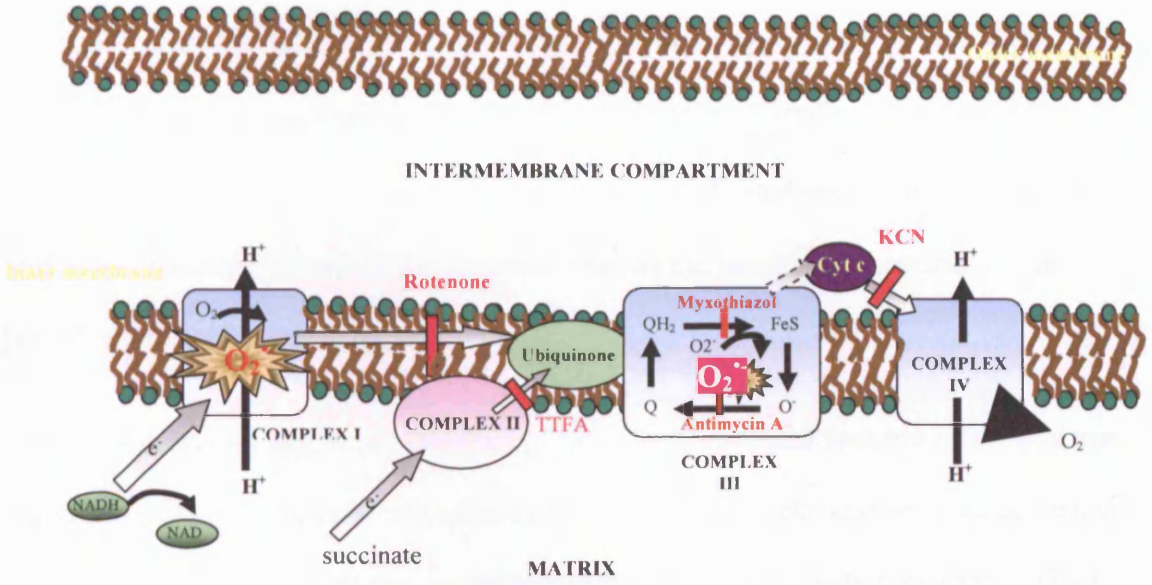


**Figure 1. 4 Mitochondrial sites of superoxide formation as adapted from http://www.ruf.rice.edu/~bioslabs/studies/mitochondria/mitets.html.** Inhibition of electron flow upstream of ubiquinone decreases $O_2^{\bullet-}$ whilst downstream inhibition enhances $O_2^{\bullet-}$ formation. In the presence of succinate (Complex II substrate), thenoyl trifluoracetone which inhibits succinate dehydrogenase prevents $O_2^{\bullet-}$ formation.

## 1.8.2 COMPLEX III AND SUPEROXIDE PRODUCTION

The Q-cycle describes the general mechanism of electron and proton transfers within the cytochrome bc1 complex. Quinol is oxidised and quinone reduced at two separate sites, the $Q_o$ and $Q_i$ sites, respectively [Mitchel, P., 1976]. The oxidation of quinol at the $Q_o$ site entails an obligatory bifurcation of the two electrons. The first electron from the quinol is transferred to the iron - sulfur center and then to cytochrome $c_1$. The electron on the semiquinone product is transferred to heme $b_L$ and from there proceeds to the $Q_i$ site via heme $b_H$. Even though, antimycin and myxathiazol are two of complex III inhibitors they have different effects on $O_2^{\bullet-}$ production [Slater, EC., 1973] [Figure 1.4]. Blocking electron passage out of cytochrome $b_H$ prevents the semiquinone at the $Q_o$ site from donating its electron and therefore inhibition with antimycin produces a tenfold increase in $O_2^{\bullet-}$ from complex III. Inhibition by myxathiozol produces little or no increase in $O_2^{\bullet-}$ formation, because it prevents ubisemiquinone formation at the cytosolic side of the inner mitochondrial membrane [Li, Y., *et al.*, 1999; Raha, S., *et al.*, 2000].

Studies [Matsuno-Yagi, A., & Hatefi, Y., 1996] have revealed features of the electron transfer system of bovine mitochondrial ubiquinol-cytochrome *c* oxidoreductase (complex III, $bc_1$ complex) that are incompatible with the Q cycle hypothesis. Firstly, it was shown that in bovine-heart submitochondrial particles, the inhibition of complex III by either antimycin or myxathiozol was incomplete. In addition, cytochrome *b* of complex III was partially reduced via cytochrome $c_1$ and the Reiske iron sulfur protein by ascorbate, and this reaction was inhibited more strongly by antimycin than by myxothiazol [Miki, T., *et al.*, 1994].

The results of carefully examining the efficacy of various complex III inhibitors on $O_2^{\bullet-}$ production in isolated whole mitochondria, compared with Mn - SOD - depleted submitochondrial particles also suggests that there is a sidedness to $O_2^{\bullet-}$ production [Raha, S., *et al.*, 2000]. That much of $O_2^{\bullet-}$ produced by the respiratory chain under physiological conditions is generated at the matrix side of the membrane is likewise suggested by the presence of Mn - SOD in the mitochondrial matrix and the comparatively low levels of $O_2^{\bullet-}$ production by whole mitochondria containing Mn - SOD [Raha, S., *et al.*, 2000]. When this enzyme is physically removed, the rates of $O_2^{\bullet-}$ produced by mitochondria are significantly increased [Raha, S., *et al.*, 2000].

## 1.9 OXIDATIVE STRESS AND MITOCHONDRIA

Mitochondria, is the most prominent cellular site of $O_2^{\bullet-}$production in mammalian cells, and the steady state concentration of $O_2^{\bullet-}$ in the mitochondrial matrix is about 5 - to 10 - fold higher than that in the cytosolic and nuclear spaces [Richter, C., *et al.*, 1988; Richter, C., *et al.*, 1995]. Mitochondria are sensitive to changes in the redox state of the cell. Several studies have demonstrated that when there is mitochondria dysfunction under conditions of oxidative stress this can lead to apoptosis [Zamzami, N., *et al.*, 1995; Zamzami, N., *et al.*, 1996; Green, DR., & Reed, JC., 1988; Susin, SA., *et al.*, 1998; Morel, Y., *et al.*, 1999]. Under severe oxidative stress, the mitochondrial permeability transition (PT) opens. PT involves a sudden increase of the inner mitochondrial membrane permeability to solutes greater than 1500 Da. When the PT pore is defective and it opens to larger molecules, it also causes uncoupling of the respiratory chain resulting in overproduction of ROS, cessation of ATP synthesis, matrix $Ca^{2+}$ outflow and depletion of reduced glutathione and other reductants. After matrix solutes are released from the inner membrane, a colloidal

osmotic pressure arises in the mitochondrial matrix due to the high concentrations of proteins, that are slow to equilibrate [Igbavboa, U., *et al.,* 1989; Gunter, TE., & Pfeiffer, DR., 1990; Richter, C., *et al.,* 1995]. To compensate for this osmotic imbalance, the diffusion of $H_2O$ results in a massive swelling of the mitochondria [Gunter, TE., & Pfeiffer, DR., 1990]. This change in membrane potential predisposes these cells to oxidative damage by impairment of endogenous antioxidant defence mechanisms [Petit, PX., *et al.,* 1996; Zamzami, N., *et al.,* 1997; Marzo, I., *et al.,* 1998; Yang, JC., & Cortopassi, GA., 1998]. Alteration of the $\Delta\psi_m$ is another factor changed during mitochondrial impaired function [Zamzami, N., *et al.,* 1995; Zamzami, N., *et al.,* 1996; Green, DR., & Reed, JC., 1988; Susin, SA., *et al.,* 1998; Morel, Y., *et al.,* 1999]. An increase in $\Delta\psi_m$ can induce oxidative stress and cell death [Ling, YH., *et al.,* 2003]. It has been reported [Li, P., *et al.,* 1999] that p53 – induced apoptosis occurs via an increase in the generation of ROS and the disruption of mitochondrial membrane potential. These events indicate that ROS generation and an increase in $\Delta\psi_m$ are the early and necessary events for the initiation of apoptotic signalling.

Calcium is another important mediator of apoptosis [Soabo, L., & Zoratti, M., 1992; Petrollini, V., *et al.,* 1993] and its status is closely linked with oxidative stress in many isolated cell systems with the best example being isolated rat hepatocytes [Gutirrez, PL., & Bachur, NR., 1983]. When cells are deprived of calcium, mitochondria become sensitive to this calcium-deficient state and their calcium regulatory mechanism is disturbed. Calcium omission results in a marked decline of mitochondrial $\Delta\psi_m$, leading to oxidative stress and induction of programmed cell death. Therefore, calcium homeostasis via mitochondria and endoplasmic reticulum is vital to the function and survival of the cell [Thomas, D., & Hanley, MR., 1994].

## 1.10 EFFECTS OF REACTIVE OXYGEN SPECIES

Reactive oxygen species generated by mitochondria, or from other sites within or outside the cell, can cause damage to mitochondrial and other intracellular components and initiate degradation and apoptotic mechanisms. Although mild oxidative damage such as that experienced during exercise training may actually be the stimulus for physiological mitochondrial biogenesis via superoxide production from ubisemiquinone. More severe or more prolonged oxidative shock is clearly damaging and such toxic events contribute significantly to the aging process. The relation between free radicals and process of ageing is now well established [Jame, AM., *et al.,* 2005]. Studies in a variety of different animal species have shown that animals with more rapid rates of basal metabolism have faster rates of ROS production and shorter life span [Barja, G., & Herrero, A., 2000; Lass, A., & Sohal, RS., 1999]. There is strong evidence that damage to proteins and DNA is cumulative with age, and that mutations and deletions, especially in mitochondrial DNA, are much more frequent in the aged compared with the young of most species [Barja, G., & Herrero, A., 2000]. These data have been interpreted as indicating that life span is influenced by mitochondrial DNA deletions and mutations accumulated through exposure to oxygen free radical damage, and that this is a function of the endogenous rate of electron transport mediated by the fixed electron-transport intermediary ubiquinone [Lass, A., & Sohal, RS., 1999]. The faster the rate of metabolism, the faster is the rate of electron transport and the rate of generation of superoxide, thus leading to free radical damage to proteins, lipids and DNA by superoxide and its downstream reactive metabolites.

In order to prevent excessive oxidative stress and tissue injury, organisms specifically synthesise molecules that fight against active oxygen species by developing a balance between the generation of reactive oxygen species and the tissue antioxidant defence mechanism. Glutathione is one of the most important molecules that protect cells against oxidative stress.

## *1.11 GLUTATHIONE*

Glutathione (GSH) [Figure 1.5] is a tripeptide of glutamate, cysteine and glycine that contains a $\gamma$-peptide bond between glutamate and cysteine [Griffith, OW., & Meister, A., 1985], which prevents GSH from being hydrolysed by most peptidases.

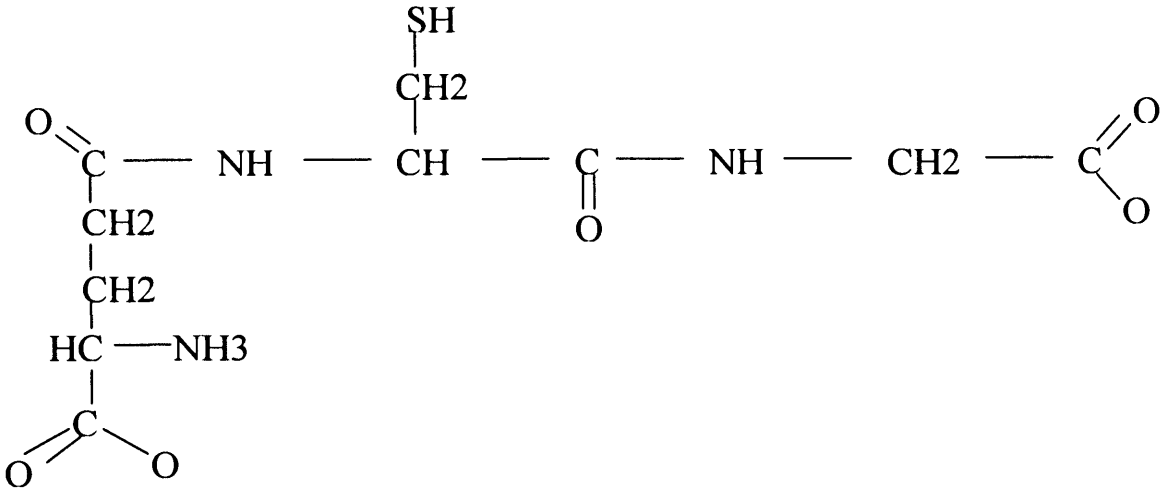


**Figure 1. 5 Chemical structure of glutathione (GSH).**

GSH is the most abundant intracellular thiol that is found in mammalian and prokaryotic cells. GSH has several important cellular functions, including its participation as a coenzyme responsible for amino acid transport and its involvement in metabolism and the maintenance of the thiol moieties of proteins. Probably its most important function relies on the protection mechanism that provides against oxidative damage caused by ROS formed normally during cell metabolism.

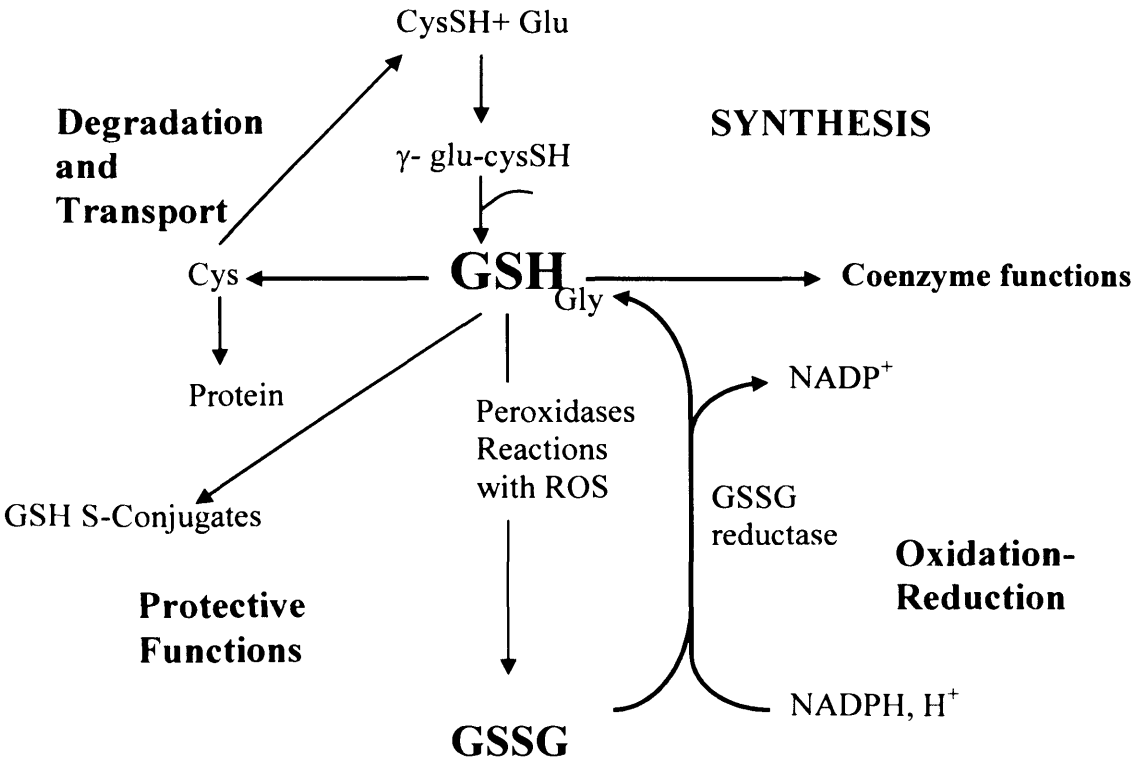


**Figure 1. 6 Summary of GSH synthesis and redox.**

GSH reacts rapidly and non-enzymatically with hydroxyl radical, the cytotoxic Fenton reaction product, and with $N_2O_3$ and peroxynitrite, cytotoxic products formed by the reaction of nitric oxide with $O_2$ and superoxide, respectively [Kalyanaraman, B., *et al.*, 1996; Luperchio, S., *et al.*, 1996; Brivida, K., *et al.*, 1999]. In reactions catalysed by glutathione peroxidase, GSH also participates in the reductive detoxification of hydrogen peroxide and lipid peroxides [Ursini, F., *et al.*, 1995]. Each of these reactions leads directly or indirectly to the formation of glutathione disulfide (GSSG) that is reduced intracellularly to GSH by glutathione reductase in a NADPH - dependent reaction [Kehrer, JP., *et al.*, 1994]. At normal levels of oxidative stress,

glutathione reductase activity and NADPH availability are sufficient to maintain [GSH] / [GSSG] in a ratio of approximately 100 : 1 [Akerboom, TP., *et al.,* 1982] and under these conditions there is no net loss of GSH through oxidation. However, if stress levels increase or GSSG reductase is limited, GSSG accumulates. This has two important consequences: (i) the thiol redox status of the cell will shift, activating certain oxidant response transcriptional elements [Sen, CK., & Packer, L., 1996; Muller, JM., *et al.,* 1997], (ii) GSSG will be secreted from the cell, and (iii) protein mixed disulfides will form [Akerboom, T., & Sies, H., 1990]. As GSSG is not taken up by cells, but rather is actively transported out of cells and degraded extracellularly, loss of GSSG from cells under conditions of oxidative stress increases cellular requirements for de novo GSH synthesis [Figure 1.6].

### 1.11.1 GLUTATHIONE BIOSYNTHESIS

GSH is synthesised intracellularly by the consecutive actions of γ-glutamylcysteine synthase (GCS) and GSH synthases:

$$\text{L-Glu} + \text{L- Cys} + \text{ATP} \xleftrightarrow{\text{GCS}} \text{L-}\gamma\text{-Glu} — \text{L-Cys} + \text{ADP} + \text{Pi}$$

$$\text{L-}\gamma\text{-Glu} — \text{L-Cys} + \text{Gly} + \text{ATP} \xleftrightarrow{\text{GSH synthase}} \text{GSH} + \text{ADP} + \text{Pi}$$

Cysteine is usually the limiting substrate and GCS the rate limiting enzyme in the synthesis of GSH. Intracellular GSH is exported from some cells, but it is not significantly taken up by cells under normal conditions [Meister, A., 1991]. Once outside of the cell, the γ-glutamyl bond of GSH is cleaved by the membrane bound γ-glutamyl transpeptidase. The product of this reaction is a γ-glutamyl enzyme, which accepts an amino acid to form γ-glutamyl amino acid. This amino acid is cleaved by γ-glutamyl cyclotransferase to yield free amino acid and 5-oxoproline. One of the best

acceptor amino acids for transpeptidases is cysteine, thus its product is γ-glutamylcysteine [Thompson, GA., 1976].

GSH, is synthesised from its constituent amino acids by the sequential action of cytosolic enzymes γ-glutamylcysteine synthase (γ-GCS) and glutathione synthase [Griffith, OW., & Mulcahy, RT., 1999; Meister, A., 1994]. Mammalian γ-GCS is a heterodimer comprised of a catalytically active heavy subunit (MW 73000 Da) that includes all substrate binding sites and a light subunit (MW 31000 Da) that modulates the affinity of the heavy subunit for substrates and inhibitors [Yan, N., & Meister, A., 1990; Gipp, JJ., *et al.,* 1992; Huang, CS., *et al.,* 1993]. γ-GCS is involved in the chemical mechanism in which, L-glutamate and ATP first react to form tightly bound γ-glutamylphosphate, and that intermediate then reacts with L-cysteine to form the final products. In addition, mammalian gluathione synthase is a homodimer with each subunit (MW 52 000 Da) containing about 2 % carbohydrate [Oppenheimer, L., *et al.,* 1979; Huang, CS., *et al.,* 1995] and catalyses the ATP - dependent formation of GSH from γ-glutamylcysteine and glycine.

### 1.11.2 THE IMPORTANCE OF MITOCHONDRIAL GLUTATHIONE

It has been reported that glutathione deficiency produced in guinea pigs and newborn rats leads to death within a few days; adult mice and rats exhibit morbidity associated with damage to various tissues, including lung and certain organs of the gastrointestinal tract [Meister, A., 1991]. L-buthionine-sulfoximine (BSO), a synthetic amino acid that depletes glutathione by irreversibly inhibiting γ-glutamylcysteine, when administered to newborn rats leads to cataracts [Calvin, HL., *et al.,* 1986] and long term treatment with BSO produces severe GSH deficiency. The cellular damage found after administration of BSO mostly involves the mitochondria. The considerable cellular damage found in glutathione deficiency reflects the extensive formation of ROS, which occurs normally in the mitochondrial compartment. In addition, it was found that mitochondrial glutathione decreases much more slowly than total cell glutathione after giving BSO [Griffith, OW., & Meister, A., 1985], suggesting that there is a separate mitochondrial pool of glutathione. Furthermore, it was reported that mitochondria do not synthesize GSH, but they obtain their GSH from other intracellular GSH [Griffith, OW., & Meister, A., 1985]. Reversible conversion of GSH to GSSG occurs in the cytosol and in the mitochondria, however, GSH synthesis occurs only in the cytosol, which is transported in the mitochondria [Figure 1.7].

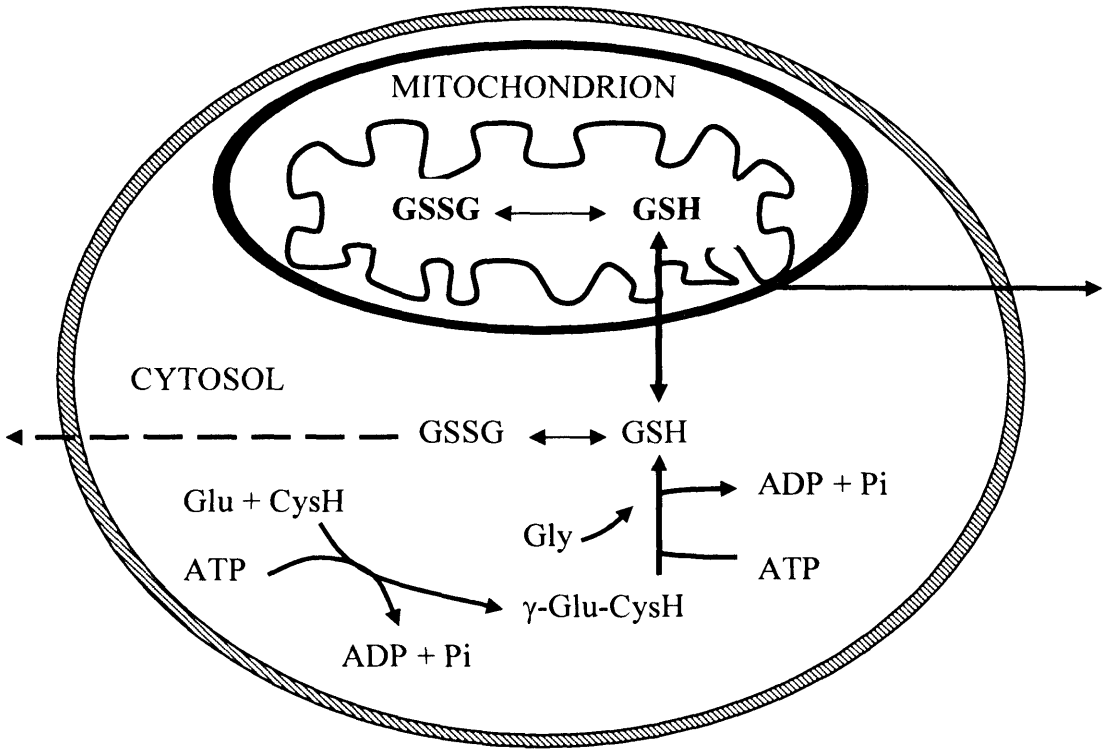


**Figure 1. 7 Glutathione transport from the cytosol into mitochondria.** Glutathione is formed by glutamate and cysteine through the action of two sequential ATP – dependent enzymatic reactions catalysed by γ-glutamylcysteine synthase. Mitochondria do not synthesise GSH, because it does not contain γ-glutamylcysteine synthase [Griffith, OW., & Meister, A., 1985]. Therefore, the mitochondrial pool is derived from the activity of a mitochondrial transporter that translocates GSH from the cytosol into the mitochondrial matrix.

Transport of GSH from the cytosol across the inner mitochondrial membrane must occur to supply the mitochondria with its pool of GSH. Studies have shown that GSH does not diffuse passively across the inner mitochondrial membrane. Rather, because mitochondria possess a membrane potential with the matrix space being negative relative to the cytoplasm and because GSH is a negatively charged molecule at

physiological pH, GSH must be transported actively or in exchange with another anion [Smith, CV., *et al.,* 1996]. Examples of these carriers include the dicarboxylate carrier (DCC) and the oxoglutarate carrier (OGC), which are responsible for at least 80 % of the total uptake of cytoplasmic GSH into renal cortical mitochondria [McKernan, TM., *et al.,* 1991; Chen, Z., & Lash, LH., 1998; Chen, Z .,*et al.,* 2000].

The electron transport system is a source of $O_2^{\bullet-}$. Since mitochondria do not contain catalase, they depend upon GSH peroxidase and non-enzymatic reaction with GSH to protect against peroxide toxicity. In cases where GSH levels are severely depleted, mitochondria swell and cells contain vacuoles, indicating endogenous oxidative stress [Martensson, J., & Meister, A., 1989; Martensson, A., *et al.,* 1991]. This oxidative stress can be reversed by administering ascorbate or other GSH esters. The use of BSO to produce a model of GSH deficiency has led to interesting data that elucidate some of the functions of GSH and provides a model to test therapies designed to increase cellular GSH levels. One such disease that is associated with GSH deficiency is thought to be nephrolithiasis.

## 1.12 Hypothesis and Aims

COM crystals in the renal tubule form the basis of most kidney stones. It is now established that exposure of renal cells to CaOx results in a free-radical mediated oxidative stress. In view of the ability of COM crystals to elicit $O_2^{\bullet-}$ production in renal epithelial cell mitochondria, the aim of this study is to further investigate whether this phenomenon is common to other crystals or micro-particles.

In addition, oxalate transport into the mitochondria may also prove important for the development and thus treatment of stone disease. Therefore, this study aims to examine mitochondrial transport systems for oxalate and its role in the mitochondrial membrane potential and superoxide production.

Finally, mitochondrial dysfunction caused by crystal formation may contribute to pathological events during clinical conditions where tubular crystal-cell interactions are uncontrolled. To further develop these studies an *in vivo* animal model is employed to investigate how specific agents that can induce kidney stone formation may trigger free radical production by altering cell homeostasis and function.

# CHAPTER 2

## METHODS AND MATERIALS

## 2.1 Materials

All materials were purchased from Sigma-Aldrich Chemical Company Ltd unless otherwise stated. All tissue culture plastic was acquired from Greiner Laboratories or Fisher Scientific.

## 2.2 Cell culture

Madin-Darby canine kidney type -I (MDCK) distal-collecting duct cells, and Lewis Lung Carcinoma Pig kidney (LLC-PK1) proximal tubule renal epithelial cells, were maintained and grown in Dulbecco's modified Eagle's minimal essential medium (DMEM). Human kidney (HK2) cells were maintained and grown in keratinocyte serum free medium (SFM). All of the cell lines were supplemented with 8 % foetal calf serum (FCS), 2 mM glutamine, and penicillin streptomycin (100 U/ml/100 μg/ml), and maintained in T80 flask, at 37 °C under 5 % $CO_2$ / 95 % air. When cells were 80 % confluent, they were washed in 1 x phosphate buffer saline (PBS) and harvested using 500 μl of trypsin / versin. T80 flasks were then kept in the incubator for 10 min for the cells to become detached from the surface of the flask. After this time, 10 ml of 8 % FCS medium was added and resuspension of the mix was achieved, using a 10 ml sterile syringe and a quill, to disperse and produce a single cell suspension. After counting the cells 1 ml of the resuspended cells were then transferred (at a density of 2.5 x $10^6$ cells/dish) to 35 mm dishes and an additional volume of 1 ml of 8 % FCS medium was added to ensure an even distribution on the surface of the 35mm dishes. This resulted after cell adhesion in confluent monolayers of cells.

Cells were also grown and maintained on polycarbonate cell culture inserts (Becton Dickinson, Belgium) [Figure 2.1]. After cell counting, 1ml of pre-warmed medium

was added to each well of a six-well plate and the insert was gently placed into the well. Cells at density 2.5 x $10^6$ were added into the insert and cells were cultured under the conditions described above.

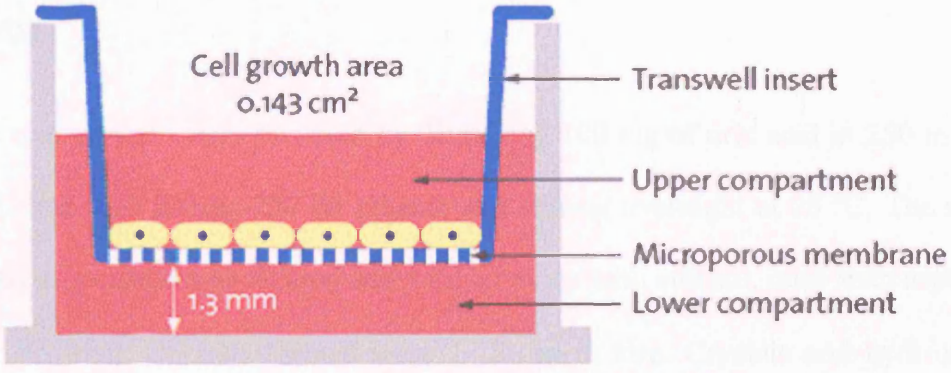


**Figure 2. 1 Polycarbonate membrane supports.** MDCK cells were seeded on the microporous membrane to form polarised monolayers that separate the cell culture medium into a basolateral and luminal side.

## 2.3 Cell treatment

After 48 h incubation of cultured cells on 35 mm dishes, cells were treated with calcium oxalate monohydrate (COM) (Merck Eurolab Supplies, UK) crystals or sodium oxalate (NaOx). Before treatment, cells cultured in 35 mm dishes were washed with PBS to remove any unattached or dead cells. Treatment of the cells with COM or NaOx followed. Sterile COM (25 mg/ml) was suspended in water and stored at 4 °C, and sterile sodium oxalate (150 mM) was prepared in water and adjusted to pH 6.8. Before treatment of cells COM was diluted to the final required concentration (250 µg/ml) in DMEM containing 2 % FCS which was continually stirred during the addition procedure. COM at 250 µg/ml is equivalent to 28.4 µg/cm$^2$ in a 35 mm dish.

Similarly, NaOx was prepared and used at a final concentration of 750 μM to 1.5 mM in 2 % FCS containing DMEM. COM treated cells were incubated for 4 h at 37 °C to allow crystals to attach to the cells, and cells treated with NaOx were pre-incubated for 15 min. Finally, control (untreated) cells were also kept in 2 % FCS containing DMEM.

Uric acid crystals were prepared by dissolving 100 mg of uric acid in 250 ml $H_2O$ at 60 °C and then adding 250 ml ethanol and stirring overnight at 25 °C. The resulting crystal suspension was filtered and washed twice with ethanol, once with acetone and then air-dried. Crystals formed were 1- 8 μm in size. Crystals and hydroxyapatite particles (Merck Eurolab Supplies, UK) were suspended in water and adjusted to pH 6.8.

Unless otherwise stated COM and other particulates were used at 250 μg/ml, equivalent to 28.4 $\mu g/cm^2$ in a 35-mm dish. Finally, crystals and particulates were added for 4 - 6 h and free oxalate 15 min before $O_2^{\bullet-}$ measurement. Additional treatment with specific inhibitors, or $Ca^{2+}$ chelators, were carried out in the manner described above, either added prior to $O_2^{\bullet-}$ measurement, or pre-incubated for the stated period of time. Table 2.1, lists details of these agents, including the concentration used.

**Table 2. 1 Details of the reagent used**

| Reagent | Final Concentration |
|---|---|
| Superoxide Dismutase (SOD) | 300mU/ml |
| Mn(III) tetrakis(1-methyl-4-pyridyl) porphyrin (MnTMPyP) | 200μM |
| Rotenone | 20μM |
| Antimycin A | 30μM |
| Carbonylcyanide chlorophenylhydrazone (CCCP) | 100μM |
| Thenoyl trifluoracetone (TTFA) | 10μM |
| 4-hydroxyccinamic acid | 500μM |
| Pyruvate | 300μM |
| Nordihydroguaiaretic acid (NDGA) | 250μM |
| Oligomycin | 10μM |
| Indomethacin | 10μM |

| | |
|---|---|
| *N,N'* dicyclohexylcarbodiimide (DCCD) | 50μM |
| Nigericin | 10μM |
| Uric acid | 250μg/ml |
| Zymosan | 250μg/ml |
| Hydroxyapatate | 250μg/ml |
| Latex Beads | 250μg/ml |
| Ethylenediminetraacetic acid (EDTA) | 1mM |
| Ethylene glycol-bis(β-aminoethyl ether-N,N',N'-tetraacetic acid (EGTA) | 1mM |
| Citrate | 1mM |
| Ascorbate | 1mM |
| Desferall | 1mM |
| (N-2[Hydroxyethl)]piperazine-N'-[2-ethanesulfonic acid]) (HEPES) | 3mM |
| (3-[N-Morppholino]propanesulfonic acid) (MOPS) | 5mM |

## 2.4 Chemiluminescence technique used for monitoring ROS production

Detection and measurement of the flux of reactive oxygen species within cells is of critical importance for investigating the patho - physiological consequences resulting from altered cellular reactive oxygen homeostasis. Therefore, the chemiluminescence technique, along with a selection of probes, has been used extensively in the measurement of ROS production. Chemiluminescence (CL) occurs whenever a molecule emits a photon of light as a result of an exergonic chemical reaction that generates an intermediate or end - product in an electronically excited state. The relaxation of the excited state molecule to ground state results in the emission of a photon [Allen, RC., 1986; Trush, MA., 1987].

As discussed earlier, there are many potential cellular sources of ROS production, however, mitochondrial respiration consuming approximately 90 % of the $O_2$ utilised by cells is generally considered to be the major source of cellular ROS. As such, mitochondria -derived ROS have frequently been implicated in a number of diseases and disorders most prominent being cancers, ischemia / perfusion injury. Thus, the need for detection and measurement of mitochondria-generated ROS has led to the development of different probes and techniques that can specifically monitor mitochondrial ROS generation. Lucigenin, pholasin and luminol are chemiluminescence probes that have been widely used for the detection of ROS production in various cellular systems [Faulkner, K., &. Fridovich, I., 1993; Roberts, PA., *et al.*, 1987].

### 2.4.1 Lucigenin-Derived Chemiluminescence (LDCL)

Lucigenin (bis-*N*-methylacridinium) - derived chemiluminescence is widely used as a specific assay for superoxide formation in mitochondria. The mechanism of LDCL depends on the fact that superoxide is capable of reducing lucigenin to its semiquinone in the following reaction [1]:

$$O_2^{\bullet-} + Luc^{2+} \longleftrightarrow O_2 + Luc^{\bullet+} \qquad [1]$$

The ability of lucigenin to function as a probe of mitochondrial superoxide generation should be dependent on its relative proximity to the mitochondrial electron transport activity. Therefore, lucigenin must first enter the cell and cross the plasma membrane. Once inside the cell it has been shown that lucigenin accumulates in the mitochondria, due to an ionic attraction between the positively charged lucigenin molecule and the negatively charged mitochondria. Once inside the mitochondria, lucigenin can undergo a one - electron reduction catalysed by components of the mitochondria electron transport chain, yielding the lucigenin cation radical [Figure 2.2]. The latter then reacts with the $O_2^{\bullet-}$, to yield an unstable dioxetane intermediate. The lucigenin dioxetane decomposes to produce two molecules of *N*-methylacridone, one of which is in an electronically excited state, which upon relaxation to the ground state emits a photon [Figure 2.3].

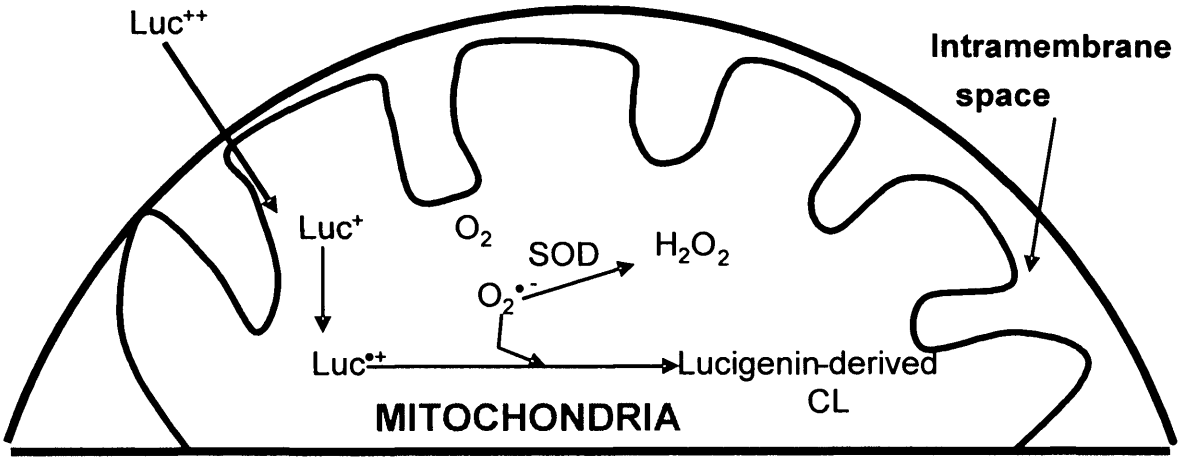


**Figure 2. 2 Diagram illustrating how lucigenin – derived CL detects mitochondrial ROS production.**

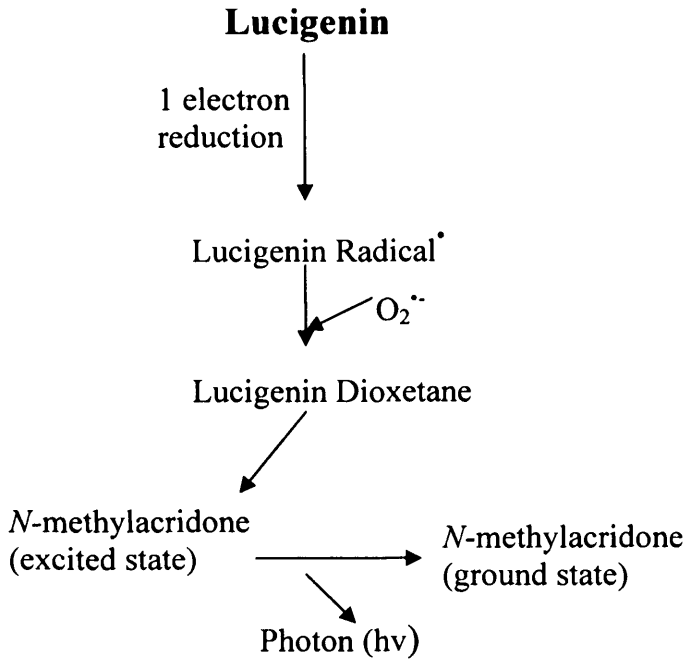


**Figure 2. 3 Schematic illustration of the chemical reaction pathways leading to lucigenin - derived CL.**

### 2.4.2 Superoxide Measurement

Cells cultured in 35 mm dishes were used for lucigenin-chemiluminescence measurement in a photon counting device comprising a gallium arsenate photo multiplier tube (Hamamatsu R943), thermoelectrically cooled to –20 °C. CL emission from samples in dishes maintained at 37 °C in a thermostatic light sealed chamber and was reflected and focused onto the photo multiplier tube [Figure 2.4]. After treatment with COM and NaOx, media from the cells was removed. Control and treated cells were washed in PBS to remove unattached crystals, and 1 ml of respiration buffer (RB), pH 7.4, was added [Table 2.2].

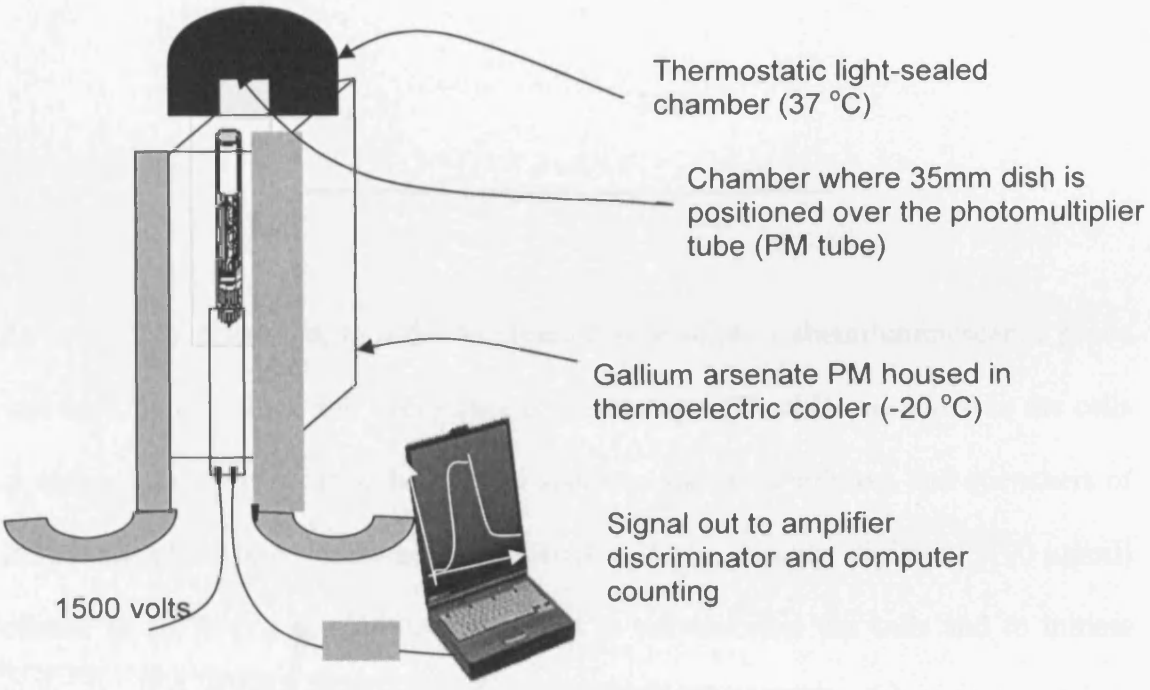


**Figure 2. 4 Schematic illustration of the chemiluminescence photon counting device.**

**Table 2. 2 Respiration Buffer at pH 7.4**

| REAGENTS | CONCENTRATION |
|---|---|
| Sucrose | 70mM |
| Mannitol | 220mM |
| EDTA | 1mM |
| $KH_2PO_4$ | 2.5mM |
| HEPES | 2mM |
| $MgCl_2$ | 1mM |

As previously discussed, in order to measure superoxide a chemiluminescence probe was used. Lucigenin at sub - recycling concentrations (20 μM) was added to the cells to obtain light derived from the $O_2^{\bullet-}$. In addition, specific inhibitors and quenchers of ROS were added prior to chemiluminescence counting. Finally, digitonin (100 μg/ml) diluted in 50 % (v / v) DMSO was added to permeabilize the cells and to initiate lucigenin chemiluminescence signal. Instrument readings (100 x 0.1 secs) were taken every 2 min.

## 2.5 MTT assay

Cell viability and functionality were tested using the MTT (3-(4, 5-dimethylthiazole-2yl)-2, 5-diphenyl tetrazolium bromide) reduction assay according to the method of Hansen *et al* [Hansen., *et al.,* 1989]. The MTT cell proliferation assay is a colorimetric assay system that measures the reduction of a tetrazolium component (MTT) into an insoluble formazan product by reductive enzymes in the mitochondria of viable cells. After incubation of the cells with the MTT reagent for approximately 2 to 4 h, DMSO was added to lyse the cells and solubilise the coloured crystals. The samples were read using a plate reader at a wavelength of 540 nm.

MTT was dissolved in RPMI (Roswell Park Memorial Institute) medium at a concentration of 0.5 mg/ml. MDCK cells were transferred in a density of $10^5$ cells / well into 96 well - plate and were incubated for one day before the experimental treatment. Once cells adhered on to the wells, they were treated with 250 μg/ml COM or with 1.5 mM NaOx for 24 h. Three hours before the incubation, treatment was removed and 100 μl / well of MTT in RPMI were added. Cells were then incubated for three hours at 37 °C. After three-hour incubation, MTT-containing medium was removed, cells washed once in PBS and 100 μl / well of DMSO was added. The plate was shaken and incubated for a further 30 min, and absorbance values determined at 540 nm using a Victor2, Wallac 1420 Multilabel counter.

## 2.6 Scanning Electron Microscopy

MDCK cells were grown on Thermenox coverslips and treated with COM for 10 to 240 min. The coverslips were then washed 3 times in PBS to remove unattached COM and cells were fixed in half-strength Karnowsky's fixative (1 % (v /v)

paraformaldehyde and 1.5 % (v/v) glutareldeyhde). After cells were washed they were dehydrated through a graded series of ethanol starting at 30 % and progressing through 50, 70, and 90 % up to 3 x 100 % (v / v). The cells were then transferred to amyl acetate and then placed into a critical point dryer (CPD7501; Polaron LTD). Drying was carried out using carbon dioxide as the drying fluid. Fragments of coverslips were then mounted onto stubs using colloidal silver dag. The cells were then coated with gold using a sputter coater (Polaron Ltd.) and finally observed in a Jeol JSM6310 scanning electron microscope.

## 2.7 Preparation of Radioactive COM crystal suspension

Radioactive sodium oxalate was prepared by adding 1 ml of 0.37 MBq/ml [$^{14}$C] oxalic acid (Amersham Pharmacia Biotech, UK) to 0.5 ml of 200 mM sodium oxalate. A calcium chloride solution was prepared by adding 0.5 ml 200 mM calcium chloride to 8 ml distilled water. After mixing the two solutions at room temperature (final concentration of 10 mM for both calcium and oxalate), radio labelled COM crystals were formed immediately. The crystal suspension was allowed to equilibrate for 3 days, and finally washed 3 times with calcium oxalate saturated distilled water and finally resuspended in 5 ml of this solution.

## 2.8 COM Dissociation

The release of free oxalate from COM was determined in RB in the absence and presence of different chelators using [$^{14}$C] - COM (Amersham Bioscience, UK) prepared from [$^{14}$C] -sodium oxalate. The dissociation of [$^{14}$C]-COM (250 μg/ml, specific activity 74 KBq/mg) was determined after equilibration in RB containing EDTA, EGTA, desferrioxamine (Desferal) (CIBA Laboratories, UK), citrate, and

ascorbate (1 mM) for 10 min at 37 °C by centrifugation of un-dissociated COM at 1000 x g for 10 min. The supernatant (free dissociated oxalate) and pellet (un-dissociated COM) were counted in a Beckman LS 6500 scintillation counter. The concentration of free oxalate was calculated from the supernatant counts relative to the un-dissociated [$^{14}C$] -COM standard (no chelators with 100 μM $CaCl_2$).

## 2.9 Confocal Microscopy

Confocal images were produced using the Zeiss LSM 510 laser scanning microscope. This is based around a Zeiss Axiovert 100 M inverted epifluorescence microscope equipped with x 40 and x 63 oil immersion lenses (NA 1.3 and 1.4, respectively) as well a x 63 water immersion lens (NA 1.2). The water immersion lens was corrected for chromatic aberration. Fluorescence was excited using one or more of three laser types – a UV argon (lines at 351 and 364 nm), an argon (lines at 458, 488 and 514 nm) and two helium-neon lasers (lines at 543 and 633 nm).

The confocal principle is based around the use of a point source of excitation illumination in combination with an adjustable aperture (the 'pinhole diaphragm') placed in the emission light pathway [Figure 2.5]. The laser light source is focused on the specimen so that only a small fraction is illuminated at any one time and a scanning module (a silvered mirror) rapidly scans this point back and forth across the area being imaged. The emission signal is scanned concurrently by the same module and the pinhole placed in the emission pathway limits the light falling on the PMT to a similar single point. Thus, light from out of focus layers is rejected, resulting in images that are less blurred, and allowing optical sections of the preparation to be obtained non-invasively (in practice, optical sections of around 1 μm thickness were

imaged). In addition, the fact that the LSM 510 is equipped with four lasers and four PMTs allows truly simultaneous imaging using up to seven excitation wavelengths and up to four emission wavelengths. The presence of an acousto-optic tuneable filter meant that the intensity of each laser line could be independently controlled.

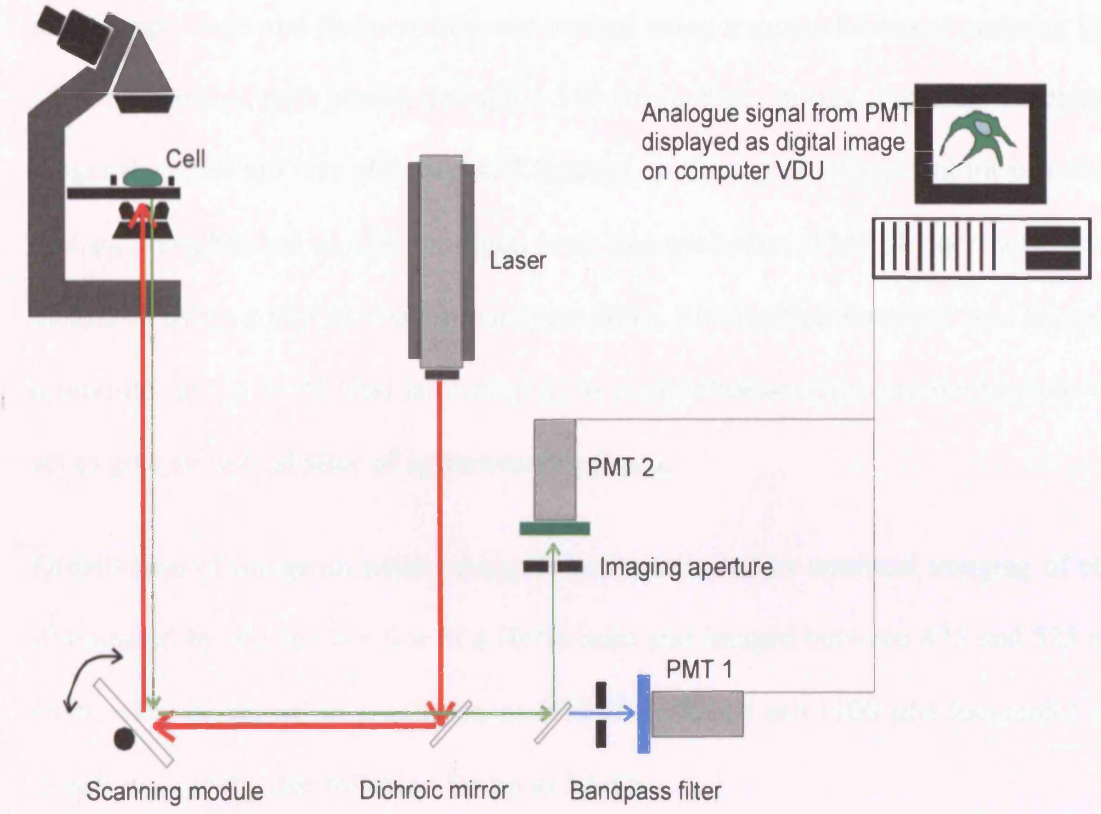


**Figure 2. 5 Schematic diagram of confocal setup.** For clarity, only one laser and two PMTs are shown. The Zeiss LSM 510 has four of each allowing truly simultaneous imaging of several fluorescent probes.

### 2.9.1 Measurement of mitochondrial membrane potential ($\Delta\psi_m$)

Cells were loaded with the membrane potential-sensitive dye tetramethylrhodamine methyl ester (Molecular probes, Netherlands) (TMRM; 20 nM in HEPES-buffered salt solution). Digital imaging of TMRM-loaded cells was performed using either a cooled CCD camera (Hamamatsu 4880) or a Zeiss 510 CLSM confocal microscope equipped with x 40 and x 63 oil immersion, quartz objectives lenses. For the cooled CCD system, coverslips were placed in a custom-made chamber and mounted on the microscope stage and fluorescence was excited using a monochromator emitting light of 490 nm which then passed through a 510 nm dichroic mirror. Light of wavelength longer than 590 nm was collected and focused on the camera. Confocal measurement of $\Delta\psi_m$ was obtained at 488 nm argon laser line excitation. TMRM fluorescence was measured using a 505 to 550 nm bandpass filter. Illumination intensity was kept to a minimum (at 0.1 % of total laser output) to avoid phototoxicity and the pinhole was set to give an optical slice of approximately 2 μm.

Distribution of lucigenin within the cells was monitored by confocal imaging of cells illuminated by the 364 nm line of a HeNe laser and imaged between 475 and 525 nm. Cells were immersed in a solution of HEPES-buffered salt (100 μM lucigenin) and distribution of the dye followed for up to 30 min.

### 2.9.2 Cytosolic calcium $[Ca^{2+}]_c$ measurements

Fluorescence cytosolic calcium concentration ($[Ca^{2+}]_c$) measurements were obtained using a Nikon Diaphot (Tokyo, Japan) epifluorescence inverted microscope with a x 20 fluorite objective. Excitation light from a xenon arc lamp was selected using 10 nm bandpass filters centred at 340 and 380 nm housed in a computer-controlled filter wheel (Cairn Research, Faversham, UK). Emitted light passed through a long-pass

filter to a cooled charge-coupled device (CCD) camera (Orca ER; Hamamatsu, Welwyn Garden City, UK). All imaging data were collected at intervals of 15 s, digitised, and analysed using Kinetic Imaging (Wirral, UK) software. Cells were protected from phototoxicity and photobleeching by interposing a shutter in the light path to limit exposure between the acquisitions of successive images.

Cells were loaded for 30 min at room temperature with 5 μM Fura-2 AM (Molecular Probes, Netherlands) and 0.005 % Pluronic F-127 in a HEPES-buffered salt solution composed of 156 mM NaCl, 3 mM KCl, 2 mM $MgSO_4$, 1.25 mM $KH_2PO_4$, 2 mM $CaCl_2$, 10 mM glucose, and 10 mM HEPES, adjusted to pH 7.4. Cells were then washed and imaged in 0.5 ml of this solution at room temperature. Traces, obtained using the cooled CCD imaging system are presented as ratios of excitation at 340 and 389 nm, both with emission beyond 515 nm. Cells were imaged for several minutes before the addition of either COM (250 μg/ml) as 2 μl aliquots. All imaging data presented here were from at least 3 coverslips and 2 or 3 different cell preparations.

## *2.10 Animals and tissue sampling*

All animals were handled according to UK Home Office approved guidelines. This rat model of calcium oxalate nephrolithiasis employed ethylene glycol (EG) to induce hyperoxaluria and 1, 25-dihydroxycholecalciferol (DHC) to initiate hyper-calciuria [Okada, Y., *et al.*, 1985].

Male Sprague-Dawley rats (36 x 200 g) were maintained under constant conditions and were divided into 4 groups (control, EG, DHC and EG + DHC) of 9 animals each. Each group was then subdivided into 3 sub - groups, of 3 animals each, with the above treatments for 1, 2 and 3 weeks.

Controls animals received water, whereas in EG and EG+ DHC experimental groups 0.5 % (v / v) of EG was administered in drinking water. Fluid intake was monitored in all groups. DHC (1, 25-dihydroxycholecalciferol 50 ng / 100 g of body weight) was administered intraperitonial every other day to the EG + DHC (starting 24 h after first exposure to EG) and DHC groups. After 7, 14 and 21 days of treatment animals were anaesthetised with halothane and urine was taken directly by a needle from the bladder. The anaesthetised animals were sacrificed by cervical dislocation and the kidneys removed. The right kidney and urine sample were immediately frozen in liquid nitrogen and the left kidney was washed in saline solution at 4 °C, trimmed of adipose and connective tissue, weighed and homogenised 1 : 9 (w/v) in buffer containing 0.25 M sucrose, 5 mM HEPES, 1mM EDTA and 0.1 % (w /v) BSA pH 7.2 with protease inhibitor cocktail in a Teflon-glass Potter/Elvehjem homogeniser [Table 2.3].

The whole homogenate was centrifuged at 500 x g for 10 min at 4 °C to remove the nuclear fraction and cell debris. 1 ml of the resulted homogenate (supernatant) was kept to process for total cytosolic and mitochondrial glutathione. The remaining supernatant was then fractionated by centrifugation at 10,000 x g for 15 min to isolate the cytosolic and mitochondrial components. Mitochondria were resuspended 1:1 (12 - 15 mg protein / ml) in original homogenisation media.

**Table 2. 3 Table showing the individual components of the protease inhibitor cocktail with their concentrations and inhibitory properties.**

| Inhibitors | Concentration | Inhibitory properties |
|---|---|---|
| AEBSF | 104 mM | Serine proteases, such as trypsin and chymotrypsin |
| Aprotinin | 80 μM | Trypsin, chymotrypsin, plasmin trypsinogen, urokinase and kallikrein |
| Leupeptin | 2.1 mM | Serine and cysteine proteases, such as calpain, trypsin, appain, and cathepsin |

## *2.11 Urinary oxalate and calcium*

The oxalate concentration of urine was measured in supernatants prepared from samples centrifuged at 10,000 x g for 1 min by ion chromatography with suppressed conductivity detection on an IonPac AS4A anion chromatographic column using a Dionex high-performance pump. Urinary calcium was measured in the same sample using an ion-selective electrode. Oxalic acid and calcium chloride were used as standards.

## 2.12 Bicinchoninic acid (BCA) protein assay

The principle of the BCA assay is similar to the Lowry procedure [Lowry OH *et al.*, 1951], in that both rely on the formation of a $Cu^{2+}$-protein complex under alkaline conditions, followed by the reduction of $Cu^{2+}$ to $Cu^{+}$. The amount of reduction is proportional to the protein present. BCA forms a purple-blue complex with $Cu^{+}$ in alkaline environments, thus providing a basis to monitor the reduction of alkaline $Cu^{2+}$ by proteins.

The BCA Working Reagent was first prepared by mixing 50 parts of Reagent A (bichinconinic acid, sodium carbonate, sodium tartrate, and sodium bicarbonate in 0.1 N NaOH) with 1 part of Reagent B (4 % w/v copper (II) sulphate pentahydrate). 25 µl of sample and 175 µl of BCA Working Reagent were added in to its well of a 96-well plate. The microplate was then shaken and incubated at 37 °C for 30 min. After incubation the plate was allowed to cool at room temperature. Absorbance was the measured at 562 nm on a Wallac Victor plate reader.

## 2.13 Tissue section preparation

Longitudinal kidney sections (5 µm ) were taken using a cryostat (Bright, UK) and thaw mount onto Vectabond coated slides. The slides were then air-dried for 15 - 20 min and then baked at 56 °C for 30 min in order for the sections to be affixed well.

## 2.14 Haematoxylin and Eosin staining

Changes of renal histopathology were visualised using haematoxylin and eosin (H & E) staining. After placing the slides with sections in a rack, the tissues were re-hydrated in deionised water for 3 min. Excess water was blotted from the slide and the sections were placed in Harris haematoxylin (Lerner Laboratories, UK) for 5 min

followed by rinsing with deionised water and a 5 min wash in running tap water in order to allow the satin to develop. This was followed by dipping the slides 12 times in 1 % acid alcohol and again washing with running water for 2 min and then with deionised water for a further 2 min. Excess water was blotted and the slides were incubated in 1 % - filtered eosin (Sigma, UK) for 5 min. Sections were then washed in running tap water until the water became clear. Sections were then dehydrated through a series of ascending alcohol solutions; 3 min in 70 % (v / v) ethanol, 3 min in 95 % (v / v) ethanol, and 3 min in absolute ethanol. Finally, the slides were cleared by incubation in histoclear for 2 min. Sections were left to air - dry thoroughly followed by mounting with Permount (Fisher, UK). The location of the birefringent crystals was examined under plain and polarised light microscopy.

## 2.15 Preparation of mitochondrial and cytoplasmic fractions for glutathione assay

Whole homogenates of fresh kidney were prepared, as described in section 2.10, and immediately processed for mitochondrial and cytoplasmic total glutathione (GSH + GSSG) measurements. 1 ml of whole homogenate was incubated with 20 µl of digitonin (10 mg/ml) for 20 s with vortexing, and was then centrifuged at 14,000 x g for 20 s. To the resultant cytosolic fraction (supernatant) 50 µl of 5 % (v / v) metaphosphoric acid (MPA) was added. The unsuspended pellet was then washed with 200 µl MOPS buffer pH 7.4 [Table 2.4], followed by 5 s centrifugation at 14, 000 x g. The supernatant was discarded and the resultant pellet was finally resuspended in 250 µl of MOPS buffer. Cytosolic and mitochondrial fractions were then processed for total glutathione measurements.

**Table 2. 4 MOPS buffer at pH 7.4.**

| Reagents | Concentration |
|---|---|
| EDTA | 19.8 mM |
| Mannitol | 250 mM |
| MOPS | 19.8 mM |
| EGTA | 19.8 mM |

## *2.16 Total Glutathione assay*

This GSH assay is a carefully optimised enzymatic recycling method using glutathione reductase for the quantification of GSH [Figure 2.6] [Tietze, F., 1969; Eyer, P., & Podhrasky, D., 1986; Baker, MA., *et al.,* 1990]. The sulfhydryl group of GSH reacts with DTNB (5,5'-dithiobis-2-nitrobenzoic acid, Ellman's reagent) and produces a yellow coloured 5-thiol-2-nitrobenzoic acid (TNB). The mixed disulfide, GSTNB (between GSH and TNB), that is concomitantly produced is reduced by glutathione reductase to recycle the GSH and produce more TNB. The rate of TNB production is directly proportional to this recycling reaction, which is in turn directly proportional to the concentration of GSH in the sample. Measurement of the absorbance of TNB at 414 nm provides an accurate estimation in the sample.

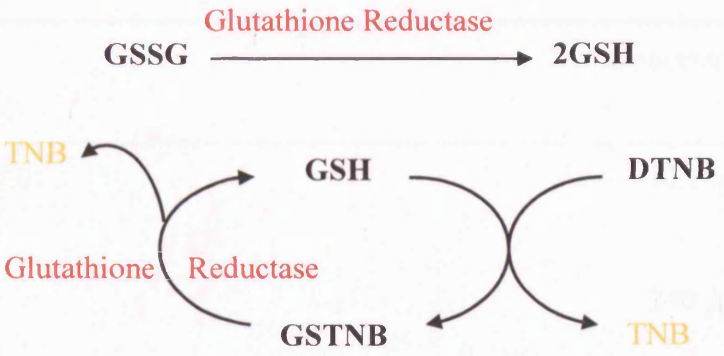


**Figure 2. 6 GSH Recycling.**

GSH is oxidised to the disulfide dimer GSSG. GSSG is produced during the reduction of hydroperoxides by glutathione peroxidase. GSSG is reduced to GSH by glutathione reductase and it is the reduced form that exists mainly in biological systems. Because of the use of glutathione reductase in this assay, both GSH and GSSG are measured and the assay reflects total glutathione.

Total glutathione was measured based on the above described principle. 20 µl of homogenate, cytosolic and mitochondrial fractions (were prepared as described in section 2.10) were added to 180 µl of glutathione assay solution [Table 2.5]. The rate of 5, 5'-dithiobis-(2-nitrobenzoic acid) DNTB reduction was measured over 5 min at 412 nm in a Wallac Victor reader plate. The rate of reaction using standards of oxidised glutathione in 0.5 % MPA was used to calculate total glutathione (reduced + oxidised) expressed as µmoles per mg of tissue.

**Table 2. 5 Glutathione assay solution.**

| Reagents | Concentration |
|---|---|
| $KPO_4$ pH 7.0 | 0.1 M |
| NADPH | 240 μM |
| DNTB | 76 μM |
| Glutathione Reductase | 1.0 mU/ml |

## *2.17 Antioxidant enzyme activities in the kidney fractionates*

The activity of antioxidant enzymes was monitored in the kidney by measuring the glutathione peroxidase, glutathione reductase and glucose-6-phosphate dehydrogenase (G6PDH). Glutathione peroxidase assay (GPx) catalyses the reduction of hydroperoxides, including hydrogen peroxides, by reduced glutathione and functions to protect the cell from oxidative damage. This assay measures GPx activity indirectly by a coupled reaction with glutathione reductase (GR). Oxidised glutathione (GSSG), produced upon reduction of an organic hydroperoxide by GPx, and is recycled to its reduced state by GR and NADPH. The oxidation of NADPH to NAD+ is accompanied by a decrease in absorbance at 340 nM. The rate of decrease in the A340 is directly proportional to the GPx activity in the sample [Paglia, DE., & Valentine, WN., 1967].

To measure glutathione peroxidase, 10 µl of the mitochondrial fraction were added to 1.25 ml of glutathione peroxidase assay solution [Table 2.6], followed by 5 min incubation at 25 °C. After incubation, 10 mM cumene-hydroperoxide was added and the change in absorbance at 340 nm was monitored.

**Table 2. 6 Glutathione Peroxidase assay solution.**

| Reagents | Concentration |
|---|---|
| $KPO_4$ pH 7.0 | 0.1 M |
| EDTA | 100 mM |
| KCN | 100 mM |
| NADPH | 2 mg/ml |
| GR | 5 µl |
| Cumene-peroxide | 10 mM |

In addition, glutathione reductase activity was monitored in the kidney mitochondrial fraction. Glutathione reductase is a flavoprotein that catalyses the NADPH-dependent reduction of oxidised glutathione (GSSG) to glutathione (GSH) [Carlberg, I., & Mannervik, B., 1985]. This enzyme is essential for the GSH redox cycle, which maintains adequate levels of reduced cellular GSH. A high GSH/GSSG ratio is essential for protection against oxidative stress. This assay measures GR activity by

measuring the rate of NADPH oxidation. To measure the oxidation of NADPH to $NAD^+$, 5 µl of mitochondrial fraction was added to 1.25 ml of glutathione reductase assay solution [Table 2.7]. Since GR is present at rate limiting concentrations, the rate of decrease in the Absorbance 340 is directly proportional to the GR activity in the sample.

**Table 2. 7 Glutathione Reductase assay solution.**

| Reagents | Concentration |
|---|---|
| Tris/HCl pH 8 | 1 M |
| EDTA | 100 mM |
| FAD | 1 mM |
| GSSG | 30 mM |
| NADPH | 2 mg/ml |

Finally, glucose 6 phosphate dehydrogenase (G6PDH) activity was determined by measuring the rate of $NADP^+$ reduction to NADPH in the presence of glucose 6 phosphate. 50 µl of kidney cytosolic fraction was added to 1.25 ml of G6PDH assay solution [Table 2.8]. In all of the above assays the change in absorbance at 340 nm was continuously monitored in a Cary 1 double beam spectrophotometer.

**Table 2. 8 G6PDH assay solution.**

| Reagents | Concentration |
|---|---|
| Glycyl-Glycyl/MgCl | 0.25 M |
| $NADP^+$ | 2 mg/ml |
| Glucose-6-phosphate | 50 mM |

## 2.18 Mitochondria oxygen consumption rates

Much of our knowledge of electron transport in mitochondria and chloroplasts comes from oxygen electrode recordings. The oxygen concentration in a sealed incubation chamber is continuously monitored, and the effects of making various additions to the chamber can be observed. A cross section through a typical apparatus is shown below [Figure 2.7]:

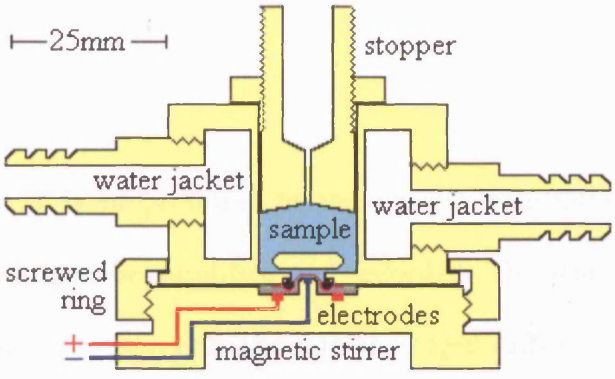


**Figure 2. 7 Schematic diagram of a Clark electron device.** The upper section containing a transparent, thermostated sample chamber is secured to the lower electrode assembly with a screwed ring. A thin Teflon membrane is trapped between the two sections and separates the isotonic incubation medium from the strong KCl electrolyte in the electrode compartment. The adjustable stopper is used to seal the incubation chamber and prevent room air dissolving during the experiments. The small hole in the centre of the stopper permits the expulsion of air bubbles and allows small volumes of reagents to be added with a microlitre syringe. The contents of the chamber are stirred continuously with a magnetic flea. Image adapted from http://www.bmb.leeds.ac.uk/illingworth/oxphos/oxygraph.htm

A small polarising voltage (ca. 0.6 volt) is applied between the silver anode (+) and the platinum cathode (-). Oxygen diffuses through the Teflon membrane and is reduced to water at the platinum cathode:

$O_2 + 4H^+ + 4e^{-1} = 2H_2O$

The circuit is completed at the silver anode, which is slowly corroded by the KCl electrolyte:

$$Ag + Cl^{-} = Ag\,Cl + e^{-1}$$

The resulting current is proportional to the oxygen concentration in the sample chamber. This signal can be amplified and recorded. The whole process is totally dependent on the supply of oxygen. The rate of oxygen diffusion to the cathode (and hence the current) depends on the oxygen concentration in the main incubation chamber. It also depends on several other factors: temperature, membrane thickness and permeability, sample viscosity and stirring speed. In contrast to pH electrodes which measure an equilibrium position, oxygen electrodes measure the velocity of a physico-chemical process that is far from equilibrium. pH electrodes have an intrinsic thermodynamic response which is relatively insensitive to temperature and sample composition, but there is no intrinsic calibration to an oxygen electrode - at regular intervals, or if the instrument is dis-assembled, it must be re-calibrated against a known standard, usually air. It is particularly important to control the temperature.

If mitochondria are incubated in an oxygen electrode in an isotonic medium containing substrate and phosphate, then addition of ADP causes a sudden burst of oxygen uptake as the ADP is converted into ATP [Figure 2.8]:

The actively respiring state is sometimes referred to as "state 3" respiration, while the slower rate after all the ADP has been phosphorylated to form ATP is referred to as "state 4".

State 4 respiration is usually faster than the original rate before the first addition of ADP because some ATP is broken down by ATPase activities contaminating the

preparation, and the resulting ADP is then re-phosphorylated by the intact mitochondria.

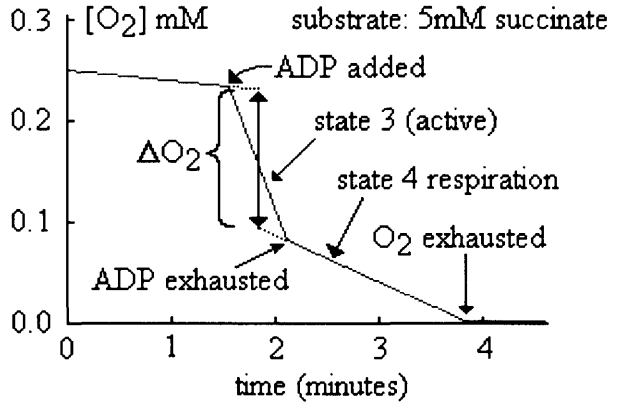


**Figure 2. 8 Representative graph of Oxygen Electron recordings as adapted from http://www.bmb.leeds.ac.uk/illingworth/oxphos/oxygraph.htm.**

The ratio [state 3 rate] : [state 4 rate] is called the respiratory control index and indicates the tightness of the coupling between respiration and phosphorylation. With isolated mitochondria the coupling is not perfect, probably as a result of mechanical damage during the isolation procedure.

It is possible to calculate a P:O ratio (the relationship between ATP synthesis and oxygen consumption) by measuring the decrease in oxygen concentration during the rapid burst of state 3 respiration after adding a known amount of ADP. It is necessary to subtract the basal respiration due to imperfect coupling and the recycling of ATP, as shown in the graph above. The change in concentration must then be multiplied by the chamber volume, so that the answer (in micro-*atoms* of oxygen) can be related to the quantity of ADP added. The quantity of oxygen in the chamber is calculated from published oxygen solubility data at the appropriate temperature.

Oxygen consumption in freshly isolated mitochondria (1-1.5mg protein/ml) in 1.5ml of respiration buffer [Table 2.2] was assayed using a Clark electrode device (Rank Brothers, UK). Malate plus pyruvate at 5 and 2mM respectively (complex I), or succinate at 5mM (complex II) were used as reducing substrates and ADP (100μM) were used to measure state 3 and state 4 respiration.

## 2.19 Statistics

All values shown are means ± standard deviation (SD). Student's t-test was used to determine whether there was a significant difference between two groups ($p < 0.05$). When multiple means were compared, significance ($p < 0.05$) was determined by one-way ANOVA followed by t-test and p values corrected for multiple comparisons using the method of Bonferroni.

# CHAPTER 3

## Method development and optimisation for monitoring $O_2^{\bullet-}$ production in calcium oxalate monohydrate (COM) and sodium oxalate (NaOx) treated MDCK cells

## 3.1 INTRODUCTION

The interaction between crystals and urothelial cell membrane is considered an essential and critical event in the development of the renal calculi [Weissner, JH., *et al.,* 2001]. The use of renal epithelial cells in tissue culture is widely accepted as a powerful tool in physiological and cell biological studies. In recent years, it has been established that renal tubular cells can provide insight into the conditions under which stones can develop. Since it is difficult to study these mechanisms *in vivo*, cultured renal tubular cells have become increasingly popular for the study of physiological and cell biological processes that are linked to stone disease. It has been known that CaOx crystals and free oxalate are injurious to renal epithelial cells and can induce lipid peroxidation [Huang, HS., *et al.,* 2003]. However, in order to understand the mechanisms involved in crystal retention within the kidneys, it is necessary to identify the initial site and causes of crystal deposition within the kidneys. So far many investigators have used a number of renal epithelial cells to identify the initial site and the detailed mechanism involved in crystal deposition within the tubules. The most widely used cell type to conduct these experiments is Madin Darby Canine Kidney (MDCK) cells.

To identify mechanisms by which crystal deposition and its subsequent pathology, can contribute to the reported cellular transformation during the development of renal calculi, it was necessary to develop a method that would answer the questions arising from the current work.

## 3.2 The effect of digitonin on lucigenin-derived chemiluminescence

It has been previously shown [Li, Y., *et al.*, 1999] that superoxide formation can be measured directly by employing the lucigenin-derived chemiluminescence technique. Specifically, Li Y *et al.*, 1999 suggested that intact MDCK cells can take up lucigenin and therefore give rise to a chemiluminescence (CL) signal. On the contrary, a more recent study has shown [Khand, FD., *et al.*, 2002] that intact MDCK cells either in the presence or absence of COM were unable to take up lucigenin. However, the same authors demonstrated that when the cells were permeabilised with digitonin, lucigenin uptake was facilitated and superoxide production was observed.

To investigate the effect of digitonin on lucigenin – derived chemiluminescence (LDCL), MDCK cells were incubated with 20 μM lucigenin for 20 min at 37 °C in order to allow time for lucigenin to enter the intracellular compartments. Media was then removed and respiration buffer was added to the lucigenin pre-incubated cells. A lack of detectable CL signal was observed, implying either the inability of MDCK cells to uptake this specific chemiluminescence probe or the requirement of prolonged incubation.

To investigate the latter, a time course of lucigenin treatment was performed. MDCK cells incubated with lucigenin, in the same manner as described above, for 20, 30, 40, and 60 min (data not shown). Once again the absence of CL signal further supported the initial findings. Thus, having confirmed that in MDCK cells lucigenin is incapable of penetrating the intracellular compartments, further experiments were performed to investigate the means of lucigenin uptake.

Digitonin is a solubilisation agent that interacts with membrane cholesterol causing permeabilisation by creating pores and allowing the release of diffusible molecules outside the cell. Therefore digitonin was employed to permeabilise MDCK cells. When 100 μg/ml of digitonin was added in COM treated MDCK cells, supplemented with respiration buffer, a clear lucigenin CL signal was detected [Figure 3.1], which lasted for approximately 10 min, after which time lucigenin CL signal was decreased. Hence, the non-ionic detergent digitonin was able to permeabilise the cells, and therefore facilitate lucigenin entry into the cells. In contrast to this observation, when MDCK cells were treated with COM and in the absence of digitonin, the CL signal was monitored at basal levels.

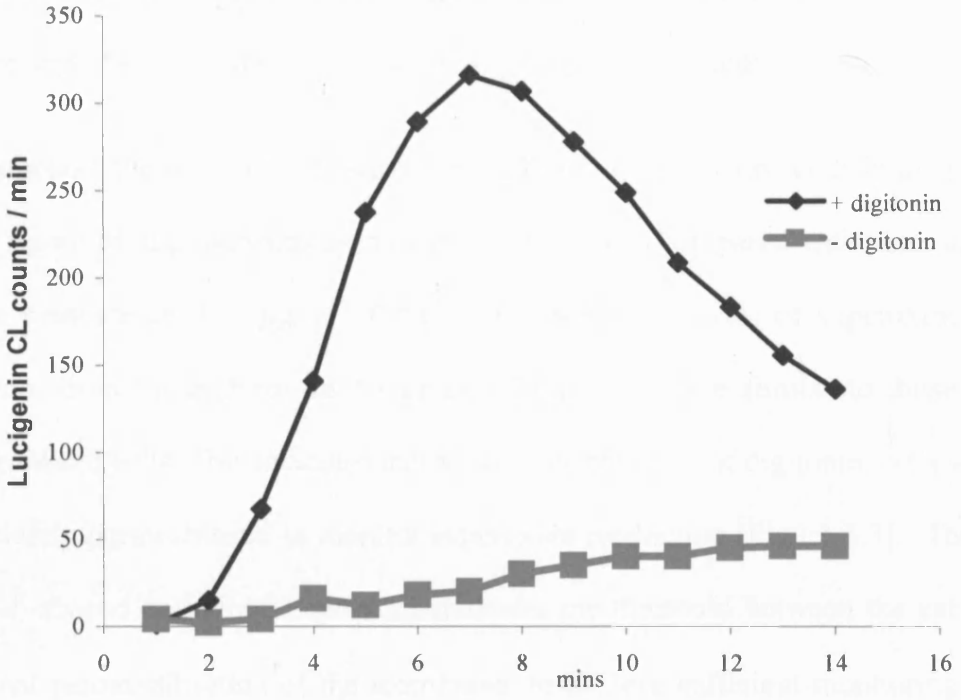


**Figure 3. 1 Lucigenin CL mediated by digitonin.** Lucigenin-enhanced chemiluminescence counts of COM treated cells in the presence (+) and absence (-) of 100 μg/ml digitonin.

Having shown the permeabilisation of cells by using 100 μg/ml of digitonin, further experiments were performed to investigate how different concentrations of digitonin might influence the lucigenin CL signal. As illustrated in Figure 3.2, when COM treated cells were permeabilised by using lower concentrations of digitonin, a greater lucigenin CL signal was observed than that seen at 100 μg/ml digitonin. A peak at 40 μg/ml of digitonin was observed. This suggests that concentrations of digitonin higher than that of 40 μg/ml may cause changes in the membrane potential across the inner mitochondrial membrane, and therefore reducing the total proton motive force that determines the rate of electron leakage to $O_2^{\bullet-}$. This in turn results in the observed

decrease of the chemiluminescence signal. In addition, it was observed that the lower the concentration used the later the peak of CL signal appeared.

Nevertheless, the lucigenin CL signal derived from COM treated cells in the presence of 10 μg/ml of digitonin was significantly lower when compared with untreated cells in the presence of 100 μg/ml of digitonin. Moreover, levels of superoxide counts resulting from the addition of 10 μg/ml of digitonin were similar to those of non permeablised cells. This indicates that at this concentration of digitonin, cells were not sufficiently permeabilised to monitor superoxide production [Figure 3.3]. Therefore, the bell-shaped pattern of Figure 3.3 indicates the threshold between the excess and minimal permeabilisation of the membrane, to achieve sufficient monitoring of $O_2^{\bullet-}$ production.

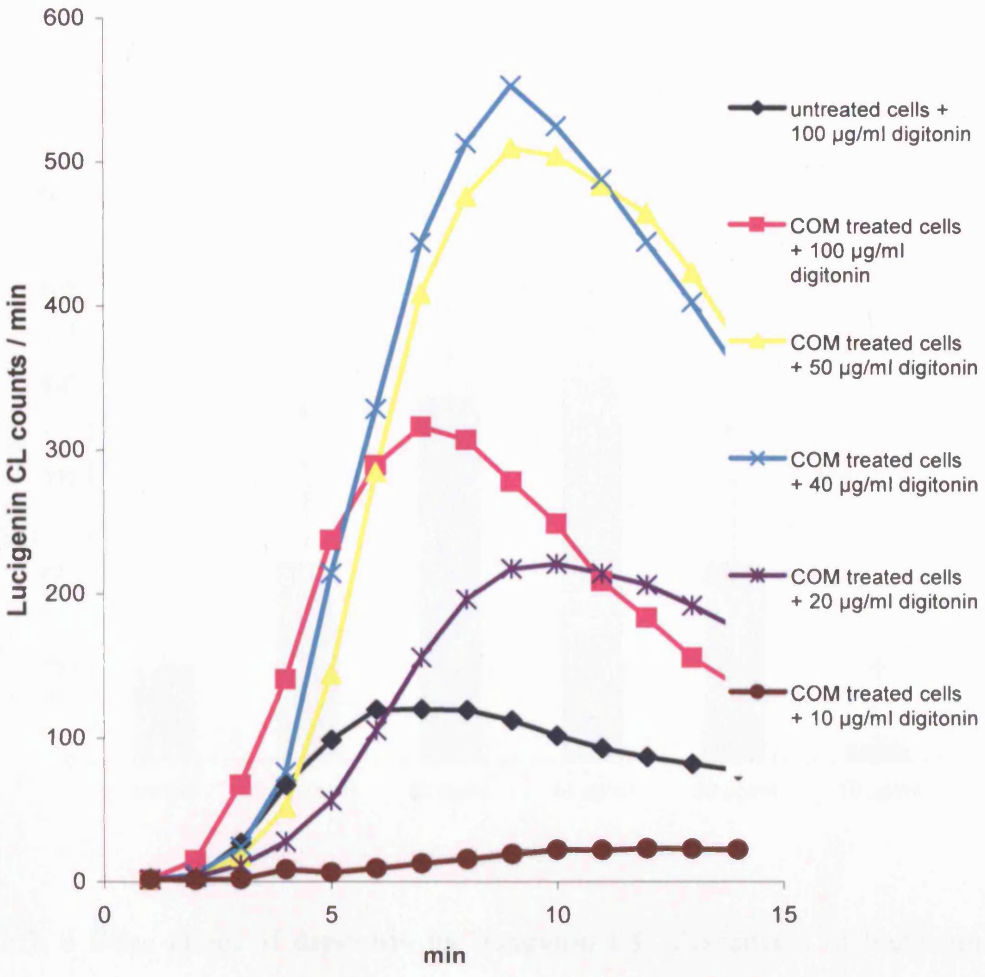


**Figure 3. 2 Effect of digitonin concentration on COM mediated lucigenin CL signal.** MDCK cells were treated with 250 µg/ml COM for 4 h. Lucigenin-enhanced chemiluminescence counts were taken in the presence of different concentration of digitonin (100 – 10 µg/ml) in the respiration buffer. Values are compared with untreated cells in the presence of 100 µg/ml digitonin (control).

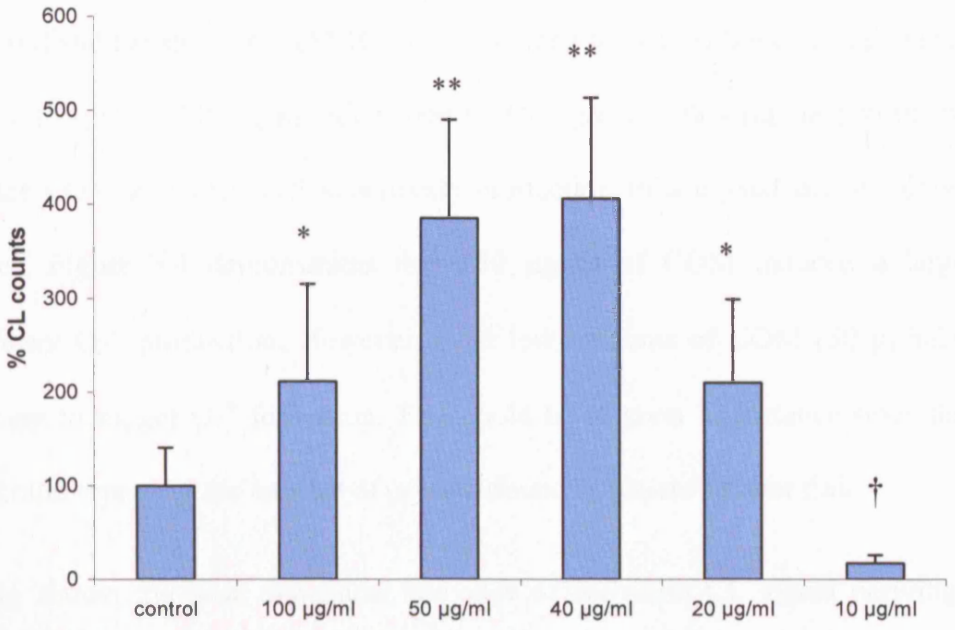


**Figure 3. 3 Dose effect of digitonin on lucigenin CL.** Percentage of lucigenin CL counts monitored by using different concentrations (100 – 10 µg/ml) of digitonin on COM treated cells. Control is untreated cells in the presence of 100 µg/ml of digitonin. Data are mean ± SD for n=20; ** $p < 0.01$ * $p < 0.05$ and † $p < 0.01$ vs control.

## 3.3 Dose-dependent effect of COM on MDCK cells

Having optimised the conditions by which lucigenin chemiluminescence signal is observed and therefore able to measure superoxide production, it is of critical importance to identify the dose dependent effect of COM on MDCK cells.

Cells of distal tubular origin (MDCK) were treated for 4 h with increasing amounts of COM (50 μg/ml - 250 μg/ml equivalent to 5.7 μg/cm$^2$ - 28.4 μg/cm$^2$) to investigate whether COM activated cell superoxide production in a crystal density dependent manner. Figure 3.4 demonstrates that 250 μg/ml of COM induced a large and significant $O_2^{\bullet-}$ production. However, even low amounts of COM (50 μg/ml) were sufficient to trigger $O_2^{\bullet-}$ formation. This could be of great importance since this low level could represent the amount of crystals found in patient tubular fluid.

Having shown the dose dependent response of lucigenin CL signal deriving from various concentration of COM, it was important to investigate the effects of COM treatment time, to elucidate the time of exposure sufficient to cause $O_2^{\bullet-}$ formation. Therefore experiments were performed where cells were incubated for 10 min and 4 h with COM. In addition, experiments were included where COM was added just after cells were permeabilised. The data in Figure 3.5, shows a 3 - fold increase in $O_2^{\bullet-}$ after 4 h COM treatment, whereas no rise in lucigenin chemiluminescence signal was shown when cells were only incubated for a short period of time (10 min). This may be due to the fact that prior to chemiluminescence assay, cells were washed with PBS and thus non - attached COM was removed. However, when COM was added to digitonin permeabilised cells (no incubation) high levels of $O_2^{\bullet-}$ were observed. This finding indicates that the presence of crystals is essential for the $O_2^{\bullet-}$ formation and 10 min is not adequate to achieve COM binding to cells.

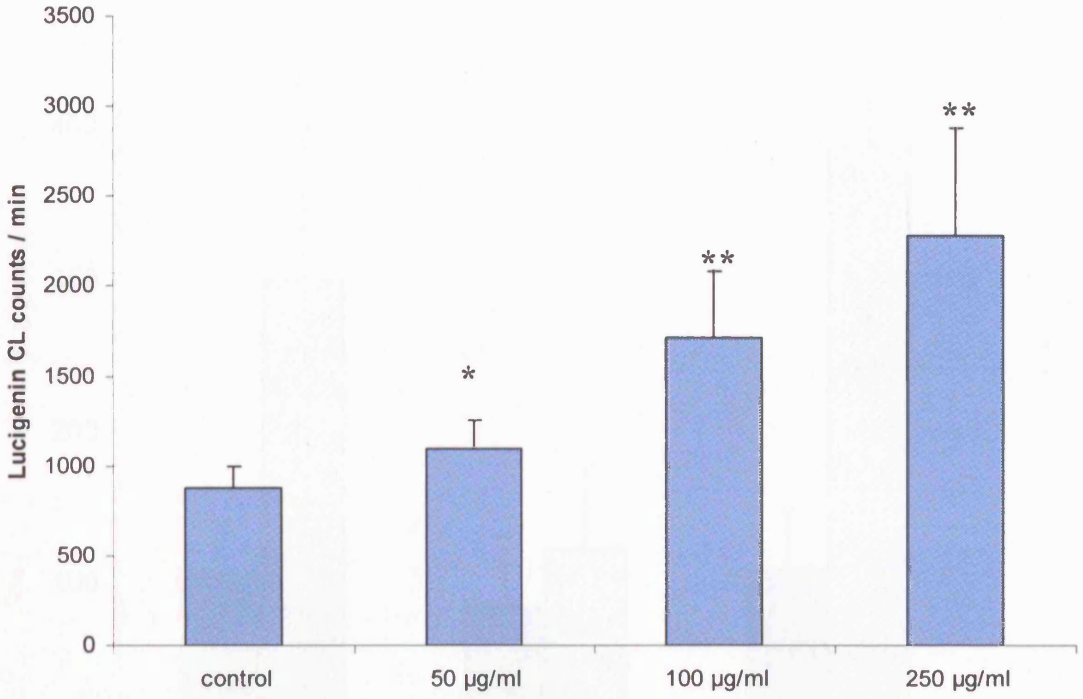


**Figure 3. 4 Effect of different COM concentration on lucigenin CL.** MDCK cells treated with 50 µg/ml - 250 µg/ml of COM and incubated for 4 h. Lucigenin-enhanced chemiluminescence counts were monitored per minute. Data are mean ± SD for n=20; * $p < 0.05$ and ** $p < 0.01$ vs untreated MDCK cells (control).

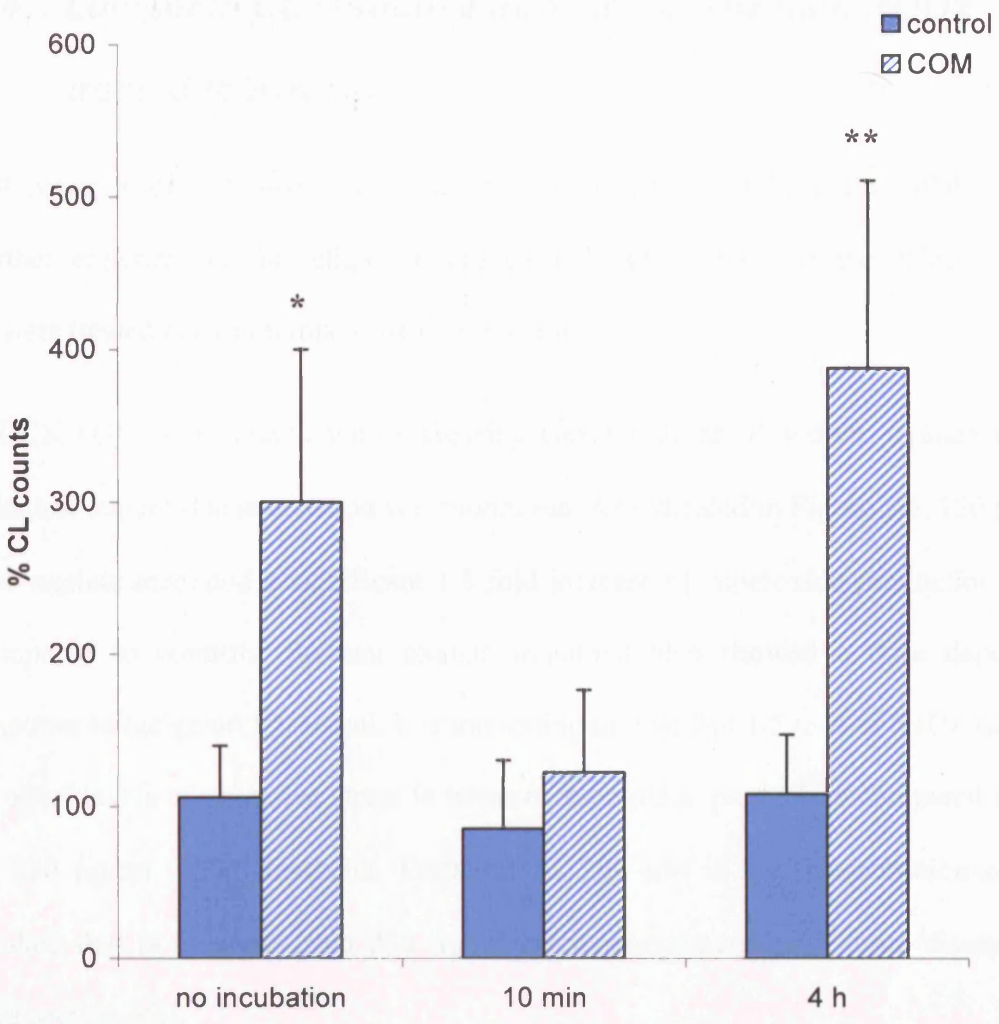


**Figure 3. 5 Effect of COM incubation times on lucigenin CL.** Percentage of lucigenin chemiluminescence counts when MDCK cells were treated with 250 μg/ml COM without incubation (zero time), 10 min and 4 h incubation. Lucigenin-enhanced chemiluminescence counts were monitored per minute. Data are mean ± SD for n=20; * $p < 0.05$, and ** $p < 0.01$ vs control.

## 3.4 Lucigenin CL response from sodium oxalate (NaOx) treated MDCK cells

Following studies of superoxide production derived from COM treated MDCK cells, further experimental investigation was carried out to examine the effect of free oxalate treated cells in terms of oxidative stress.

MDCK cells were treated with increasing concentrations of sodium oxalate for 15 min, and superoxide production was monitored. As indicated in Figure 3.6, 750 μM of free oxalate mediated a significant 1.5 fold increase of superoxide production when compared to controls. Sodium oxalate treatment also showed a dose dependent response in lucigenin CL signal. It is interesting to note that 1.5 mM of NaOx resulted in equal levels of oxidative stress in terms of superoxide production compared to that of 250 μg/ml COM treatment. Furthermore, 750 μM is the concentration of free oxalate that is released from 250 μg/ml calcium oxalate monohydrate dissociation (see section 4.4).

Additional, experiments were performed to examine whether time of NaOx incubation had any significant effect on the lucigenin chemiluminescence signal. As shown in Figure 3.7, incubation of MDCK cells with 750 μM NaOx for 15 min caused the cells to respond similarly in terms of superoxide production compared with those treated for 4 h. This absence of difference with treatment time was expected, since NaOx represents the free form of oxalate that is transported into the cells. Thus, there is no requirement for crystal-cell interactions to occur as in the case with COM treatment.

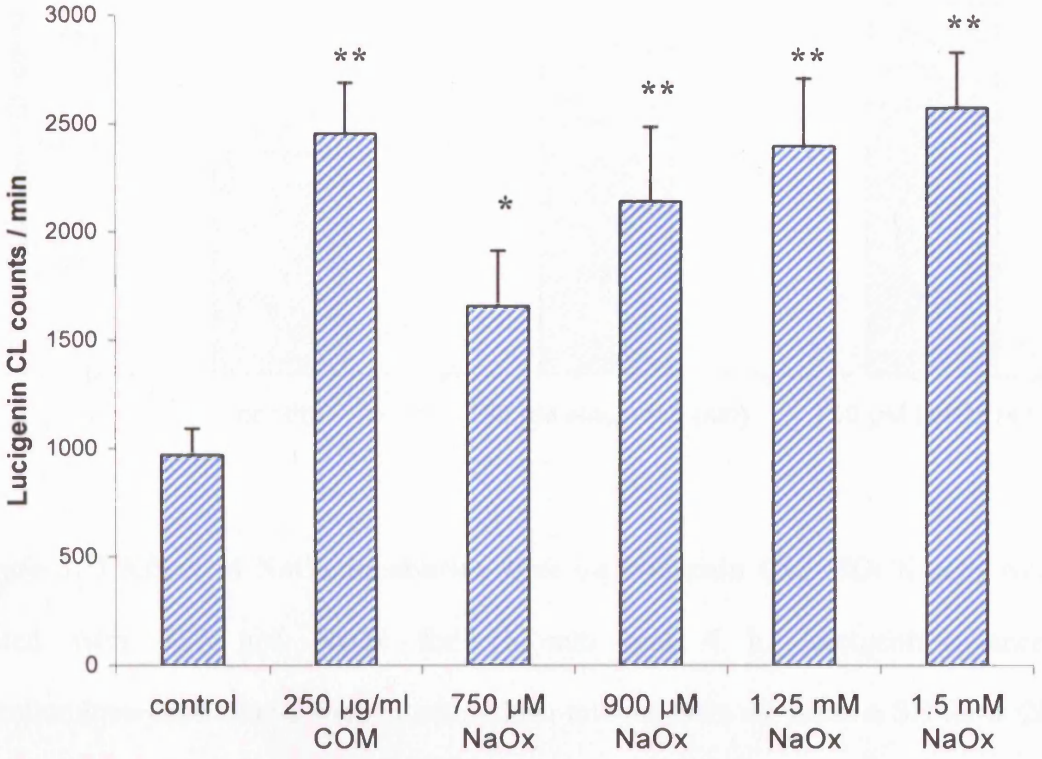


**Figure 3. 6 Dose-dependent effect of NaOx on lucigenin CL.** MDCK cells were treated with 250 µg/ml COM for 4 h. MDCK cells were also treated with increasing amounts (750 µM – 1.5 mM) of NaOx for 15 min. Lucigenin-enhanced chemiluminescence counts were monitored per minute. Data are mean ± SD for n=20; ** $p < 0.01$ and * $p < 0.05$ vs control.

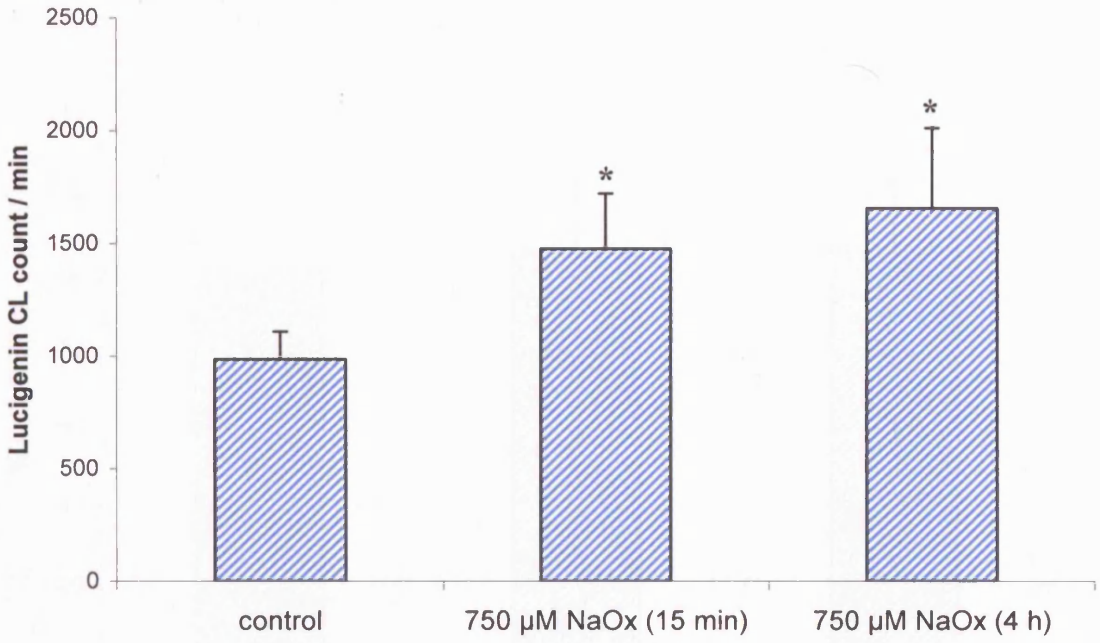


**Figure 3. 7 Effect of NaOx incubation time on lucigenin CL.** MDCK cells were treated with 750 µM NaOx for 15 min and 4 h. Lucigenin-enhanced chemiluminescence counts were monitored per minute. Data are mean ± SD for n=20; * $p < 0.05$ vs control.

## 3.5 Cytotoxicity of COM or NaOx in MDCK cells

The optimal concentration and the incubation times of COM or NaOx treatment for cells to initiate a significant superoxide production monitored by lucigenin chemiluminescence have been optimised. The next question to be addressed, in order to further investigate this phenomenon was to examine the cytotoxic effects of the proposed doses and treatment time of COM and NaOx.

The MTT assays, a functional and survival method were carried out on cells receiving 1.5 mM NaOx or 250 µg/ml COM treatment for 24 h. As shown in Figure 3.8, no significant change was observed.

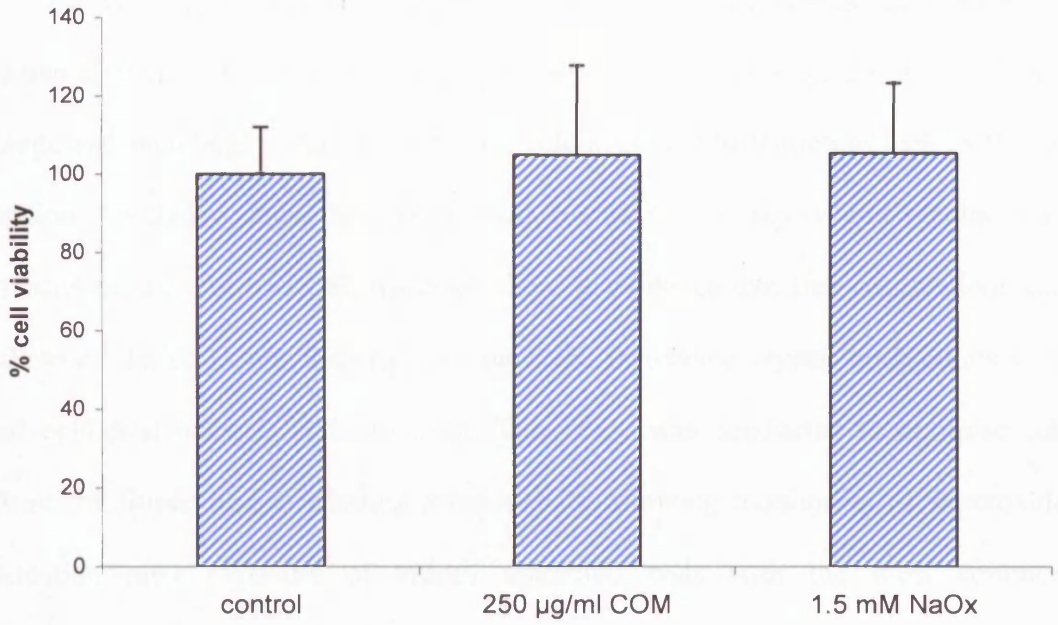


**Figure 3. 8 Cell toxicity after COM and NaOx treatment.** MDCK cells were treated with 250 µg/ml COM or 1.5 mM NaOx for 24 h and MTT assay was performed. Values presented as a percentage of cell viability. Data are Mean ± SD for n=5.

Therefore, no cell death occurred when cells were treated with the aforementioned doses and treatment times. This outcome indicates that in the cell – crystal model the superoxide production monitored is a result of the crystal-cell interaction effect of COM or the effect of free oxalate, and not due to overall cell cytotoxicity.

## 3.6 DISCUSSION

It is now well established that cell injury is central to the process of urolithiasis [Wiessner, JH., *et al.,* 2001]. An injury to the epithelial cells results in membrane damage and shedding, which play a critical role in crystal formation as well as crystal retention. Oxidative stress is a recognised source of cell injury and results from increased production of ROS. Although there is evidence that free oxalate ions can mediate oxidative insult, the origin of the ROS in oxalate crystal interactions with renal epithelial cells, is still unknown. This study was conducted to optimise cell culture conditions and to develop a method for allowing monitoring of superoxide production after exposure of kidney epithelial cells with the most common constituents of kidney stones.

It is now established that exposure of renal epithelial cells to COM crystals results in a free radical mediated oxidative stress [Muthukumar, A., & Selvam, R., 1998; Muthukumar, A., & Selvam, R., 1997]. Muthukumar and Selvam have reported oxalate–mediated oxidative stress by showing that during the development of calcium oxalate stones in ethyl glycol fed rats, GSH was depleted leading to mitochondrial dysfunction with observed lipid peroxidation and oxidation of protein thiols. In order to monitor oxidative stress, in this study the lucigenin-derived chemiluminescence method was employed. Lucigenin is a well validated chemiluminegenic probe for detecting superoxide formation [Li, Y., *et al.,* 1998; Rembish, AJ., & Trush, M., 1994; Faulkner, K., & Fridovich, I.,; 1993]. This was based on the observation that in several in vitro enzymatic systems such as xanthine oxidase or glucose oxidase that produce little $O_2^{\bullet-}$, lucigenin may itself act as a source of $O_2^{\bullet-}$ via autoxidation of the lucigenin cation radical. The lucigenin cation radical produced by these systems can

reduce $O_2$ to $O_2^{\bullet-}$ and therefore give artifictual positive results. However, other studies by Li, Y., *et al.,* [1999] have shown that lucigenin participates in redox–cycling is dependent on the concentrations of lucigenin used. To investigate this, the authors measured KCN-resistant $O_2$ consumption rates for increasing amounts of lucigenin (5 μM-100 μM) and the results were compared with 5 μM benzo(α)pyrene-1,6-quinone (BPQ), as a positive control. BPQ is a chemical known to undergo redox cycling in the mitochondria and the authors have shown that using 5μM BPQ, there was a dramatic increase in KCN-resistant $O_2$ consumption rates. This observation was compared with 50 μM – 100 μM lucigenin which showed a similar response in the KCN-resistant $O_2$ consumption rates. However, at a concentration of 20 μM and lower the levels of $O_2$ consumption rates were non-detectable, indicating that at these concentrations, lucigenin does not undergo redox cycling. The same authors have also suggested that lucigenin redox cycling also depends on the charge of lucigenin and the intermediates. Because of the opposite charges of the lucigenin cation radical and $O_2^{\bullet-}$ and the unstable dioxetane intermediate produced from the reaction of lucigenin cation radical with $O_2^{\bullet-}$ , both the molecular binding affinity and the rate constant of the reaction between the lucigenin cation radical and $O_2^{\bullet-}$ may be much higher than those between the lucigenin cation radical and $O_2$. This may explain the inability of luginenin below certain concentrations to undergo redox cycling in the $O_2^{\bullet-}$ generating systems.

Furthermore, in this work it was shown that when intact treated or untreated MDCK cells were incubated with 20 μM lucigenin, a chemiluminescence signal was not detected. This indicates the inability of lucigenin to penetrate into the intracellular compartments. This contrasts with the findings of Li, Y., *et al.,* [Li, Y., *et al.,* 1998], who observed uptake of lucigenin by intact cell lines. To further support the finding

that intact cells do not uptake luginenin, MDCK cells were incubated with 20 μM lucigenin for several time points. Even after 1 h incubation a chemiluminescence signal was absent. However, when MDCK cells were permeabilised with 100 μg/ml of digitonin a clear lucigenin - derived chemiluminescence signal was detected. Digitonin is a detergent which replaces cholesterol in the membrane and creates pores. In order to determine the optimum digitonin concentration and to avoid perturbations of mitochondrial membrane, different concentrations of digitonin were used and superoxide was monitored. When increasing amounts of digitonin were tested it was shown that digitonin at concentrations of 40 - 50 μg/ml, resulted in the highest recorded levels of superoxide production, whereas below this, 10 μg/ml of digitonin did not induce a chemiluminescence signal. This indicates that cell permeabilisation by digitonin at concentrations of 40 - 50 μg/ml did not seem to disturb the mitochondrial membrane potential, therefore increased levels of superoxide were observed. In contrast, 100 μg/ml of digitonin has resulted in lower but significant levels of superoxide formation, which indicates disturbance in the balance between cell permeability and damage of the inner mitochondrial membrane. However, it has been reported that by measuring $O_2$ consumption in a Clark oxygen electrode, digitonin at a concentration of 100 μg/ml did not cause mitochondrial uncoupling [Khand, FD., *et al.*, 2002]. In addition other studies have also reported the use of digitonin to study pathological processes that influence mitochondrial functions. Specifically, Floryk, D., & Houstek, J., [1999] have described a method suitable for sensitive measurement of mitochondrial membrane potential in different types of cultured cells by using digitonin [Floryk, D., & Houstek, J., 1999]. The same authors have also reported that digitonin influence on mitochondrial enzymatic

activities at concentrations lower than 100 μg/ml did not significantly disturb the mitochondrial membrane potential.

Even though, 40 - 50 μg/ml digitonin appeared to be the optimal digitonin concentration, experiments performed prior to this study were carried out at using 100 μg/ml of digitonin. This however, did not interfere with the interpretation of the results. Therefore, due to time limitation to repeat most of the earlier experiments and in order to keep consistency between the results obtained from this thesis, 100 μg/ml of digitonin was used throughout the whole study.

Furthermore, when MDCK cells were treated with 50 - 250 μg/ml COM, cell superoxide production was activated in a dose dependent manner. Even at a low COM concentration of 50 μg/ml superoxide levels were significantly increased compared to untreated cells. This could be of clinical importance, since 50 μg/ml COM is more likely to represent the amount of COM crystals found in stone patients tubular fluid than that of 250 μg/ml COM. In addition, other reports from this laboratory have shown that even concentrations as low as 25 μg/ml resulted in a significant increase of superoxide formation [Khand, FD., *et al.*, 2002]. For this activation to occur in this model, MDCK cells had to be treated with COM crystals for up to 4 h, a time period at which COM crystal adherence to the cells is fully achieved. Prior to superoxide measurements, MDCK cells were washed with PBS and non - attached crystals were removed. When COM crystals were added to MDCK cells just 10 min prior to superoxide assay, no chemiluminescence signal was detected, since un-attached COM crystals were removed by washing before the superoxide assay. However, increased superoxide levels were observed when COM crystals were added without subsequent washing and immediately prior to digitonin permeabilisation. This indicates that the

physical presence of COM crystals is an absolute requirement to initiate oxidative stress and for this manifestation to occur.

In addition, different concentrations of sodium oxalate were used to investigate whether free oxalate elicited the same response. MDCK cells were treated with 1.5 mM - 750 μM NaOx and also showed a dose dependent response with respect to superoxide formation. NaOx concentration of 750 μM, represents the free oxalate released from COM dissociation as reported in the oxalate dissociation studies (Chapter 4). In contrast to 4 hr COM treatment, NaOx incubation time was independent with respect to lucigenin chemiluminescence. Even when NaOx was added 10 min to MDCK cells prior to the superoxide assay, the resulting superoxide formation was at similar levels with those observed with 4 h NaOx treatment. This finding was predicted as NaOx is the free form of oxalate and there is no requirement for crystal-cell interaction to occur. In addition oxalate is known to be rapidly transported into renal epithelial cells [Cao, LC., *et al.*, 2004].

Furthermore, to assess the cytotoxicity of COM and NaOx treatments at concentrations of 250 μg/ml and 1.5 mM respectively, an MTT assay was performed. MDCK cells were treated at the above concentration for up to 24 h and it was observed that there was no difference in the viability of cells when compared to untreated MDCK cells. This validates the use of this model system since it indicates that superoxide production did not arise as a result of cell death and apoptosis at these treatment times and concentration. In addition, since the MTT assay is a functional mitochondrial assay, the indications are that at the above concentration of COM and NaOx used no uncoupling of the mitochondria occurs and the intra-mitochondrial redox remains much as it is in control cells. Furthermore, SEM data also showed (see

Chapter 5) that cells survive and divide in culture despite the presence of internalised COM crystal, thus providing evidence that the crystals are not toxic for these renal cells. Similar results were also observed in previous studies [Verkoelen, CF., *et al.*, 1996] where they showed that 32 $\mu g/cm^2$ of COM treated MDCK cells, did not result in increased levels of brush border and cellular enzymes. Therefore there was no evidence of cellular damage or mitochondrial metabolism alteration. This observation is still in line with the theory that for crystal adherence to occur, renal cells must undergo injury and oxidative damage [Muthukumar, A., & Selvam, R., 1998; Scheid, C., *et al.*, 1996]. Evidence that oxidative stress and cell damage is initiated by COM binding or free oxalate exposure to MDCK cells arose from studies that showed elevated total glutathione levels [Muthukumar, A., & Selvam, R., 1998; Lash, LH., *et al.*, 1998].

At this part of the study it has been shown that COM and NaOx and different concentrations and time course treatments elicit oxidative stress by means of superoxide production. It is therefore, of critical importance to address the question of whether the above response is specific to COM and NaOx or whether other particles can mediate the same response. Further studies of how crystal internalisation and/or availability of oxalate can mediate oxidative stress, were subsequently performed.

# CHAPTER 4

## Superoxide formation mediated by crystal and microparticles adherence on MDCK cells

## 4.1 INTRODUCTION

A kidney stone is a hard mineral and crystalline material formed within the kidney or urinary tract. The chemical composition of stones depends on the chemical imbalance in the urine. Although the majority of renal stones contain calcium oxalate, other crystalline components can also contribute to renal stone formation. These include calcium phosphate, uric acid, and cystine stones [Herring, LC., 1962]. The mechanism by which stones develop in the kidney is still poorly understood. However, there is strong evidence that tubular dysfunction or damage is involved in COM binding and subsequent pathology [Selvam, R., & Devaraj, S., 1991]. As it has been shown in Chapter 3, COM crystals mediate oxidative stress in the form of $O_2^{\bullet-}$ production. It is therefore, important to examine whether crystal internalisation occurs at the time points where oxidative stress is observed and the consequences of such an action. In addition, this part of the study examines whether other micro-particles can elicit the same response.

## 4.2 COM binding and internalisation

Having shown in the previous section that COM treated cells undergo oxidative stress in terms of $O_2^{\bullet-}$ production, further experiments were performed to investigate whether COM binding and internalisation occurs during this process. To examine COM binding to MDCK cells, SEM was used. Electron micrographs obtained, showed a COM attachment to MDCK cell monolayers after 15 min [Figure 4.1 B] and this attachment process appeared to cause proliferation of cell microvilli. After 60 min a region of the plasma membrane invaginates and forms a membrane vesicle to endocytose COM crystals [Figure 4.2 A]. By 120 min COM crystals were internalised [Figure 4.2 B]. After 4 h of COM incubation, crystals were completely enclosed within the cell membrane [Figure 4.3 A]. Finally, after cell permeabilisation with digitonin in COM treated cells, crystals remained within the intra-cellular milieu [Figure 4.3 B].

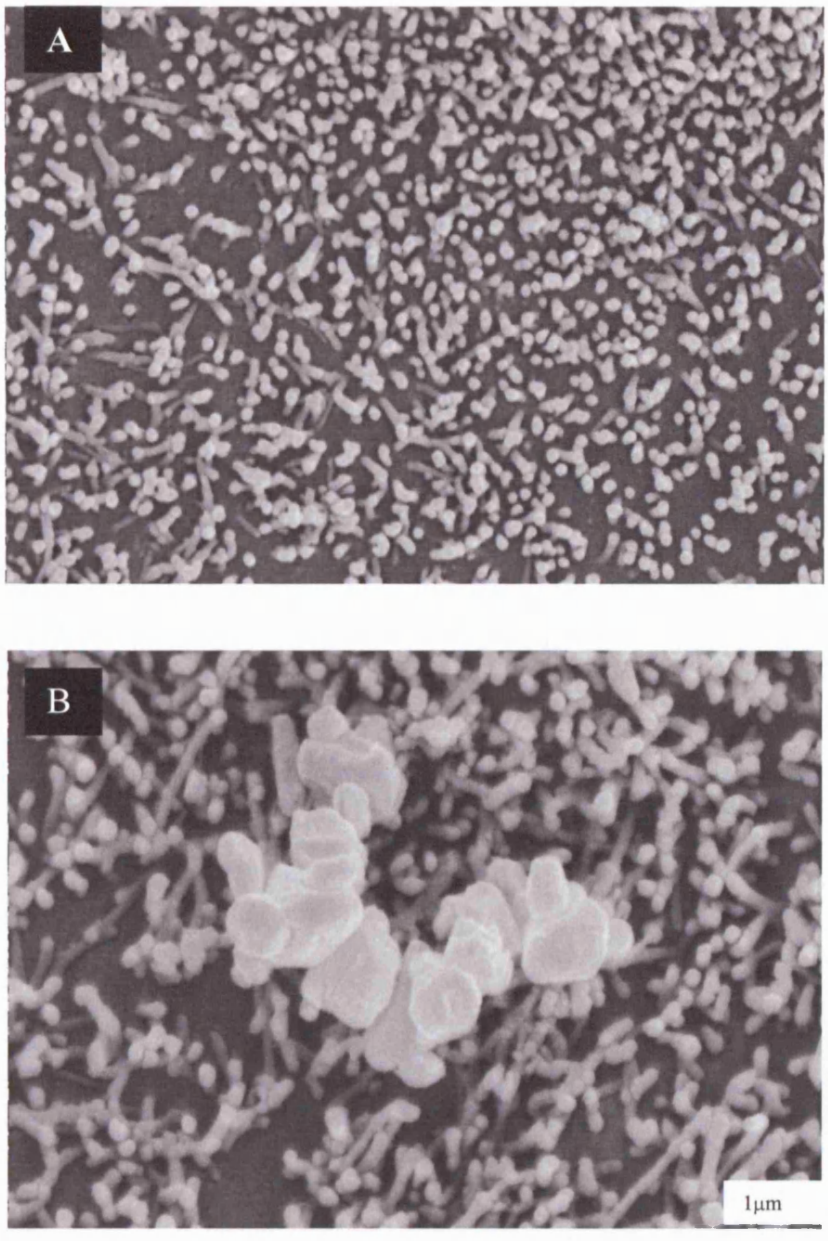


**Figure 4. 1 Scanning electron microscopy of MDCK cells.** (A) Untreated MDCK cells were grown on Thermenox coverslips and examined under scanning electron microscopy (B) MDCK cells were grown on Thermenox coverslips and incubated with 250 μg/ml of COM for 15 min showing microvilli being projected towards the crystal surface.

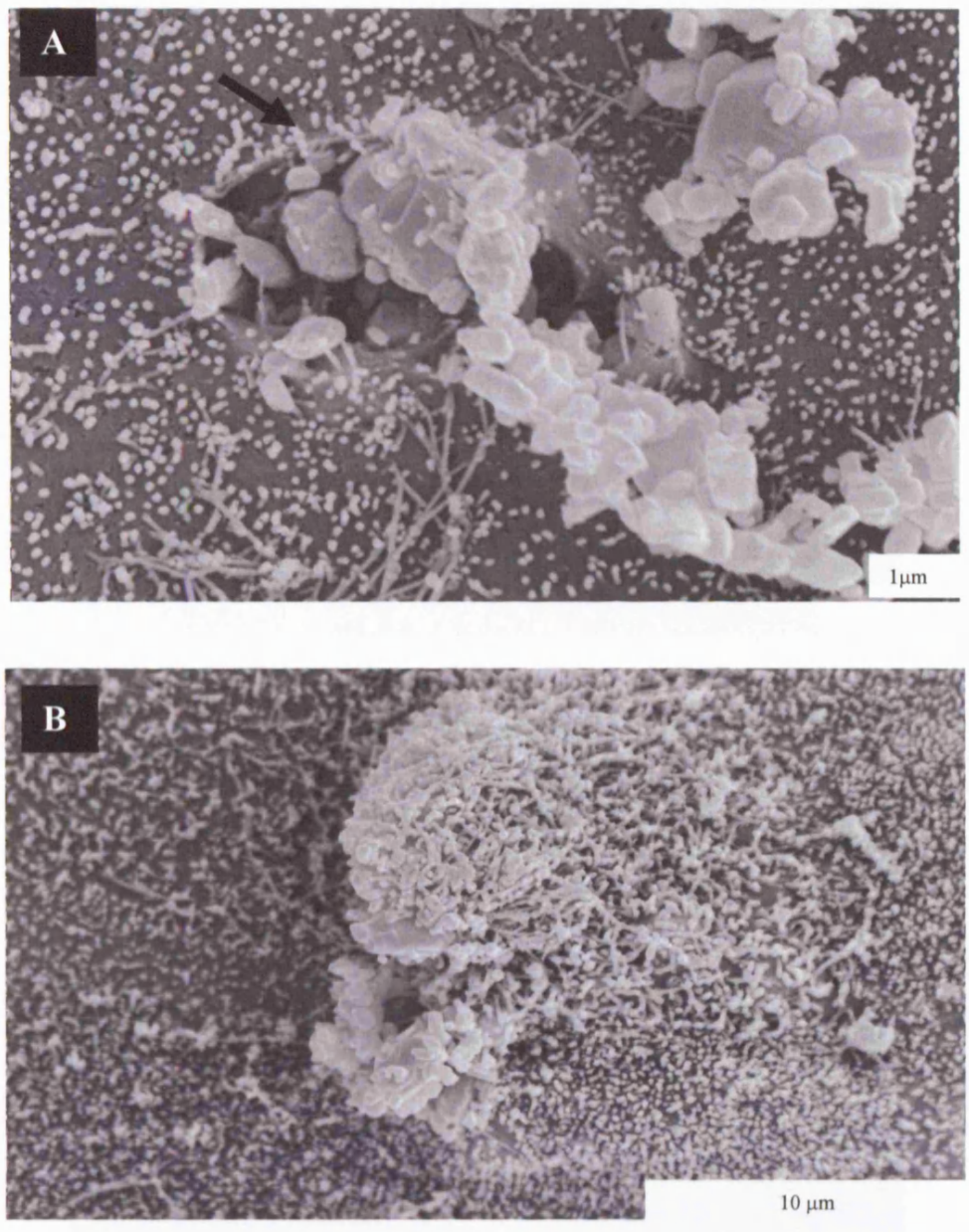


**Figure 4. 2 Scanning electron microscopy of MDCK cells.** MDCK cells were grown on Thermenox coverslips and incubated with 250 μg/ml of COM for (A) 60 min, crystal endocytosis and (B) for 120 min, crystal phagocytosis.

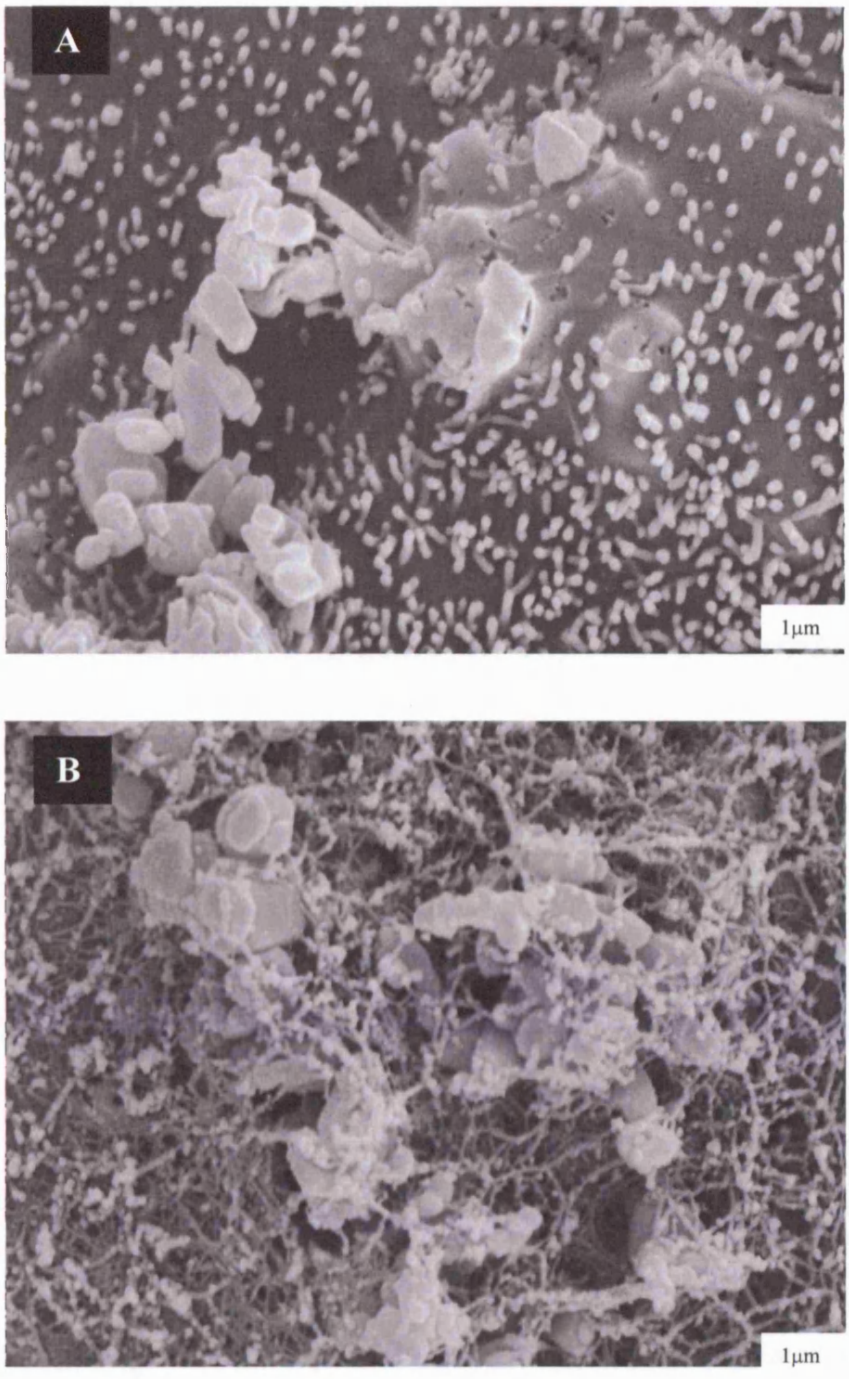


**Figure 4. 3 Scanning electron microscopy of MDCK cells.** COM treated MDCK cells for 240 min where crystals were fully engulfed (A) and crystals remain within intracellular structures after membrane permeabilisation with digitonin (B).

The above results indicate that up to 4 h of COM exposure, crystals were internalised resulting in oxidative stress as indicated by superoxide production measurements at the same time point.

As these measurements were carried out in permeabilised cells, respiration buffer containing EDTA (1 mM) was used to conserve mitochondrial integrity. EDTA is a strong calcium chelator, indicating that internalised COM crystals, calcium dissociates and free oxalate is transported into the mitochondria. To confirm this hypothesis, further experiments were performed by omitting EDTA from the respiration buffer.

## 4.3 Effect of Calcium Chelators on superoxide formation

COM crystal attachment and internalisation in renal epithelial cells, may result in dissociation to $Ca^{2+}$ and free oxalate and therefore in free oxalate entry into mitochondria. To investigate this hypothesis and whether release of free oxalate from COM, due to a shift in the dissociation equilibrium resulting from calcium chelation was contributing to CL, identical measurements were made in the presence and absence of EDTA.

As illustrated in Figure 4.4, omitting EDTA from the respiration buffer caused a small but significant decrease in superoxide production ($\approx$ 15 %) in untreated cells. By contrast, the absence of EDTA caused an abrogation of COM-mediated superoxide production. However, there remained a small but significant increase in chemiluminescence signal, above that of the control minus EDTA. This outcome strongly suggests that $Ca^{2+}$ chelation was essential for the observed COM effect.

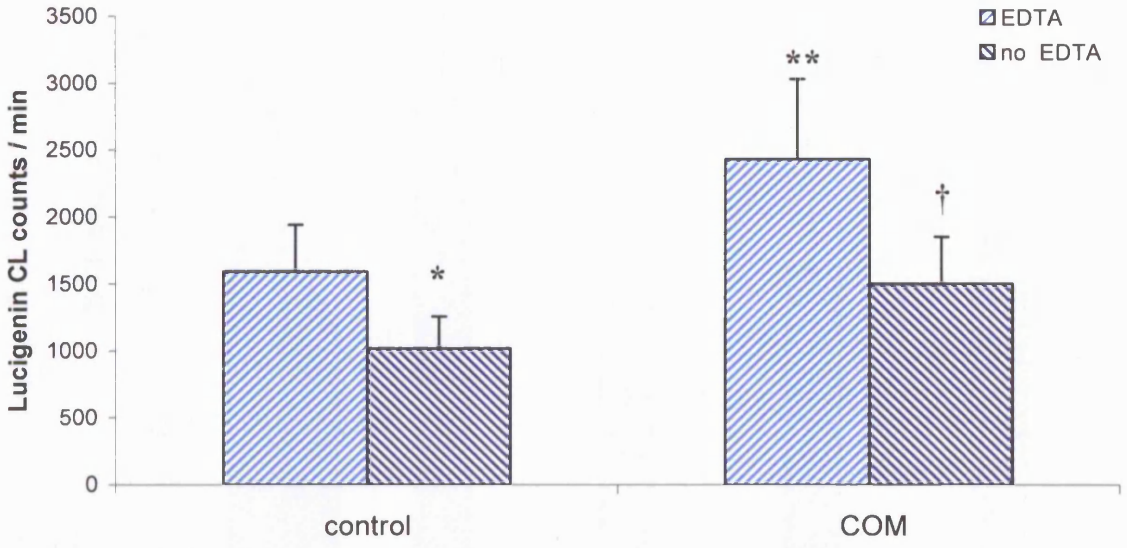


**Figure 4. 4 Effect of EDTA on COM mediated lucigenin–CL.** Lucigenin-enhanced chemiluminescence counts measured in the presence and absence of EDTA in untreated and COM treated cells. Data are mean ± SD for n=20; * $p < 0.05$ vs control with EDTA, ** $p < 0.01$ vs control with EDTA, † $p < 0.01$ vs COM with EDTA.

Further experiments were also performed to restore the abrogated superoxide signal by employing other chelators such as EGTA, desferal, citrate and ascorbate. When re-introduction of different chelators into the system was employed, it was observed that only EGTA proved to be effective in restoring superoxide formation, probably a reflection on its calcium chelation properties. On the other hand, neither citrate nor ascorbate, both weaker calcium chelators, nor desferal, an iron chelator were able to significantly restore any component of the COM mediated superoxide increase [Figure 4.5].

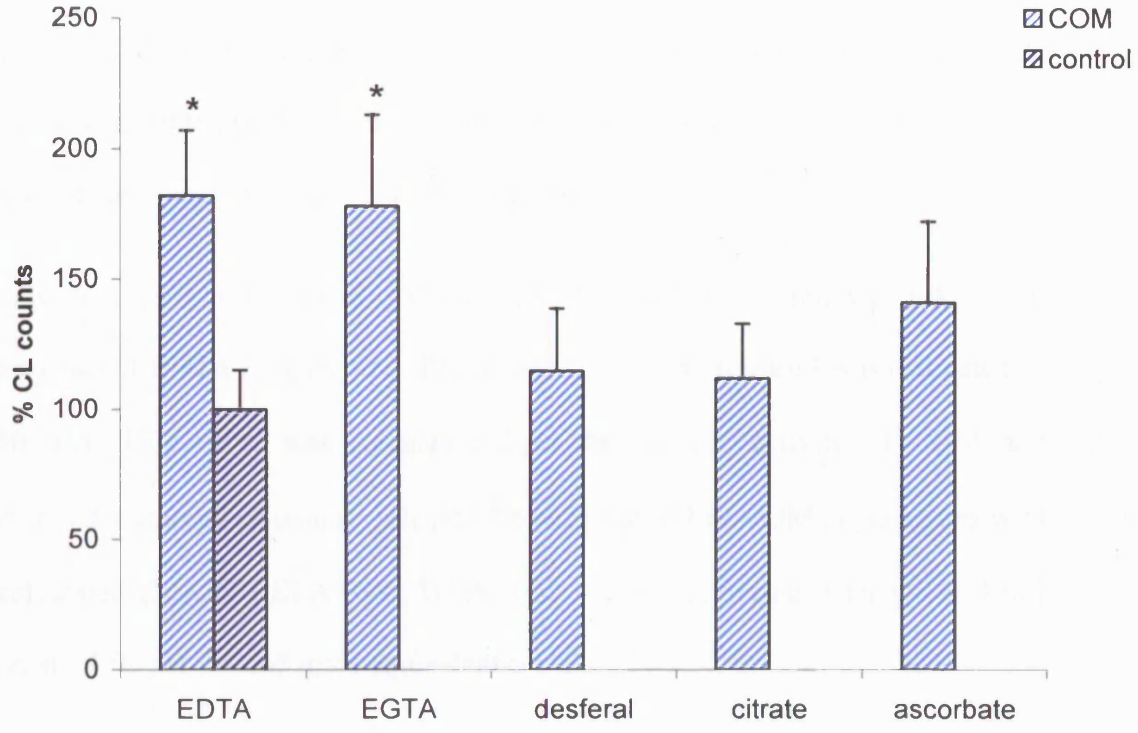


**Figure 4. 5 Effect of calcium chelators on COM mediated lucigenin - CL.** MDCK cells treated with COM and a superoxide assay was performed in the presence of EDTA, EGTA, desferal, citrate, ascorbate, in the RB, and in COM treated MDCK cells. Values expressed as a percentage of lucigenin CL counts. Data are mean ± SD for n=20; * $p < 0.05$ vs control with EDTA.

## 4.4 COM dissociation

To establish that free oxalate indeed is released from COM, [$^{14}$C] - COM (250 μg/ml) was incubated with respiration buffer in the presence and absence of 1 mM EDTA. This was then centrifuged and the radioactive content of the soluble and crystalline components analysed by liquid scintillation counting.

When MDCK cells were treated with COM, 50 % of [$^{14}$C] - oxalate was released in the presence of EDTA [Figure 4.6]. The amount of oxalate released was estimated as ≈ 750 μM. This value was calculated from the specific activity of COM and represents the amount of oxalate released from 250 μg/ml of COM. This agrees with the calculated (MAXCHELATOR, WinMAxC v 2.40) buffering capacity of 1mM EDTA at 37 °C pH 7.4 and ionic equivalent 0.142.

In addition to EDTA, EGTA is also a potential chelator resulting in COM dissociation and ≈ 37 % of the oxalate from COM was released, whereas, other chelators such as ascorbate, desferal or citrate, did not initiate oxalate dissociation from the calcium crystal form.

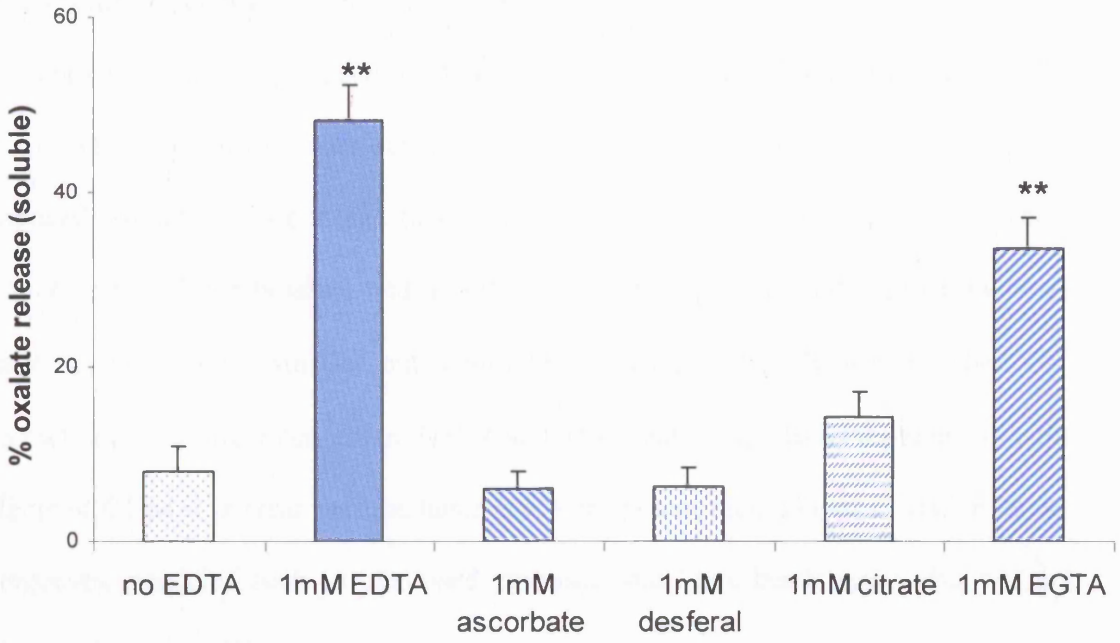


**Figure 4. 6 Percentage of [$^{14}$C] - oxalate release from [$^{14}$C]-COM in the presence of different chelators.** [$^{14}$C] - oxalate dissociation from [$^{14}$C]-COM in respiration buffer containing different chelators. Data are mean ± SD for n=5; ** $p \leq 0.01$ vs RB without EDTA.

## 4.5 Superoxide activation by other crystal forming agents

Having established patho-physiological levels of COM that induce superoxide production, further experiments were performed to investigate whether other crystals or free oxalate in renal stones produced similar amounts of $O_2^{\bullet-}$. Sodium oxalate (NaOx), uric acid (UA) crystals, brushite, zymosan, latex beads (LB) and hydroxyapatite (HA) were employed to investigate this.

This was accomplished by treating MDCK cells with the above particulates at concentrations equal to those of COM (250 µg/ml) and a pre-incubation time of 4 h. Nevertheless, NaOx treatment occurred as previously described, at 1.5 mM

concentration and for 15 min incubation. In addition, superoxide production was measured in digitonin permeabilised cells by lucigenin chemiluminescence. Results demonstrated that at the same density as COM crystals (28.4 $\mu g/cm^2$), hydroxypatite produced a much lower but significant enhancement of superoxide production, whilst neither uric acid nor brushite had an effect [Figure 4.7]. Free oxalate, as previously observed, produced a smaller but significant increase in CL. However, when $O_2^{\bullet-}$ production, resulting from either NaOx and HA treatment, was compared with the effects of COM it is clear that the latter is a more potent mediator of oxidative stress. Phagocytic particles such as opsinised zymosan and latex beads were also without effect on lucigenin CL.

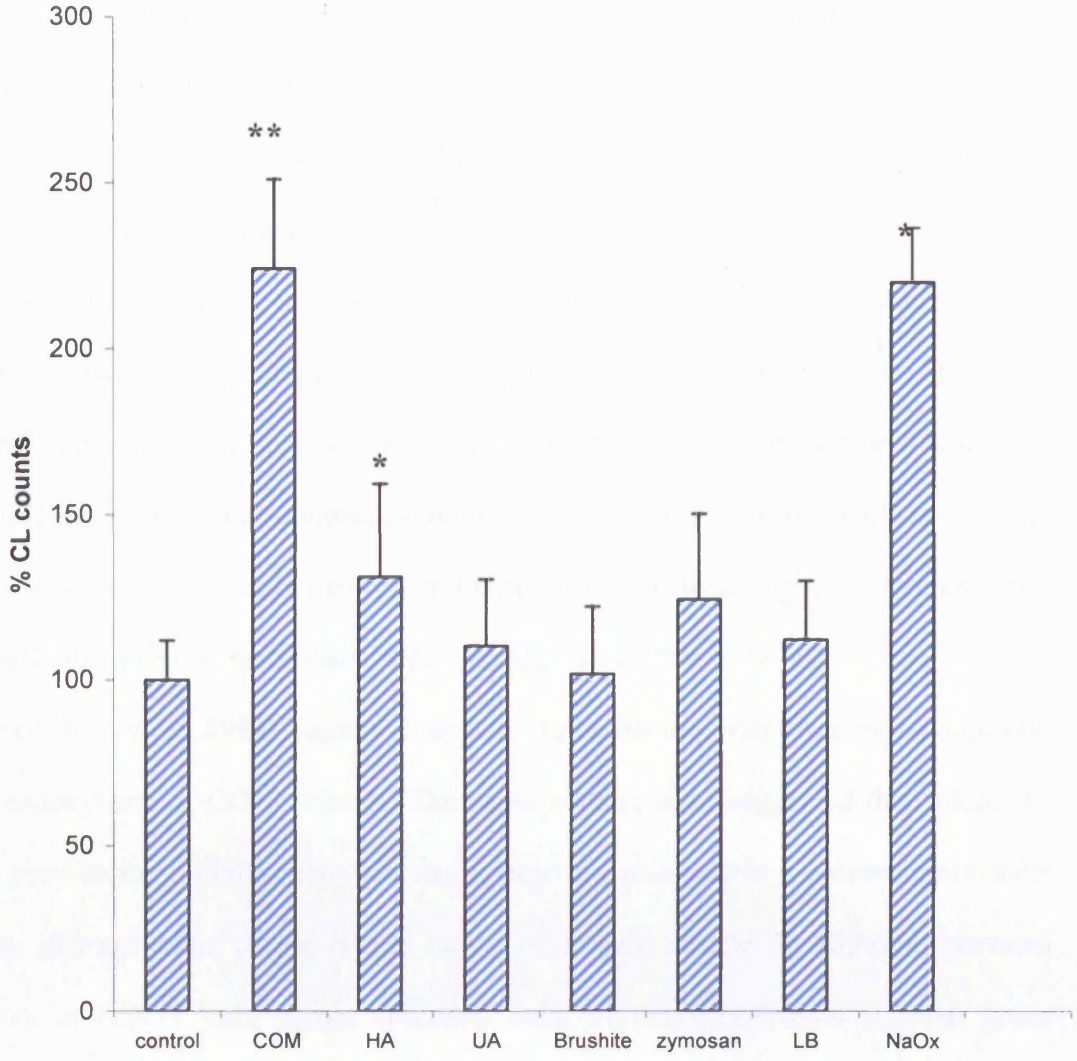


**Figure 4. 7 Superoxide activation by other crystal forming agents.** Lucigenin-enhanced chemiluminescence counts were taken after 4 h treatment with crystals and microparticles. NaOx was added 15 min prior to superoxide assay. HA, hydroxyapatite; UA uric acid; LB latex beads. Values expressed as percentage of activation. Data are mean ± SD for n=20; $^{**}p<0.01$, $^{*}p< 0.05$.

## 4.5 DISCUSSION

To evaluate the rate of COM attachment and internalisation in this model, electron microscopy was employed. The scanning micrographs showed that after 15 min of COM incubation, crystal cell microvilli changes were observed. This resulted in an increase of the cell surface, and therefore in an increase in the affinity of crystal binding. The subsequent cell internalisation occurred over a period of 30 to 240 min, where crystals were entrapped by the microvilli and then moved into the cells. Specifically at 60 min, many of the microvilli of the cells had already been elongated towards the crystals and microvillar projections covered the crystal surface. At later times when microvilli appeared to contribute to phagocytosis, crystals were engulfed beneath the plasma membrane. Interestingly, as it has previously been reported [Lieske, JC., *et al.,* 1994], microvilli appear to play an important role in the adhesion and endocytosis of COM crystals. The same authors have suggested that microvilli may provide the initial binding site and appear to participate in a process that results in the internalisation of the crystal into a membrane vesicle. In addition, previous studies in BSC-1 cells (renal epithelial cells of non-transformed African green monkey lines) [Lieske, JC., & Toback, FG., 1993] and in primary cultures of rat inner medullary collecting duct cells [Riese, RJ., *et al.,* 1998] suggested that COM binds to specific receptors. The number of these receptors may be influenced by the distribution of apical and basolateral proteins found in the plasma membrane. Under normal circumstances these receptors may be small in number but could increase upon injury.

It is now established that crystal formation and retention are critical events for the formation of kidney stones. As discussed before, COM crystals are injurious to renal

epithelium, and membranes of injured cells promote crystal adherence and retention. In addition, COM adherence results in oxidative stress and manifest via superoxide production. However, data that links superoxide formation with other forms of crystals and micro-particles is currently unavailable. A part of this work investigated the effect of other constituents found in tubular fluid that are known to be involved in the kidney stones, on superoxide production. Calcium phosphate crystals, the second most common crystal present in urine and kidney stones [Smith, LH., & Werness, PG., 1982] were employed to investigate their injurious effect on renal epithelial cells. When MDCK cells were treated with brushite and hydroxyapatite crystals at the same density as COM (28.4 $\mu g/cm^2$), only the hydroxyapatite produced a significant enhancement of superoxide production. However, this increase of superoxide production was lower than that observed with COM treatment. The absence of chemiluminescence signal with brushite treatment may be due to the fact that calcium phosphate crystals form in different locations in the kidney. Supersaturation for calcium phosphate crystals is reached more likely where urine is alkaline and therefore in early segments of the nephron, whereas calcium oxalate crystals reach supersaturation where urine is acidic, therefore distal tubules and collecting ducts [Fasano, JM., & Khan, SR., 2001; Asplin, JR., *et al.*, 1996]. In addition, it has also been shown that COM and hydroxyapatite crystals share the same binding sites, and they are both endocytosed and induce cell proliferation [Khan, SR., 2004; Mandel, NS., 1994; Lieske, *et al.*, 1992; Mandel, NS., & Riese, R., 1991]. Therefore, crystal cell interactions are based upon specific molecular contacts between the cell and crystal surfaces and upon the nature of the crystals and cell types [Mandel, NS., 1994; Mandel, NS., & Riese, R., 1991]. Recently it has been reported that when MDCK or LLC-PK1 cells were treated with brushite at a similar density to that used in this study

(28.4 μg/cm$^2$) and at the same time periods (4 hr), LDH release and $H_2O_2$ levels were increased [Aihara, K., *et al.*, 2003]. However, MDCK cells showed less sensitivity to brushite crystals in terms of LDH release and $H_2O_2$ production. This study by Aihara reports oxidative stress mediated by brushite crystals in intact cells due to cytosolic sources, whereas in this current study, the effect of the same crystal was investigated in digitonin permeabilised cells and therefore principally in the mitochondrial compartment. Furthermore, a specific cell can respond differently to different types of crystal [Umekawa, T., *et al.*, 2003], and also to different forms of the same type of crystal [Weisner, J., *et al.*, 1988]. As other crystals have been reported to bind and be internalised by MDCK cells in a similar time frame to these experiments [Koka, R., *et al.*, 2000; Aihara, K., *et al.*, 2003], it is unlikely that an endocytotic/phagocytotic phenomenon is the sole trigger of mitochondrial superoxide production. A recent study [Koka, RM., *et al.*, 2000] has also suggested that interaction between renal epithelial cells and COM or HA crystal differs from that of UA crystals. Specifically, COM and HA crystals behave as if they are positively charged which bind to negatively charged molecules that constitute the apical surface of the plasma membrane. On the other hand UA crystals appear to be electrostatically neutral, suggesting that charge does not play a major role in interaction between UA crystals and cells. Specifically, Koka, RM., *et al.*, [2000] have proposed that UA have a perfect hydrogen bonding system and that the apical cell surface more likely has organic molecules organised according to a motif that satisfies a demand of the UA crystalline lattice for hydrogen bonding interaction. Therefore it is not surprising that hydrogen rather ionic bonding appears to play a role in UA crystal cell-interaction. Since COM and HA crystals share the same mechanistic interaction with the cell membrane and respond with similar levels of superoxide formation, this may suggest

that there is a relationship between the manner of adhesion and oxidative stress. In addition, another study [Bigelow, MW., *et al.,* 1997] has also provided evidence that lipid components from the plasma membrane may play a role during adhesion of different crystals to renal cells. In the present study, digitonin was used to permeabilise cells in order to monitor superoxide production. This membrane poration will have an effect on the cholesterol component of the plasma membrane and therefore affect the types or the quantity of cell surface anionic receptor molecules. This consequently may influence the adhesion capacity of different crystals to retain binding to the renal epithelial cells, therefore creating a favourable environment for COM binding in the plasma membrane.

To investigate the mechanism by which COM crystals contribute to mitochondrial superoxide formation, it is important to study the fate of COM crystals once engulfed in the plasma membrane. The hypothesis suggested in this work, was that COM once internalised dissociates to $Ca^{2+}$ and free oxalate. To explore this, experiments were carried out in the absence of EDTA and presence of other chelators in the respiration buffer. Interestingly, the COM-mediated rise in superoxide was lower in respiration buffer containing EGTA compared with EDTA. This may be due to the fact that $Ca^{2+}$ complex of EGTA, in contrast to EDTA, is 100,000 times more stable than its $Mg^{2+}$ complex [Bers, DM., *et al.,* 1994]. Alternatively the EGTA difference may arise because of $Mg^{2+}$-mediated decrease in respiration [Sordahl, LA., & Silver, BB., 1975]. Therefore, the ablated chemiluminescence signal in the absence of strong calcium chelators, indicates that dissociation of COM to free oxalate is a necessary and an important step in enhanced superoxide formation. This was further supported by the observation that at the level of free oxalate released from COM by EDTA in the respiration buffer calculated from the radioactive release from crystal to aqueous

phase, although a significant rise in superoxide occurs, production is only ≈ 30 % of that apparent with crystals. This again implies that the physical presence of crystals as well as free oxalate is important, and that a critical concentration of free oxalate is needed to trigger this synergy.

As it was shown in Chapter 3, the absence of lucigenin chemiluminescence signal when cells were not permeabilised with digitonin indicates no extracellular sources of superoxide were evident, when MDCK cells were treated with COM. Plasma membrane NAD(P)H oxidase is recognised as a major source of superoxide production in non-inflammatory cells. However, absence of lucigenin chemiluminescence signal, without cell permeabilisation, implies that superoxide formation resulting from COM exposure originates from intracellular sources. Therefore, further studies were performed to identify the intracellular origin of superoxide and possible consequences of this pathology.

# CHAPTER 5

## Intracellular origins of MDCK cell superoxide production in response to exposure to calcium oxalate; mechanisms of free oxalate transport into mitochondria

## 5.1 INTRODUCTION

Generation of calcium oxalate monohydrate crystals results from a series of key events occurring in renal epithelial cells. These include supersaturation of tubular fluid with respect to calcium oxalate ions, crystal nucleation and crystal adherence to the surface of renal epithelial cells. Therefore, there is strong evidence that tubular dysfunction results from COM-cell interactions [Grases, F., *et al.,* 1998; Selvam, R., & Devaraj, S., 1991].

It is now established that exposure of renal cells to CaOx results in a free radical mediated oxidative stress [Muthukumar, A., & Selvam, R., 1998]. This oxidative stress results from increased production of reactive oxygen species (ROS). These species initiate diverse cellular effects ranging from upregulation of key transcription factors, through gene induction, to cell proliferation or necrotic or apoptotic cell death [Hensley, K., *et al.,* 2000]. ROS are also formed endogenously in resident non-inflammatory cells. This may occur via two pathways: (i) either through dysregulation of oxidative enzymes, such as xanthine oxidase, cyclooxygenase, lipoxygenase, and plasma membrane $Cyt_{b558}$NADH oxidase [Griendling, KK., *et al.,* 1994; Bayraktutan, U., *et al.,* 1998], or (ii) due to continuous leakage from the mitochondrial electron transport chain [Chance, B., *et al.,* 1979].

In previous chapters it was shown that calcium oxalate is the form of crystals that mediate the main oxidative insult in terms of superoxide formation. Previous work in this laboratory has showed that the origin of this insult originates mainly from the mitochondria [Khand, FD., *et al.,* 2002]. Therefore, the aim of the work presented in this chapter focuses initially to confirm the above findings and to correlate them with subsequent mitochondria responses upon crystal deposition.

## 5.2 Lucigenin-derived chemiluminescence monitors mitochondrial $O_2^{\bullet -}$ production

In order to demonstrate that the lucigenin CL signal is derived primarily from mitochondrial $O_2^{\bullet -}$, superoxide dismutase (SOD) or Mn(III)tetrakis(1-methyl-4-pyridyl) porphyrin (MnTMPyP), a SOD mimetic, were used. In digitonin permeabilised COM treated cells, CL was inhibited 27 % by SOD (300 mU/ml) and 95 % by the cell permeable SOD mimetic MnTMPyP [Figure 5.1]. Exogenous SOD in plasma membrane permeabilised cells is unable to access the mitochondrial matrix, but may have limited access to the cytoplasmic compartment and to the inner membrane space of the mitochondria. Therefore, lucigenin CL signal was monitored at high and non-significant levels when compared with that of COM treated cells and in the absence of SOD. By contrast, the membrane-permeable SOD mimetic MnTMPyP that penetrates the mitochondrial compartment effectively inhibited the CL signal. Furthermore, it was observed that superoxide formation in the presence of MnTMPyP was lower than that resulting from control cells, confirming MnTMPyP's permeability property, and its ability to inhibit endogenous basal levels of $O_2^{\bullet -}$ production. This provides strong evidence that (i) lucigenin CL signal arises due to $O_2^{\bullet -}$ and, (ii) a membrane enclosed subcellular compartment is responsible for the $O_2^{\bullet -}$ production.

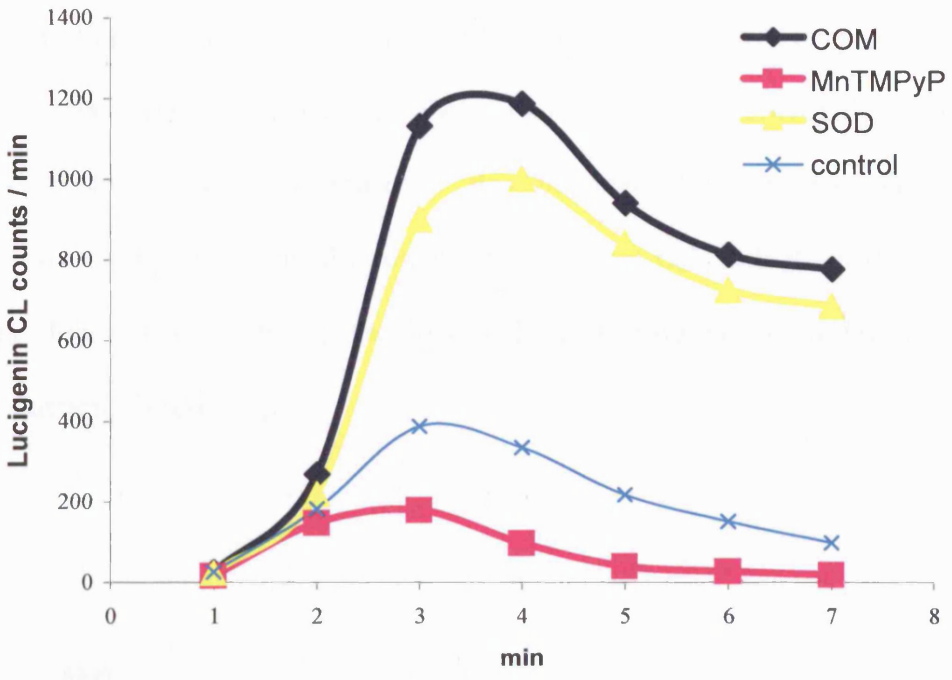


**Figure 5. 1 Lucigenin signal derived from intracellular $O_2^{\bullet-}$.** Lucigenin-enhanced chemiluminescence counts after permeabilisation of COM treated MDCK cells. SOD and MnTMPyP were used at 300 U/ml and 2 μM, respectively and lucigenin-enhanced chemiluminescence counts were monitored for 7 minutes at 1 minute intervals.

## 5.3 *Mitochondrial origin of $O_2^{\bullet-}$*

As suggested in section 5.2, $O_2^{\bullet-}$ formation in this model originates from the mitochondria. To further support this finding, a range of mitochondrial and non-mitochondrial inhibitors were employed to establish the intra-cellular origin of enhanced $O_2^{\bullet-}$ formation in renal epithelial cells mediated by COM crystals. Inhibitors that targeted known non-mitochondrial $O_2^{\bullet-}$ producing enzyme systems failed to abrogate lucigenin CL. Nordihydroguaiaretic acid (NDGA) [Figure 5.2], a

lipoxygenase inhibitor, and indomethacin [Figure 5.4], a potent inhibitor of prostaglandin-forming cyclooxygenase showed no effect on COM-enhanced $O_2^{\bullet-}$ production. Furthermore, hydralazine, and oxypurinol, a NADH oxidase and a xanthine oxidase inhibitor respectively showed no inhibition of superoxide production upon COM treatment. In contrast, to this nominal effect on CL, employing mitochondrial inhibitors resulted in dramatic changes in $O_2^{\bullet-}$ formation. Rotenone, a complex I inhibitor which blocks the flow of electrons towards complex III, inhibited $O_2^{\bullet-}$ production [Figure 5.3].

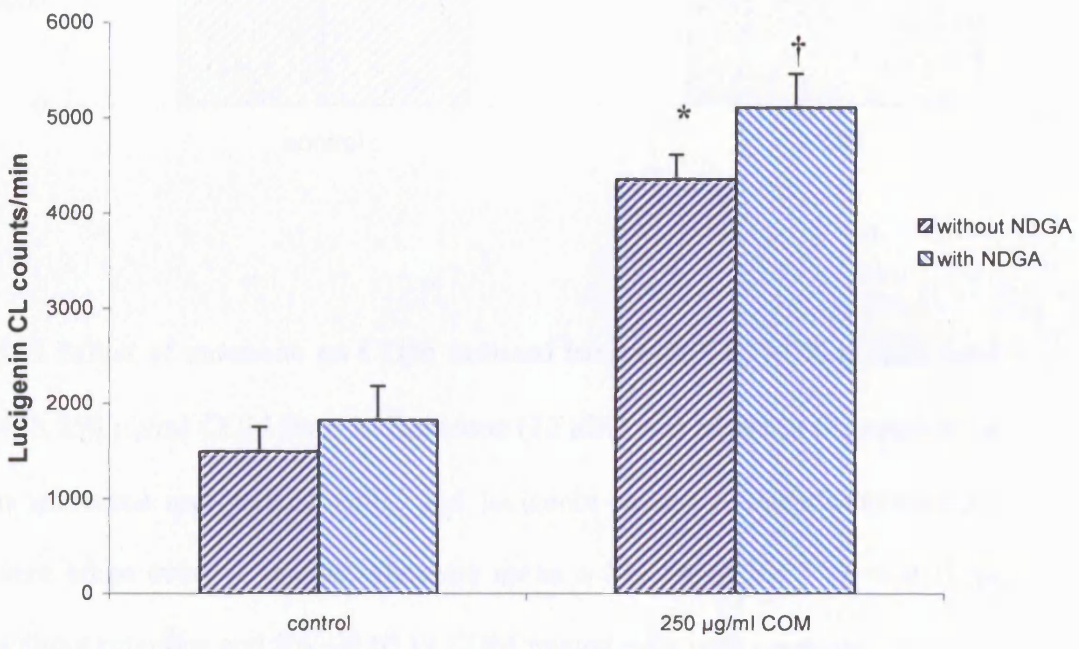


**Figure 5. 2 NDGA effect on lucigenin CL.** MDCK cells treated with 250 µg/ml COM for 4 h. 250 µM NDGA was added in the respiration buffer prior to superoxide assay. Lucigenin-enhanced chemiluminescence counts were taken every 1 minute. Data are mean ± SD for n=20; ** $p < 0.01$ vs untreated MDCK cells (control) without NDGA and † $p < 0.01$ vs untreated MDCK cells in the presence of NDGA.

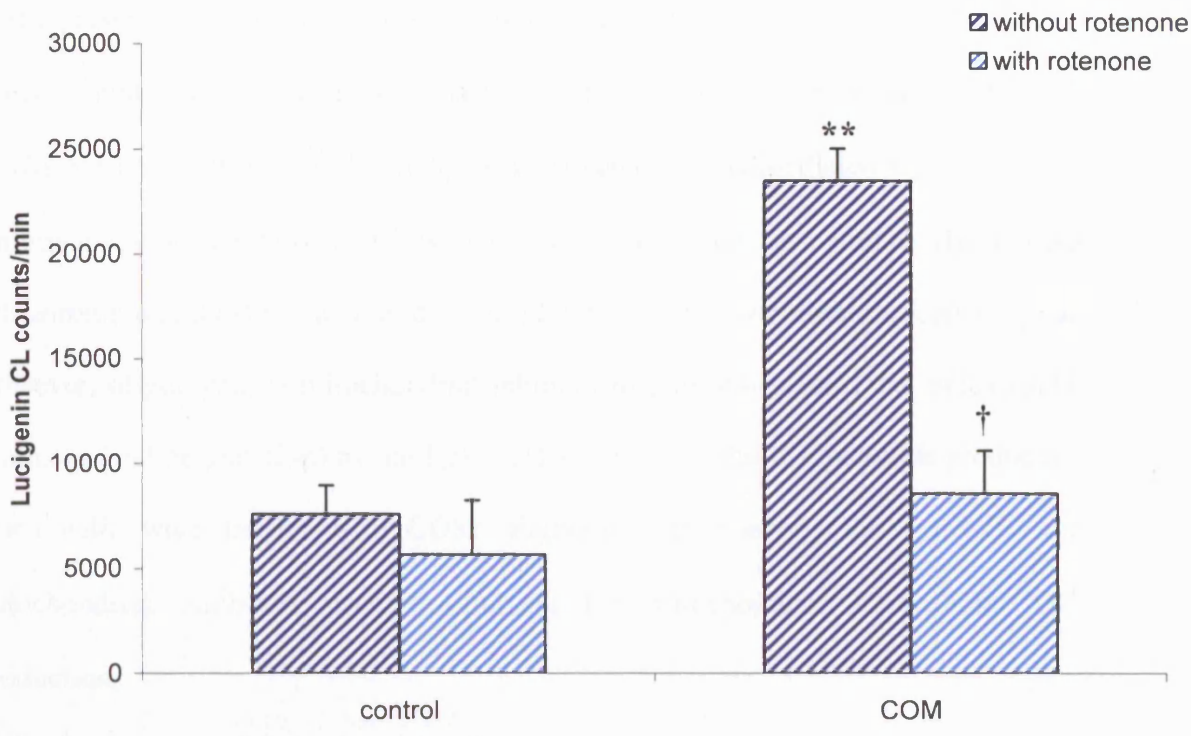


**Figure 5. 3 Effect of rotenone on COM induced lucigenin CL.** MDCK cells were treated with 250 μg/ml COM for 4 h. Rotenone (20 μM) was added in the respiration buffer to untreated and treated cells, and lucigenin-enhanced chemiluminescence counts were taken every 1 minute. Data are mean ± SD for n=20; ** $p < 0.01$ vs control without rotenone and † $p < 0.05$ vs COM treated cells with rotenone.

In addition, of particular interest was the protonophore carbonylcyanide m-chlorophenylhydrazone (CCCP), which dissipates the mitochondrial proton gradient and therefore, as would be expected severely inhibits the $O_2^{\bullet-}$ formation. Furthermore, in the presence of succinate (complex II substrate), thenoyl trifluoracetone (TTFA) which inhibits succinate dehydrogenase together with 4-hydroxyccinamic acid which blocks pyruvate entry from the cytoplasm, prevented COM mediated $O_2^{\bullet-}$ formation. Antimycin A, an inhibitor that blocks the respiratory chain at complex III between cytochrome b and cytochrome $c_1$ did not inhibit lucigenin chemiluminescence signal. However, oligomycin, a mitochondrial inhibitor of phosphorylation that blocks ATP synthesis (and degradation) by the $F_0/F_1$ ATPase did not inhibit superoxide production when cells were treated with COM. Figure 5.4 summarises the cytosolic and mitochondrial inhibitors used to confirm the mitochondrial intracellular $O_2^{\bullet-}$ production.

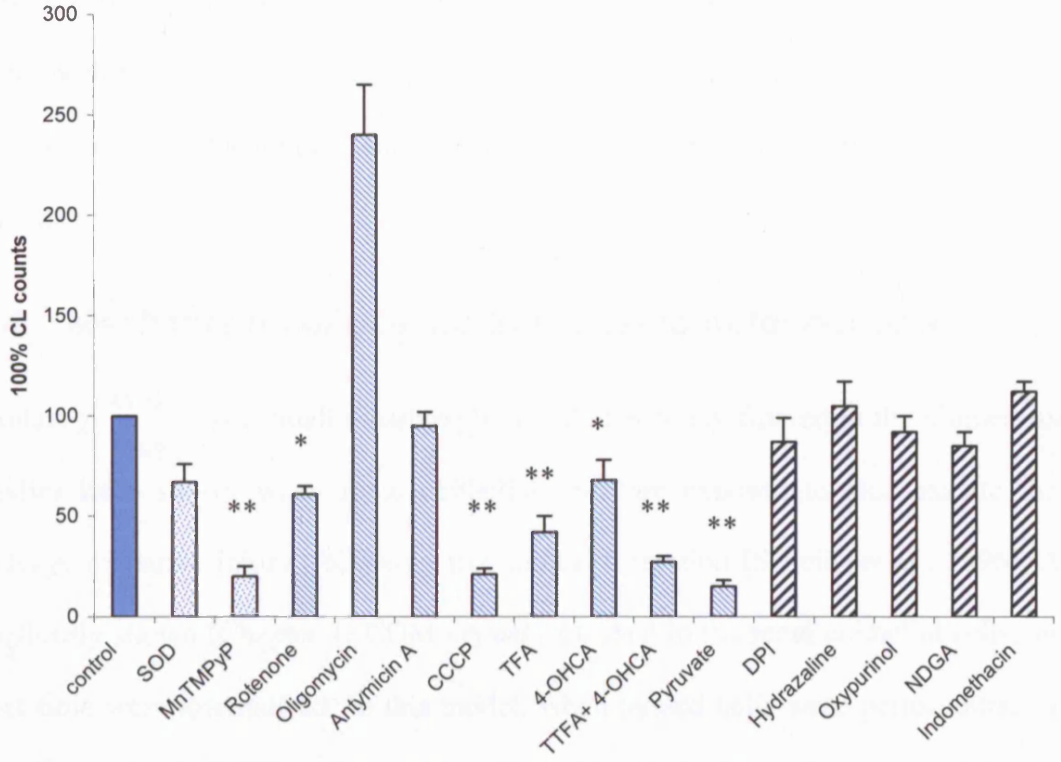


**Figure 5. 4 Effect of cytosolic and mitochondrial inhibitors on COM enhanced CL.** MDCK cells were treated with 250 μg/ml COM for 4 h (control). Cytosolic and mitochondrial inhibitors were added in the respiration buffer to COM treated cells, and lucigenin-enhanced chemiluminescence counts were taken every 1 minute. Values are expressed as a percentage of CL counts in respect to control. Data are mean ± SD for n=20; ** $p < 0.01$ and * $p < 0.05$ vs control.

Having confirmed the mitochondrial origin of superoxide upon crystal deposition combined with the data shown in chapter 4 showing that oxalate is released in the presence of EDTA when MDCK cells were treated with COM, further experiments were performed to investigate possible mechanisms by which oxalate may be transported to mitochondria and initiate oxidative stress in terms of superoxide production.

## 5.4 Mechanisms of oxalate transport to mitochondria

Oxalate ( $\begin{matrix} COO^- \\ \| \\ COO^- \end{matrix}$ ) is a small dicarboxylic ion that is freely filtered at the glomerulus. Studies have shown when renal epithelial cells are exposed to free oxalate they undergo oxidative injury, following free radical formation [Scheid, *et al.*, 1996]. As previously shown (Chapter 4) COM crystals attached to the renal epithelial cells, and over time were internalised. In this model, when treated cells were permeabilised in the presence of EDTA, free oxalate was released in the cells. Interest in this dicarboxylic transport arose from data in this study demonstrating that the mitochondrial electron transport chain is the most probable origin of free radicals. Therefore, the initial question was to identify the mechanism of the oxalate transport into the mitochondria, and investigate whether it is associated with free radical production that could lead to renal cellular injury.

It has been suggested that oxalate can be transported by the dicarboxylic carrier in kidney mitochondria by three mediator systems [Liu, G., *et al.*, 1996]. These include electron-neutral transport, the dicarboxylate carrier and the Inner Membrane Anion Channel (IMAC). Firstly, electrophoretic transport via IMAC was examined. To investigate this, *N,N'* dicyclohexylcarbodiimide (DCCD), a selective IMAC inhibitor was employed and $O_2^{\bullet -}$ was monitored [Figure 5.5].

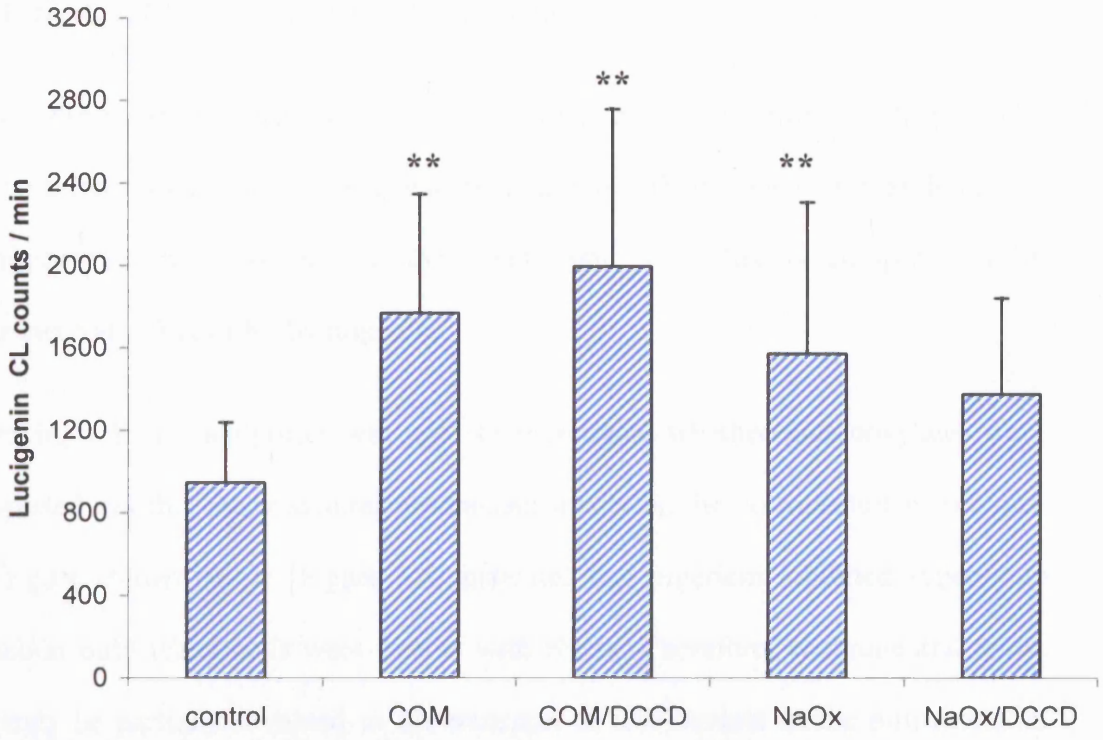


**Figure 5. 5 Effect of IMAC inhibition by DCCD on lucigenin CL.** Lucigenin chemiluminescence was performed in MDCK cells treated with COM or NaOx in the presence and absence of 50 μM DCCD. Data are mean ± SD for n=20; ** $p < 0.01$ vs control.

This data demonstrates that in COM treated cells, DCCD did not have an inhibitory effect on superoxide formation. This indicates that free oxalate originating from COM crystals was not transported into the mitochondria via IMAC. On the contrary to the COM effect, in NaOx treated cells, DCCD inhibited the formation of superoxide.

Further experiments were carried out to investigate other forms of dicarboxylic transport. Energised mitochondria generate a high membrane potential that drives the electrophoretic influx of $K^+$. In the steady state this flux is compensated by electroneutral efflux of $K^+$ by nigericin.

Nigericin, a $K^+/H^+$ antiporter was used to investigate whether dicarboxylates were transported via this electroneutral mechanism involving the co-transport of protons. The figure shown below [Figure 5.6] indicates that nigericin inhibited superoxide formation only when cells were treated with NaOx. Therefore, electroneutral anion flux may be partially involved in the transport of free oxalate in the mitochondria. Hence, the data collected using DCCD and nigericin implies that COM and NaOx act differently once they are found in the intracellular matrix milieu.

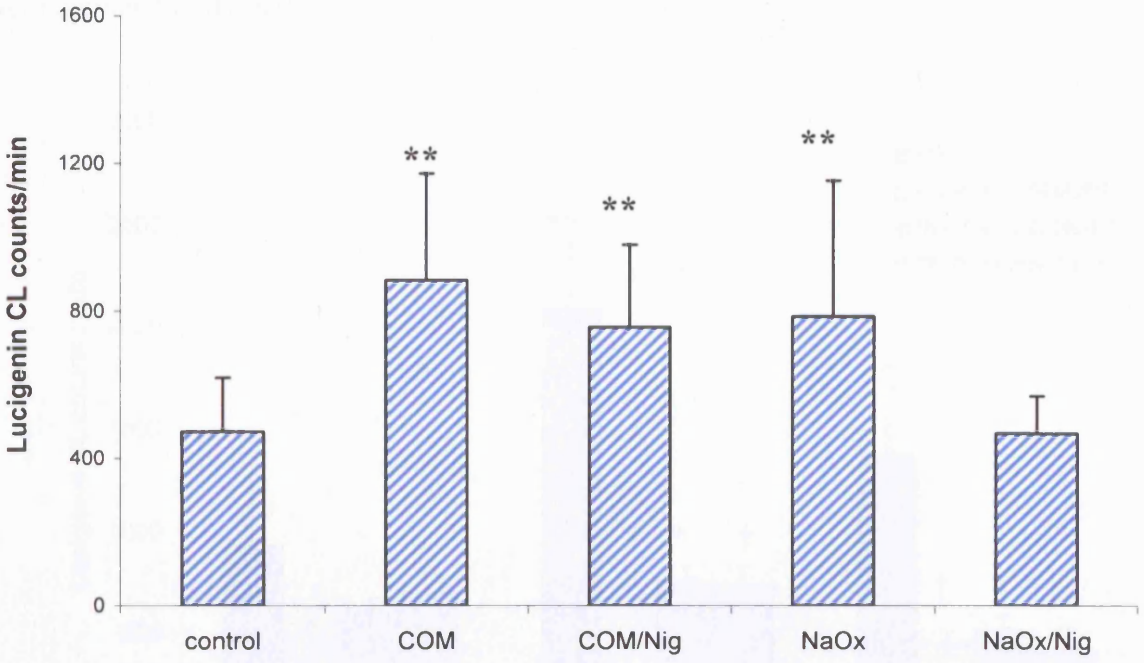


**Figure 5. 6 Effect of nigericin on lucigenin CL.** Chemiluminescence was performed in MDCK cells treated with COM or NaOx in the presence and absence of 10 μM nigericin. Data are mean ± SD for n=20; ** $p < 0.01$ vs control.

Finally, mitochondrial transport via the dicarboxylate carrier was investigated. This carrier mediates electroneutral exchange of dicarboxylates for inorganic phosphate (Pi). When phosphate was omitted, the dicarboxylic acid transport was disrupted, leading to inhibited formation of $O_2^{\bullet-}$ [Figure 5.7]. In order to avoid pH alterations by omitting phosphate in the buffer, 5 mM MOPS, 3 mM HEPES or 3 mM Tris-HCl were included in the RB.

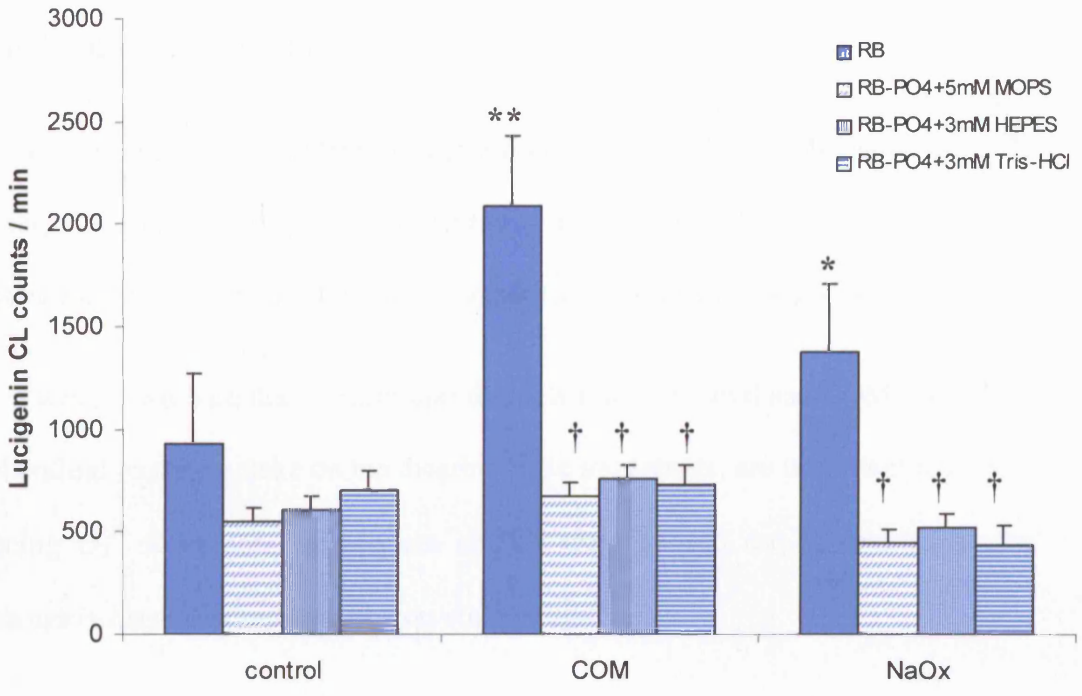


**Figure 5. 7 Superoxide production in the absence of phosphate.** Lucigenin chemiluminescence was performed when MDCK cells were treated with COM or NaOx and omitting phosphate from the respiration buffer (RB). Phosphate was replaced with 5 mM MOPS, 3 mM HEPES, or 3 mM Tris-HCl. Data are mean ± SD for n=20; ** $p$ <0.05 and * $p$ < 0.01 vs control, † $p$ < 0.01 vs COM and NaOx treated cells in phosphate containing RB.

To confirm the above finding, further experiments were performed by employing mersalyl which, is commonly used as a specific inhibitor of dicarboxylate-phosphate transport. Therefore, by including 150 μM mersalyl in the respiration buffer, there was a significant decrease (50 %) in superoxide production evoked by COM treatment. The same effect was also observed when MDCK cells treated with NaOx (30 % decrease) [Figure 5.8]. Furthermore, this abrogation in superoxide signal observed in COM and NaOx treated cells by omission of phosphate, was not observed in control cell superoxide formation.

Therefore, this data illustrates that the disruption of the dicarboxylic transport when Pi is absent, abrogated COM and NaOx treated cells to produce $O_2^{\bullet-}$. This indicates the importance of this transporter for oxalate uptake in the mitochondria of MDCK cells.

Thus, it was shown here that intracellular dissociation of internalised COM, as well as mitochondrial oxalate uptake on the dicarboxylate transporter, are important factors in enhancing $O_2^{\bullet-}$ formation. Subsequent studies were carried out to investigate the mitochondria responses mediated by crystal toxicity.

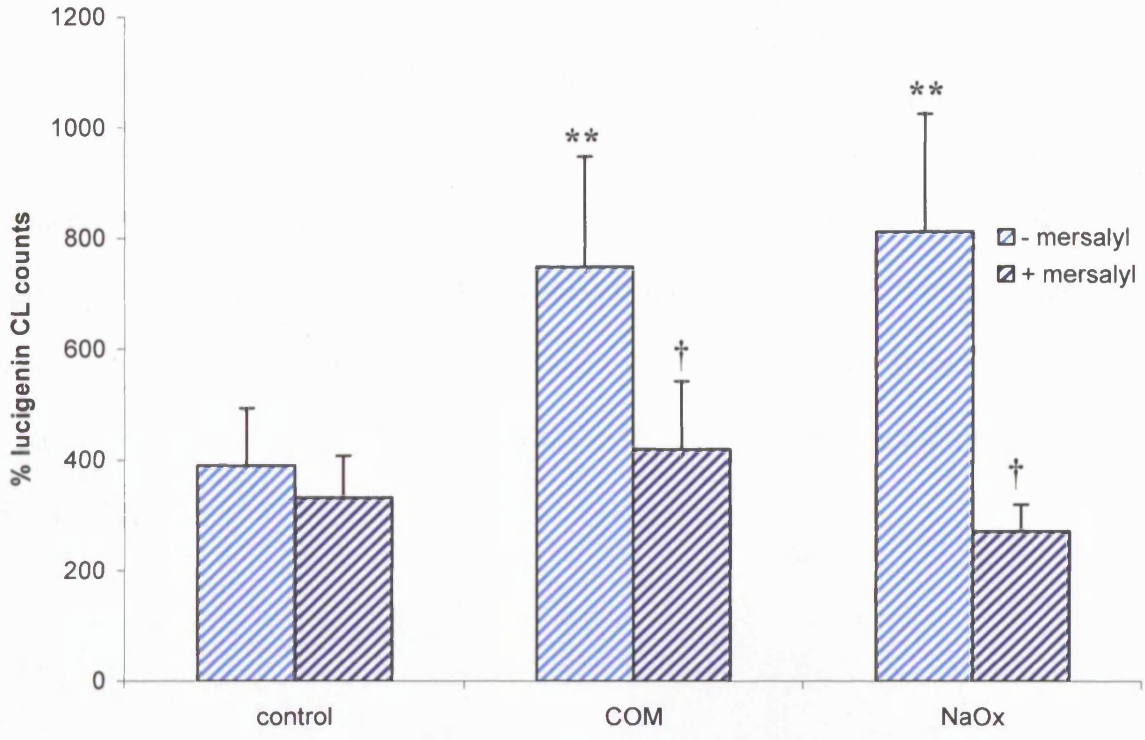


**Figure 5. 8 Superoxide production in the presence and absence of mersalyl.** Lucigenin chemiluminescence was performed when MDCK cells were treated with COM or NaOx and using 150 μM mersalyl as a phosphate inhibitor. Data are mean ± SD for n=20; ** $p$ and * $p < 0.01$ vs control, † $p < 0.01$ vs COM and NaOx treated cells in mersalyl included conditions.

mediated by changes in $\Delta\psi_m$. In order to investigate whether COM exposure is accompanied by similar changes in $\Delta\psi_m$, a membrane potential-sensitive dye TMRM together with confocal microscopy, were employed.

When concentrated, TMRM exhibits auto-quenching, such that the fluorescence signal becomes a non–linear function of dye concentration [Dutchen, MR., & Biscoe, TJ., 1992; Bunting, JR., *et al.,* 1989]. Mitochondrial depolarisation causes loss of mitochondrial dye, and dilution into the cytosol where the signal therefore increases. Untreated MDCK cell monolayers contained only weakly polarised mitochondria [Figure 5.9]. However, some cells differentiated into tubular zones forming rings, containing mitochondria in which the $\Delta\psi_m$ was much greater [Figure 5.10]. Furthermore, in confluent COM treated MDCK cells, $\Delta\psi_m$ was increased dramatically [Figure 5.11].

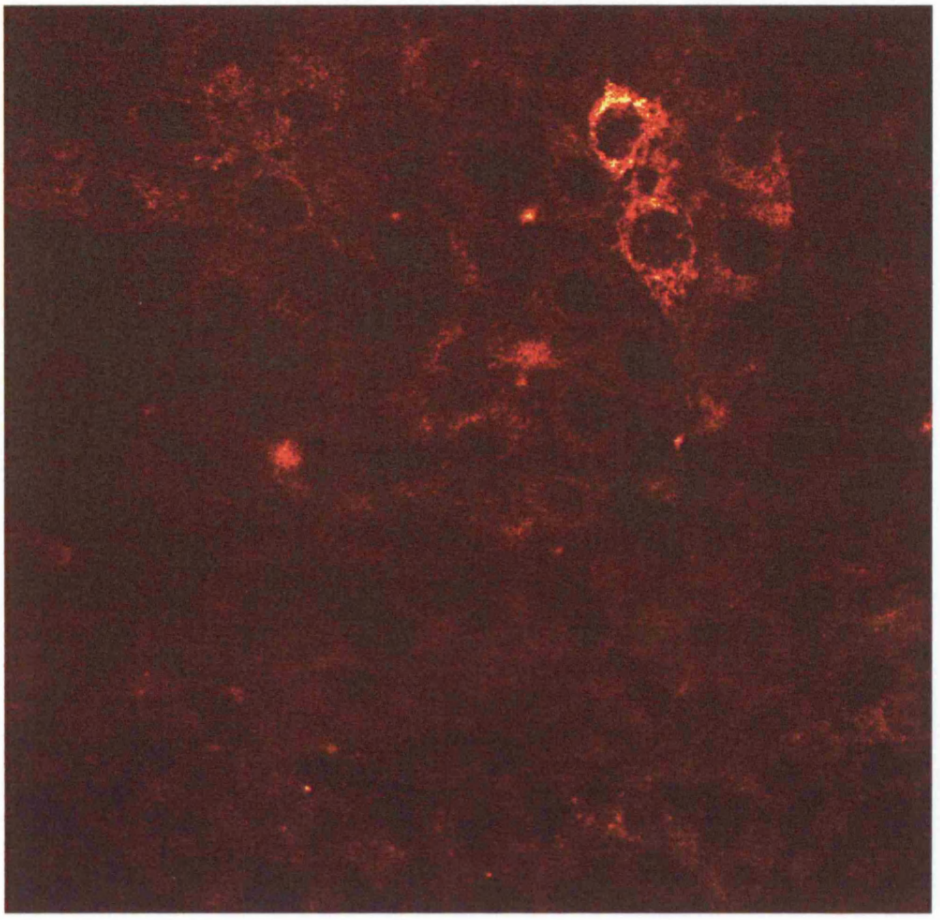

**Figure 5. 9 Fluorescence imaging of mitochondrial membrane potential in untreated confluent MDCK cells.** Cells were loaded with TMRM (20nM in HEPES-buffered salt solution). Illumination intensity was 0.1 % of total laser output and the pinhole was set to give an optical slice of ~ 2 μm.

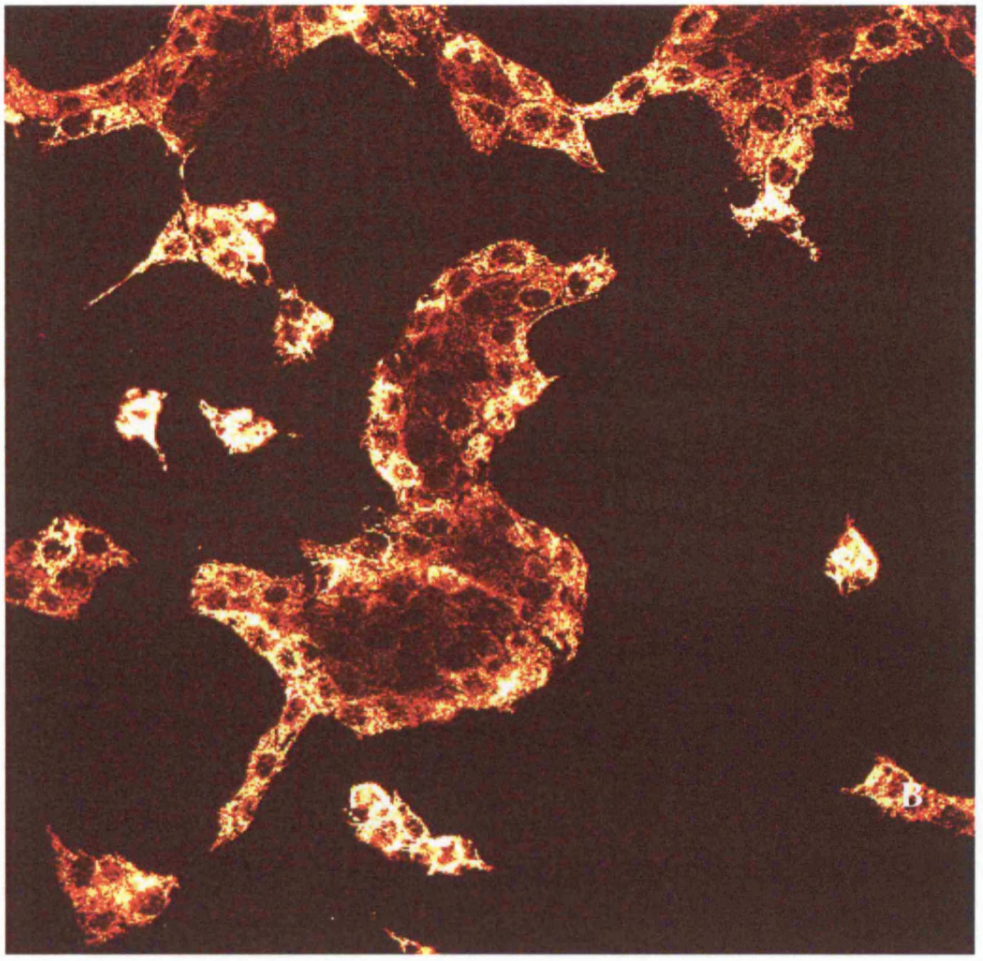

**Figure 5. 10 Fluorescence imaging of mitochondrial membrane potential in untreated non-confluent MDCK cells.** Cells were loaded with TMRM (20nM in HEPES-buffered salt solution). Illumination intensity was 0.1 % of total laser output and the pinhole was set to give an optical slice of ~ 2 μm.

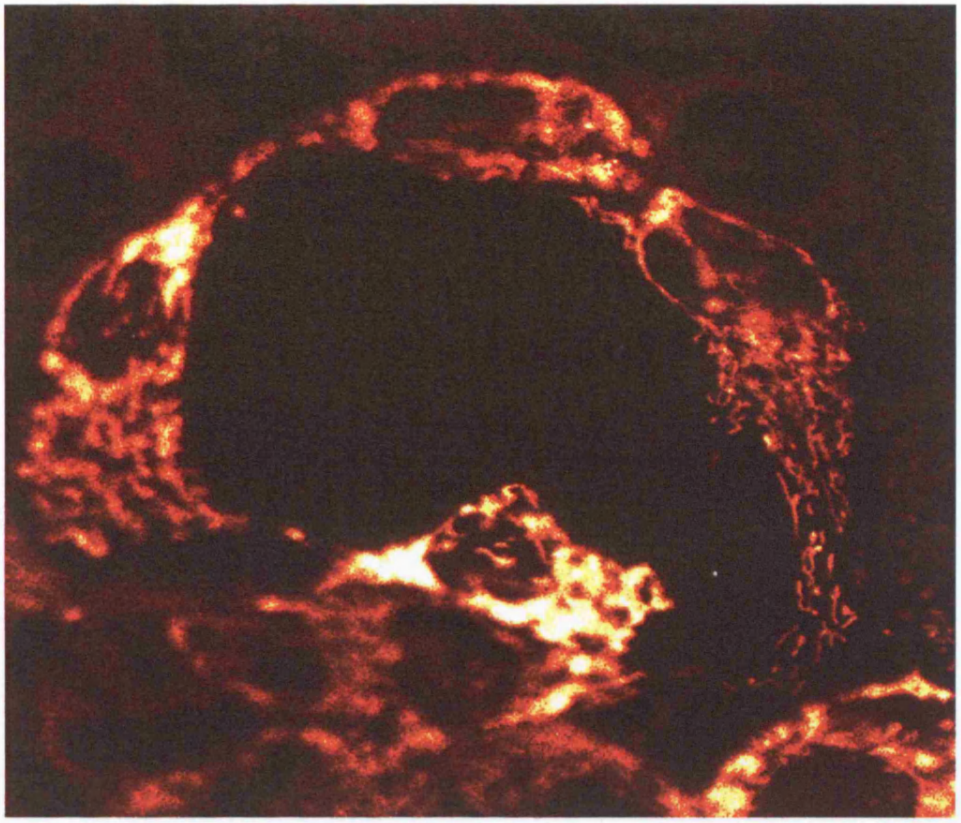

**Figure 5. 11 Fluorescence imaging of mitochondrial membrane potential in COM-treated MDCK cells.** Cells were treated with COM and loaded with 20 nM TMRM. Illumination intensity was 0.1 % of total laser output and the pinhole was set to give an optical slice of ~ 2 μm.

Moreover, Figure 5.12 A and B show TMRM fluorescence and light images, respectively, which when superimposed [Figure 5.12 C] show a clear association between crystal attachment and increased TMRM signal localised to mitochondria. In contrast, when crystals did not attach to MDCK cells the mitochondrial fluorescence signal was minimal.

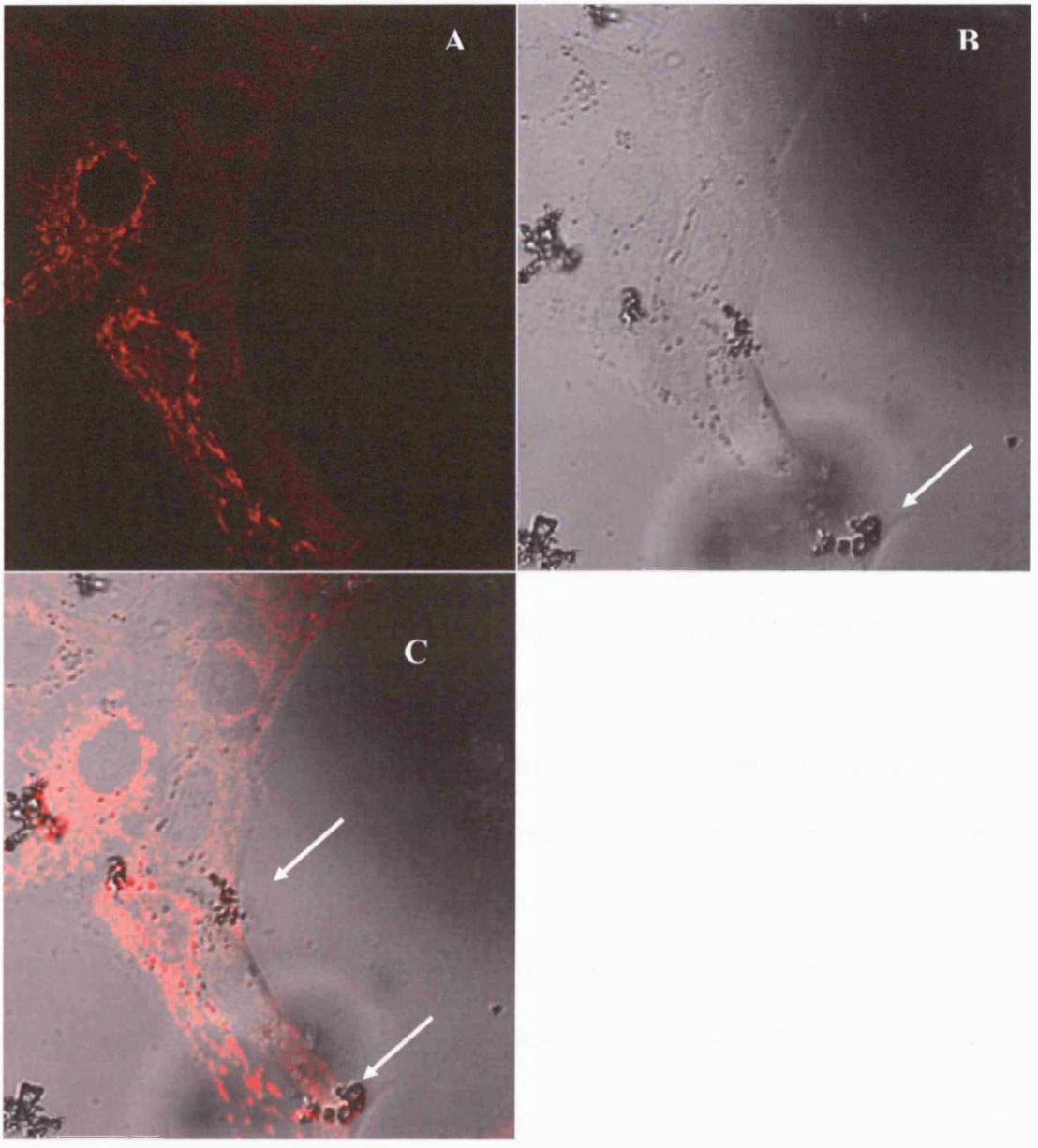

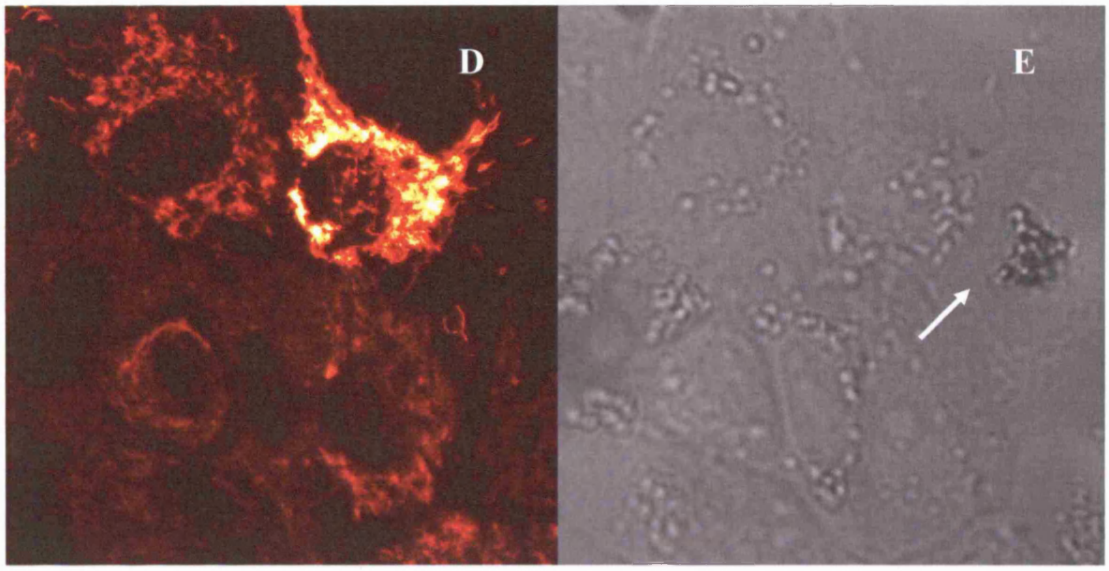


**Figure 5. 12 Fluorescence imaging of mitochondrial membrane potential in COM-treated MDCK cells.** Cells were loaded with TMRM (20 nM in Hepes-buffered salt solution). Illumination intensity was 0.1% of total laser output and the pinhole was set to give an optical slice of ~ 2 μm. **(A)** Increased TMRM fluorescence and distinct mitochondria in the cells on the left of the field, where COM crystals have attached (see transmitted light image, **B**). In contrast, cells to the upper right of the field, where crystals are absent, display much lower TMRM signal. **(C)** Superimposition of the fluorescence and transmitted light images. **(D)** Increased TMRM fluorescence where COM crystals have attached. **(E)** Transmitted light image showing crystal presence. Arrows indicate presence of crystals and the line represents 10 μm.

Therefore, significant changes in mitochondrial potential after COM treatment was observed when compared to untreated MDCK cells in 4 different cell populations (n = 4), including 200 cells in each group [Figure 5.13].

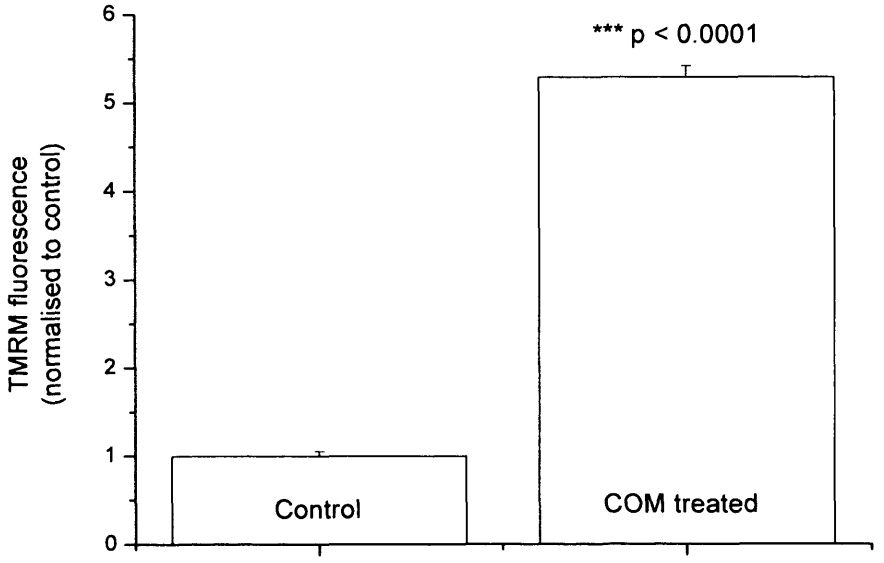


**Figure 5. 13 Effects of COM treatment on mitochondrial membrane potential.** Confocal microscopy performed on control and COM treated MDCK cells. Mean ± SEM (n ≈ 200 individual cells) of TMRM fluorescence over single cells.

An increase in intracellular TMRM fluorescence can either be derived from changes in mitochondria $\Delta\psi_m$ or from plasma membrane hyperpolarisation [Duchen, MR., *et al.*, 2003]. However, accumulation of intracellular dye in response to a hyperpolarized plasma membrane results in a more homogenous dye distribution than that caused by mitochondrial hyperpolarisation, and hence the ratio of the standard deviation (SD) of the fluorescence signal across the whole cell to the mean whole cell signal can be used to distinguish between the two phenomena [Duchen, MR., *et al.*, 2003]. In the MDCK cells images observed here this SD/mean ratio was significantly increased

indicating that with COM treatment a mitochondrial hyperpolarisation occurs [Figure 5.14].

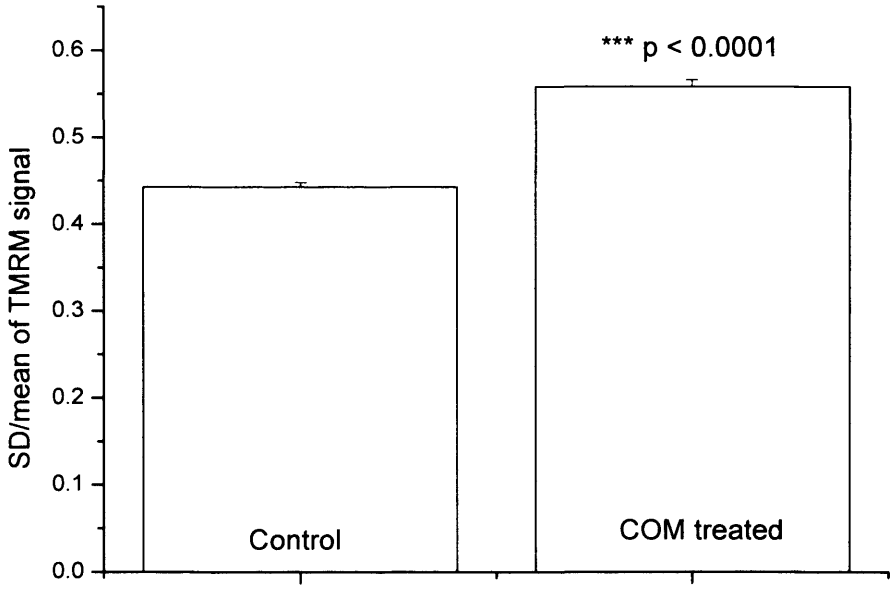


**Figure 5. 14 Effects of COM treatment on mitochondrial membrane potential.** Confocal microscopy performed on control and COM treated MDCK cells. Increased SD TMRM signal/mean TMRM ratio of every cell upon COM application.

Furthermore, a linear increase in $\Delta\psi_m$ was observed during continuous monitoring by a CCD camera when COM crystals were applied by micropipetting, [Figure 5.15]. In contrast to this mitochondrial response derived within minutes of crystal attachment, untreated cells manifested a steady significant decrease in TMRM fluorescence, which may be due to photobleaching [Figure 5.16].

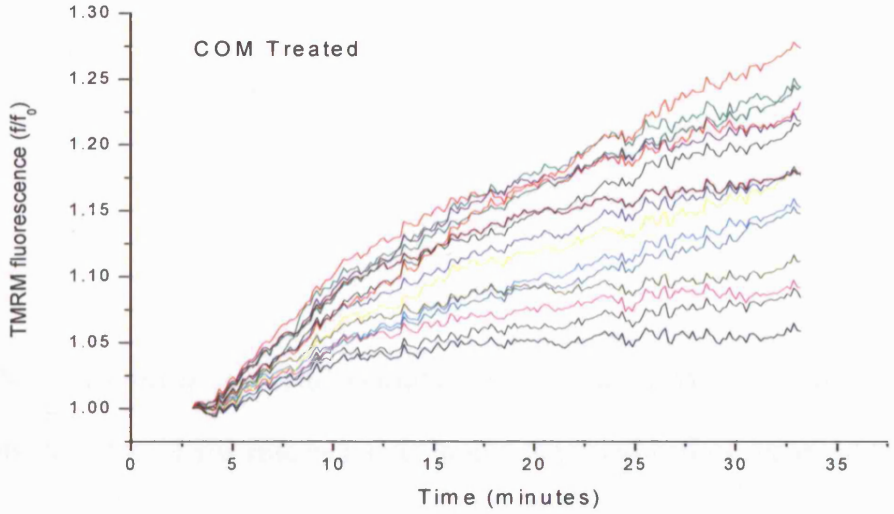


**Figure 5. 15 Changes in Δψm mediated by COM treatment.** Each trace represents the TMRM fluorescence over single COM treated cell as recorded by a CCD camera.

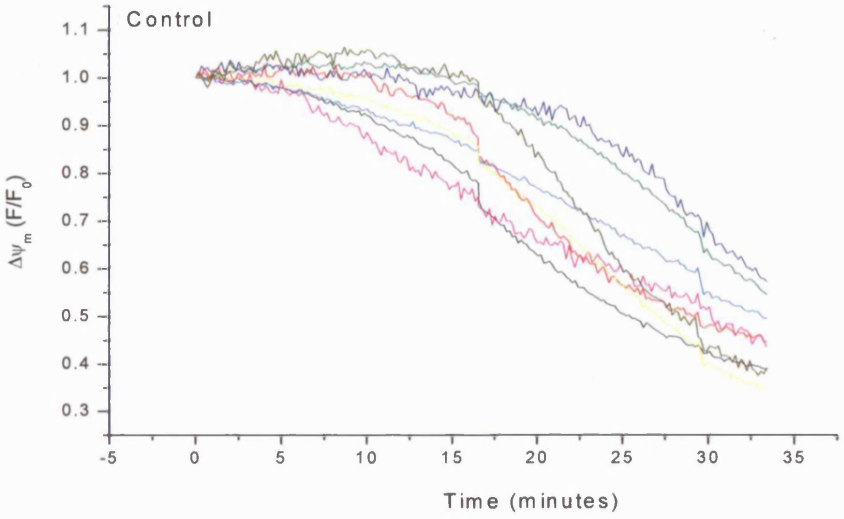


**Figure 5. 16 Changes in Δψm mediated by untreated MDCK cells.** Each trace represents the TMRM fluorescence over single untreated cell as recorded by a CCD camera.

## 5.6 $Ca^{2+}$ signalling upon COM binding

Mitochondria are key modulators of intracellular [$Ca^{2+}$] and it is well established that regulation of intracellular [$Ca^{2+}$] is disrupted in oxidative stress [Jacobson, J., & Duchen, MR., 2002]. Consequently, further experiments were performed to examine whether $Ca^{2+}$ signalling is altered due to oxidative stress caused by COM treatment.

Changes in intracellular $Ca^{2+}$ in MDCK cells exposed to COM were investigated by employing the $Ca^{2}$-sensitive dye Fura-2 AM and the ratio of fluorescence excited at 340 nm and emission at 380 nm was measured. When COM was applied to MDCK cells, $Ca^{2+}$ pulse signals were rapidly induced after 2-3 min [Figure 5.17].

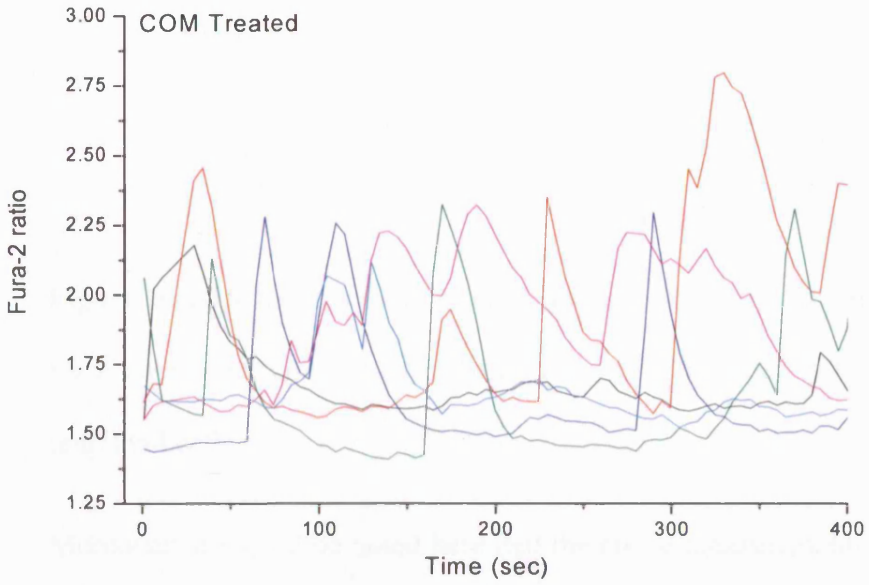


**Figure 5. 17 Changes in [$Ca^{2+}$] transients mediated by COM treatment.** Each trace represents the ratios of excitation of Fura-2 at 340 and 380 nm over single COM treated cell.

These $Ca^{2+}$ oscillations derived from COM treatment were cyclical, and were observed rising and falling over individual cells for up to 45 min after the addition of the COM. Untreated MDCK cells, however, did not respond to any rise in signal of Fura-2 ratio signal [Figure 5.18].

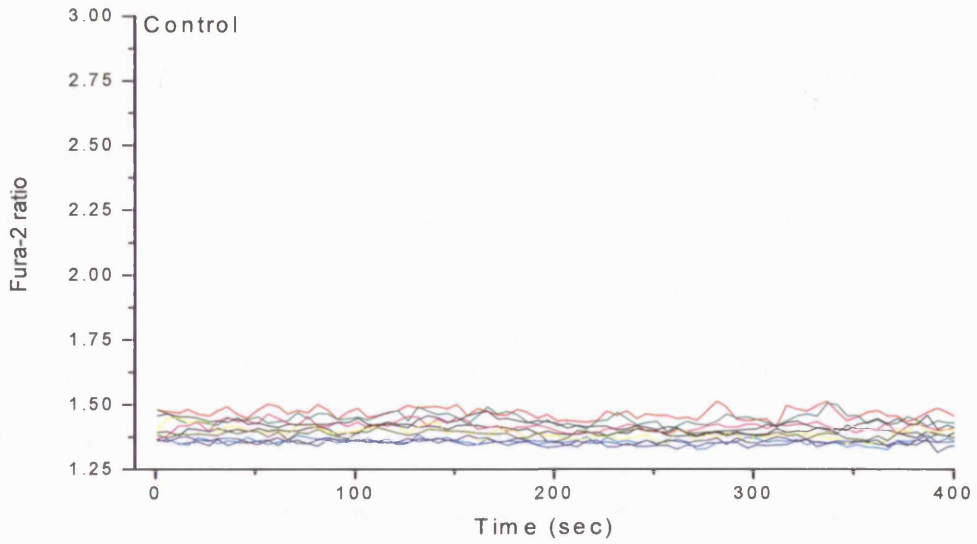


**Figure 5. 18 Changes in [Ca2+] transients observed in untreated MDCK cells.** Each trace represents the ratios of excitation of Fura-2 at 340 and 380 nm over single untreated cell.

Moreover, it should be noted here that the above measurements were made in HEPES buffer containing calcium without EDTA, thus dissociation of calcium and oxalate from the COM treatment would not occur. This indicates that crystal mediated changes of mitochondrial membrane potential and [$Ca^{2+}$] rises could contribute to formation of superoxide. In addition, these are dependent on COM crystal adherence.

## 5.7 DISSCUSSION

It is now well established that cell injury is central to the process of urolithiasis [Wiessner, JH., *et al.,* 2001]. An injury to the epithelial cells results in membrane damage and shedding, which play a critical role in crystal formation as well as crystal retention. Oxidative stress is a recognised source of cell injury and results from increased production of ROS. Although there is evidence that free oxalate ions can mediate oxidative insult, the origin of the ROS in oxalate crystal interactions with renal epithelial cells, is still unknown. This study was conducted to examine and confirm the findings that ROS mainly originates from the mitochondrial compartment.

In order to demonstrate that in this model the lucigenin chemiluminescence signal is derived from the mitochondria, superoxide dismutase (SOD), and MnTMPyP, a small molecular weight cell permeable SOD mimetic were used. Data presented here, showed that the lucigenin chemiluminescence signal was reduced greatly by the membrane permeable SOD mimetic, whereas SOD resulted in a non-significant decrease of the chemiluminescence signal. This non-inhibitory effect of SOD is due to its ability to penetrate only the porated plasma but not the intact mitochondrial membrane. Thus, this confirms that the cytosol is not the primary site of superoxide formation in this model. In contrast to SOD, MnTMPyP can penetrate the mitochondrial membrane and therefore dismutate the superoxide formed in the mitochondria. In addition, incubation of COM treated MDCK cells with MnTMPyP resulted in less superoxide detection than those observed in untreated (control) MDCK cells, implying that MnTMPyP was able to inhibit superoxide derived from

mitochondria under control conditions. Thus, it is now evident that lucigenin-chemiluminescence signal arises due to mitochondrial superoxide.

To further support this finding, selective mitochondrial and cytosolic inhibitors were employed. Results presented here, show that by using cytosolic inhibitors, such as indomethacin, hydrazaline, NDGA, DPI, and oxypurinol, this resulted in increased superoxide formation. This indicates that the lucigenin chemiluminescence signal, derived from COM exposure on MDCK cells, was not due to cytosolic sources of superoxide. On the contrary, employment of mitochondrial inhibitors diminished the chemiluminescence signal, indicating the mitochondrial source of superoxide. It is now established that, in non-inflammatory cells, electron leakage at NADH-ubiquinone reductase (complex I), and ubiquinone-cytochrome c reductase (complex III) during electron transport contribute to superoxide generation [Turrens, JF., *et al.*, 1985; Liu, SS., 1997]. Therefore, when rotenone, a complex I inhibitor, was employed, superoxide production was decreased. In addition, pyruvate diminished chemiluminescence signal by decreasing NADH, and when COM treated MDCK cells were incubated with 4-OHCA that inhibits pyruvate transport into mitochondria, the levels of superoxide formation were further decreased. Furthermore, to investigate whether COM activated superoxide, CCCP, a mitochondrial uncoupler, was used and resulted in abrogated chemiluminescence signal. This indicates a coupled electron transport chain is a requirement for the superoxide production. Similar results were also obtained when TFA, a succinate dehydrogenase inhibitor was used. When oligomycin was employed in the same study, superoxide formation was increased. Oligomycin inhibits ATP synthesis and therefore backs-up electron flow from complex III. In addition, when antimycin A was employed levels of superoxide production were still increased. Antimycin A is a complex III inhibitor, blocks

electron transport from cytochrome b to ubiquinone which is behind the site of superoxide formation in complex III. The presence of antimycin A therefore would cause the electrons to build up, leading to increased superoxide production. This data presented here combined with a previous report by Khand, FD., *et al.,* 2002, confirms and establishes the mitochondrial origin of superoxide under COM exposure on MDCK cells.

In addition, it has been shown in Chapter 4 that COM crystals once internalised into the cells undergo dissociation to free calcium and free oxalate. This part of the study also examined the fate of oxalate once it dissociates from COM and transported into the mitochondria. Further evidence that free oxalate is transported into mitochondria and initiate superoxide formation was provided by the studies with different dicarboxylate transport inhibitors. DCCD, an IMAC inhibitor, and nigericin, a $K^+/H^+$ antiporter inhibitor, both were able to inhibit oxalate transport into mitochondria resulting in no effect on superoxide production mediated by COM. However, both of these inhibitors showed to decrease the levels of superoxide production when MDCK cells were treated with NaOx. However, when these studies were repeated in the same laboratory these findings were not reproducible with DCCD and nigericin showing no distinguishable effect on superoxide formation when MDCK cells were treated with either COM or NaOx. Omitting phosphate from the medium or using mersalyl to inhibit the mitochondrial phosphate-dependent dicarboxylate transporter caused a significant decrease in the superoxide production evoked by COM or NaOx treatment. Mechanisms for the transport of dicarboxylic acids into mitochondria isolated from a wide range of tissues have been demonstrated [Karniski, LP., 1998; Kakhniashvilli, D., *et al.,* 1997; LaNoue, KF., & Schoolwerth, AC., 1979]. In mammalian mitochondria, dicarboxylate transport is mediated by a phosphate-dicarboxylate

exchange [Robinson, BH., & Williams, GR., 1970]. Further evidence for the importance of phosphate-dicarboxylate exchange resulting from the mersalyl experiments, may arise from the sensitivity of dicarboxylate accumulation to uncouplers (CCCP). This type of inhibitor can directly affect internal phosphate uptake, and thus lower the amount of internal phosphate available for exchange with external dicarboxylates such as oxalate.

It has been suggested earlier in this chapter and in other reports from this laboratory [Khand, FD., *et al.,* 2002] that mitochondria are a significant source of the superoxide that is produced in renal cells following exposure to oxalate or to COM crystals. Since perturbations in mitochondrial function, in particular a loss of mitochondrial membrane potential ($\Delta\psi_m$,) are a common occurrence in cell death [Lemaster, JJ., *et al.,* 1999; Kim, JS., *et al.,* 2003], further experimental work was performed to investigate whether COM treatment of renal epithelial cells could trigger a change in $\Delta\psi_m$. A recent study by Cao *et al.,* 2004, has shown that when MDCK cells were exposed to oxalate there was a reproducible decrease in $\Delta\psi_m$. This was assessed by shifts in JC-1 (1,1',3,3'-tetraethylbenzimidazolylcarbocyanine iodide) fluorescence ratios, suggesting that mitochondria are targets for oxalate-induced toxicity [Cao, LC., *et al.,* 2004]. JC-1 is a green fluorescent probe which exists as a monomer at low membrane potentials and forms aggregates at higher potentials. Even though JC-1 has been widely used to estimate qualitative changes in $\Delta\psi_m$ it has been noted [Reers, M., *et al.,* 200] that the equilibrium between monomers, dimmers and polymers may not be solely influenced by changes in $\Delta\psi_m$, since JC-1 is pH-sensitive and its absorption spectrum may be affected by the osmolarity of its environment or by the presence of a dissociated acid. This disadvantage of JC-1 may result in underestimation of the actual changes in $\Delta\psi_m$. Furthermore, in the same study the authors did not account

for any crystals that might have been formed due to the calcium, oxalate and hydrogen ion concentrations in the media. Microcrystals may well have formed and potentially influence cellular processes [Cao, LC., *et al.,* 2004]. It has been shown here for the first time an increase caused by COM crystals on renal mitochondrial polarisation. By employing TMRM, a specific intramitochondrial dye, it was shown that COM causes a marked change in the $\Delta\psi_m$ of cells onto which COM has been attached. It has been known that $\Delta\psi_m$ is a component of the overall proton force that drives the ATP generation in mitochondria [Polyak, K., *et al.,* 1997]. Therefore, this increase in proton gradient is a significant finding as it is known to result in increased electron leakage from the electron transport chain especially during State 4 respiration [Jacobson, J., & Duchen, MR., 2002]. The reasons for this increase in $\Delta\psi_m$ are currently unknown but any inhibition of steps downstream of complex III are potential candidates. In addition, this increase in $\Delta\psi_m$ could be due to disruption of mitochondrial functions on the inner membrane, including the reduction of mitochondrial electron transport flow rate and the instability of $F_0F1$–ATPase to effectively pump protons to the mitochondrial matrix [Gottlob, K., *et al.,* 2001]. An alternative mechanism that could cause the increase in $\Delta\psi_m$ could be due to a defect in adenine nucleotide translocator (ANT) on the inner mitochondria membrane or in the voltage-dependent anion channel (VDAC) on the mitochondrial outer membrane [Vender Heinden, MG., *et al.,* 2000]. A defect in the properties of ANT or VDAC permeabilities may result in the disruption of mitochondrial ATP/ADP exchange with the cytosol [Vender Heinden, MG., *et al.,* 2000]. The inhibition of cytochrome c oxidase by oxalate [Muthukumar, A., & Selvam, R., 1998] may account for the increased electron leakage at ubiquinone oxidoreductase in the inner mitochondrial membrane.

Mitochondrial ROS have previously been shown to induce perturbations in $Ca^{2+}$ signalling [Jacobson, J., & Duchen, MR., 2002]. ROS and mitochondrial $Ca^{2+}$ overload in combination can induce cell death by both apoptotic and necrotic routes. As ROS derived from mitochondria have been shown to induce $Ca^{2+}$ release from intracellular stores, possibly by thiol group modulation [Richter, C., *et al.,* 1995], experiments to investigate whether COM treatment induced cytosolic $Ca^{2+}$ signalling were carried out. Calcium movements of intracellular origin were apparent in cells pre-treated with COM for 4 h and within minutes of applying COM. It should be noted that these measurements were made in HEPES-buffered salts containing calcium without EDTA, and therefore dissociation to oxalate would have not occurred. The absence of EDTA and digitonin in this series of experiments is of great importance, since these conditions mimic physiological ones encountered in human renal tubular cells. In addition, absence of EDTA supports the findings that depolarised mitochondria and changes in $Ca^{2+}$ transients are phenomena observed upon crystal exposure. In contrast, work from this laboratory (data not shown) demonstrated that addition of NaOx (750 μM) induced much smaller $[Ca^{2+}]_c$ signals in a subpopulation of the cells, which were cyclical in some cells but more sustained in others. Furthermore, as the signals were still apparent in the presence of the mitochondrial protonophore FCCP, in which ROS production ceases [Scheid C *et al.,* 1996], the increased production of superoxide is not the cause of large amplitude $[Ca^{2+}]_c$ oscillations. However, it is known that FCCP results in a rapid rise in cytosolic $Ca^{2+}$ originating from the decrease in the proton gradient [Friel, DD., & Tsien, RW., 1994], which could block any potential diminution of the $[Ca^{2+}]_c$ signals resulting from lowered superoxide release. Mitochondria seem to play a role in modulating the COM-induced $Ca^{2+}$ fluctuations, as the $[Ca^{2+}]_c$ rises were more

sustained in the FCCP-treated cells, with fewer repetitive $Ca^{2+}$ oscillations. Previous work [Rizzuto, R., *et al.,* 1998] suggested a privilege access of ER $Ca^{2+}$ to mitochondria. More recent data [Jacobson, J., & Dunchen, MR., 2002] has also shown that oxidative stress increases the probability of $Ca^{2+}$ release from ER. These authors showed that the very close proximity of ER and mitochondria means that $Ca^{2+}$ is accumulated by nearby mitochondria and further sensitises the mitochondria to ROS. Therefore, to investigate whether this also applies in the current study, additional experiments were performed. Specifically, to investigate whether the changes in $[Ca^{2+}]_c$ were due to $Ca^{2+}$ influx from the plasma membrane or were a result of intracellular signalling events resulting in $Ca^{2+}$ release from intracellular $Ca^{2+}$ stores, cells were treated with sarcoplasmic/endoplasmic reticulum calcium ATPase inhibitor thapsigagrin. Thapsigargin induces emptying of intracellular $Ca^{2+}$ stores by blocking reuptake of cytosolic $Ca^{2+}$. Thapsigargin completely prevented COM-induced $Ca^{2+}$ fluctuations in MDCK cells and produced a profile identical to that of control cells (data not shown). This confirms that the $[Ca^{2+}]_c$ signals derived from intracellular stores rather than through extracellular influx or $Ca^{2+}$ derived directly from the COM crystal itself. Dissipation of the mitochondrial proton gradient with FCCP had no effect in the amplitude of these transients. However, their rises were sustained for longer periods, indicating that polarised mitochondria are not necessary for the release of stored $Ca^{2+}$ (data not shown). This observation together with the fact that the fura-2 ratio was initially higher over the FCCP treated cells, implies that MDCK mitochondria take up cytosolic $Ca^{2+}$, modulating the cell signalling cascade induced by COM crystal adherence.

# CHAPTER 6

## Oxalate – mediated stress from renal epithelial cells of different origin and morphology

## 6.1 Introduction

The most widely used cell type to conduct experiments to identify the pathology of the kidney stone disease is the Madin Darby Canine Kidney (MDCK) cells. This cell line forms tight junctions, has the morphological properties of distal tubular epithelial cells and lacks several proximal tubular enzyme markers [Rindler, MG., *et al.*, 1979]. When the cells are cultured on filter membranes, the MDCK cells obtain a morphology that resembles more the *in vivo* situation, and form confluent monolayers, composed of morphologically and functionally polarised cells, with apical and basolateral domains [Barker, G., & Simmons, NL., 1981]. Therefore, this cell line has been used frequently for studies of cellular processes in epithelial cells, and is so far the best characterised epithelial cell line [Simons, K., & Fuller, SD., 1985].

In addition to MDCK cells, Lewis Lung Carcinoma Pig Kidney cells (LLCPK-1), a cell line of renal proximal tubule epithelial cells, is also widely employed to study cell injury when exposed to free oxalate or CaOx crystals. It is thus important to determine the differences in oxidative stress response by epithelial cells lining along various sections of nephron.

The aim of the study presented in this chapter is to demonstrate whether the observed superoxide production is influenced by cell culture on solid plastic culture dishes or on polycarbonate membranes. In addition, this study was conducted to show whether COM and free oxalate treatment on MDCK and human renal epithelial (HK2) cells result in the same degree of oxidative stress in terms of superoxide production.

## 6.2 Oxalate toxicity in MDCK and HK2 cells

Previous work in this laboratory [Khand, FD., *et al.*, 2002], has shown that 250 μg/ml of COM and 1.5 mM of NaOx treatment on MDCK cells cultured on 35 mm dishes, responded to a three-fold increase of superoxide production when compared to untreated cells. To investigate and compare the effect of COM and NaOx treatment between MDCK and HK2 cells, lucigenin-dependent chemiluminescence was used to monitor superoxide production. Specifically, HK2 and MDCK cells were cultured in 35 mm dishes and were pre-incubated with 250 μg/ml COM or 1.5 mM NaOx for 4 h or 15 min, respectively. As indicated in Figure 6.1, superoxide production was significantly increased in COM or NaOx pre-treated HK2 cells. It was also observed that in these human kidney proximal originating cells, free oxalate resulted in a higher, however not significant, production of superoxide than that monitored with COM crystals. Higher levels of superoxide formation were also observed in NaOx treated HK2 cells when compared with NaOx treated MDCK cells.

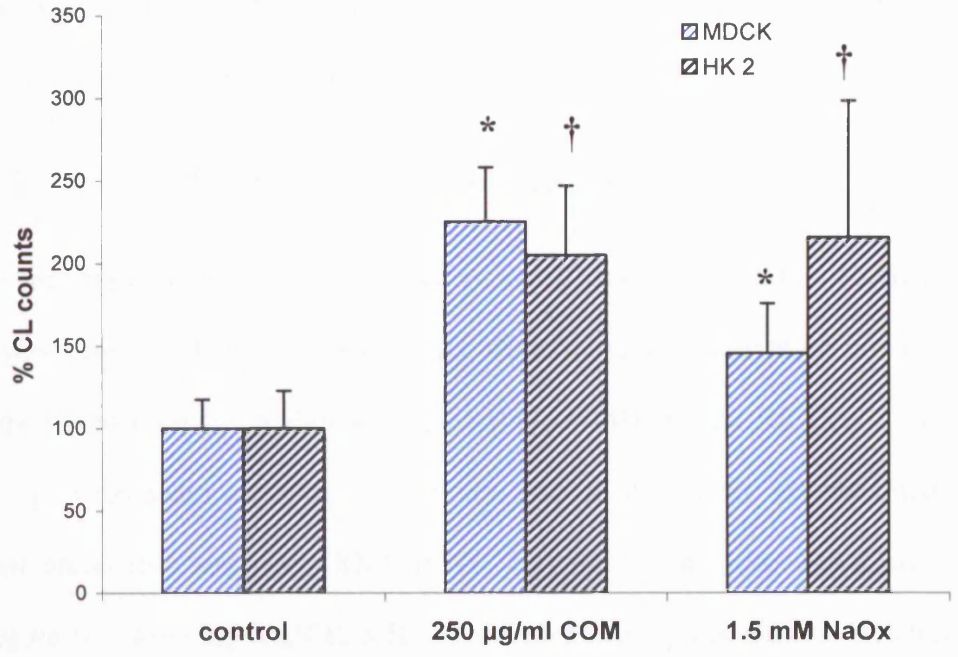


**Figure 6. 1 Superoxide production after COM or NaOx pre-treatment of MDCK and HK2 cells cultured on 35mm dishes.** Percentage of lucigenin chemiluminesence counts after MDCK and HK2 cells were treated with 250 µg/ml COM or 1.5 mM NaOx for 4 h and 15 min respectively. Data are mean ± SD for n=5. *$p<0.05$ and †$p<0.05$ compared with corresponding values for untreated MDCK and HK2 cells, respectively.

In addition, as shown in Figure 6.1, when both MDCK and HK2 cells were treated with COM this resulted in similar levels of superoxide production. This indicates that both cell lines, despite their different origins, resulted in the same response of oxidative damage in terms of levels of superoxide formation detected by lucigenin-dependent chemiluminescence.

## 6.3 Oxalate toxicity in polarised cells

Further experiments were performed to investigate the effect that COM crystals and NaOx have on MDCK and HK2 cells, when these are cultured on porous membrane supports to provide conditions of polarisation. MDCK and HK2 cells were cultured on polycarbonate membrane supports and treated with normal media on the basolateral side and with COM or NaOx at the luminal side. As it can be seen in Figure 6.2, growing MDCK cells on membrane supports did not interfere with the oxidative stress caused by COM crystals or free oxalate. HK2 cells grown on membrane supports responded in similar levels of superoxide formation when exposed to COM crystals, however when treated with free oxalate, superoxide levels were not significantly different compared to the untreated cells.

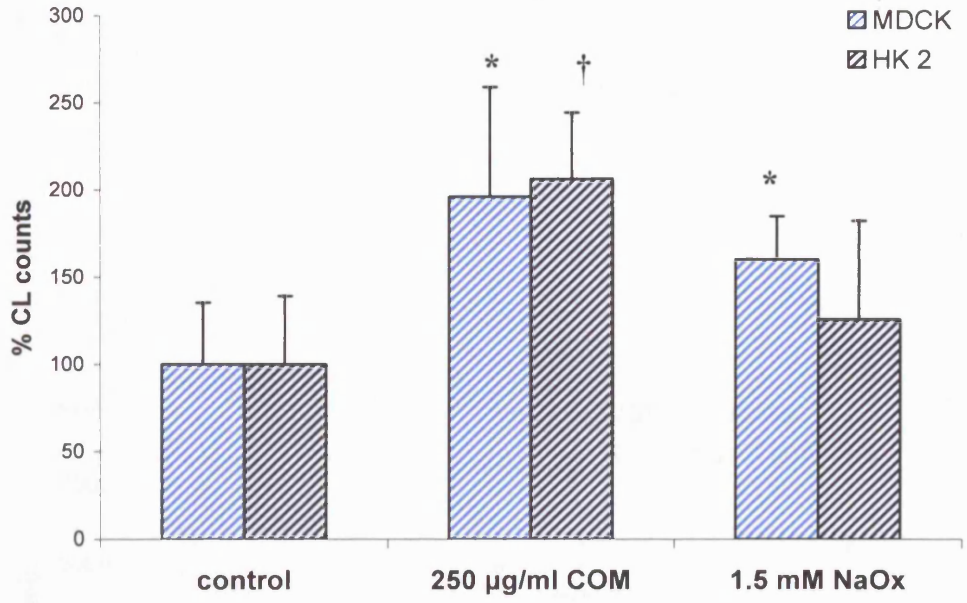


**Figure 6. 2 Superoxide production after COM or NaOx pre-treatment of MDCK and HK2 cells cultured on a polycarbonate membrane.** MDCK and HK2 cells were cultured on a polycarbonate membrane support and were pre-incubated with COM or NaOx for 4 h or 15 min respectively. Data are mean ± SD for n=5 *$p<0.05$ and †$p<0.05$ compared with corresponding values for untreated MDCK and HK2 cells respectively.

In addition, a comparison was made [Figure 6.3] between MDCK cells cultured on a plastic surface or on a polycarbonate membrane support. There was no apparent difference in the levels of superoxide formation between polarised and non-polarised MDCK cells. It was therefore concluded that cell polarisation did not affect the process by which oxalate mediated the mitochondrial superoxide production.

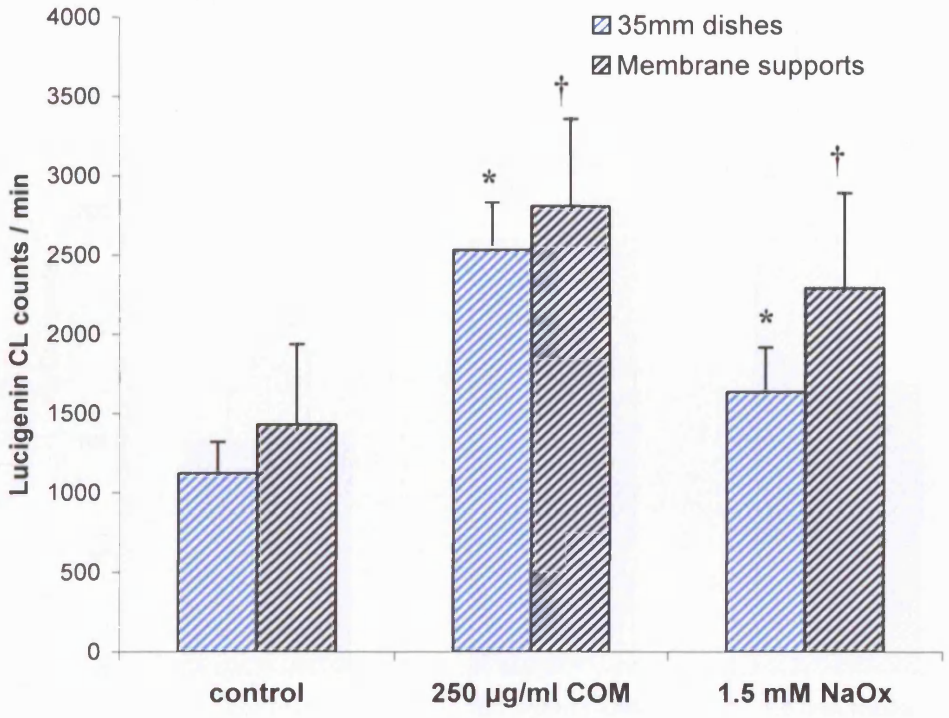


**Figure 6. 3 Superoxide production after COM or NaOx pre-treatment of MDCK cells cultured on a 35 mm dish or on a polycarbonate membrane.** MDCK cells were cultured on a 35 mm dish or on a polycarbonate membrane support and were pre-incubated with 250 µg/ml COM or 1.5 mM NaOx for 4 h or 15 min, respectively. Data are mean ± SD for n=5 *$p<0.05$ and †$p<0.05$ compared with corresponding values for untreated MDCK cells.

The same comparison was performed for HK2 cells. The results [Figure 6.4] demonstrated that oxidative stress manifest by elevated levels of superoxide, was diminished when HK2 cells were cultured on a porous membrane surface and exposed with free oxalate. This indicates that changes of HK2 cell polarity may result in altered oxalate transport mechanism into the cells and subsequently into the mitochondria.

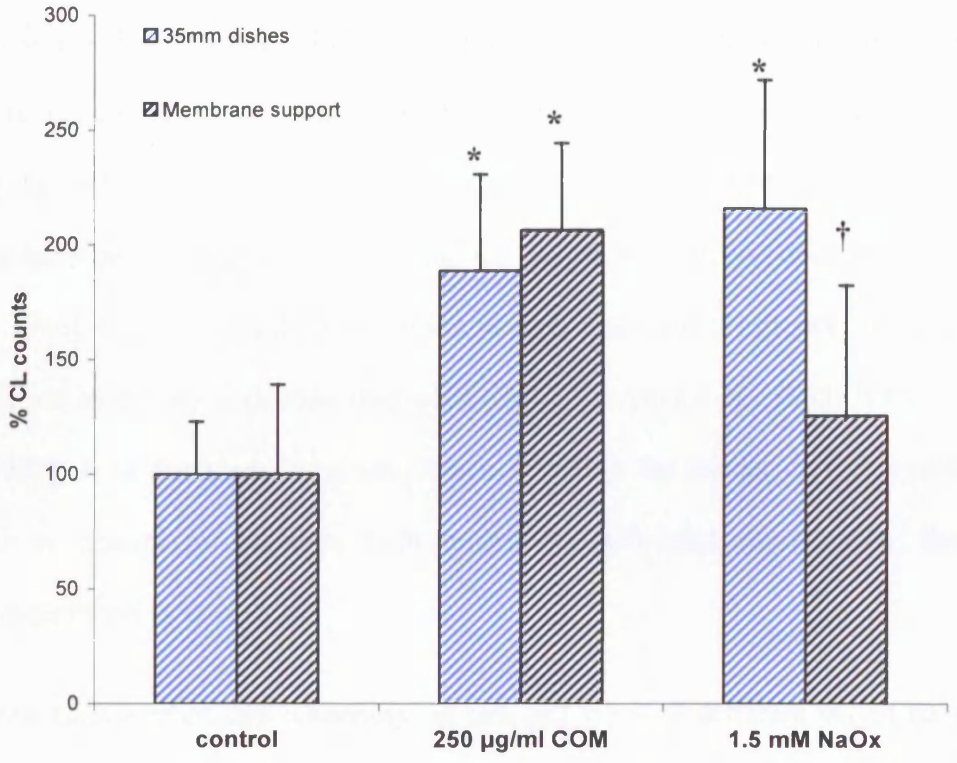


**Figure 6. 4 Superoxide production after COM or NaOx pre-treatment of HK2 cells cultured on a 35mm dish or on a polycarbonate membrane.** HK2 cells were cultured on a 35 mm dish or on a polycarbonate membrane support and were pre-incubated with 250 µg/ml COM or 1.5 mM NaOx for 4 h or 15 min, respectively. Data are mean ± SD for n=5. *$p<0.05$ compared with corresponding values for untreated HK2 cells and †$p<0.05$ compared with oxalate treated cells in 35 mm dish.

## 6.4 DISCUSSION

During the past 100 years, stone formation in the urinary tract has become an increasing problem in most countries of the world [Coe, FL., *et al.*, 2005]. Calcium oxalate monohydrate crystals are the commonest component of kidney stones and their presence in renal cells are known to contribute to the pathology of the disease. The use of renal epithelial cells in tissue culture is an accepted powerful tool used to study physiological and biological cell functions. A number of cell lines with distinct nephron segmental characteristics have been used in the past to study the pathology of kidney stones. For example, LLC-PK1 cells of proximal tubular origin have been used to study oxalate transport mechanisms [Koul, H., *et al.*, 1994; Verkoelen, CF., *et al.*, 1993]. In addition, MDCK cells derived from a normal adult male cocker spaniel kidney have been widely used as a model for the distal collecting duct [Gausch, CR., *et al.*, 1966]. Crystal-cell interactions have also been studied in primary cultures of rat renal inner medullary collecting duct cells (IMCD) [Mandel, N., 1995; Riese, RJ., *et al.*, 1988]. It is therefore important, when selecting the model culture system, to mimic as closely as possible, both morphologically and functionally, the cell phenotype found *in vivo*.

Previous studies from this laboratory on two cell types of different origin had been employed to investigate the effect of crystal-cell interaction in terms of oxidative stress [Khand, FD., *et al.*, 2002]. These authors showed that when MDCK and LLC-PK1 cells were treated with 250 μg/ml COM or 1.5 mM NaOx, a three-fold increase of superoxide formation was observed. Increased levels of superoxide indicate that at this concentration of COM or NaOx, renal cells even of different origin, could undergo oxidative stress mediated cellular injury. Thamilselvan *et al.*, [1999] have

reported cellular injury by demonstrating increased levels of LDH release when both LLC-PK1 and MDCK cells were exposed to COM and NaOx. Furthermore, they have shown that treatment of COM and NaOx together resulted in a more pronounced LDH release from LLC-PK1 cells than that of MDCK cells. Data from this laboratory [Khand, FD., *et al.,* 2002], have also demonstrated that at the lowest and patho-physiological relevant levels of COM (25 μg/ml COM), LLC-PK1 cells loose their sensitivity in terms of oxidative stress and superoxide levels are monitored at basal levels. This indicates that cells of proximal tubule origin are less susceptible to COM initiated oxidative stress at low crystal deposition, implying that in the proximal tubule region of the kidney, patho-physiological levels of calcium oxalate crystals are unlikely to cause damage.

Both of the cell model systems employed in these studies originate from animal cell lines. In order to confirm the above findings and validate the model system used to study oxidative stress in cultured renal epithelial cells mediated by crystal-cell interaction, it is important to examine if a cell line originating from human epithelial (HK2) cells, elicits the same response. Data shown in this chapter, demonstrated that when HK2 and MDCK cells were treated with 250 μg/ml COM or 1.5 mM NaOx, a response with similar significantly increased superoxide levels when compared to untreated cells was observed. In addition, there was no significant difference in oxalate mediated oxidative stress in terms of superoxide production, between COM treated MDCK and HK2 cells. Therefore, the MDCK cell line can be considered as a valid system of study since it performs comparably to that of a human cell phenotype. Furthermore, the distal tubule is the most likely location within the nephron for COM crystal exposure to arise. Supersaturation of tubular fluid with respect to calcium oxalate, at the end of the descending limb of the Loop of Henle indicates that calcium

oxalate may nucleate in this region [Asplin, JR., *et al.,* 1996; Kok, DJ., & Khan, SR., 1994].

The experimental studies carried out in this work, have been performed in cell culture on 35 mm plastic culture dishes. It has been shown that cells cultured on a permeable substrate obtain higher levels of differentiation than cells cultured on solid plastic dishes [Handler, JS., 1989]. This cell polarisation has been shown to lead to alteration of binding properties of crystals [Verkoelen, CF., *et al.,* 1997]. In order to examine whether different culture conditions may lead to different experimental behaviour, both MDCK and HK2 cells were cultured on polycarbonate membrane supports. Treatments were performed in an identical way as mentioned above and superoxide formation was monitored. Results shown here, demonstrated a two-fold increase of superoxide production when COM treated cells were grown on membrane supports compared to untreated cells. In addition, there was no significant difference when superoxide levels were compared between COM treated cells cultured on 35 mm dishes and COM treated cells grown on membrane supports. This indicates that in this study, binding of crystals did not depend on the polarity of the surface on which crystals attach. This finding contrasts with that reported by Verkoelen, CF., *et al.,* [1997], were they showed that the ability of crystals to adhere to the cells, varied according to culture protocols used. This difference in observations may be due to different cell density and culture duration. In particular, in the work of Verkoelen [1997] cells were seeded at 1 x $10^6$ density and cultured from 0-10 days and this author showed that after 4 days in culture, crystal binding was different between cell growth conditions. In this study, cells were seeded at twice the cell density and were cultured for only two days prior to treatment. At this time-point where MDCK cells were grown to form confluent monolayers, Verkoelen *et al.,* [1997] had also reported

the same crystal binding ability on different growth substrates. However, in the same study these authors suggested that when MDCK cells continued to proliferate and form multilayers, crystal binding was decreased. This crystal adherence property exhibited by intact monolayers did not differ between cells cultured on permeable or impermeable growth substrates. This indicates that surface differences on which cells were grown did not contribute to COM-cell interactions. This includes changes to intercellular junctions as well as polarisation associated with dome cell–formation [Rothen-Rutishauser, *et al.,* 1998]. Therefore, the present study demonstrated that these changes in cellular differentiation had no quantitative or qualitative effects on COM – mediated superoxide production.

From the above findings it was concluded that MDCK, LLC-PK1 and HK2 cell lines provide a suitable model system to study cellular processes involved in renal stone pathology. In addition, having shown how a cell line of human origin responds in the tissue culture environment, it is important to examine how this is related to the *in vivo* studies.

# CHAPTER 7

## Changes in mitochondrial glutathione and energy homeostasis in a rat model of calcium oxalate urolithiasis

## 7.1 INTRODUCTION

Kidney stone formation is a complex process and involves a cascade of events, including crystal nucleation, growth and aggregation, retention within the renal tubules, and migration to the renal papillary surfaces [Khan, SR., 1995]. Hyperoxaluria is a major risk factor of human idiopathic calcium oxalate disease and leads to increased calcium oxalate supersaturation and calcium oxalate stone formation [Asplin, JR., 2002]. In addition, hyperoxaluria can provoke calcium oxalate nephrolithiasis in both humans and rats. Oxalate metabolism is considered to be almost identical between rats and humans. Thus, there are many similarities between experimental nephrolithiasis induced in rats and human kidney stone formation. A rat model of calcium oxalate nephrolithiasis has been used to investigate the mechanisms involved in human CaOx kidney stone formation.

Previous reports have shown that CaOx kidney stones in rats can be produced by the induction of acute or chronic hyperoxaluria using a variety of agents such as sodium oxalate, ethylene glycol (EG), and glycolic acid [Khan, SR., 1991; Khan, SR., & Hacket, RL., 1987]. Furthermore, other studies have shown that hyperoxaluria together with hypercalciuria can also contribute to the pathogenesis of kidney stones [Halabe, A., 2003; de Water, R., *et al.,* 1996]. Specifically, administering rats with vitamin $D_3$ which plays an important role in calcium homeostasis, can induce hypercalciuria. Hence, in a chronic rat model based on EG and vitamin $D_3$ diet, crystal deposition was observed.

As it has been shown in a previous chapter (Chapter 3), using MDCK cells exposed to COM as a model, an increased oxidative stress in terms of superoxide production was observed. In addition, it has been shown that increased levels of superoxide in

response to injury, originates from the mitochondria, which consequently results in depletion of mitochondrial glutathione.

According to the above findings, the aim of the current study was to examine whether oxidative stress, which occurs as a result of the interaction between calcium oxalate crystals and tubular epithelial cells in culture, also occurs in an animal model of hyperoxaluria and hypercalciuria.

## 7.2 Urinary oxalate and calcium concentrations

Early urine crystal formation was checked by light microscopy. Freshly passed urine collected 24 h after the start of EG feeding was clear of crystals and throughout the study urine remained either free of crystals or exhibited only slight crystal presence. Three hours after administration of DHC in EG-fed animals, crystal formation was observed (data not shown), whereas in animals treated only with DHC, crystal formation was either not detected or slight crystal nucleation was observed. This situation maintained throughout the 3 weeks of treatment.

The concentration of urinary free oxalate [Table 7.1] was also measured by conductivity after ion chromatography, ionised calcium concentrations, and urine pH as shown in Table 7.2, and Table 7.3. The crystalluria group (EG + DHC) had significantly lower oxalate levels than the EG alone group. This is a result of a proportion of the free oxalate being excreted as crystals, which are removed from the urine before analysis.

**Table 7. 1 Urinary oxalate (mM) in hyperoxaluric, calciuric and crystalluric animals.** Values are means ± SD. EG, ethylene glycol; DHC, 1,25 – dihydroxycholecalciferol.

| | Week1 | Week2 | Week3 |
|---|---|---|---|
| Control | 0.91±0.11 | 1.12±0.16 | 140±23 |
| EG | 6.3±0.75 | 7.03±0.66 | 158±19 |
| DHC | 1.1±0.19 | 0.89±0.14 | 411±56 |
| EG+DHC | 4.2±0.60 | 4.6±0.78 | 345±60 |

**Table 7. 2 Urinary ionised Calcium (µM) in hyperoxaluric, calciuric and crystalluric animals.** Values are means ± SD. EG, ethylene glycol; DHC, 1,25 – dihydroxycholecalciferol.

| | Week1 | Week2 | Week3 |
|---|---|---|---|
| Control | 185±31 | 156±29 | 0.95±0.12 |
| EG | 144±19 | 165±23 | 7.11±0.86 |
| DHC | 475±32 | 466±55 | 1.25±1.9 |
| EG + DHC | 401±58 | 396±61 | 4.71±0.54 |

**Table 7. 3 Urinary pH in hyperoxaluric, calciuric and crystalluric animals.** Values are means ± SD. EG, ethylene glycol; DHC, 1,25 - dihydroxycholecalciferol

| | Week1 | Week2 | Week3 |
|---|---|---|---|
| Control | 7.1±0.4 | 7.4±0.5 | 6.9±0.4 |
| EG | 7.6±0.5 | 8.2±0.5 | 8.4±0.6 |
| DHC | 6.4±0.4 | 6.9±0.6 | 6.8±0.6 |
| EG + DHC | 7.3±0.3 | 7.2±0.3 | 7.8±0.6 |

## 7.3 Kidney hypertrophy in nephrolithic rats

As shown in biodata [Table 7.4], animal body weight did not differ between experimental groups and throughout treatment. On the contrary, kidney hypertrophy was observed by the end of the treatment course [Figure 7.1] in the crystalluric (EG + DHC) experimental group. Kidney weight was significantly increased by the end of week 1 in hyperoxaluric (EG), hypercalciuric (DHC), and crystalluric groups when compared with the untreated group (control) [Figure 7.2]. In the following weeks 2 and 3 this increase was only observed in the EG + DHC group whereas in EG and DHC groups, kidney weight maintained at the control levels. Fluid intake was also significantly increased in the EG + DHC group but not with the EG or DHC treatment alone [Table 7.4].

**Table 7. 4 Changes observed in animal weight (g), kidney weight (g), and water intake per ml per rat per day, throughout the 3 week course treatment.**

| | | Control | EG | EG+ DHC | DHC |
|---|---|---|---|---|---|
| **week 1** | Rat weight (g) | 262 ± 9.07 | 250 ± 14.98 | 227 ± 23.67 | 253 ± 5.29 |
| | Kidney weight (g) | 0.66± 0.03 | 1.00± 0.12 | 1.43 ± 0.01 | 0.87 ± 0.09 |
| **week 2** | Rat weight (g) | 293 ± 4.73 | 299 ± 15.87 | 221 ± 17.52 | 281 ± 9.07 |
| | Kidney weight (g) | 0.86 ± 0.13 | 1.00 ± 0.13 | 1.70 ± 0.1 | 0.97 ± 0.07 |
| **week 3** | Rat weight (g) | 264 ± 60.81 | 301 ± 4 | 257 ± 11.02 | 296 ± 3.4 |
| | Kidney weight (g) | 1.03 ± 0.04 | 1.04 ± 0.07 | 1.71 ± 0.04 | 0.95 ± 0.11 |
| | Water intake (over 3 weeks) (ml/rat/day) | 32.8 ± 8 | 40 ± 9 | 56 ± 13 | 39 ± 7 |

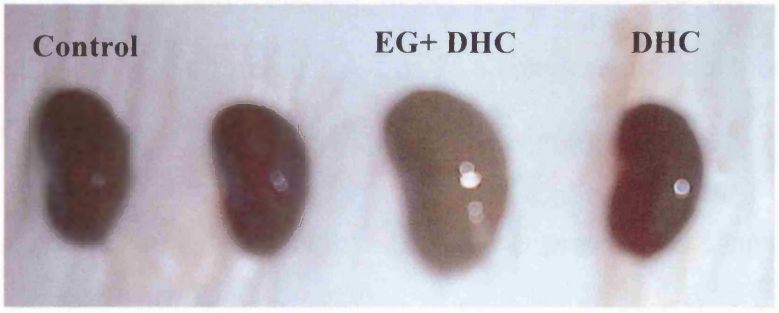


**Figure 7. 1 Kidney hypertrophy in the crystalluric group.** Photographic images of the kidneys from control, ethyl glycol fed (EG), ethyl glycol + DHC (EG + DHC), and 1, 25-dihydroxycholecalciferol (DHC) groups excised at the end of experimental week 3.

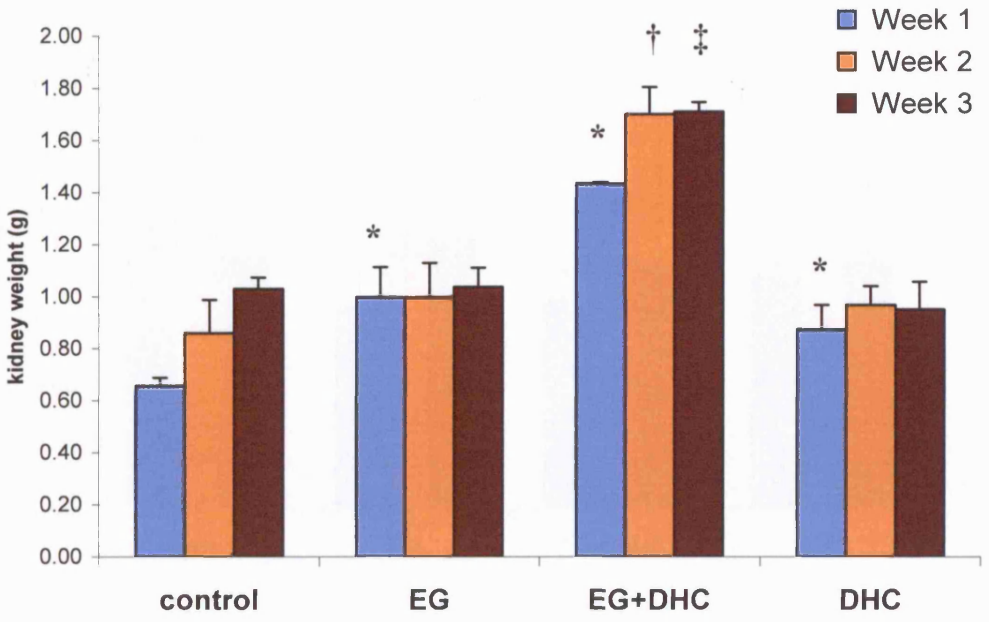


**Figure 7. 2 Changes in kidney weight during the 3 weeks treatment.** Kidneys from control, ethyl glycol fed (EG), ethyl glycol + DHC (EG + DHC), and DHC groups, excised at the end of experimental weeks 1, 2, and 3 and their weight (g) was determined. Mean ± SD for n=3; * $p < 0.05$ vs untreated animals (control) at week 1, † $p < 0.05$ vs control at week 2, and ‡ $p < 0.05$ vs control at week 3.

To investigate kidney hypertrophy formation, protein concentration in kidney homogenates was measured. As shown in Figure 7.3, protein concentration in the kidney did not change between the experimental groups and throughout the 3 week treatment course. Therefore, total kidney protein does not account for kidney hypertrophy. On the contrary, fluid intake was significantly increased by 70 % in the EG + DHC treated rats but not in the groups treated with EG and DHC alone. Therefore, increase in weight of the nephrolithic (EG + DHC) kidney may be due to water retention [Table 7.4]. This is in line with reports showing that hypercalciuria is known to lead to tubular fluid retention [Lieske, JC., & Toback, FG., 2000].

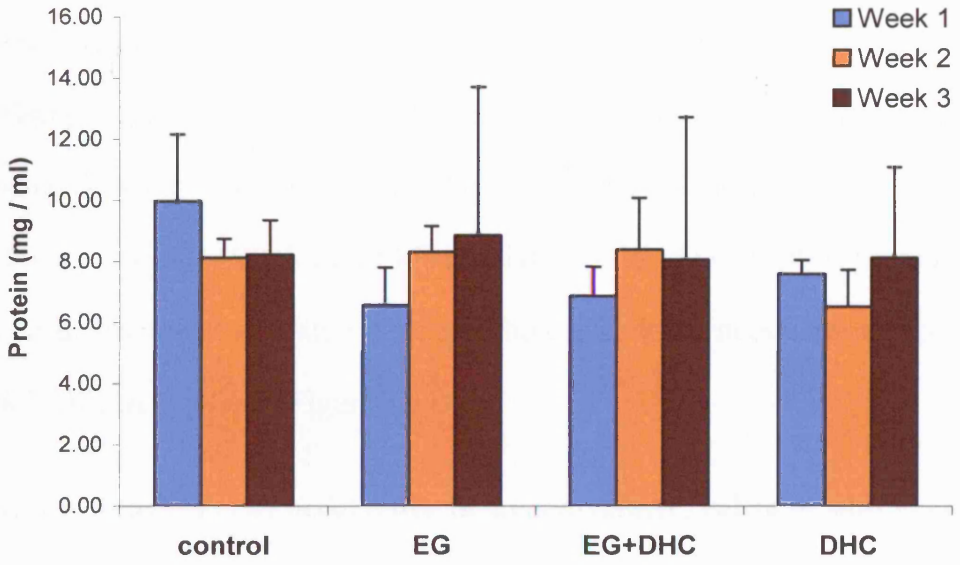


**Figure 7. 3 Total kidney protein in hyperoxaluric, calciuric and crystalluric animals.** Kidneys from control, ethyl glycol fed (EG), ethyl glycol + DHC (EG + DHC), and DHC groups, homogenised and protein concentration (mg / ml) was determined using the BCA protein assay. Mean ± SD for n=3.

## 7.4 Kidney morphology and pathology

To examine renal histopathology, H & E stained sections of kidney were examined by polarisation and light microscopy (all data are summarised in Table 7.5). Histological examination revealed that kidney tubules from EG + DHC treated animals after week 1 treatment, were distended when compared with the compact and higher density of distal tubules from untreated animals [Figure 7.4 A]. In addition, crystal formation was observed in the lumen and within tubular cells even after week 1 in EG + DHC treatment [Figure 7.4 B]. Renal crystal formation was increased at 2 weeks after EG + DHC as was the tubular distension. Interstitial inflammation with focal infiltrates of

inflammatory cells consisting largely of polymorphic granulocytes and lymphocytes was also observed after 2 weeks EG + DHC treatment [Figure 7.4 C and Figure 7.4 D]. These changes were even more prominent by week 3 of treatment with the kidney containing larger crystals and widely distended tubules. Furthermore, loss of renal epithelial cells was observed by the end of week 3 EG + DHC treatment [Figure 7.5 A and Figure 7.5. B]. Histology of kidney tissue of the EG or DHC treated animals showed an absence of crystals and no morphological differences when compared with controls [Figure 7.5 C and Figure 7.5 D].

**Table 7.5 Renal crystal occurrence in hyperoxaluric, calciuric and crystalluric animals**. —,Absent; +, small and infrequent crystals; + +, medium-sized and moderate crystal occurrence; + + +, large and frequent crystal occurrence

| | Control | 0.5% EG | DHC | EG + DHC |
|---|---|---|---|---|
| Week 1 | — | — | — | + + |
| Week 2 | — | + | + | + + + |
| Week 3 | — | + | + | + + + |

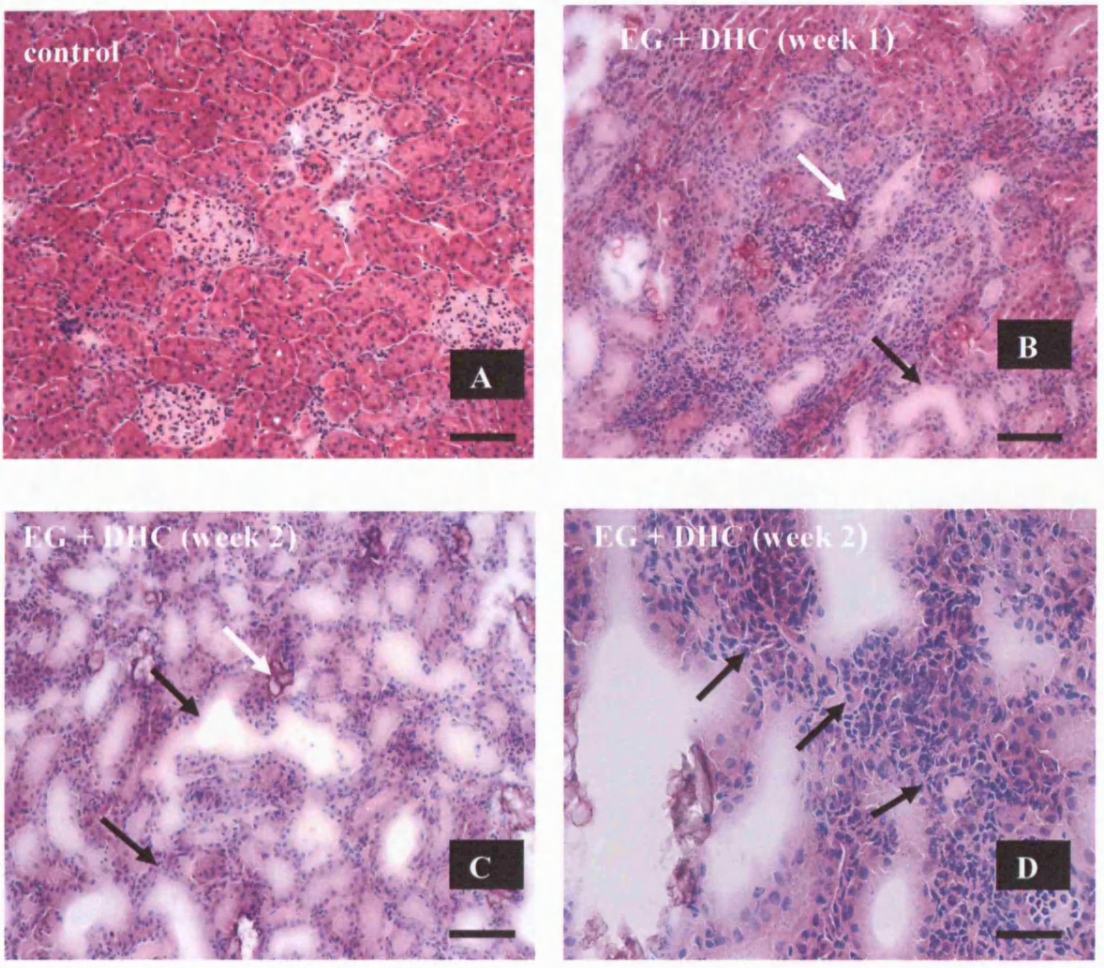


**Figure 7. 4 Haematoxylin staining of kidney tissue from hyperoxaluric, calciuric, and crystalluric animals. (A)** Histological examination of control kidney with compact distal tubules **(B)** kidney sections of EG + DHC treated group at week 1 with white arrows showing crystal deposition and black arrows distended distal tubules **(C)** kidney sections of EG + DHC treated group at week 2 with white arrows showing increased crystal formation and black arrows pronounced tubular distension **(D)** kidney sections of EG + DHC treated group at week 2 with black arrows showing inflammatory cells. Scale bars represent 100 μm.

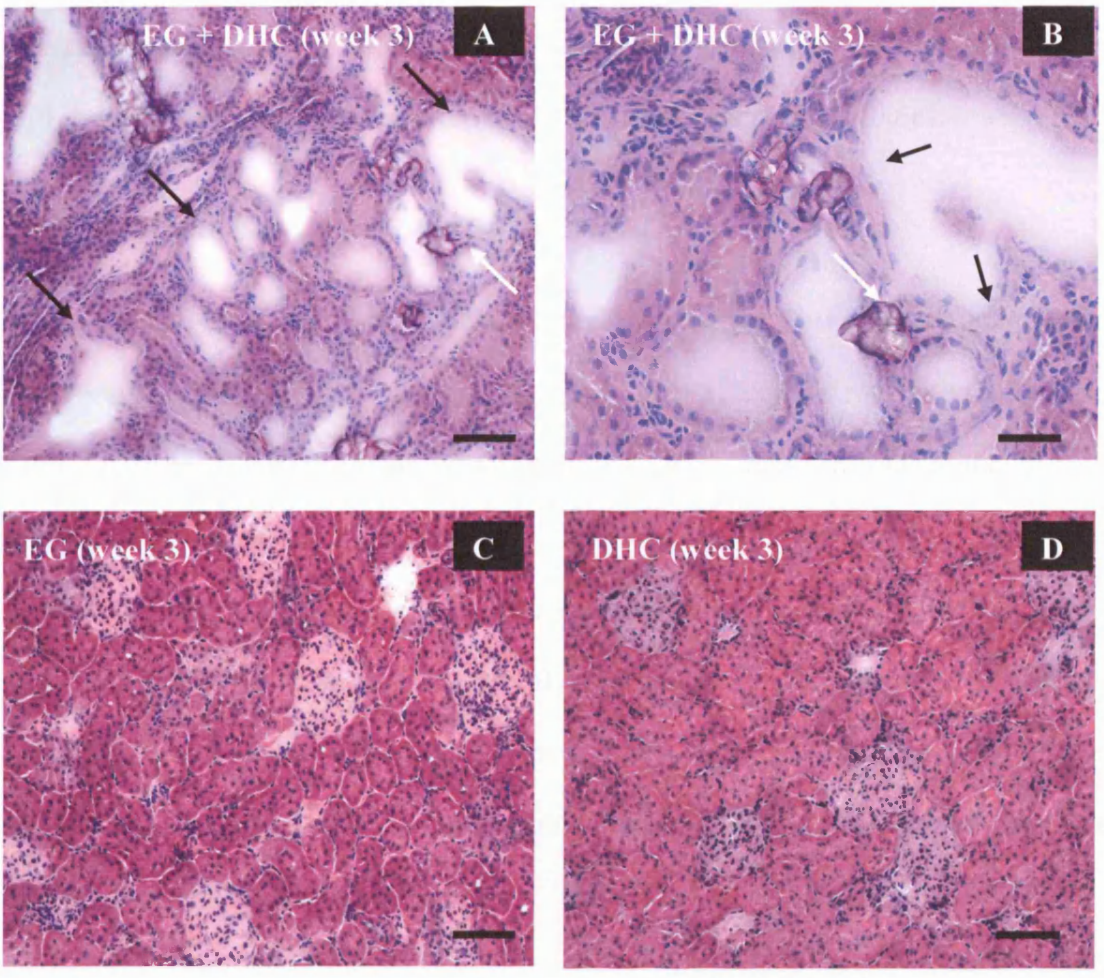


**Figure 7. 5 Haematoxylin staining of kidney tissue from hyperoxaluric, calciuric, and crystalluric animals at week 3. (A)** kidney sections of EG + DHC treated group at week 3 with white arrows showing increased crystal formation and black arrows pronounced tubular distension and **(B)** loss of epithelial cells indicated by black arrows. Histology of kidney tissues of the EG **(C)** and DHC **(D)** treated groups at week 3 treatment. Scale bars represent 100 μm.

Having observed these morphological changes and differences between the nephrolithic and non-nephrolithic groups, further studies were performed to assess changes occurring at the cellular and biochemical level under the oxidative insult initiated by the deposition of calcium oxalate crystals in the renal tubules.

## 7.6 Glutathione in nephrolithic rats

Total cell and mitochondrial glutathione levels, over the 3 weeks treatment were monitored to investigate any changes occurring in the kidneys of rats with crystalluria during the process of stone formation. There was a decrease in total mitochondrial glutathione by week 1 in all of the experimental groups [Figure 7.6], but it was most severely depleted in the EG + DHC group. After weeks 2 and 3, the EG + DHC treated group had retained these markedly low levels of glutathione, indicating an excessive oxidative stress. In the EG or DHC fed groups, total glutathione was restored back to the control levels, implying that they were able to recover from the initial hyperoxaluric and calciuric shock.

In addition, glutathione in the whole homogenate [Figure 7.7] and cytosolic fractions [Figure 7.8] were also measured and showed a similar pattern of decrease throughout the three-week course treatment in the EG + DHC group.

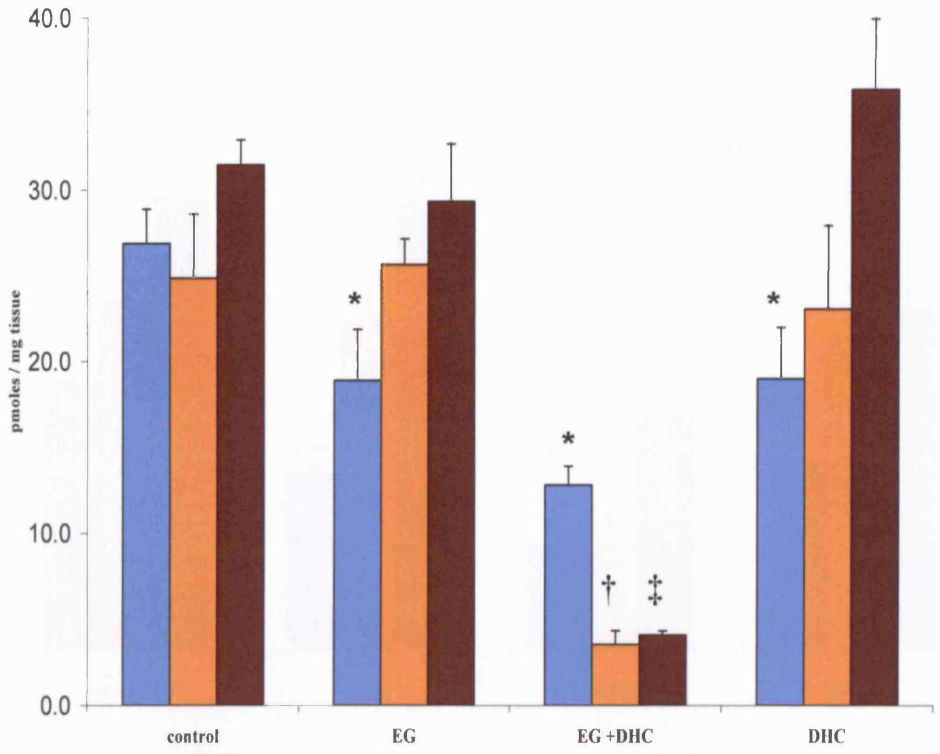


**Figure 7. 6 Total mitochondrial GSH levels in hyperoxaluric, calciuric, and crystalluric kidneys**. Total glutathione measured in the mitochondrial fractions of experimental groups (control, EG, EG + DHC, and DHC) at the end of week 1, 2, 3. Values presented as a percentage relative to the controls. Mean ± SD for n=3; * $p <$ 0.05 vs control at weeks 1, † $p$ and ‡ $p < 0.01$ vs control at weeks 2, 3 respectively.

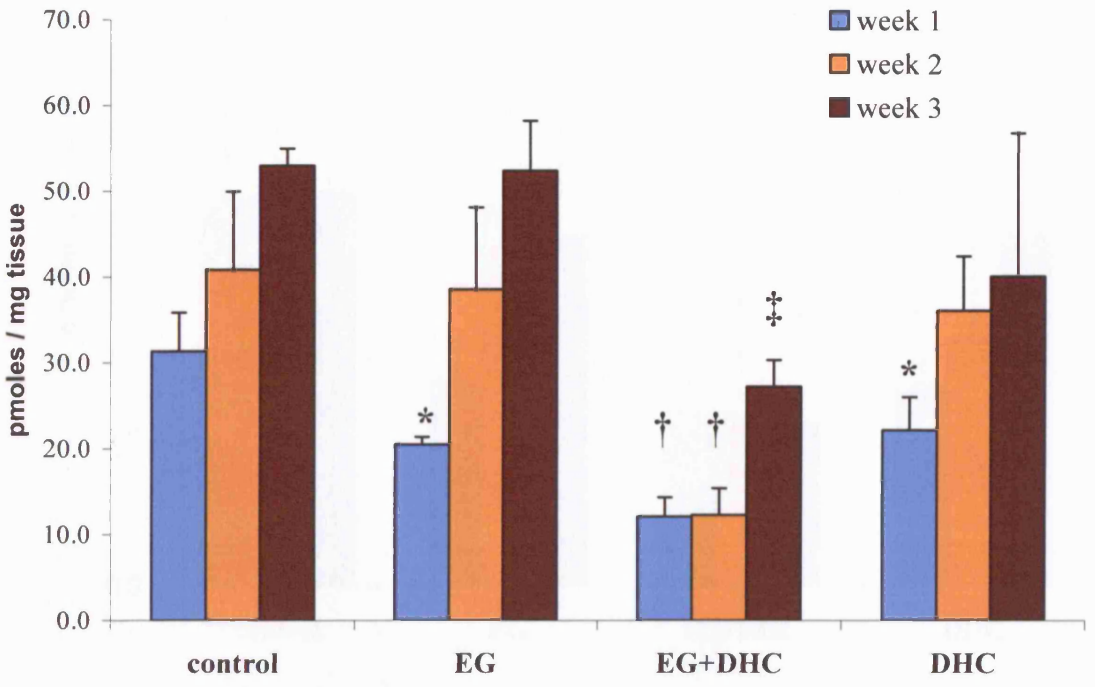


**Figure 7. 7 Total whole homogenate GSH levels in hyperoxaluric, calciuric, and crystalluric kidneys.** Total glutathione measured in the whole homogenate fractions of experimental groups (control, EG, EG + DHC, and DHC) at the end of week 1, 2, 3. Values presented as pmoles / mg of tissue. Mean ± SD for n=3; * $p < 0.05$ vs control at weeks 1, † $p$ and ‡ $p < 0.01$ vs control at weeks 1, 2, 3.

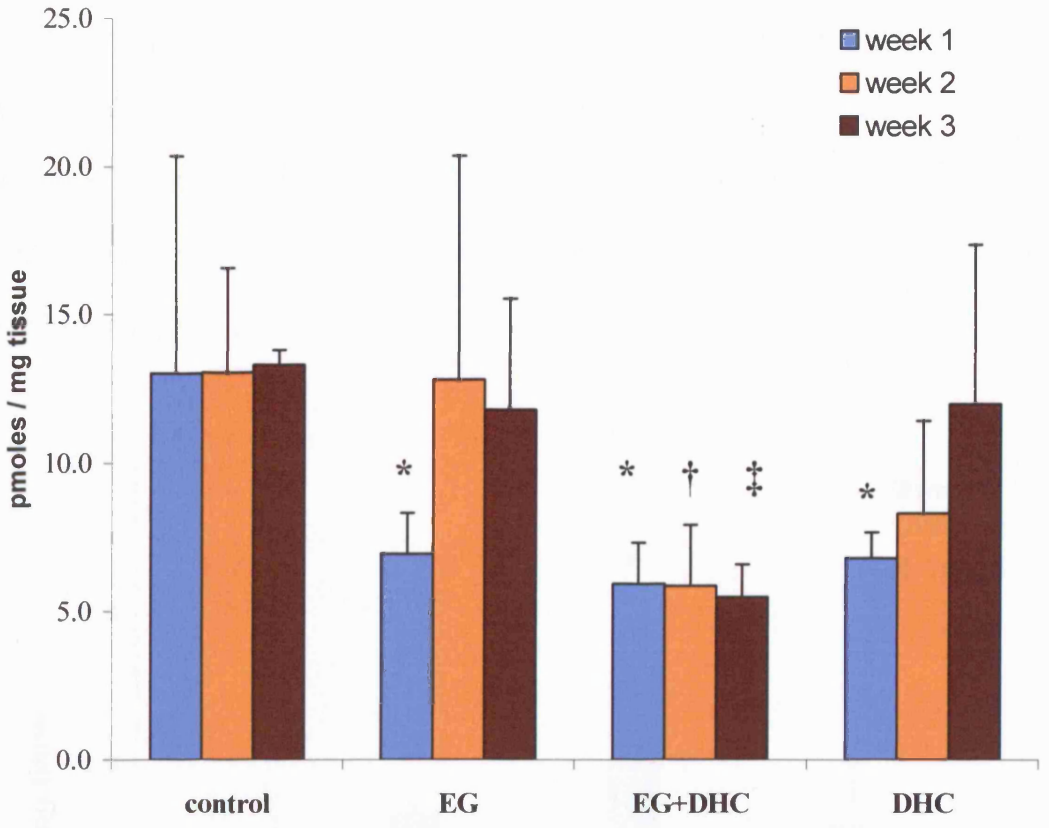


**Figure 7. 8 Total cytosolic GSH levels in hyperoxaluric, calciuric, and crystalluric kidneys.** Total glutathione measured in the whole cytosolic fractions of experimental groups (control, EG, EG + DHC, and DHC) at the end of week 1, 2, 3. Values presented as pmoles / mg of tissue. Mean ± SD for n=3; * $p < 0.05$ vs control at weeks 1, † $p$ and ‡ $p < 0.05$ vs control at weeks 2, 3.

## 7.7 Antioxidant enzymes in nephrolithic rats

To further confirm that crystal deposits and crystalluria initiate an oxidative insult, experiments were carried out to examine the levels of antioxidant enzymes responding to this insult. Specifically, glutathione peroxidase [Figure 7.9] and glutathione reductase [Figure 7.10] were measured in the mitochondrial fraction and showed similar profiles.

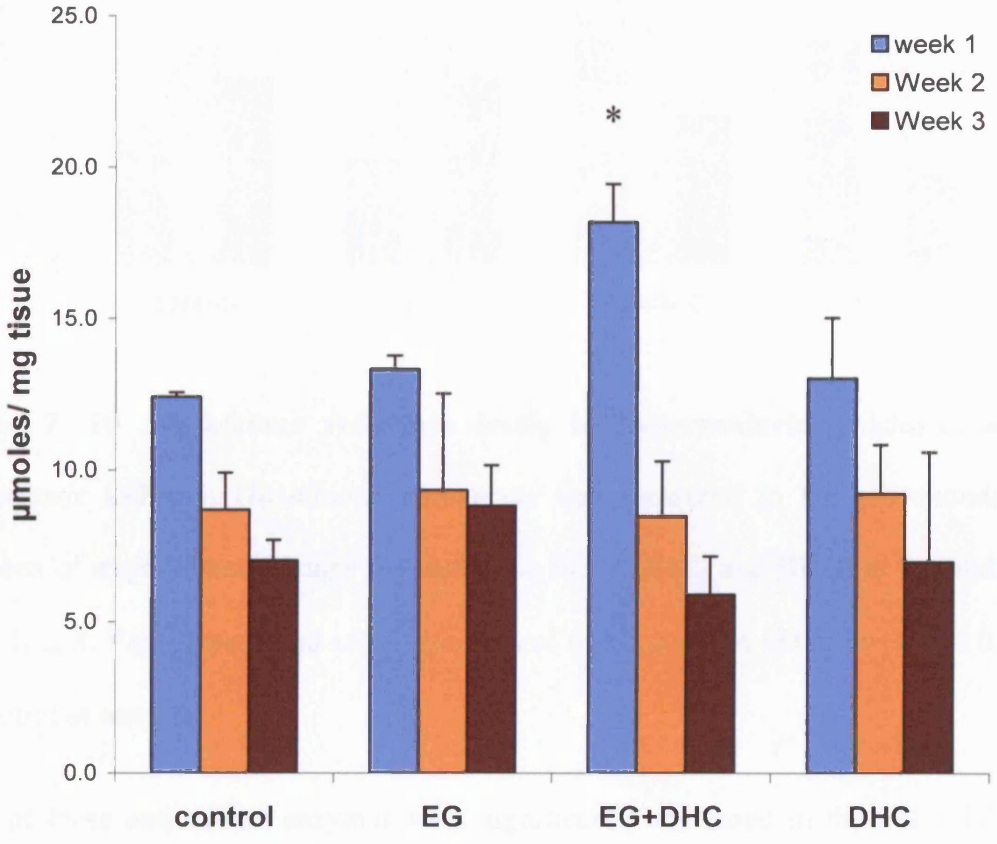


**Figure 7. 9 Glutathione peroxidase levels in hyperoxaluric, calciuric, and crystalluric kidneys.** Glutathione peroxidase was measured in the mitochondrial fractions of experimental groups (control, EG, EG + DHC, and DHC) at the end of week 1, 2, 3. Values presented as µmoles / mg of tissue. Mean ± SD for n=3; * $p <$ 0.05 vs control at weeks 1.

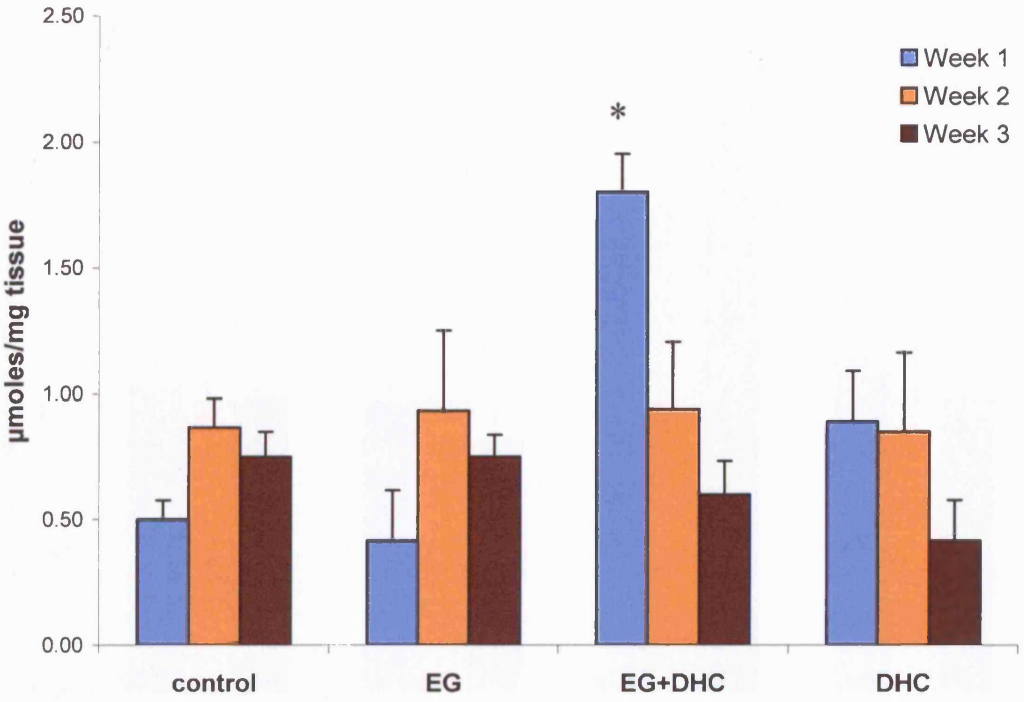


**Figure 7. 10 Glutathione reductase levels in hyperoxaluric, calciuric, and crystalluric kidneys.** Glutathione peroxidase was measured in the mitochondrial fractions of experimental groups (control, EG, EG + DHC, and DHC) at the end of week 1, 2, 3. Values presented as µmoles / mg of tissue. Mean ± SD for n=3* $p < 0.05$ vs control at week 1.

Both of these antioxidant enzymes were significantly increased in the EG + DHC group after week 1 of treatment, indicating that the kidney initially increased antioxidant activity to cope with increased oxidative stress. However, in the following weeks glutathione peroxidase and reductase were restored to control levels. G-6PDH levels were markedly increased in the EG + DHC group throughout the whole 3 weeks treatment [Figure 7.11], hence maintaining reduced glutathione and a supply of reducing equivalents in the form of NADPH.

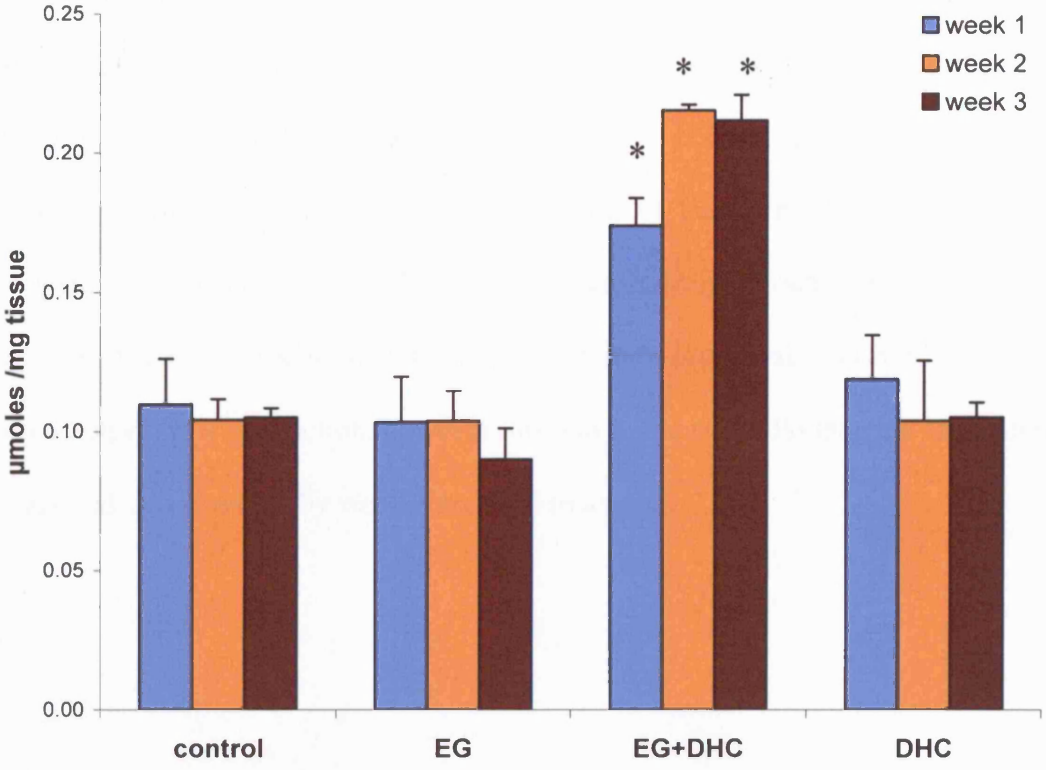


**Figure 7. 11 Glucose-6-phosphate dehydrogenase (G-6PDH) levels in hyperoxaluric, calciuric, and crystalluric kidney.** G-6PDH measured in the cytosolic fractions of experimental groups (control, EG, EG + DHC, and DHC) at the end of week 1, 2, 3. Values presented as µmoles / mg of tissue. Mean ± SD for n=3; * $p < 0.05$ vs control at weeks 1, 2, 3.

## 7.7 Superoxide Monitoring

In order to provide further evidence of oxidative stress in this nephrolithic animal model, superoxide production was also monitored in the kidney mitochondria. Mitochondrial superoxide production from the EG + DHC group was markedly decreased (> 90 %) throughout the whole course of treatment [Figure 7.12]. This phenomenon implies that EG + DHC causes severe kidney mitochondrial damage. At week 1 both the hyperoxaluria and the hypercalciuria groups also showed decreased levels of superoxide production, however this was lower (< 40 %) than the crystalluria animals and was reversed by week 2 and 3 of treatment.

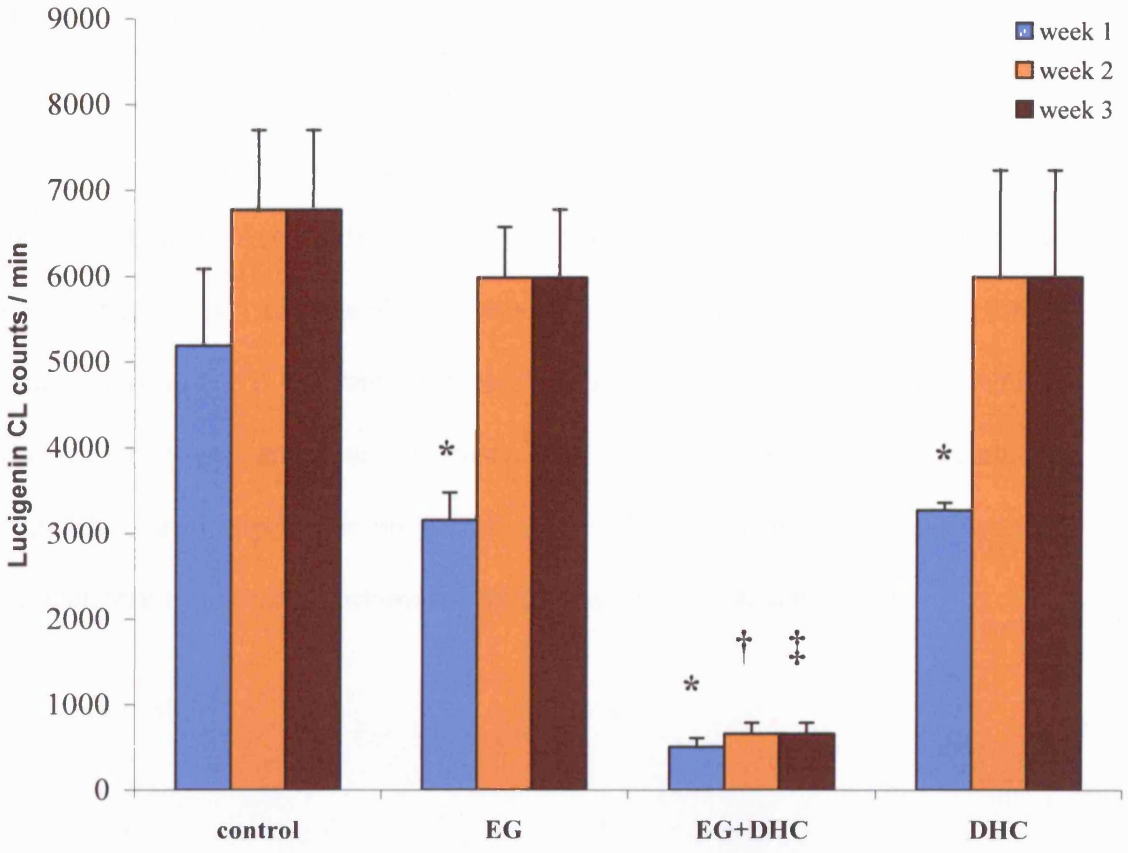


**Figure 7. 12 Superoxide production in hyperoxaluric, calciuric, and crystalluric kidneys.** Superoxide formation as measured by lucigenin chemiluminescence in the mitochondrial fractions of experimental groups (control, EG, EG + DHC, and DHC) at the end of week 1, 2, 3. Mean ± SD for n=3; * $p$, †$p$, and ‡ $p < 0.01$ vs control at weeks 1, 2, 3.

## 7.9 Oxygen consumption rates

Mitochondrial oxygen consumption was measured to investigate if the electron transport chain was a potential source of the observed changes in superoxide production. Oxygen consumption in kidney mitochondria of EG or DHC groups and in the presence of malate and pyruvate, complex I substrates, was not significantly changed compared to the control [Figure 7.13 and Figure 7.14]. However, in the nephrolithic kidney (EG + DHC) group, the rate that oxygen was consumed in the presence of complex I substrates, was reduced to 80 % after weeks 2 and 3. Using succinate, a complex II substrate, [Figure 7.15 and Figure 7.16] the same level of diminution of oxygen rates was observed. The oxygen consumption data combined with monitoring of superoxide production provide strong evidence that nephrolithic kidneys undergo a severe mitochondrial dysfunction in this animal model.

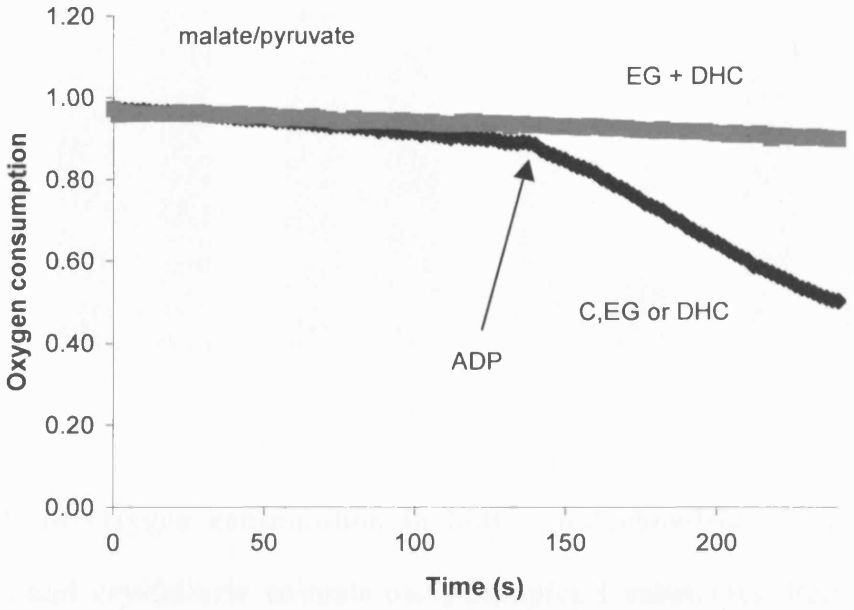


**Figure 7. 13 Oxygen consumption rates in hyperoxaluric, calciuric, and crystalluric kidneys at week 1 using complex I substrates.** Representative plot of oxygen consumption by mitochondria from control, EG or DHC treated animals using malate/pyruvate; lower line and EG + DHC; upper line. Addition of ADP (state III respiration) denoted by arrow.

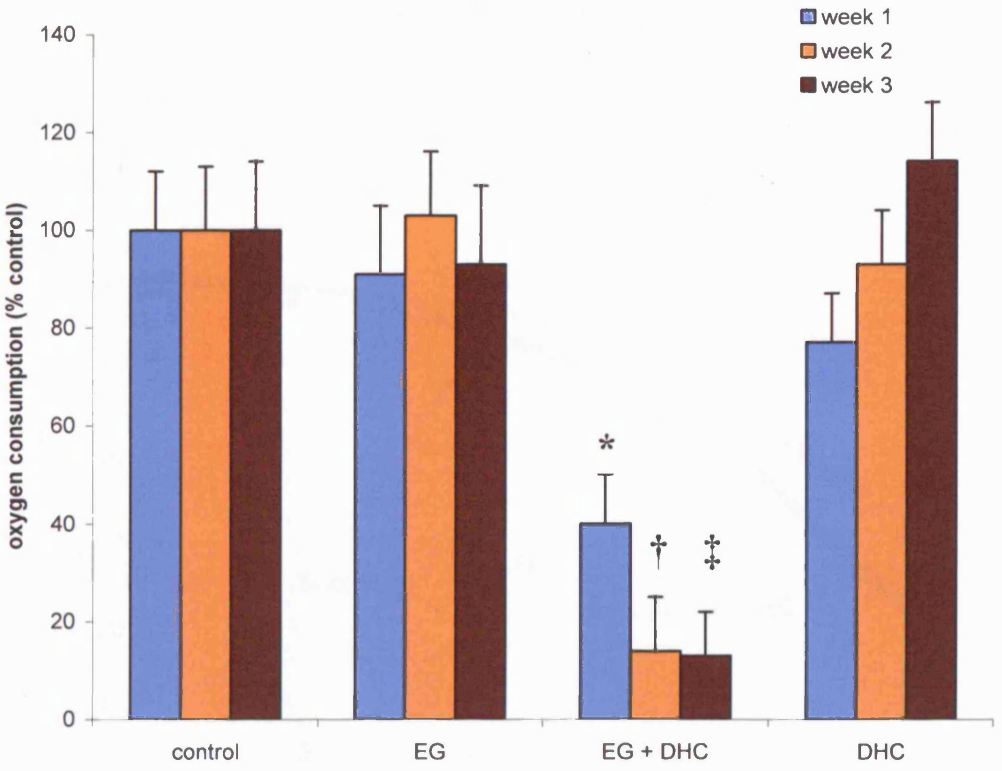


**Figure 7. 14 Oxygen consumption in kidney mitochondria of hyperoxaluric, calciuric, and crystalluric animals using complex I substrates.** Rates of oxygen consumption during state III respiration using malate/pyruvate. Values are means ± SD for n=3 expressed as a percentage of oxygen consumption rate in respective control kidney. Open bars week 1, closed bars week 2 and shaded bars week 3. *, †and ‡ $p<0.01$ v control at week 1, 2 and 3 respectively.

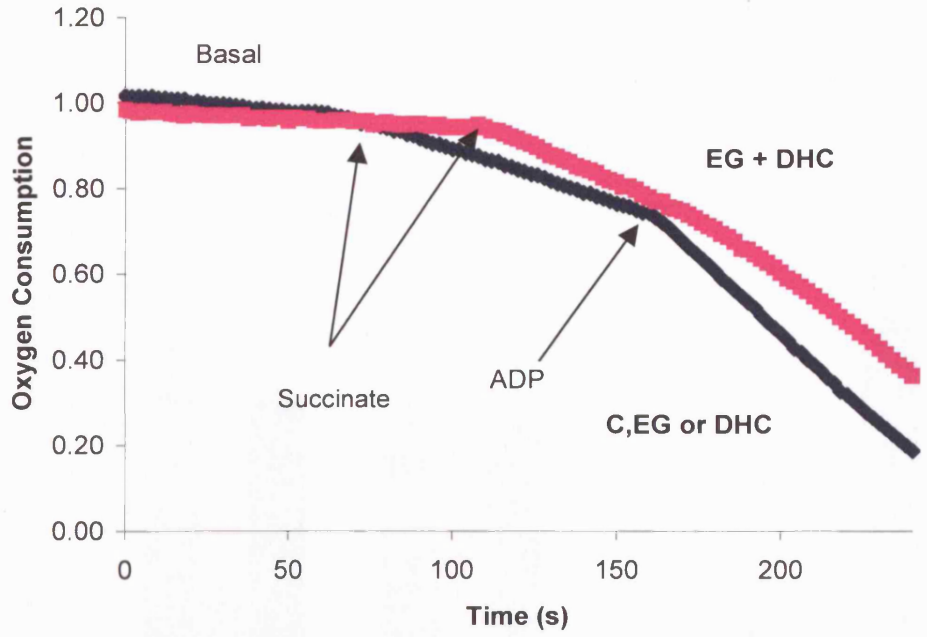


**Figure 7. 15 Oxygen consumption rates in kidney mitochondria at week 1 using complex II substrates.** Representative plot of oxygen consumption by mitochondrial from control, EG or DHC treated animals using succinate; lower line and EG + DHC; upper line. Addition of ADP (state III respiration) denoted by arrow.

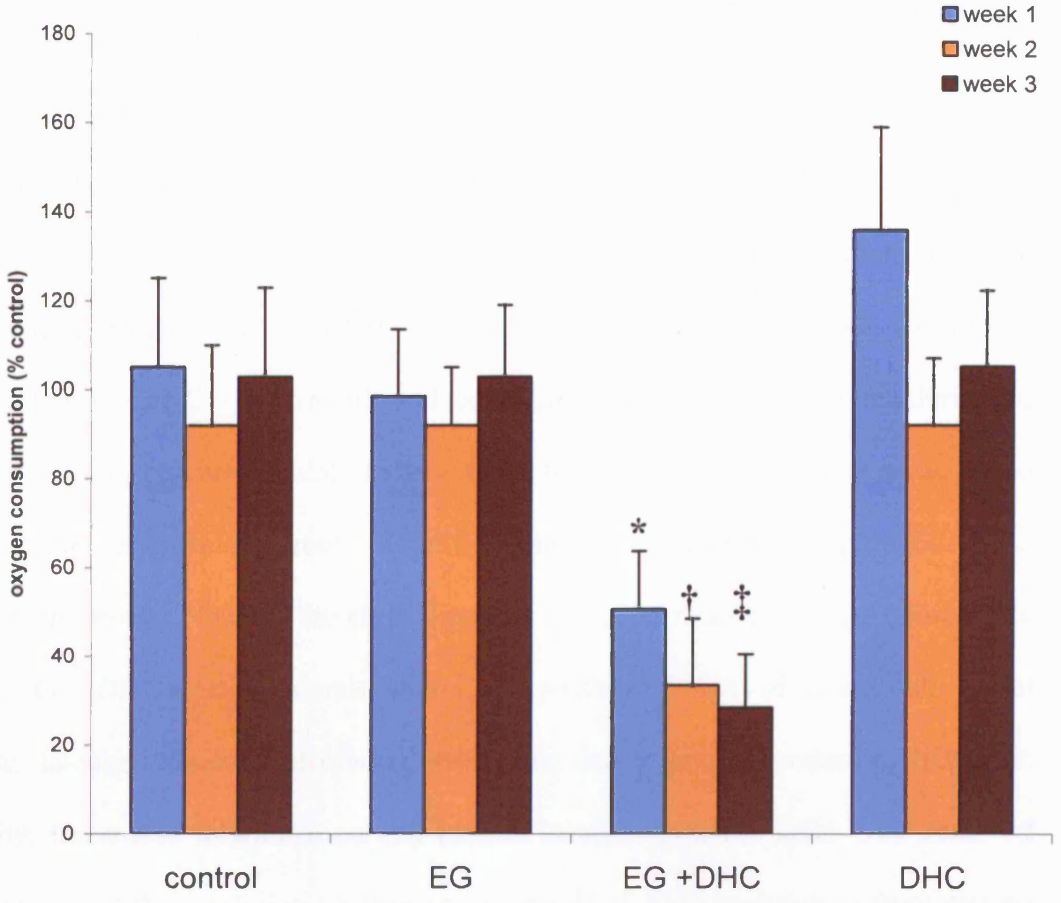


**Figure 7. 16 Oxygen consumption in kidney mitochondria using complex II substrates.** Rate of oxygen consumption during state III respiration using succinate. Values are means ± SD for n=3 expressed as a percentage of oxygen consumption rate in respective control kidney. Open bars week 1, closed bars week 2 and shaded bars week 3. *, †and ‡ $p<0.01$ v control at week 1, 2 and 3, respectively.

## 7.10 DISCUSSION

This study examined whether this oxidative stress, which occurs as a result of the interaction between COM and tubular epithelial cells in culture, also occurs in an animal model of crystalluria arising from hyperoxaluria and hypercalciuria. To achieve this, a rat COM crystalluria model was used, comprising a low (0.5 %) ethylene glycol feeding which raises urinary oxalate [Lee, YH., *et al.,* 1996] and 1,25-dihydroxycholecalciferol the active form of Vitamin $D_3$, to raise calcium levels in tubular fluid [Horst, R., *et al.,* 2000]. In this model of hyperoxaluria (EG - treatment), hypercalciuria (DHC - treatment), and crystalluria (EG + DHC, hyperoxaluria and hypercalciuria), calcium oxalate kidney stone formation occurred after week 1 and only in the crystalluria group. Crystal formation became more pronounced in subsequent weeks. None of the control groups exhibited renal pathology comparable to the EG + DHC treated animals whose kidneys showed signs of hypertrophy, renal tubular damage consisting of tubular obstruction due to crystal formation, dilatation, atrophy, interstitial inflammation and loss of tubular epithelial cells. The observed hypertrophy of the crystalluria animals was a result of fluid retention as there was no change in kidney protein content. This is despite an increase in renal workload demonstrated by the increased fluid intake and distended bladders.

The appearance of calcium oxalate crystals in the kidney by the end of week 1 is rapid relative to other reported studies of rat nephrolithiasis, where higher ethylene glycol treatments (0.75 %) were used without simultaneous raising the urinary calcium (without any forms of Vitamin D). Under these circumstances intra-renal crystal appearance was slower and appeared later than week 1 [Huang, HS., 2002]. In the current study, calcium oxalate crystals began to aggregate in the tubular lumen

causing widening of the interstitial space. However, histological studies of kidneys from animals fed with only 0.5 % ethylene glycol did not show any morphological differences. Findings from this study also differ from those of de Water *et al.,* [de Water, R., *et al.,* 1996] who showed using $VitD_3$ and 0.5 % EG that only some of the rats showed calcium oxalate deposits in the renal cortex or medulla after 4 weeks. When 0.75 % EG was used, the amount of kidney-associated crystals was proportionally higher. This disparity is most probably a result of differences in the potential of different forms of $VitD_3$ used, to raise urinary calcium. In addition, in another study where rats were fed with 0.75 % EG and 2 % $NH_4CL$, these animals showed poor renal function even as early as day 10 of treatment [Huang, HS., *et al.,* 2002]. Furthermore, Lee YH *et al.,* [1996] have shown the presence of kidney stones in animals fed with 0.5 % EG alone. However, this study was conducted over a longer period of 4 weeks. This demonstrates the ability to achieve crystalluria and kidney stones formation at lower and potential sub-cytotoxic doses of EG, making this animal model appropriate to investigate the mechanisms involved in human kidney stone formation.

Changes in total glutathione levels in both mitochondria and the cytosol indicate a considerable oxidative stress imposed in the kidneys of animals exhibiting crystalluria, which is absent from the other treatment groups. This indicates the importance of crystalline oxalate rather than the free ion in the pathological process. The smaller decrease apparent at week 1 in the EG treated group may result either from the initial hyperoxaluric stress or from circulating levels of EG and/or its subsequent metabolites (including oxalate). The reversal of this phenomenon at weeks 2 and 3 indicate that this is a transient event, and is certainly not related to crystalluria, which is absent from this group. Antioxidant enzyme activity can be

increased when damage of oxidative modification occurs. Glutathione peroxidase (GPx), glutathione reductase (GR) and glucose-6-phosphate dehydrogenase (G-6PDH) were used as specific indicators of responses to oxidative stress in renal tubular injury induced by EG + DHC treatment in this nephrolithiasis rat model. In this study, kidney mitochondrial GPx and GR were elevated by the end of week 1 in the crystalluria group, where in the rest of experimental groups (EG or DHC) antioxidant activities remained the same as those in the control group indicating no forms of oxidative stress. However, by the end of weeks 2 and 3 the nephrolithic rat group showed gradual attenuation of antioxidant enzyme activities indicating impairment of the defence mechanism of the kidney in response to persistent oxidative stress. On the contrary to GPx and GR, cytosolic G-6PDH levels were significantly increased in the crystalluria group throughout the whole course treatment. G-6PDH is important in supplying redox equivalents, in the form of NADPH, for thiol maintenance and is a marker routinely observed to be induced under oxidative stress conditions [Salvemini, F., *et al.,* 1999]. Previous literature usually describes this enzyme as unchanged or decreased. However, this is the first time this enzyme has been investigated in a model employing DHC. Vitamin $D_3$ and its analogues have been shown to both upregulate and activate (via a calcium dependent-mechanism) G-6PDH and at the doses used in this study, no changes were observed in animals treated with DHC alone. Although, it is possible that the combination of DHC with oxidative stress in the form of kidney crystals, may contribute to the increased activity of G-6PDH.

It has previously been observed that mitochondrial derived superoxide was the source of oxidative stress in renal epithelial cells treated with COM *in vitro*. Mitochondrial oxygen consumption and superoxide formation were investigated in this model to

determine whether the electron transport chain was compromised, and if mitochondria were also the source of oxidative stress *in vivo*. Oxygen consumption in kidney mitochondria of EG or DHC groups in the presence of malate/pyruvate (complex I substrates) and succinate (complex II substrate), was not significantly changed compared to the control, indicating that hyperoxaluria or hypercalciuria alone were ineffective in changing mitochondrial function. By contrast, in the nephrolithic kidney (EG + DHC) group, the rate at which oxygen was consumed in the presence of complex I and complex II substrates, was severely decreased. The restriction in electron flow, which was apparent mainly during state III respiration with complex I substrates, is normally associated with an increased incidence of electron leakage, therefore superoxide formation. This is a consequence of the decreased flow of electrons and results from an increased concentration of ubisemiquinone of complex II during the Q cycle [Turrens, JF., & Boveris, 1980]. However this did not appear to be the case in this model as superoxide formation was decreased to a greater extent than oxygen consumption. This indicates that the redox state of ubiquinone (ratio of oxidised ubiquinone to ubisemiquinone to reduced ubiquinol) remained oxidised due to impaired mitochondrial reductive capacity (complex I and/or II). A study by Huang *et al.,* [2000] has shown elevated luminol chemiluminescence levels of renal venous samples, in the 7-day 0.75 % EG treated rats. They have also suggested that free radicals induced by hyperoxaluria in the early stages in this animal model. This, along with the observation of mitochondrial impairment at week 1, may suggest that in the current accelerated nephrolithic model, superoxide measurements should have been taken earlier than the end of week 1 treatment. Furthermore, no other studies in my knowledge have reported attempts of measurement of superoxide in kidney tissues.

Finally, this data indicates that electron leakage from the electron transport chain did not result from impaired electron flow. Thus, mitochondrial dysfunction caused by crystal formation may contribute to pathological events during clinical conditions where tubular crystal-cell interactions are uncontrolled, as in renal stones disease.

# CHAPTER 8

## Discussion and Future work

## 8.1 Summary

Cultured renal tubular cells serve as tools in experimental studies to further explore the mechanisms of urolithiasis. In this work, it is confirmed and established that MDCK cells could be used as a model system for the distal/collecting duct studies. Initially, in the attempt to provide a link between kidney stone disease and oxidative stress, this work confirmed and further optimised technical conditions to study oxidative damage under crystal deposition. Detection and measurement of fluxes of reactive oxygen species within the cells are of critical importance for investigating the patho-physiological consequences resulting from altered cellular reactive oxygen homeostasis. Due to their sensitivity, both lucigenin and luminol chemiluminescence techniques have extensively been used to assess ROS generation by various cellular systems. In this study particularly, lucigenin-chemiluminescence was employed to show that COM crystals, free oxalate and to a lesser extent hydroxyapatite crystals initiate oxidative damage in terms of superoxide production. Lucigenin has been questioned by many due its autoxidation ability above certain concentrations however it is now characterised as the most appropriate probe for measuring superoxide production. In contrast, it has been reported that luminol-derived CL reflects the $H_2O_2$ released from the mitochondria and should not be used to assess biological derived $O_2^{\bullet-}$ generation [Li, Yi., *et al.*, 1999]. In addition, it has been reported that uptake of lucigenin by mitochondria appears to depend on the membrane potential [Li, Y., 1999]. Based on these observations and the immediate connection of lucigenin and mitochondria employing lucigenin was of critical importance since one of the aims of the current work was to identify the main origin of oxidative damage occurring upon crystal deposition. Furthermore, the involvement of the mitochondrial electron transport chain in the generation of the lucigenin derived chemiluminescence was

further confirmed by employing a number of agents that modulate mitochondrial respiration at selective sites of the mitochondrial electron transport chain. In particularly it was shown that in the presence of rotenone, a complex I inhibitor, the electron flow from NADH/iron-sulphur clusters to ubiquinone is blocked, leading to reduction of both membrane potential and $O_2^{\bullet-}$ production by the electron transport components, particularly complex III. In contrast to the effects of rotenone, antimycin A blocks the electron transport from cytochrome $b_{562}$ to ubiquinone, which is downstream the site of $O_2^{\bullet-}$ formation in complex III. The presence of antimycin A therefore would cause the electrons to build up, leading to the increased univalent reduction of $O_2$ to $O_2^{\bullet-}$. In summary, these data demonstrate that lucigenin uptake and accumulation by mitochondria appear to occur via an ionic attraction between the positively charged lucigenin molecule and the negatively charged mitochondrial inner membrane. Once inside the mitochondria, lucigenin undergoes a one electron reduction catalysed by components of the mitochondria electron transport chain, yielding the lucigenin cation radical. The lucigenin cation radical then reacts specifically with the $O_2^{\bullet-}$ derived from the mitochondria electron chain, leading to lucigenin-derived chemiluminescence. Therefore, besides $O_2^{\bullet-}$ production by the mitochondria, the lucigenin-derived chemiluminescence appears to be determined by two other factors: the mitochondrial membrane potential and the one electron reduction of lucigenin.

Even though, lucigenin has been proven to be a good chemilumigenic probe to assess mitochondria derived ROS, uptake of lucigenin by mitochondria in intact cells was uncomplicated. Data from the current work showed that intact cells were not able to uptake lucigenin and therefore monitor superoxide production. Other studies however, have shown that intact mitochondria can take up lucigenin and therefore give rise to a

chemiluminescence signal [Li, Y., *et al.,* 1999]. This indicates that lucigenin is unable to penetrate the plasma membrane and therefore to achieve the mitochondria-lucigenin charge attraction. To facilitate such an action to occur, digitonin, a solubilisation agent, was employed in the current work. Digitonin is able to cause cell permeabilisation by creating pores of the plasma membrane, and allowing entry of lucigenin into the cytosolic compartment and in close proximity with the mitochondria. This extensive membrane poration was also confirmed by the scanning electron micrographs of COM treated MDCK cells. However, permeabilising the cells with digitonin may have two consequences. Firstly, the concentration of digitonin can be crucial in the monitoring of $O_2^{\bullet-}$ formation and therefore in the interpretation of the results. Specifically, digitonin at high (< 100 μg/ml) concentrations could cause mitochondrial perturbations and disturb the mitochondrial membrane potential therefore lowering the levels of $O_2^{\bullet-}$ formation. A recent study however has shown that by measuring $O_2$ consumption in a Clark oxygen electrode digitonin up to100 μg/ml did not cause mitochondria uncoupling [Khand, FD., *et al.,* 2002]. The integrity of the mitochondria has also been shown by the effect of mitochondrial inhibitors in the formation of $O_2^{\bullet-}$. In the case where mitochondria were uncoupled due to the digitonin effect, mitochondria transport chain would have also been compromised and an effect of mitochondrial inhibitors would not have been shown.

Another important consequence that digitonin may have on the cells, could be that of a structural change of the cell membrane. Results obtained from the present study showed that COM crystals are the most potent constituents of kidney stone to initiate oxidative stress in terms of significantly higher levels of $O_2^{\bullet-}$ formation. Free oxalate and hydroxyapatite crystals were also shown to induce high levels of $O_2^{\bullet-}$, whereas other micro-particles such as uric acid crystals, brushite, zymosan and latex beads had

no effect. This difference in effect may arise from the fact that digitonin contributes to the alteration of the lipid composition of the MDCK cells and therefore affects the manner of adhesion. The effect of cell surface molecules on the affinity of crystals has been studied by many. Mandel's group [Weissner, JH., *et al.*, 2001; Bigelow, MW., *et al.*, 1997] have reported that the plasma membrane phospholipids have an important role in the attachment of COM crystals. In particular they revealed that the expression of phosphatidylserine at the cell surface greatly enhanced crystal binding. The same authors also proposed that under pathological conditions, the appearance of phosphatidylserine at the surface of the epithelial cells occurs and this contributes to crystal retention. Recently, the group of Scheid demonstrated that the same effects of phosphatidylserine exposure and crystal binding were observed after exposing MDCK cells to toxic oxalate concentrations [Cao, LC., *et al.*, 2001]. Furthermore, other reports by Lieske *et al.*, [1996] have shown the effect of charged compounds on the adherence of COM crystals to MDCK cells. These authors proposed two populations of anions; one anchored to the apical plasma membrane and the other free in tubular fluid, can be viewed as competitors for the crystal surface. Alteration in the quality and quantity of either population of anions could alter this competitive balance and thereby determine whether or not crystals bind to the cell surface. This may also explain the effect of digitonin in this balance. Incubation of MDCK cells with digitonin can cause changes in the phospholipid membrane composition and favour COM crystal adhesion. On the contrary digitonin could also affect the quantity of anionic presented molecules of the cell surface and therefore inhibit adhesion of crystals or other micro-particles such as brushite or zymosan.

In addition to digitonin, the culture conditions in which cells were grown could also affect crystal binding and its consequences. In particular, epithelial cells cultured on

porous supports in a two-compartment system tend to form highly polarised and differentiated monolayers. Results presented in this work showed that MDCK and HK2 cells when cultured on membrane supports, $O_2^{\bullet-}$ production levels were at similar levels with those resulted from MDCK and HK2 cells cultured in plastic dishes. This indicates that COM binding was not affected by the different cell growth methodology. In contrast, different culture substrates seemed to interfere with the NaOx effect observed in MDCK and HK2 cells. In particular, results from this work showed that NaOx treated MDCK cells grown on both different substrates initiate similar levels of $O_2^{\bullet-}$ production, whereas the NaOx effects on HK2 cells grown on porous supports were lost. This indicates that different culture substrates may interfere with oxalate transport. Oxalate transport to the tubular fluid requires its crossing of the basolateral plasma membrane and the apical plasma membrane which faces the tubular fluid. The transport of oxalate across these membranes is mediated by anion-exchange mechanisms. Therefore, when HK2 cells of proximal origin are cultured on membrane supports the anion exchange transport mechanisms are functional and under external NaOx stimuli, this would facilitate cellular exit of the oxalate at the apical membrane. This may indicate that oxalate levels passing through the epithelial cells were not high enough to initiate mitochondrial oxidative stress due to continuous oxalate outflow.

Even though the effect of COM on MDCK and HK2 cells grown on different culture substrates was not lost it could be of great importance to investigate how other crystalline forms such as brushite, or hydroxyapatite, respond under these conditions. This could lead to important observations since important surface molecules would be different, critically altering the crystal binding sites therefore promoting or inhibiting binding of such micro-particles. Furthermore, cell culture on membrane supports

could also be used in studies on oxalate transport into the mitochondria. In the current work it was shown that oxalate transport into the mitochondria is mediated via the dicarboxylate-phosphate transport mechanism when cells are grown on plastic surfaces. Therefore, by introducing anion exchange mechanisms between the basolateral and apical membrane, this could lead to an oxalate competition for oxalate transport between the mitochondria and oxalate outflow in the tubular fluid. This potentially could result in a different cell pathology.

In addition, in the present work, an overall scheme in which COM crystals, as opposed to other endocytic particles bind to and are internalised in renal epithelial cells is proposed. Under circumstances during which free oxalate is released via dissociation, COM enters the mitochondrion via the phosphate-dependent dicarboxylate transporter. This leads to an increase in the mitochondrial membrane potential with a resultant rise in electron leakage and mostly mitochondrial matrix superoxide production. This together with a non-mitochondrial mechanism, which, because of its rapidity is crystal - attachment, initiates intracellular calcium transients. This has the potential to damage the renal epithelium.

Finally, to provide a link between *in vitro* and *in vivo* studies and to investigate whether the effects observed due to crystal-cells interactions in tissue culture also occur in an animal model, a rat crystalluria model was used. In this *in vivo* crystalluria model of kidney stones, it was observed that nephrolithic kidney underwent oxidative stress. Specifically, in the EG + DHC treated animals, this oxidative insult was manifest by a decrease in mitochondrial total GSH concentration, as well as an increased activity of G-6PDH, both important in maintaining cell redox. Severe kidney damage at the mitochondrial level was a key observation, indicated by the

diminished oxygen consumption. Although the above observations do not share the same response as shown *in vitro* studies this indicates severe renal damage and the mitochondria being the primary site. Furthermore, the above findings observed only in animals of crystalluria, suggest that damage related events result directly from the occurrence of COM crystals in kidney distal tubules. This has clinical importance for whole cell and mitochondrial antioxidant therapies in conditions mimicked by this model and of particular significance to primary and enteric hyperoxaluria and the acute situations in idiopathic stone formers.

## 8.2 Future work

Post-translational modification of proteins (glycation, oxidation and nitration), are common events during patho-physiological age related disease. The elevation of products derived during oxalate metabolism and increased oxidative stress, both events associated with calcium oxalate crystalluria, mimic conditions associated with these modifications, and the onset of such diseases. Therefore, by employing the animal model studied in this work, it would be important to investigate whether specific proteins undergo post-translational modification. Specifically, the level of expression of heat shock protein (Hsp)-25 from kidney tissue, which is the kidney form of a protein known to be a powerful protectant against stress events, could be examined. In addition, the level of expression of Hsp-25 would be compared with other Hsps such as Hsp70 and Hsp60, which have been reported not to change their expression under similar insult conditions [Muller, E., *et al.*, 1996]. Since, mitochondria integrity has been shown to be impaired in the animal model employed in this work, it could be further tested by assessing the activity and expression of adenine nucleotide translocase 1 (ANT1), a mitochondrial protein, [Yan, LJ., &

Sohal., RS, 1998]. Furthermore, levels of oxidation, nitration, and glycation of Hsp-25 and ANT1, could be examined to identify post-translational modifications occurring during nephrolithiasis. These studies might explain why tubular damage is evident and would provide a suitable target for protection.

In addition, microarray technology is a now well established technique that enables the screening of thousands of genes simultaneously and could provide information on diseased mechanisms, and therefore enabling the development of effective therapeutics. Therefore, to obtain a more detailed insight into the pathogenesis of nephrolithiasis, it would be very informative to examine gene expression profiles in the kidney of the rat CaOx nephrolithiasis model developed in the current study, using cDNA microarrays. Specifically, generation of a list of genes that are upregulated or downregulated upon EG, or DHC and EG + DHC treatment would provide useful information. Cluster analysis of the differentially expressed genes may reveal changes in gene expression that could correlate with the biochemical and histopathological findings observed in the current study. Therefore, by employing a cDNA microarray approach, it would further enhance our understanding of specific gene functions in the progression of nephrolithiasis.

# CHAPTER 9

## REFERENCES

Aihara, K., Byer, KJ., Khan, SR., 2003. Calcium phosphate-induced renal epithelial injury and stone formation: Involvement of reactive oxygen species. *Kidney Int* **64**: 1283-1291.

Akerboom, T & Seis, H., 1990. Glutathione transport and its significance in oxidative stress. In: Vina J ed. *Glutathione: metabolism and physiological functions.* Boca Raton: CRC Press 45-55.

Akerboom, TP., Bilzer, M., Sies, H., 1982. The relationship of bilary glutathione disulfide efflux and intracellular glutathione disulfide content in perfused liver. *J Biol Chem* **257**: 4248-4252.

Allison, MJ., Dawson, KA., Mayberry, WR., Foss, JG., 1985. *Oxalobacter formigenes*: Oxalate degrading bacteria that inhabit the gastrointestinal tract. *Arch Microbiol* **141**: 1-7.

Alstrand, C., Larsson, L., Tiselius, HG., 1984. Variations in urine composition during the day in patients with calcium oxalate stone disease. *J Urol* **131**: 77-81.

Aronson, PS., 1989. The proximal tubule: a model for diversity of ion exchangers and stilbene-sensitive anion transporters. *Annu Rev Physiol* **51**: 419-423.

Aronson, PS., Kuo, SM., 1989. Heterogeneity of anion exchangers mediating chloride transport in the proximal tubule. *Ann N Y Acad Sci* **574**: 96-101.

Asimos, DG., Goodman, HO., Holmes, RP., 1997. Hyperoxaluria: Advances in medical therapy. *Contemp Urol* December: 47-60.

Asplin, JR., 2002. Hyperoxaluric calcium nephrolithiasis. *Endocrinol Metab Clin North Am.* **31**(4):927-49.

Asplin, JR., Mandel, NS., Coe, FL., 1996. Evidence for calcium phosphate supersaturation in the loop of Henle. *Am J Physiol* **270**: F604-613.

Atmani, F., Lacour, B., Jungers, P., Drueke, T., Daudon, M., 1994. Reduced inhibitory activity of uronic-acid-rich protein in urine of stone formers. *Urol Res* **22**: 257-260.

Atmani, F., Mizon, J., Khan, SR., 1996. Identification or uronic-acid ruch protein as urinary bikunin, the light chain of inter-α-inhibitor. *Eur J Biochem* **236**: 984-990.

Atmanni, F., Opalko, FJ., Khan, SR., 1996. Association of urinary macromolecules with calcium oxlate crystals induced *in vivo* in normal human and rat urine. *Urol Res* **24**: 45-50.

Ayatse, JOI., & Kwan, JTC., 1991. Relative sensitivity of serum and urinary retinal binding protein and alpha-1 microglobulin in the assessment of renal function. *Ann Clin Biochem* **28**: 514-516.

Baggio, BG., Gambaro, E., Ossi, S., Borsati, A., 1983. Increased urinary excretion of renal enzymes in idiopathic calcium oxalate nephrolithiasis. *J Urol* **129**: 1161-1162.

Baillie, TA., & Slatter, JG., 1991. Glutathione: A vehicle for the transport of chemically reactive metabolites in vivo. *Acc. Chem. Res*; **24**: 264-270.

Barja, G., & Herrero, A., 2000. Oxidative damage to mitochondria DNA is inversely related to maximum life span in the heart and brain of mammals. *FASEB J* **14**: 312-318.

Bayraktutan, U., Draper, N., Lang,, D., Shah, AM., 1994. Expression of functional neutrophil type NADPH oxidase in cultured vascular smooth muscle cells. *Circ. Res.* **74**: 1141-1148.

Bers, DM., Patton, CW., Nuccitelli, R., 1994. A practical guide to the preparation of Ca2+ buffers. *Methods Cell Biol* **40**: 3-29.

Betteridge, DJ., 2000. What is oxidative stress? *Metabolism* **49**: 3-8.

Beyer, R., 1991. An analysis of the role of coenzyme Q in free radical generation and as an anti-oxidant. *Biochem Cell Biol* **70**: 390-443.

Bezeaud, A., & Guillin, MC., 1984. Quantitation of prothrombin activation products in human urine. *Br J Haematol* **58**: 597-606.

Bigelow, MW., Wiessner, JH., Kleinman, JG., Mandel, NS., 1996. Calcium oxalate crystal membrane interactions, dependence on membrane lipid composition. *J Urol* **155**: 1094-1098.

Bigelow, MW., Wiessner, JH., Kleinman, JG., Mandel, NS., 1997. Surface exposure of phosphatidylserine increases calcium oxalate crystal attachment. *Am J Physiol* **272**: F55-F62.

Boveris, A., & Cadenas, B., 1977. Mitochondrial production of superoxide readical and hydrogen peroxide. In *Tissue Hypoxia and Ischemia* 67-82, Plenum Press.

Boveris, A., & Chance, B., 1973. The mitochondrial generation of hydrogen peroxide. General properties and effect of hyperbaric oxygen. *Biochem J* **134**: 707-716.

Brivida, K., Klotz, LO., Sies, H., 1999. Defences against peroxynitrite. *Meth Enymol* **301**: 301-311.

Bunting, JR., Phan, TV., Kamali, E., Dowben, RM., 1989. Fluorescent cationic probes of mitochondria. Metrics and mechanism of interaction. *Biophys J* **56**: 979-993.

Calvin, HL., Medvedovsky, C., Worgul, BV., 1986. Near total glutathione depletion and age-specific cataracts induced by buthionine sulfoximine in mice. *Science* **233**: 553-555.

Cao, LC., Honeyman, TW., Cooney, R., Kennington, L., Scheid, CR., Jonassen, JA., 2004. Mitochondrial dysfunction is a primary event in renal cell oxalate toxicity. *Kidney Int* **66**: 1890-1900.

Cao, LC., Jonassen, J., Honeyman, TW., Scheid, C., 2001. Oxalate-induced redistribution of phospho tidylserine in renal epithelial cells: implications for kidney stone disease. *Am J Nephrol* **21**: 69-77.

Chae, HZ., Kang, SW., Rhee, SG., 1999. Isoforms of mammalian peroxiredoxin that reduce peroxides in presence of thioredoxin. *Methods Enzymol* **300**: 219-226.

Chae, HZ., Kim, HJ., Kang, SW., Rhee, SG., 1999. Characterisation of three isoforms of mammalian peroxiredoxin that reduce peroxides in the presence of thioredoxin. *Diabetes Res Clin Pract* **45**: 101-112.

Chakraborty, J., Below, AA., Solaiman, D., 2003. Tamm-Horsfall protein in patients with kidney damage and diabetes. *Urol Res* In press.

Chen, Z., & Lash, LH., 1998. Evidence of mitochondrial uptake of glutathione by dicarboxylaet and 2-oxoglutarate carriers. *J Pharmacol Exp Ther* **285**: 608-618.

Chen, Z., Putt., DA, Lash, LH., 2000. Enrichment and functional reconstitution of glutathione transport activity from rabbit kidney mitochondria: further evidence for the role of the dicarboxylate and 2-oxoglutarate carriers in mitochondrial glutathione transport. *Arch Biochem Biophys* **373**: 193-202.

Coe, FL., & Parks, JH., 1988. *Nephrolithiasis: Pathogenesis and Tretament* (2nd ed) Chicago, Year book Medical Publishers.

Coe, FL., Evan, A., Worcester, E., 2005. Kidney stone disease. *J Clin Invest* **115**: 2598-608.

Cohen, TD., & Preminger, GM., 1996. Struvite calculi. *Semin Nephrol* **16**(5): 424-434.

Colussi, G., DE Ferrari, ME., Brunati, C., Civati, G., 2000. Medical prevention and treatment of urinary stone. *J Nephrol* **13** Suppl 3:S65-S70.

de Water, R., Boeve, ER., van Miert, PP., Deng, G., Cao, LC., Stijnen, T., de Bruijn, WC., Schroder, FH., 1996. Experimental nephrolithiasis in rats: the effect of ethylene glycol and vitamin D3 on the induction of renal calcium oxalate crystals. *Scanning Microsc.*:; **10**(2): 591-601.

Doane, LA., Liebman, M., Caldwell, DR., 1989. Microbial oxalate degradation: Effects on oxalate and calcium balance in humans. *Nutr Res* **9**: 957964.

Doyle, IR., Marshall, VR., Dawson, CJ., Ryall, RL., 1995. Calcium oxalate crystal matrix extract: the most potent macromolecular inhibitor of crystal growth and aggregation yet tested in undiluted human urine *in vitro* . *Urol Res* **23**: 53-62.

Doyle, IR., Ryall, RL., Marshall, VR., 1991. Inclusion of proteins into calcium oxalate crystals precipitated from human urine: A highly selective phenomenon. *Clin Chem* **37**: 1589-1594.

Du, G., 1998. Generation of superoxide anion by mitochondria and impairment of their functions during anoxia and reoxygenation in vitro. *Free Radic Biol Med* **25**: 1066-1077.

Duchen, MR., & Biscoe, TJ., 1992. Relative mitochondrial membrane potential and [Ca2+]i in type I cells isolated from the rabbit carotid body. *J Physiol* **450**: 33-61.

Duchen, MR., Surin, A., Jacobson, J., 2003. Imaging mitochondrial function in intact cells. *Methods Enzymol* **361**, 353-389.

Dussol, B., & Berland, Y., 1996. Urinary kidney stone inhibitors. Where are we? *Nephrology, Dialysis, Transplantation*, **11**: 1222-1224.

Elliot, JS., & Rabinowitz, IN., 1976. Calcium oxalate crystalluria. *J Urol* **116**: 773-775.

Evan, AP., Coe, FL., Rittling, SR., Bledsoe, SM., Shao, Y., Lingeman, JE., Worcester, M., 2005. Apatite plaque particles in inner medulla of kidneys of calcium oxalate stone formers: Osteopontin localisation. *Kidney Int* **68**: 145-154.

Fassano, JM., & Khan, SR., 2001. Intratubular crystallisation of calcium oxalate in the presence of membrane vesicles: an in vitro study. *Kidney Int* **59**: 169-178.

Faulkner, K., & Fridovich, I., 1993. Luminol and lucigenin as detectors for O2•-. *Free radical biology and medicine* **15**: 447-451.

Finlayson, B.,& Reid, S., 1978. The expectation of free and fixed particles in urinary stone disease. *Invest Urol* **15**: 442-448.

Floryk, D., & Houtek, J., 1999. Tetramethyl Rhodamine Methyl Ester (TMRM) is suitable for cytofluorometric measurements of mitochondrial membrane potential in cells treated with digitonin. *Bioscience reports* **19**: 27-34.

Floyd, RA., 1990. Role of oxygen free radicals in carcinogenesis and brain ischemia. *FASEB J* **4**: 2587.

Gahtan, E., Auerbach, JM., Groner, Y., Segal, M., 1998. Reversible impairment of long-term potentiation in transgenic Cu/Zn-SOD mice. *Eur J Neurol* **10**: 538-544.

Gausch, CR., Hard, WL., Smith, TF., 1966. Characterisation of an established line of canine kidney cells (MDCK). *Proc soc Exp Biol Med* **122**: 931-935.

Gill, WB., Jones, KW., Ruggiero, KJ., 1981. Protective effects of heparin and other sulphated glycosaminoglycans on crystal adhesion to injured urothelium. *J Urol* **127**: 152-154.

Gipp, JJ., Chang, C., Mulcahy, RT., 1992. Cloning and nucleotide sequence of a full-length cDNA for human liver $\gamma$-glutamylcysteine synthetase. *Biochem Biophys Res Commun* **185**: 29-35.

Golenser, J., Peled-Kamar, M., Schwartz, E., Friedman, I., Groner, Y., Pollack, Y., 1998. Transgenic mice with elevated level of CuZnSOD are highly susceptible to malaria infection. *Free Radic Biol Med* **24**: 1504-15010.

Goodman, HO., Holmes. RP., Assimos, DG., 1995. Genetic factors in calcium oxalate stone disease. *J Urol* **153**:301–7.

Gottlob, K., Majewski, N., Kennedy, S., Kandel, E., Robey, RB., Hay, N., 2001. Inhibition of early apoptotic events by Akt/PKB is dependent on the first committed step of glycolysis and mitochondrial hexokinase. *Genes Dev* **15**: 1406-1418.

Graces, F., Garcia-Ferragut, L., Costa-Bauza, A., 1998. Development of calcium oxalate crystals on urothelium: effect of free radicals. *Nephron* **78**: 296: 301.

Green, DR., & Reed, JC., 1988. Mitochondria and apoptosis. *Science* **281**: 1309-1311.

Griendling, KK., Miniei, CA., Ollerenshaw, JD., Alexander, RW., 1994. Angiotensin II stimulates NADH and NADH oxidase activity in cultured vascular smooth muscle cells. *Circ Res* **74**: 1141-1148.

Griffith, OW., & Meister, A., 1985. Origin and turnover of mitochondrial glutathione. *Biochem J* **94**: 705-711.

Griffith, OW., & Mulcahy, RT., 1999. The enzymes of glutathione biosynthesis: $\gamma$-glutamylcysteine synthetase. *Adv Enzymol Relat Areas Mol Biol* **73**: 209-267.

Grover, PK., Noritz, RL., Simpson, RJ., Ryall, RL., 1988. Inhibition of growth and aggregation of calcium oxalate crystals *in vitro*: A comparison of four human proteins *Eur J Biochem* **253**: 637-644.

Gunter, TE., & Pfeiffer, DR., 1990. Mechanisms by which mitochondria transport calcium. *Am J Physiol* **258**: C755-C786.

Gutierrez, PL., & Bachur, NR., 1983. Free radicals in quinone containing antitumor agents. The nature of the diaziquone 93,6-diaziridinyl-2,5-bis(carboethoxyamino)-1,4-benzoquinone) free radical. *Biochim Biophys Acta* **758**: 37-41.

Hackett, RL., Shevock, PN., Khan, SR., 1994. Calcium oxalate crystals and oxalate ion are injurious to renal epithelial cells. In: Ryall (ed) Urolithiasis 2. Plenum Press, New York, 325-345.

Halliwell, B., 1987. Oxidants and human disease: some new concepts.*FASEB J* **1**: 358-364.

Han, JZ., Zhang, X., Li, JG., Zhang, YS., 1995. The relationship of Oxalobacter formigenes and calcium oxalate calculi. *J Tongji Med Univ* **15**: 249-52.

Handler, JS., 1989. Overview of epithelial polarity. *Annu Rev Physiol* **51**: 729-740.

Hansen, C., Fraiture, B., Rouhi, R., Otto, E., Froster, G., Kahaly, G., 1997. HPLC glycosaminoglycan analysis in patients with Grave's disease. *Clin Sci* **92**: 511-517.

Harris, LR., Cake, MH., Macey, DJ., 1994. Iron release from ferritin and its sensitivity to superoxide ions differs among vertebrates. *Biochem J* **301**: 385-389.

Hatch, M., & Freel, RW., 1996. Oxalate transport across intestinal and renal epithelia. In: *Calcium Oxalate in Biological Systems*, edited by Khan S, Boca Raton FL, CRC Press, 217-238.

Hatch, M., Freel, RW., Vaziri, ND., 1993. Characteristics of the transport of oxalate and other ions across rabbit proximal colon. *Pfluggers Arc* **423**: 206-208.

Hensley, K., Robinson, KA., Gabbita, SP., Salsman, S., Floyd, RA., 2000. Reactive oxygen species, cell signalling, and cell injury. *Free radic. Biol. Med.* **28**: 1456-1462.

Herring, LC., 1962. Observations on the analysis of the thaousand urinary calculi. *J Urol* **88**: 545-562.

Hess, B., 1994. Tamm-Horsfall glycoprotein and calcium nephrolithiasis. *Mineral and Electrolyte Metabolism*, **20**: 393-398.

Hess, B., Nakagawa, Y., Parks, JH., Coe, FL., 1991. Molecular abnormality of Tamm-Horsfall glycoprotein in calcium oxalate nephrolithiasis. *American Journal of Physiology*, **260**: F569-F578.

Hogg, N., & Kalyanaraman, B., 1998. Nitric oxide and low-density lipoprotein oxidation. *Free Radic res* **28**593-600.

Holland, PC., Clark MG., Bloxham, DP., Lardy HA., 1973. Mechanism of action of the hypoglycemic agent diphenyleneiodonium *J Biol Chem* **248**: 6050-6056.

Holmes, RP., Goodman, HO., Assimos, DG., 1995. Dietary oxalate and its intestinal absorption. *Scann Microsc* **9**: 1109-1120.

Horst, R., Prapong, S., Reinhardt, T., Koszewski, N., Knutson, J., Bishop, C., 2000. Comparison of the relative effects of 1,24-dihydroxyvitamin D(2) [(1,24-(OH)(2)D(2)], 1,24- dihydroxyvitamin D(3) [(1,24-(OH)(2)D(3)], and 1,25-dihydroxyvitamin D(3) [(1,24-(OH)(2)D(3)] on selected vitamin D-regulated events in the rat. *Biochem Pharmacol* **60**: 701-714.

Huang, CS., Anderson, ME., Meister, A., 1993. Amino acid sequence and function of the light subunit of rat kidney $\gamma$-glutamylcysteine synthetase. *J Biol Chem* **268**: 20578-20583.

Huang, CS., He, W., Meister, A., Anderson, ME., 1995. Amino acid sequence of rat kidney glutathione synthetase. *Proc Natl Acad Sci USA* **92**: 1232-1236.

Huang, HS., Chen, CF., Chien, CT., 2000. Possible biphasic changes of free radicals in ethylene glycol-induced nephrolithiasis in rats. *Br J Urol* **85**: 1143-1154.

Huang, HS., Ma, MC., Chen, CF., Chen, J., 2003. Lipid peroxidation and its correlations with urinary levels of oxalate, citric acid, and osteopontin in patients with renal calcium oxalate stones. *Urology* **62**:1123-1128.

Huang, HS., Ma, MC., Chen, J., Chen, CF., 2002. Changes in the oxidant-antioxidant balance in the kidney of rats with nephrolithiasis induced by ethylene glycol. *J Urol* **167**: 2584-2593.

Igbavboa, U., Zwizinski, CN., Pfeiffeer, DR., 1989. Release of mitochondrial matrix proteins through a Ca2+ requiring, cyclosporin-sensitive pathway. *Biochim Biophys res Commun* **161**: 619-625.

Ignarro, LJ., 1990. Haem-dependent activation of guanylate cyclase and cyclic GMP formation by endogenous nitric oxide: a unique transduction mechanism for transcellular signalling. *Pharmacol Toxicol* **67**: 1-7.

Jacobson, J., Duchen, MR., 2002. Mitochondrial oxidative stress and cell death in astrocytes-requirement for stored $Ca^{2+}$ and sustained opening of the permeability transition pore. *J Cell Sc* **115**: 1175-1188.

James, AM., Cocheme, HM., Murphy, MP., 2005. Mitochondria-targeted redox probes as tools in the study of oxidative damage and ageing. *Mech Ageing Dev* **126**: 982-986.

Jonassen, JA., Cao, LC., Honeyman, T., Scheid, CR., 2003. Mechanisms mediating oxalate-induced alterations in renal cell functions. *Crit Rev Eukaryot Gene Expr*; **13**(1); 55-72.

Kaissling, B., Kriz, W., 1979. Structural analysis of the rabbit kidney. *Advances in Anatomy, Embryology and Cell Biology*: 56.

Kakhniashvilli, D., Mayor, JA., Gremse, DA., Xu, Y., Kaplan, RS., 1997. Identification of a novel gene encoding the yeast mitochondrial dicarboxylate transportprotein via overexpression, purification, and characterisation of its protein product. *J Biol Chem* 7: 4516-4521.

Kalyanaraman, B., Karoui, H., Singh, RJ., Felix, CC., 1996. Detection of thiyl radical adducts formed during hydroxyl radical and peroxynitrite mediated oxidation of thiols: a high resolution ESR spin-trapping study at Q-band. *Anal Biochem* **241**: 75-81.

Karniski, LP., 1998. Effects of sulfate and chloride on three separate oxalate transporters reconstituted from rabbit renal cortex. *Am J Physiol* **274**: F189-F196.

Kehrer, JP., Lund, LG., 1994. Cellular reducing equivalents and oxidative stress. *Free Radic Biol Med* **17**: 65-75.

Khan, SR., 1991. Pathogenesis of oxalate urolithiasis: lessons form experimental studies with rats. *Am J Kidney Dis* **17**: 398-403.

Khan, SR., 1995. Animal model of calcium oxalate nephrolithiasis. In: Khan SR, editor. Calcium oxalate in biological systems. Boca Raton, FL: CRC Press 343-59.

Khan, SR., 1997. Animal models of kidney stone formation: an analysis. *World J Urol*; **15:** 236-43.

Khan, SR., 1997. Interactions between stone-forming calcific crystals and macromolecules. *Urol Int* **59**: 59-71.

Khan, SR., 2004. Crystal-induced inflammation of the kidneys: results from human studies, animal models, and tissue-culture studies. *Clin Exp Nephrol* **8**: 75-88.

Khan, SR., Cockrell, CA., Finlayson, B., Hackett, RL., 1989. Crystal retention by injured urothelium of the rat urinary bladder. *J Urol* **142**: 846-849.

Khan, SR., Finlayson, B., Hackett, RL., 1979. Histologic study of the ealy events in oxalate induced intranephronic calculosis. *Invest Urol* **17**: 199-206.

Khan, SR., Finlayson, B., Hackett, RL., 1982. Experimental calcium oxalate nephrolithiasis in the rat, role of renal papilla. *Am J Pathol* **107**: 59-67.

Khan, SR., Hackett, RL., 1985. Calcium oxalate urolithiasis in rat: Is it a model for human stone disease. *Scanning Microsc* **2**: 759-763.

Khan, SR., Hackett, RL., 1993. Hyperoxaluria, enzymuria and nephrolithiasis. *Contrib Nephrol* **101**: 190-195.

Khan, SR., Shevock, PN., Hacket, RL., 1992. Acute hyperoxaluria, renal injury and calcium oxalate urolithiasis. *J Urol* **147**: 226-237.

Khan, SR., Shevock, PN., Hackett, RL., 1989. Urinary enzymes and calcium oxalate urolithiasis. *J Urol* **142**: 846-858.

Khan, SR., Shevock, PN., Hackett, RL., 1990. Membrane associated crystallisation of calcium oxalate *in vitro*. *Calcif Tissue Res* **46**: 116-121.

Khand, FD., Gordge, MP., Robertson, WC., Noronha-Dutra, AA., Hothersall, JS., 2002. Mitochondrial superoxide production during oxalate-mediated oxidative stress in renal epithelial cells. *Free radic Biol Med* **32**: 1339-50.

Kim, J., Cha, J., Tisher, TC., Madsen, KM., 1996. Role of apoptotic and nonapoptotic cell death in the removal of intercalated cells from developing rat kidney. *Am J Physiol* **270**: F535-F592.

Kim, JS., He, L., Lemasters, JJ., 2003. Mitochondrial permeability transition: A common pathway to necrosis and apoptosis. *Biochem Biophys res Comm* **304**: 463-470.

Kleinman, JG., Soronika, EA., 1999. Cloning and preliminary characterisation of a clcium-binding protein closely related to nucleolin on the apical surface of inner medullary collecting duct cells. *J Biol Chem* **274:** 27941-27946.

Knoll, T., Janitzky, V., Michel. MS., Alken, P., Kohrmann, KU., 2003. Cystinuria - Cystine Stones: Recommendations for Diagnosis, Therapy and Follow-up. *Aktuel Urol* **34(2)**: 97-101.

Knudson, W., Bartnik, E., Knudson, CB., 1993. Assembly of pericellular matrices by COS-7 cells transfected with CD44 lymphocyte-homing receptor genes. *Proc Natl Acad Sci USA* **90**: 4003-4007.

Kobayashi, H., Shibata, K., Fujie, M., Surgino, D., Terao, T., 1998. Identification of structural domains in inter-α-trypsin inhibitor involved in calcium oxalate crystalisation. *Kidney Int* **53**: 1727-1735.

Kohri, K., Kodama, M., Ishikawa, Y., 1991. Immunofluorescent study on the interaction between collagen and calcium oxalate crystals in the renal tubules. *Eur Urol* **19**:249-252.

Kohri, K., Nomura, S., Kitamura, Y., Nagata, T., Yoshioka, K., Iguchi, M., Yamate, T., Umekawa, T., Suzuki, Y., Sinohara, H., Kurita, T., 1993. Structure and expression of the mRNA encoding urinary stone protein (osteopontin). *J Biol Chem* **268**: 15180-15184.

Kohri, K., Suzuki, Y., Yoshida, K., Yamamoto, K., Yamate, T., Amasaki, N., Umekawa, T., Iguchi, M., Sinohara, H., Kurita, T., 1992. Molecular colning and sequencing of cDNA encoding urinary stones proteins, which is identical to osteopontin. *Biochem Biophys Res Commun* **184**: 859-864.

Kok, DJ., Khan, SR., 1994. Calcium oxalate nephrolithiasis, a free or fixed particle disease. *Kidney Int* **46**: 847-854.

Koka, RM., Huang, E., Lieske, JC., 2000. Adhesion of uric crystals to the surface of renal epithelial cells. *Am J Physiol Renal Physiol* **278**: F989-F998.

Korshunov, SS., Skulachev, VP., Starkov, AA., 1997. High protonic potential actuates a mechanism of production f reactive oxygen species in mitochondria. *FEBS Lett.* **416**: 15-18.

Koul, H., Ebisumo, SR., Yanagawa, M., Menon, M., Scheid, C., 1994. Polarised distribution of oxalate transport systems in LLC-PK1 cells a line of renal epithelial cells. *Am J Phsyiol* **266**: F266.

Kreil, G., 1995. Hyaluronidases: A group of neglected enzymes. *Protein Sci* **4**: 1666-1669.

Kuppusamy, P., Zweier, JL., 1989. Characterisation of free radical generation by xanthine oxidase. Evidence for hydroxyl radicalgeneration. *J Biol Chem* **264**: 9880-9884.

Kwak, C., Kim., HK, Kim, EC., Choi, MS., Kim, HH., 2003. Urinary oxalate levels and the enteric bacterium Oxalobacter formigenes in patients with calcium oxalate urolithiasis. *Eur Urol* **44**: 475-81.

LaNoue, KF., Schoolwerth, AC., 1979. Metabolite transport in mitochondria. *Annu Rev Biochem* **48**: 871-922.

Larsson, L ., Tiselius, HG., 1987. Hyperoxaluria. *Min Electr Metab* **13**: 242-245.

Lash, LH., Visarius, TM., Sall, JM., Qian, W., Tokartz, JJ., 1998. Cellular and subcellular heterogeneity of glutathione metabolism and transport in rat kidney cells. *Toxicology* **130**: 1-15.

Lass, A., Sohal, RS., 1999. Comparisons of Coenzyme Q bound to mitochondrial membrane proteins among different mammalian species. *Free Radic Biol Med* **27**: 220-226.

Laurent, TC., Fraser, JRE., 1992. Hyaluran. *FASEB J* **6**: 2397-2404.

Lee, YH., Huang, WC., Huang, JK., Chang, LS., 1996. Testosterone enhances whereas eostregen inhibits calcium oxalate stone formation in ethylene glycol treated rats. *J Urol* **156**: 502-510.

Lemasters, JJ., Qian, T., Bradham, CA., 1999. Mitochondrial dysfunction in the pathogenesis of necrotic and apoptotic cell death. *J Bioengerg Biomembr* **31**: 305-329.

Lenaz, G., Bovina, C., Castelluccio, G., Fato, R., Formiggini, G., Genova, ML., Marchetti, M., Pich, M., Palloti, F., Pavnti Castelli, GP,, Biagina ,G., 1997. Mitochondrial complex I defects in aging. *Mol Cell Biochem* **174**: 329-333.

Li, P., Dietz, R., von Harsdof, R., 1999. p53 regulates mitochondrial membrane potential through reactive oxygen species and induces cytochrome c-independent apoptosis blocked by Bcl-2. *EMBO J* **18**: 6027-6038.

Li, Y., Zhu, H., Kuppusamy, P., Roubaud, V., Zweier, JL., 1996. Detection of mitochondria derived reactive oxygen species production by chemilumigenic probes lucigenin and luminol. *Biochim Biophys Acta* **1428**: 1-12.

Lieberthal, W., Levine, JS., 1996. Mechanisms of apoptosis and its potential role in renal tubular epithelial cell injury. *Am J Physiol* **271**: F477-F488.

Lieberthal, W., Triaca, V., Levine, JS., 1996. Mechanisms of death induced by cisplatin in proximal tubular epithelial cells: Apoptosis vs necrosis. *Am J Physiol* **270**: F700-F708.

Lieske, JC., Leonard, R., Toback, FG., 1995. Adhesion of calcium oxalate monohydrate crystals to renal epithelial cells is inhibited by specific anions. *Am J Physiol* **268**: F604-F612.

Lieske, JC., Deganello, S., 1999. Nucleation, adhesion and internalisation of calcium containing urinary crystals by renal cells. *Am Soc Nephrol* **10**: S422-S429.

Lieske, JC., Deganello, S., Toback, FG., 1999. Cell-crystal interactions and kidney stone formation. *Nephron* **81**: S8-S17. An overview of the response of renal cells to urinary crystals.

Lieske, JC., Leonard, R., Swift, H., Toback, FG., 1996. Adhesion of calcium oxalate monohydrate crystals to anionic sites on the surface of renal epithelial cells. *Am J Physiol Renal Physiol* **270**: F192-F199.

Lieske, JC., Swift, HS., Martin, T., Patterson, B., Toback, FG., 1993. Renal epithelial cells rapidly bind and internalise calcium oxlate monohydrate crystals. *Am J Physiol* **264**: F800-F807.

Lieske, JC., Toback, FG., 1993. Regulation of renal epithelial cell endocytosis of calcium oxalate monohydrate crystals. *Am J Physiol* **262**: F622-F630.

Lieske, JC., Toback, FG., 1996. Regulation of renal epithelial cell endocytosis of calcium oxalate monohydrate crystals. *Am J Physiol* **264**: F192-F199

Lieske, JC., Toback, FG., 2000. Renal cell-urinary crystal interactions. *Curr Opin Nephrol Hypertens* **9**: 349-355.

Lieske, JC., Toback, FG., Deganello, S., 2001. Sialic-acid containing glycoproteins on renal cells determines nucleation of calcium oxalate dihydrate crystals. *Kidney Int* **60**: 1784-1791.

Lieske, JC., Walsh-Reitz, MM., Toback, FG., 1992. Calcium oxalate monohydrate crystals are endocytosed by renal epithelial cells and induce proliferation. *Am J Physiol* **262**: F622-F630.

Ling, YH., Liebes, L., Zou, Y., Perez-Soler, R., 2003. Reactive oxygen species generation and mitochondrial dysfunction in the apoptotic response to Bortezomib, a novel proteasome inhibitor, in human H460 non-small cell lung cancer cells. *J Biol Chem* **278**: 33714-33723.

Linnane, AW., Zhang, C., Baumer, A., Nagley, P., 1992. Mitochondrial DNA mutation and the ageing process: bioenergy and pharmacological intervention *Mutat Res* **275**: 195-208.

Liu, SS., 1997. Generating, partitioning targeting and functioning of superoxide in mitochondria. *Biosci Rep* **17**: 259-272.

Lokeshwar, VB., Obek, C., Soloway, MS., Block, NL., 1997. Tumor-assosiated hyaluronic acid: A new sensitive and specific urinary marker for bladder cancer. *Cancer Res* **57**:773-777.

Luperchio, S., Tamir, S., Tannenbaum, SR., 1996. NO induced oxidative stress and glutathione metabolism in rodent and human cells. *Free Radic Biol Med* **21**: 513-519.

Majander, A., Finel, M., Wilkstrom, M., 1994. *J Biol Chem* **269**: 21037-21042.

Mandel N., 1994. Crystal - membrane interaction in kidney stone disease. *J Am Soc Nephrol* **5**: S37-45.

Mandel, N., Riese, R., 1991. Crystal-cell interactions: Crysatl binding to rat renal papillary tip collecting duct cells in culture. *Am J Kidney Dis* **17**: 402-406.

Martensson, J., Jain, A., Stole, E., Frayer, W., Auld, PAM., Meister, A., 1991. Inhibition of glutathione synthesis in the newborn rat: a model for endogenously produced oxidative stress. *Proc Natl Acad Sci USA* **88**: 9360-9364.

Martensson, J., Meister, A., 1989. Mitochondrial change in muscle occurs after marked depletion of glutathione and is prevented by giving glutathione monoester. *Proc Natl Acad Sci USA* **867**: 471-475.

Marzo, I., Susin, SA., Petit, PX., Ravagnan, L., Brenner, C., Larochette, N., Zamzani, N., Kroemer, G., 1997. Caspases disrupt mitochondrial membrane barrier function. *FEBS Lett* **427**: 282-286.

Mason, RP., 1982. Free radicalintermediates in the metabolism of toxic chemicals. In *free radicals in Biology*, Pryor, WA (ed) **5**, p 161. Academic Press .

Mason, RP., Chignell, CF., 1982. Free radicals in pharmacology-selected topics. *Pharmacol Rev* **33**: 189.

Mates, JM., Perez-Gomez, C., Nunez de Castro, I., 1999. Antioxidant enzymes and human diseases. *Clin Biochem* **32**: 595-603.

Matsuno-Yagi, A., Hatefi, Y., 1996. Ubiquinol-cytochrome c oxidoreductase. The redox reactions of the bis-heme cytochrome b in ubiquinone-sufficient and ubiquinone-deficient systems *J Biol Chem I* **271**: 6164-6171.

McCord, JM., Fridovich, I., 1969. Superoxide dismutase: an enzymatic function for erythrocuprein (hemocuprein). *J Biol Chem* **244**: 6049-6055 .

McIntyre, M., Bohr, DF., Dominiczak, AF., 1999. Endothelial function in hypertension. *Hypertension* **34**: 539-545.

McKee, CM., Lowenstein, CJ., Horton, MR., Wu, J., Bao, C., Chin, BY., Choi, AMK., Noble, PW., 1997. Hyaluran fragments induce nitric oxide synthase in murine macrophages through a nuclear factor kB-dependent mechanism. *J Biol Chem* **272**: 8013-8018.

McKee, CM., Penno, MB., Cowman, M., Burdick, MD., Streiter, RM., Bao, C., Noble, PW., 1996. Hyaluran (HA) fragments induce chemokine gene expression in alveolar macrophages: The role of HA size and CD44. *J Clin Invest* **98**:2403-2413.

Meister, A., 1991. Glutathione deficiency produced by inhibition of its synthesis and its reversal; applications in research and therapy. *Pharmacol Therapeut* **51**: 155-194.

Meister, A., Anderson, ME., 1983. Glutathione. *Ann Rev Biochem* **52**: 711-760.

Menon, M., Ayvazian, P., Hodapp, J., Malhotra, R., Renzulli, L., Scheid, C., Koul, H., 1993. Oxalate induced proximal tubular cell damage. *J Urol* **149**: 440.

Menon, M., Koul, H., 1992. Calcium oxalate nephrolithiasis. *J Clin Endocrin Metab* **74**: 703-707.

Menon, M., Mahle, CJ., 1992. Oxalate metabolism and renal calculi. *J Urol* **127**: 148-153.

Meredith, MJ., Reed, DJ., 1982. Status of mitochondrial pool of glutathione in the isolated hepatocyte. *J Biol Chem*; **257**: 3747-3573.

Miki, T., Miki, M., Orii, Y., 1994. Membrane potential-linked reversed electron transfer in the beef heart cytochrome bc1 complex reconstituted into potassium-loaded phospholipid vesicles. *J Biol Chem* **269**: 1827-1833.

Mitchell, P., 1976. Possible molecular mechanisms of the proton-motive function of cytochrome systems. *J Theor Biol* **62**: 327-367.

Mohazzab-H, KM., Kaminski, PM., Wolin, MS., 1994. NADH oxidoreductase is a major source of superoxide anion in bovine coronary endothelium. *Am J Physiol* **266**: H2568-H2572.

Morel, Y., Barouki., 1999. Repression of gene expression by oxidative stress. *Biochem J* **342**:481-496.

Morse, RM., Resnick, MI., 1991. A new approach to the study of urinary macromolecules as participants in calcium oxalate crystallisation *J Urol* **139**: 869-871.

Muller, E., Neuhofer, W., Ohno, A., Rucker, S., Thurau, K., Beck, FX., 1996. Heat shock proteins HSP25, HSP60, HSP72, HSP73 in isoosmotic cortex and hyperosmotic medulla of rat kidney. *Pflugers Arch* **431**: 608-617.

Muller, JM., Rupec, RA., Baeuerle, PA., 1997. Study of gene regulation by NF-kB and AP-1 in response to reactive oxygen intermediates. *Methods* **11**: 301-312.

Muthukumar, A., Selvam, R., 1997. Renal injury mediated calcium oxalate nephrolithiasis: role of lipid peroxidation. *Ren Fail* **19**: 401-408.

Muthukumar, A., Selvam, R., 1998. Role of glutathione on renal mitochondrial status in hyperoxaluria. *Mol Cell Biochem* **185**: 77-84.

Nishio, S., Takeda, H., Iseda, T., Yokoyamam, Iwata H., Takeuchi, M., 1997. Inhibitory effects of α2-HS-glycoprotein, prothrombin and osteopontin on calcium oxalate crystallisation. *J Urol* [Abstarct] **159**: 1240.

Oertli, B., Beck-Schimmer B, Fan X., Wuthrich, R., 1998. Mechanisms of hyaluran-induced-up-regulation of ICAM-1 and VCAM-1 expression by murine kidney tubular epithelial cells: Hyaluran triggers cell adhesion molecular expression through a mechanism involving activation of nuclear factor-kB and activating protein-1. *J Immunol* **161**: 3431-3437.

Okada, Y., KaWamujra, J., Kuo, YJ., Yoshida, O., 1985. Experimental and clinical studies on calcium urolithiasis: animal model for calcium oxalate urolithiasis using ethylene glycol and alpha (OHD3). *Hinyokika Kiyo*; **4**: 565-577.

Oppenheimer, L., Wellner, VP., Griffith, OW., Meister, A., 1979. Glutathione synthetase: purification from rat kidney and mapping of the substrate binding site. *J Biol Chem* **254**: 5184-5190.

Petit, PX., Susin, SA., Zamzani, N., Mignotte, B., Kroemer, G., 1996. Mitochondria and programmed celldeath: back to the future. *FEBS Lett* **396**: 7-13.

Petrollini, V., Cola, C., Bernadi, P., 1993. Modulation of the mitochondrial cyclosporin: A sensitive permeability transition pore. II. The minimal requirements for pore induction inderscore a key role for transmembrane electrical potential, matrix pH, and matrix $Ca^{2+}$. *J Biol Chem* **268**: 1011-1016.

Pitkanen, S., Merante, F., McLeod, DR., Applegarth, D., Tong, T., Robinson, BH., 1996. Familial cardiomyopathy with cataracts and lactic acidosis: A defect in complex I (NADH-dehydrogenase) of the mitochondrial respiratory chain. *Pediatr Res* **39**:513-521.

Pitkanen, S., Robinson BH., 1996. Mitochondrial complex I deficiency leads to increased production of superoxide radicals and induction of superoxide dismutase. *J Clin Invest* **98**: 345-451.

Polyak, K., Xia, Y., Zweier, JL., Kinzler, KW., Vogelstein, B., 1997. A model of p53-induced apoptosis. *Nature* **389**: 300-305.

Prien, EL., 1975. The riddle of Randall's plaques. *J Urol* **114**: 500-507.

Ragan, CI., Bloxham, DP., 1977. *Biochem J* **163**: 605-615.

Raha, S., McEachern GE., Myint, AT., Robinson, BH., 2000. Superoxides from mitochondrial complex III: the role of manganese superoxide dismutase. *Free Radic Biol Med.*

Rees, M., Smiley, ST., Mottola-Hartshorn, C., Chen, A., Lin, M., Chen, LB., 1995. Mitochondrial membrane potential monitored by JC-1 dye. *Methods Enzym* **260**: 406-417.

Rembish, SJ., Trush, MA., 1994. Further evidence that lucigenin - derived chemiluminescence monitors mitochondrial superoxide generation in rat alveolar macrophages. *Free radical biology and medicine* **17**: 117-126.

Richter, C., Gogvadze, V., Laffranchi, R., Schlapbach, R., Schweizer, M., Suter, M., Walter, R., Yaffee, M., 1995. Oxidants in mitochondria: from physiology to disease. *Biochim Biophys Acta* **1127**: 67-74.

Richter, C., Park, JW., Ames, BN., 1988. Normal oxidative damage to mitochondrial and nuclear DNA is extensive. *Proc Natl Acad Sci USA* **85**: 6465-6467.

Riese, RJ., Mandel, NS., Wiessner, JH., Mandel, GS., Becker, CG., Kleinmnn, JG., 1992 Cell polarity and calcium oxalate crystal adherence to cultured collecting duct cells. *Am J Physiol* **262**: F177-F184.

Riese, RJ., Riese, JW., Kleinman, JG., Weissner, JH., Mandel, GS., Mandel, NS., 1988. Specificity in calcium oxalate adherence to papillary epithelial cells in cultures. *Am J Physiol* **255**: F1025-F1032.

Riese, RJ., Riese, JW., Kleinman, JG., Wiessner, JH., Mandel, GS., Mandel, NS., 1988. Specificity in calcium oxalate adherence to papillary epithelial cells in culture. *Am J Physiol* **255**: F1025-F1032.

Rizzuto, R., Pinton, P., Carrington, W., Fay, FS., Fogarty, KE., Lifshitz, LM., Tuft, RA., Pozzan, T., 1998. Close contacts with the endoplasmic reticulum as determinants of mitochondrial Ca2+ responses. *Science* **280**: 1763-1766.

Roberts, PA., Knight, J., Campbell, AK., 1987. Pholasin--a bioluminescent indicator for detecting activation of single neutrophils. *Anal Biochem* **160:** 139-48.

Robertson, WG., 1969. A method for measuring calcium crystalluria. *Clin Chim Acta* **26**: 105-110.

Robertson, WG., 2004. Kidney models of calcium oxalate stone formation. *Nephron Physiol* **98**: 21-30, 2004

Robinson, BH., Williams, GR., 1971. The sensitivity of dicarboxylate anion exchange reactions to transport inhibitors in rat liver mitochondria. *Biochim Biophys Acta* **216**: 63-70.

Rothen-Rutishauser, B., Kramer, SD., Braun, A. Gunthert, M., Wunderli-Allenspach, H., 1998. MDCK cell cultures as an epithelial in vitro model: cytoskeleton and tight junctions as indicators for the definition of age-related stages by confocal microscopy. *Pharmacol Res* **15**: 964-971.

Rubbo, H., Radi, R., Anselmi, D., Kirk, M., Barnes, S., Butler, J., Eiserich, JP., Freeman, BA., 2000. Anitric oxide reaction with lipid peroxyl radicals spare alpha-tocopherol during lipid peroxidation. Greater oxidant protection from the pair nitric oxide/alpha-tocopherol than alpha-tocopherol/ascorbate. *J Biol Chem* **275**: 10812-10818.

Rumsby, G., 2000. Biochemical and genetic diagnosis of the prmary hyperoxaluria: a review. *Mol Urol* **4**: 349-354.

Ryal, RL., Grover, PK., Stapleton, AMF., Barell, DK., Tang, Y., Moritz, RL., Simpson, RJ., 1995. The urinary F1 activation peptide of human prothrombin is a potent inhibitor of calcium oxalate crystallization in undiluted human urine *in vitro*. *Clin Sci* **89**: 533-541.

Ryall, RL., 1997. Urinaty inhibitors of calcium oxalate crystallisation and their potential role in stone formation. *World J Urol* **15**:155-164.

Ryall, RL., Stapleton, AMF., 1995. Urinary macromoleculs in calcium oxalate stone and crystal matrix: Good, bad or indifferent? *Calcium Oxalate in Biological Systems*, edited by Khan SR, Boca Raton, FL, CRC Press, 265-290.

Saari, H., 1991. Oxygen derived free radicals and synovial fluid hyaluronate. *Ann Rheum Dis* **50**: 389-392.

Sakhee, K., Poindexter, JR., Park, CYC., 1989. The spectrum of metabolic abnormalities in patients with cystine nephrolithiasis. *J Urol* **141**: 819-821.

Salvemini, F., Franze, A., Lervolino, A., Filosa, S., Salzano, S., Ursini, MW., 1999. Enhanced glutathione levels and oxidoresistence mediated by increased glucose-6-phospahet dehydrogenase expression *J Biol Chem* **274**: 2750-2757.

Scheid, CR., Koul, H., Hill, WA., Luber-Narod, J., Kennington, L., Honeyman, T., Jonassen, J., Menon, M., 1996 (a). Oxalate toxicity in LLC-PK cells: Role of free radicals. *Kidney Int* **49**: 413-419.

Scheid, CR., Koul, H., Honeyman, T., Jonassen, J., Menon, M., 1996(b). Role of oxalate induced free radical production in stone disease. *Urolithiasis* 10-12.

Schwartzman, RA., & Cidlowski, JA., 1991. Apoptosis: the biochemistry and molecular biology of programmed cell death. *Endocrinol Rev* **14**: 133-151.

Scott, JE., Cummings, C., Brass, A., Chen, Y., 1991. Secondary and tertiary structures of hyaluran in aqueous solution, investigated by rotary shadowing-electron microscopy and computer simulation: Hyaluran is a very efficient network-forming polymer. *Biochem J* **274**: 699-705.

Seftel, A., & Resnick, MI., 1990. Metabolic evaluation of urolithiasis. *Urol Clin North Am* **17**: 159-169, 1990

Selvam, R., & Devaraj, S., 1991. Induction of oxalate binding by lipid peroxidation in rat kidney mitochondria. *Biochem.Int.* **24**: 857-866.

Selvam, R., &. Devaraj, S., 1991. Induction of oxalate binding by lipid peroxidation in rat kidney mitochondria. *Biochem. Int.* **24:**857–866.

Sen, CK., & Packer, L., 1996. Antioxidant and redox regulation of gene transcription. *FASEB J* **10**: 709-720.

Senekjian, HO., & Weinman, EJ., 1982. Oxalate transport by proximal tubule of the rabbit kidney. *Am J Physiol* **243**: F271-F273.

Serafini-Cessi, F., Malagolini, N., Cavallone, D., 2003. Tamm-Horsfall glycoprotein: Biology and clinical relevance. *Am J Kidney Dis.* **42(4)**: 658-76.

Shekarriz, B., & Stoller, ML., 2002. Cystinuria and other noncalcareous calculi. *Endocrinol Metab Clin North Am* **31(4)**: 951-77.

Shoffner, JM., & Wallace, DC., 1995. Oxidative phosphorylation diseases. In *The Metabolic and Molecular Bases of Inherited Disease* 7th edition McGraw Hill, 1535-1629.

Singh, A., Marshall, FF., Chang, R., 1988. Cystine calculi: clinical management and in vitro observations. *Urology* **31**(3): 207- 210.

Slater, EC., 1973. The mechanism of action of the respiratory inhibitor, antimycin *Biochim Biophys Acta* **301**: 129-154.

Slavkovic, A., Radovanovic, M., Siric, Z., Vlajkovic, M., Stefanovic, V., 2002. Extracorporeal shock wave lithotripsy for cystine urolithiasis in children: outcome and complications. *Int Urol Nephrol* **4**:457-61.

Smith, CV., Hughes, H., Mitchell, JR., 1984. Free radicals in vivo. Covalent binding to lipids. *Mol Pharmac* **26**: 112.

Smith, CV., Jones, DP., Guenther, TM., Lash, LH., Lauterburg, BH., 1996. Compartmentation of glutathione: implications for the study of toxicity and disease. *Toxicol Appl Pharmacol* **140**: 1-12.

Smith, LH., & Werness, PG., 1982. Hydroxyapatite-The forgotten crystal in calcium urolithiasis. *Trans Am Clin Climatol Assoc* **95**: 183-190.

Soabo, L., & Zoratti, M., 1992. The mitochondrial megachannel is the permeability transition pore. *J Bioenerg Biomembrl* **24**: 111-117.

Sordahl, LA., & Silver, BB., 1975. Pathological accumulation of calcium by mitochondria: modulation by magnesium. *Recent Adv Stud Cardiac Struct Metab* **6**: 85-93.

Stapleton, AM., Dawson, CJ., Grover, PK., Hohmann, A., Comacchio, R., Boswarva, V., Tang, Y., Ryall, RL., 1996. Further evidence linking urolithiasis and blood coagulation: urinary prothrombin fragment 1 is present in stone matrix. *Kidney Int* **49**: 880-888.

Stapleton, AMF., Ryall, RL., 1995. Blood coagulation proteins and urolithiasis are linked: Crystal matrix protein is the F1 activation peptide of human prothrombin *Br J Urol* **75**: 712-719.

Stapleton, AMF., Seymour, AE., Brennan, JS., Doyle, IR., Marshall, VR., Ryall, RL., 1993. Immunohistochemical distribution and quantification of crystal matrix protein. *Kidney Int* **44**: 817-824.

Suzuki, K., Moriyama, M., Nakajima, C., Kawamura, K., Miyazawa, K., Tsugawa, R., Kikuchi, N., Nagata, K., 1994. Isolation and partial characterization of crystal matrix protein as a potent inhibitor of calcium oxalate crystal aggregation: Evidence of activation peptide of human prothrombin. *Urol Res* **22**: 45-50.

Takahashi, T., Yamagucchi, T., Shitashige, M., Okamoto, T., Kishi, T., 1995. Characterization of NADPH-dependent ubiquinone reductase activity in rat liver cytosol: effect of various factors on ubiquinone-reducing activity and discrimination from other quinone reductases *Biochem J* **309**: 883-890.

Takeshiga, K., & Minakami, S., 1995. NADH and NADPH-dependent formation of superoxide anions by bovine heart submitochondrial particles and NADH-ubiquinone reductase preparation. *Biochem J* **180**: 129-135.

Thamilselvan, S., Byer, KJ., Hackett, RL., 2000. Free radical scavengers, catalase and superoxide dismutase provide protection from oxalate-associated injury to LLC-PK1 and MDCK cells. *J Urol*; **164**: 224.

Thamilselvan, S., Hackett, RL., Khan, SR., 1997. Lipid peroxidation in ethylene-glycol-induced hyperoxaluria and calcium oxalate Nephrolithiasis. *J Urol*; **157**: 1059-63.

Thamilselvan, S., Hackett, RL., Khan, SR., 1999. Cells of proximal and distal tubular origin respond differently to challenges of oxalate and calcium oxalate crystals. *J Am Soc Nephrol*; **10**: S452- S456.

Thomas, D., & Hanley, MR., 1981. Pharmacological tools for perturbing intracellular calcium storage. *Methos Cell Biol* **40**: 65-89.

Thompson, GA., 1976. Hydrolysis and transfer reactions catalysed by γ-glutamyl transpeptidase; evidence for separate substrate sites and for high affinity of L-cystine. *Bochem Biophys Res Commun* **71**: 32-36.

Tiselius, HG., & Almagard, LE., 1977. The diurnal excretion of oxalate and the effect of pyridoxine and ascorbate on oxalate excretion.*Eur Urol* **3**: 41-46.

Tiselius, HG., & Hojgaard, I., 1999. Some aspects of the intratubular precipitation of calcium salts. *J Am Soc Nephrol* **10**: S371-S375.

Tiselius, HG., & Hojgaard, I., 1999. Some aspects of the intratubular precipitation of calcium salts. *J Am Soc Nephrol* **10**: S371-S375.

Tiselius, HG., 1980. Oxalate and renal stone formation. *Scand J Urol Nephrol Suppl* **53**: 135-148.

Trush, MA., Mimnaugh, EG., Gram, TE., 1982. Activation of pharmacologic agents to radical intermediates. Implications for the role of free radicals in drug action and toxicity. *Biochem Pharmac* **31**: 3335.

Turrens, JF., & Boveris, A., 1980. Generation of superoxide anion by the NADH dehydrogenase of bovine heart mitochondria. *Biochem J* **191**: 421-427.

Turrens, JF., Alexander, A., Lehninger, AL., 1985. Ubisemiquinone is the electron donor for superoxide formation by complex III of heart mitochondria. *Arch Biochem Biophys* **237**: 408-414.

Ullrich, KJ., 1994. Specificity of transporters for "organic anions" and "organic cations" in the kidney. *Biochem Biophys Acta* **1197**: 45-62.

Umekawa, T., Chegini, N., Chan, SR., 2003. Increased expression of chemoattractant protein-1 (MCP-1) by renal epithelial cells in culture on exposure to calcium oxalate, phosphate and uric acid crystals. *Nephrol Dial Transplant* **18**: 664-669.

Ursini, F., Maiorino, M., Brigelius-Flohe, R., Auman, KD., Roveri, A., Schomburg, D., Flohe, L., 1995. The diversity of glutathione peroxidases. *Meth EnzymolI* **252B**: 38-53.

Ursini, F., Maiorino, M., Gregolin, C., 1985. The selenoenzyme phospholipid hydroperoxide glutathione peroxidase. *Biochim. Biophys. Acta*; **839**: 62-72.

Vander Heiden, MG., Chandel, NS., Li, XX., Schumacker, PT., Colombini, M., Thompson, CB., 2000. Outer mitochondrial membrane permeability can regulate coupled respiration and cell survival. *Proc Natl Acad Sci USA* **97**: 4666-4671.

Vasquez – Vivar, J., Hogg, N., Pritchard, KA Jr., Martasek, P., Kalyanaraman, B.,1997. Superoxide anion formation from lucigenin: an electron spin resonance spin-trapping study. *FEBS Lett* **403**: 127-130.

Verkoelen, CF., Romijin, JC., Cao, LC., Boeve, ER., Cao, L., de Bruijn, WC., Schroder, FH., 1996. Crystal-cell interaction inhibition by polysaaccharides. *J Urol* **155**: 749-752.

Verkoelen, CF., Romijn, JC., Bruijn, WC., Cao, LC., Schroder, FH., 1993. Absence of a transcellular oxalate transport mechanism in LLC-PK1 and MDCK cells cultured on porous supports. *Scann Microsc* **3**: 1031-1040.

Wandzilak, TR., & Williams, HE., 1990. The hyperoxaluric syndromes. *Endocr Metab Clin N Am* **19**: 851-854.

Warnholtz, A., Nickening, G., Schulz, E., Macharzina, R., Brasen, JH., Sktchkov, M., Heitzer, T., Stasch, JP., Griendling, KK., Harrison, DG., Bohm, M., Meinertz, T., Munzel, T., 1999. Increased NADH-Oxidase-Mediated Superoxide Production in the Early stages of Atherosclerosis: Evidence for involvment of the Renin-angiotensin System. *Circulation* **99**: 2027-2033.

Weissner, JH., Hasegawa, AT., Hung, LY., 2001. Mechanisms of calcium oxalate crystal attachment to injured renal collecting duct cells. *Kidney Int* **59**: 637-644.

Weissner, JH., Hasegawa, AT., Hung, LY., Mandel, NS., 1999. Oxalate-induced exposure of phosphatidylserine on the surface of renal epithelial cells in culture. *Journal Am Soc Nephrol* **10**: S441.

Wells, AF., Larsson, E., Tengblad, A., Fellstrom, B., Tufveson, G., Klareskog, L., Laurent, TC., 1990. The localisation of hyaluran in normal and rejected human kidneys. *Transplantion* **50**: 240-243.

Wessler, E., 1971. The nature of non-ultrafilterable glycosaminoglycans of normal human urine. *Biochem J* **122**: 373-384.

Wiessner, J., Mandel, G., Halverson, P., 1988. the effect of hydroxyapatite crystallinity on hemolysis. *Calcif Tissue Int* **42**: 210-219.

Wiessner, JH., Hasegawa, AT., Hung, LY., Mandel, LY., Mandel, GS., Mandel, NS., 2001. Mechanisms of calcium oxalate crystal attachment to injured renal collecting duct cells. *Kidney Int* **59**: 637-644.

Wiessner, JH., Kleinmann, JG., Blumenthal, SS., 1987. Calcium oxalate crystal interaction with rat renal inner papillary collecting tubule cels. *J Urol* **138**: 640-643.

Williams, HE., & Wandzilak, TR., 1989. Oxalate synthesis, transport and the hyperoxaluric syndromes. *J Urol* **141**: 742-746.

Williamsm AW., & Wilson, DM., 1990. Dietary intake, absorption, metabolism and excretion of oxalate. *Sem Nephrol* **10**: 2-5.

Wink, DA., & Mitchell, JB., 1998. Chemical biology of nitric oxide: insights into regulatory, cytotoxic, and cytoprotective mechanisms of nitric oxide. *Free Radic Biol Med* **25**:434-456.

Worcester, EM., Nakagawa, Y., Wabner, CL., Kumar, S., Coe, FL., 1988. Crystal adsorption and growth slowing by nephrocalcin, albumin and Tamm-Horsfall protein. *American Journal of Physiology*, **255**: F1197-F1205.

Yamate, T., Kohri, K., Umekawa, T., 1999. Interaction between osteopontin on madin darby canine kidney cell membrane and calcium oxalate crystal. *Urol Int* **62:** 81-86.

Yamate, T., Kohri, K., Umekawa, T., Amaski, N., Ishikawa, Y., Iguchi, M., Murita, T., 1996. The relation of osteopontin in adhesion of calcium oxalate crystal with Madin-Darby canine kidney cells. *Eur Urol* **30**: 388-393.

Yan, LJ., Sohal, RS., 1998. Mitochondrial adenine nucleotide translocase is modified oxidatively during aging. *Proc Natl Acad Sci U S A* **95**: 12896-12901.

Yan, N., & Meister, A., 1990. Amino acid sequence of rat kidney $\gamma$-glutamylcysteine synthetase. *J Biol Chem* **265**: 1588-1593.

Yang, JC., & Cortopassi, GA., 1998. Induction of the mitochondrial permeability transition causes release of the apoptogenic factor cytochrome c. *Free Radic Biol Med* **24**: 624-631.

Zamzami, N., Hirsch, T., Dallaporta, B., Petit, PX., Kroemer, G., 1997. Mitochondria implication in accidental and programmed cell death: apoptosis and necrosis. *J Bioenerg Biomembr* **29**: 185-193.

Zamzami, N., Marchetti, P., Castedo, M., Decaudin, D., Macho, A., Hirsch, T., Susin, SA., Petit, PX., Mignotte, B., Kroemer, G., 1995. Sequential reduction of mitochondrial transmembrane potential and generation of reactive oxygen species in early programmed cell death. *J Exp Med* **182**: 1533-1544.

Zamzami, N., Susin, SA., Marchetti, P., Hirsch, T., Gomez, I., Monterrey, Castedo, M., Kroemer, G., 1996. Mitochondrial control of nuclear apoptosis. *J Exp Med* **183**: 1533-1544.

# Renal oxidative vulnerability due to changes in mitochondrial-glutathione and energy homeostasis in a rat model of calcium oxalate urolithiasis

**Eirini Meimaridou, Edgar Lobos and John S. Hothersall**

*Am J Physiol Renal Physiol* 291:731-740, 2006. First published May 2, 2006;
doi:10.1152/ajprenal.00024.2006

*Am J Physiol Renal Physiol* 291: F731–F740, 2006.
First published May 2, 2006; doi:10.1152/ajprenal.00024.2006.

# Renal oxidative vulnerability due to changes in mitochondrial-glutathione and energy homeostasis in a rat model of calcium oxalate urolithiasis

**Eirini Meimaridou,[1] Edgar Lobos,[2] and John S. Hothersall[1]**

Available online at www.sciencedirect.com

SCIENCE DIRECT

Free Radical Biology & Medicine 38 (2005) 1553 – 1564

www.elsevier.com/locate/freeradbiomed

Original Contribution

# Crystal and microparticle effects on MDCK cell superoxide production: Oxalate-specific mitochondrial membrane potential changes

Eirini Meimaridou[a], Jake Jacobson[b], Alan M. Seddon[c], Alberto A. Noronha-Dutra[a], William G. Robertson[a], John S. Hothersall[a,*]

0891-5849/$ - see front matter 
doi:10.1016/j.freeradbiomed.2005.02.020